"A Study of the Constitution and Viscosity of the Silicate Systems."

Thesis presented for the Degree of Doctor of Philosophy by

John Rhynas Rait, B.Sc. June, 1938.

ProQuest LLC.
789 East Eisenhower Parkway
P.O. Box 1346
Ann Arbor, MI 48106 – 1346

The author wishes to express his gratitude and appreciation for the interest shown by Professor R. May in this work which was carried out in The Metallurgy Department, The Royal Technical College, Glasgow.

Part I

CONSTITUTION OF SLAG SYSTEMS.

Part II

VISCOSITY OF SLAG SYSTEMS

Part 1.

[illegible] OF FLAG SYSTEMS.

Introduction

Slags derived from the Iron and Steel Industry are chiefly composed of silicates. It has been recognised by many melters that the slag produced in the furnace is a very important factor in the correct working of the furnace charge. Different melters work their furnaces in different ways, making their additions at different times in the working of the charge. All, however, are aiming at obtaining a certain condition of the slag, which condition, they maintain, gives the best working of the charge and yields the best results in the process. In electric furnace practice, the working slag is poured off and replaced by a synthetic finishing slag and in shops equipped with tilting furnaces the working slag is poured off and a special finishing slag is employed.

Physico-Chemical considerations have also shown that due attention must be paid to the slag. According to COLCLOUGH[1] the constitution of the slag is the most important factor controlling the reactions occurring in the basic open hearth furnace. For example, a slag high in lime is necessary to remove phosphorus from the molten steel. The work of McCANCE[2] on the Physico-Chemical properties of slags has also indicated the important influence of the slag in the refining operations in the open hearth process of steel making. McCance, in reviewing the work in this field, has shown that the behaviour of the slag-metal relationships in the acid process can be accounted for in a fairly satisfactory manner on theoretical grounds but that there are anomalies in the basic process. The chief anomaly is the building up of FeO in the finishing slags. FERGUSON[3] believes that the formation of calcium ferrites has some influence on this phenomenon.

Before commencing the study of actual open hearth furnace slags it is necessary to have a knowledge of the behaviour and properties of their constituents. In the Metallurgy Department, Royal Technical College, Glasgow, a comprehensive scheme of research into slag-metal relationships has been undertaken. The three binary systems FeO-MnO, MnO-SiO_2 and FeO-SiO_2 and the ternary system FeO-MnO-SiO_2 comprised the preliminary

part of the investigation. From the refining aspect, the $CaO-Fe_2O_3$ was the next system examined.

The effect of other oxides upon the low melting compositions in the $FeO-MnO-SiO_2$ slags called for attention. Al_2O_3 was investigated. In view of the effect of Al_2O_3 on the melting points, and of the difficulty of correlating the phases present in the different melts, it was felt desirable that the systems $MnO-Al_2O_3$, $FeO-Al_2O_3$, $FeO-MnO-Al_2O_3$, $MnO-Al_2O_3-SiO_2$ and then the quaternary system $FeO-MnO-Al_2O_3-SiO_2$ should be investigated.

The scope of the present work is the experimental determination of the thermal equilibrium diagrams:-

a) Binary system $FeO-Al_2O_3$ and b) Ternary system $FeO-MnO-Al_2O_3$.

BENEDICKS and LOFQUIST[4] have indicated the need for the knowledge of the physical properties of these slag systems in the field of non-metallic inclusions in steel. Herty and his collaborators have shown in recent years that the most prolific source of non-metallic inclusions in steel is from the deoxidation process. Deoxidation is brought about in the bath by deoxidisers, chiefly manganese and silicon. But these do not remove all the FeO. To do this, additions are usually made in the ladle and it has become quite common practice to use aluminium in addition to manganese and silicon. Hence, due to this deoxidation process, Al_2O_3, MnO and SiO_2 are formed. So that in the steel there will be FeO, MnO, Al_2O_3 and SiO_2 to form non-metallic inclusions, and if these are not removed the resulting steel is 'dirty'. The elimination of these inclusions can only be effected by taking advantage of their natural tendency to rise. It can be shown that the velocity of rising of slag spheres through a liquid metal is:-

$$v = \frac{2}{9}\frac{r^2(d-d')g}{\eta}$$

where v = velocity of rising
r = radius of slag particle
d = density of metal
d' = density of slag
η = coefficient of viscosity of metal

It is, therefore, obvious that the speed of rising of the slag particles depends largely upon their size. The size of the inclusions, in turn, depends upon the degree of coalescence obtained

It is therefore obvious that the speed of rising of the slag particles depends largely upon their size. The size of the inclusions, in turn, depends upon the degree of coalescence obtained between the smaller particles, and this will be governed by the melting point of the inclusions and other physical properties such as Surface Tension, Viscosity etc. Hence, it is essential to have a knowledge of the Thermal Equilibrium Diagrams $FeO-SiO_2$, $MnO-SiO_2$, $FeO-Al_2O_3$, $MnO-Al_2O_3$, $FeO-MnO-Al_2O_3$, $FeO-MnO-SiO_2$ and $FeO-MnO-Al_2O_3-SiO_2$. Such information regarding the constitution is essential to the interpretation of the data to be obtained from the experimental work on viscosity.

Resume of Previous Work done on Thermal Equilibrium Diagrams of Slag Systems.

Many of the silicates found in the slags derived from the Iron and Steel Industry are found in rocks, so that they are of interest to petrologists and to manufacturers of refractories. It is not surprising to find that a good deal of work has been done on these substances. VOGT[5] was one of the earliest workers and another pioneer was DOERINCKEL[6] who determined the melting temperatures of various binary mixtures, and of special interest in the present field was the diagram $MnO-SiO_2$. SOSMAN and his colleagues[7] have continued and developed the work on binary and more complex systems at the Geophysical Laboratories in the U.S.A. WHITELY and HALLIMOND[8] have investigated open hearth steel furnace slags, as has HERTY and his co-workers[9]. Iron blast furnace slags have received much attention from RANKIN and WRIGHT[10], FEILD and ROYSTER[11], and McCAFFERY and his co-workers[12].

Work on FeO has been carried out by MATHEWSON, SPIRE and MILLIGAN[13], FOOTE and JETTE[14], TRITTON and HANSON[15] and their results compared with those of HAY, HOWAT and WHITE[16] in a paper published by the latter.

BENEDICKS[4] has described researches on slag systems and has propounded thermal equilibrium diagrams for various Silicate systems.

BOWEN and SCHAIRER[17] investigated slag systems and put forward a diagram for $FeO-SiO_2$ based chiefly on quenching experiments. BOWEN and GREIG[18] have fully investigated the system $Al_2O_3-SiO_2$.

In the Royal Technical College, Glasgow, ANDREW[19] developed a technique for the investigation of Thermal Equilibrium Diagrams of slag systems. Work has proceeded in this department and the technique has been modified by HAY and his co-workers[20].

ESSER, AVERDIECK and GRASS[21] have investigated M.P's of $FeO-SiO_2$.

From a survey of the research carried out in the investigation of Thermal Equilibrium Diagrams of slag systems, the chief methods of investigation are:-

a) Thermal Analysis - Time-temperature, inverse rate and differential heating and cooling curves.

b) Quenching methods.

c) Petrographic methods.

d) High-Temperature microscope.

None of these methods alone yields sufficient evidence to determine thermal equilibrium diagrams for slag systems. If necessary, all methods would be used.

a) Thermal analysis is the most common method of investigation, but does not always yield evidence of phase changes. RANKIN and WRIGHT[10] in their investigation of the ternary diagram $CaO-Al_2O_3-SiO_2$ found that in some regions of the diagram thermal curves indicated phase changes, while in other regions no phase changes were indicated by thermal curves but were shown to occur by other methods of investigation. If the slag is very viscous and tends to be glassy, crystal formation is retarded or may be prevented under the rate of cooling employed in determining cooling curves. Hence, the phase change will not be found on the curves.

However, if the slag is annealed at the temperature of crystal formation, crystals are formed and can be detected by method C.

When the thermal curves show no evidence of phase changes, the slag is heated to a given temperature and annealed for a suitable period and then quenched. By quenching from a range of temperatures and then examining the optical properties, the various phase changes can be found. This method is very useful in determining limits of solubility and other phase changes occurring below the liquidus. RANKIN and WRIGHT[10] employed this method along with thermal analysis. Although phase changes are shown by one of these methods, the other method may also be employed as a check. However, it is comparatively simple to quench slags which do not oxidise in air, but it is much more difficult to quench slags containing FeO or MnO which do oxidise in air. Fortunately, it was found that thermal curves of slags such as $FeO-Al_2O_3$ and $FeO-MnO-Al_2O_3$ showed the phase changes and hence it was not necessary to carry out quenching experiments.

c) Petrographic methods most usually employed to identify phases are Refractive Index, Pleochroisim, Angle of Extinction, Binefringence, Optical character, Polarisation Colours and colour. These properties may be investigated in the powdered slag or in thin sections. Another method is to examine a polished section of the slag by a microscope using reflected light. When the number of different phases occurring in the system is small, it is possible to identify them by this latter method. It is very useful to employ this method on a slag which has been slowly cooled, for it is then possible to find the mode of cooling. For example, in a system of two components A and B, a slag may deposit primary A and eutectic of A and B. On examination of the specimen by this method, primary phase will be distinguished. If it is not possible to identify the various phases which would be the case where there is a large number, it would be necessary to measure Refractive indices etc.

d) WHITE, HOWAT and HAY[20] designed a high temperature microscope which made it possible to examine the changes occurring in $MnO-SiO_2$ slags during heating to temperatures at which they were completely liquid. This method is only necessary in exceptional cases as described by the authors.

Methods of Investigation employed in determining the Thermal Diagrams for systems $FeO-Al_2O_3$ and $FeO-MnO-Al_2O_3$.

Determination of differential heating and cooling curves together with microscopic examination by reflected light of polished sections of slowly cooled slags was found to yield sufficient evidence.

The Apparatus.

Construction of the Furnace.

The first essential is a furnace capable of yielding a temperature of over 1600°C and whose rate of heating and cooling can be fairly accurately controlled. Few furnaces comply with these requirements. The usual experimental furnaces employed to give such temperatures are:-

1) Refractory tube wound with suitable wire in the form of a solenoid using D.C. as source of energy.
2) Carbon Granular Furnace.
3) High Frequency Induction Furnace.
4) Gas-fired Muffles.

1) was considered the most suitable since a suitable source of current was at hand and the necessary equipment was both simple and cheap. The amount of energy supplied to the furnace could be easily controlled by a rheostat and hence the rates of heating and cooling could be accurately adjusted.
The Carbon Granular and High Frequency Induction furnaces require much more expensive equipment and have the disadvantage that the rate of heating and cooling is not easy to control.

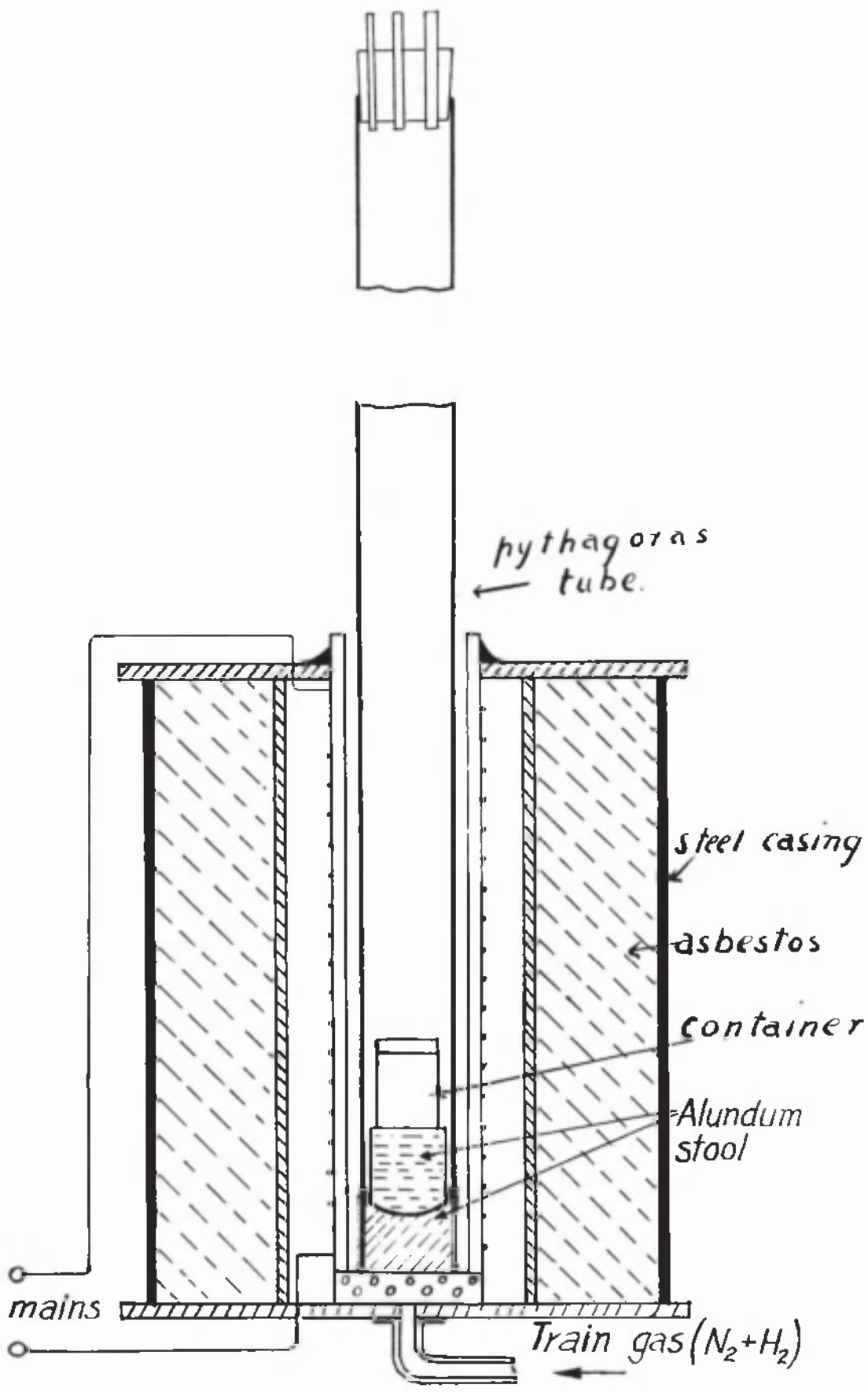
pythagoras
tube.
steel casing
asbestos
container
Alundum
stool
mains
Train gas (N_2+H_2)

fig 1.

The High Frequency Induction furnace requires also a suitable core in which the current can be induced. Such a furnace was employed by McCAFFERY[12] in which the heat was induced in the graphite slag container.

Having decided to use a wire-wound furnace, the question of suitable wire arises. Platinum, Platinum-Iridium, Tungsten and Molybdenum wires are the only ones possible. Platinum and Platinum-Iridium are seldom used to obtain a temperature of over 1600°C in such a furnace, since to yield this temperature in the furnace the wire would be at a much higher temperature and approaching its melting point. Molybdenum and Tungsten have much higher melting points and so are capable of producing a much higher temperature. However, they both have the disadvantage of oxidising when heated to over 690°C in air. This, however, can be overcome by surrounding the winding with an inert atmosphere such as hydrogen or nitrogen. Molybdenum was chosen since Tungsten wire becomes much more brittle than Molybdenum on heating. MnO with a melting point of 1795°C has been melted in a molybdenum wound furnace[16].

The furnace employed for determining the thermal data is shown in fig. 1. The casing is of mild steel ¼ inch thick; the top and bottom plates are also of mild steel, but are $\frac{3}{8}$ inch thick to minimise warping. Spigot and faucet jointing is used both at top and bottom to ensure tightness. This is particularly important in the case of the bottom joint, as leakage of air into the furnace causes rapid deterioration of the molybdenum wire winding. A welded bottom joint has been used on some of the furnaces, but as another type of bottom plate is required for certain work, interchangeability is an advantage. It is possible to make a satisfactory joint without resort to welding. The furnace element is similar to one described by ANDREW[19], although minor modifications were made to give higher temperatures and longer life. The diameter of the Alundum tube, which carries the furnace winding, was

reduced to a minimum about 2¾ ins. Such a tube is made by mixing together 90% of alundum (grade 563) with 10% of alundum (grade 562) and water to give a plastic material. An iron tube of an external diameter slightly less than the required internal diameter of the alundum tube is used as a former. Round the iron tube are wrapped three or four folds of damp brown paper. The alundum mixture is put round the wet paper and worked by hand until it is of uniform thickness of about ¼ inch. The iron tube, supported on a steel rod, is slowly dried by placing it near a hot muffle. Slow drying is essential to prevent cracking. When thoroughly dry, the tube is rubbed down with emery paper to a uniform thickness. Thick string is wound round the tube at the required spacing of winding, usually five turns to the inch. The string is fixed in position by a very thin coating of alundum. After drying the thin coating, the former with the alundum tube on it, is now placed in a large furnace and slowly heated to 1100°C. The string and paper are burned and the tube is easily removed from the iron tube. It is finally dressed and the grooves for the wire cleaned. The finished tube is about 18 ins. long by 2¾ ins. internal diameter and wall thickness less than ¼ inch.

About 45 ft. of molybdenum wire .04 inch in diameter is required to wind the furnace. The wire is first cleaned with emery to remove the graphite coating formed during drawing. The top and bottom of the winding are fixed by a binding wire consisting of a few turns of molybdenum wire. This binding wire also serves to fix the lead-in wires which are made of very heavy nichrome wire. To protect the molybdenum winding from dust, it is embedded in a coating of alundum.

The tube carrying the winding fits into a recessed groove in the bottom plate, and is thus held in position.

Another alundum tube made in a similar manner but about 4 ins. in diameter is slipped over the winding to prevent

to prevent/
the asbestos insulation (see fig. 1) coming into contact with the hot tube, which would cause slagging.

The heavy nichrome leads which project through the outer casing to brass terminals (See fig. 1) are joined to the ends of the molybdenum winding. These leads must not be strained since after being heated to 1600°C, molybdenum wire becomes brittle and is easily broken. The bottom lead and winding joint must be at such a distance from the "hot zone" of the furnace, that when it is at a temperature of about 1600°C, this connection is at a temperature below the melting point of nichrome. Quite a number of furnace failures were due to the bottom lead melting.

The most efficient wire wound furnace is one in which the wire is wound inside the alundum tube. When the wire is wound outside the alundum tube as in the furnace described previously, there is a temperature gradient through the alundum and so to attain a temperature of say 1600°C inside the furnace, the wire has to be at a much higher temperature. However, molybdenum wire becomes brittle and must be protected. It is, therefore, better to wind the molybdenum wire on a very thin walled alundum tube and then to cover it with a thick coating of alundum. With a thin walled tube there is only a small temperature gradient from the wire to the inside of the furnace and the thick alundum coat acts as a heat insulator.

The amount of energy available for heat is C^2Rt

where C = current (amps)
R = resistance (ohms)
t = time

For the furnace described above, a current of 30 amps. at 250 volts enables a temperature of over 1600°C to be attained at a speed suitable for the determination of heating curves. The rate of cooling can be adjusted by adjusting the current supplied to the furnace through a variable resistance.

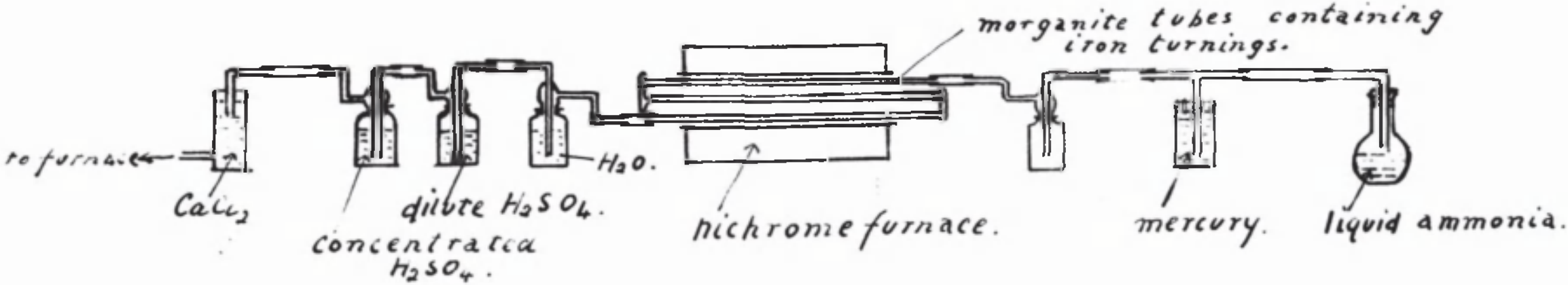
morganite tubes containing iron turnings.
to furnace
$CaCl_2$
concentrated H_2SO_4.
dilute H_2SO_4.
H_2O.
nichrome furnace.
mercury.
liquid ammonia.

fig. 2.

The resistance of the furnace winding is $\frac{250}{30}$ ohms at 1600°C. After experimenting with various diameters and lengths of winding it was found that the previously mentioned dimensions were most suitable. Molybdenum winding of smaller cross-section, having a greater resistance and so requiring a smaller current, has a short life.

No oxygen should come into contact with the molybdenum winding, since the volatile oxide MoO_2 is formed and the winding ruined. Hence an inert atmosphere is maintained in the annular space between the two alundum tubes. A stream of nitrogen and hydrogen is passed from a cracking train through the bottom of the furnace and is distributed round the heating element by means of a distributer (see fig. 1) To prevent too rapid a passage of the gas through the furnace, all joints are luted up with a mixture of fireclay and alundum.

To obtain this stream of gas, a flask containing liquid ammonia (S.G. ·88) is heated, the expelled ammonia gas passing through a trap and mercury valve and then cracked by passing over iron turnings contained in a series of "Morganite" tubes heated to 700°C in a nichrome wound furnace. Residual ammonia gas is removed by passing the gas through water and dilute sulphuric acid, and the stream of nitrogen and hydrogen is finally led through concentrated sulphuric acid and calcium chloride towers to dry before entering the furnace. The mercury valve is inserted so that if too great a resistance to the passage of the gas is set up, the gas escapes through the valve, thus preventing a building up of pressure which would lead to explosion. Dilute sulphuric acid is used to remove the final traces of ammonia gas since the ammonium sulphate formed is insoluble in concentrated sulphuric acid. Fig. II shows a diagram of the cracking train.

It may well be asked why a mixture of commercial hydrogen and nitrogen is not employed. Firstly, such a mixture contains a certain amount of oxygen which would ultimately destroy the molybdenum winding, and, secondly it is cheaper to manufacture the mixture of nitrogen and hydrogen.

"Pythagoras" Tube

The mixture of hydrogen and nitrogen gases diffuses through the porous 'Alundum' tube. The easily reducible and oxidisable nature of FeO rendered it necessary to make all determinations either in vacuo or in an inert atmosphere. It was, therefore, necessary to heat the slags containing FeO in an inner refractory tube which was impervious to gases at the temperatures employed. "Pythagoras" tubes 90 cm. long and 50 m.m. internal diameter were found to hold a vacuum up to a temperature of 1500°C., but at higher temperatures they are liable to soften and collapse. It would have been preferable to carry out the determinations in vacuo, but to prevent collapse of the tubes, nitrogen was maintained at a pressure of 1 atmosphere for all determinations. To remove the residual oxygen, the nitrogen was passed over copper turnings in a Morganite tube heated to about 700°C. This was necessary as the residual oxygen attacked the molybdenum-tungsten thermocouple wires. The tube was evacuated and slowly filled with oxygen-free nitrogen at a pressure of 1 atmosphere. If the pressure were allowed to increase on heating, then, since the tube softens at about 1500°C., it would tend to blow out. The pressure was kept constant by means of a mercury manometer, which allowed the gas to escape when the pressure increased beyond 1 atmosphere. When the"Pythagoras" tube is allowed to rest in the furnace, it deforms under its own weight at 1500°C., so to increase the life of the tube and to prevent loss of shape, it was suspended in the furnace by means of a lever and counterpoise system.

Slag Containers

Suitability of containers for molten slags is one of the problems to be encountered in this type of work. The container must be sufficiently refractory and must withstand the corrosive action of slags. Pure electrode graphite can be used if there are no constituents present which can be reduced by the carbon. In earlier work[20] on the system MnO-SiO_2,

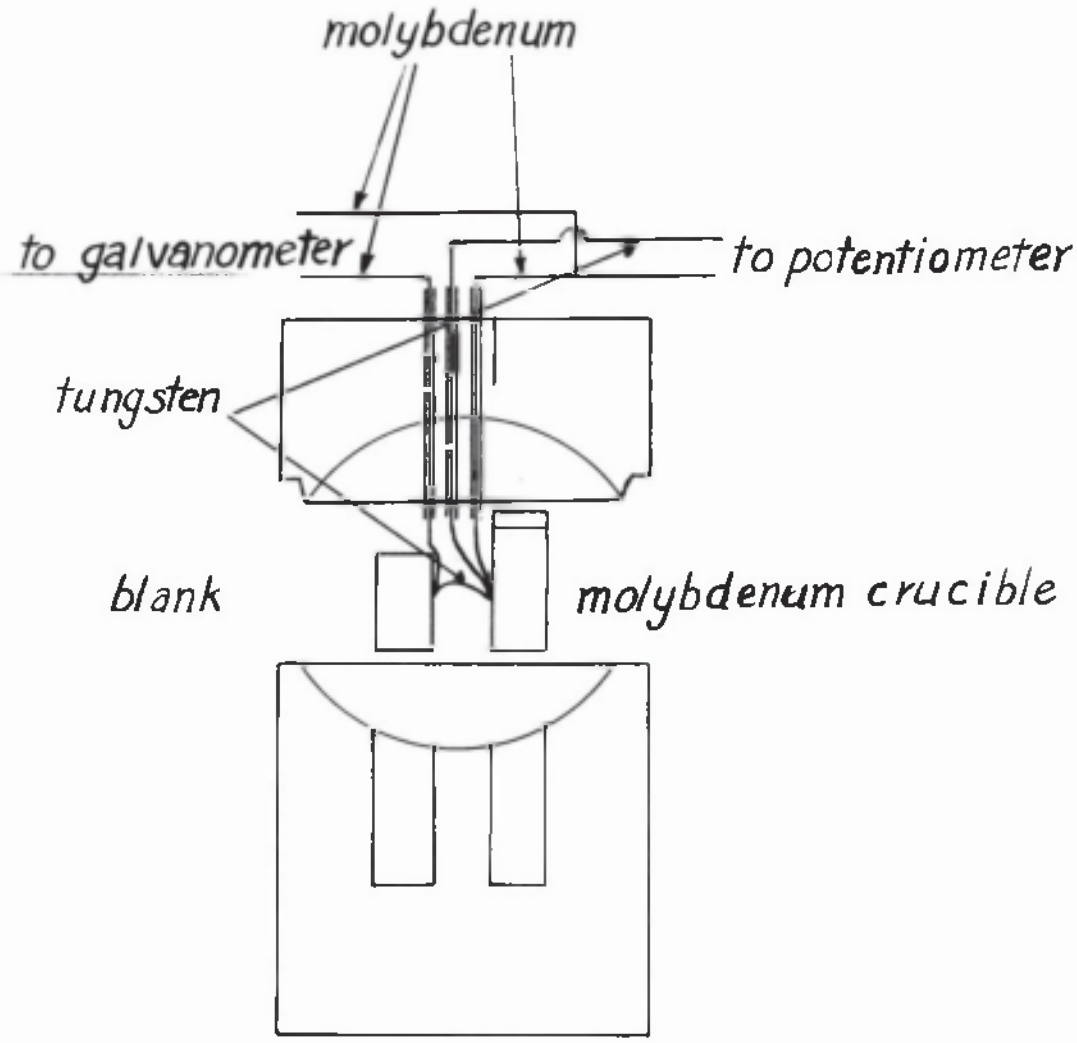
molybdenum
to galvanometer
to potentiometer
tungsten
blank
molybdenum crucible

fig. 3.

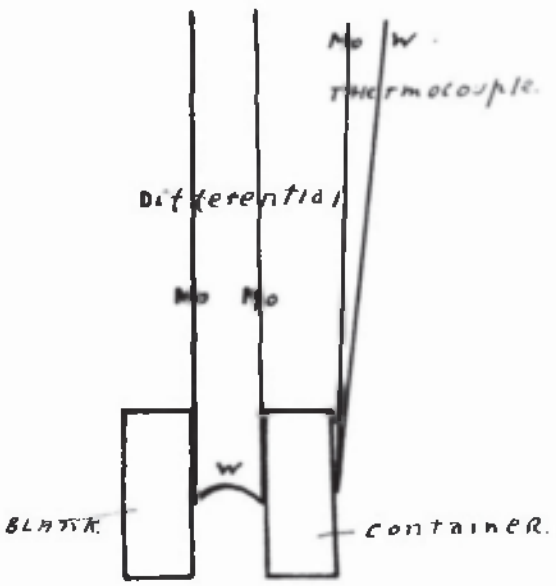

fig. 4.

salamander crucibles were found to withstand the corrosive action of the slag, but MnO was reduced to manganese by the carbon. FeO is also reduced by carbon. When using other types of refractory material it is very necessary to be certain that they do not contaminate the melt and so seriously alter its properties. Small molybdenum crucibles, drilled from solid rod, were found to meet all requirements. These crucibles are 1¼ in. long and $\frac{5}{16}$ in. in diameter, and hold about 2 grams of material. A Hilger spectrograph and various highly sensitive chemical tests have been employed in order to detect any contamination of the melts. Furthermore, analysis of the material was carried out after fusion, which showed that no serious change in composition had occurred during melting.

Temperature Measurement.

A molybdenum-tungsten thermocouple was employed. Owing to the smallness of the heat change in many of the systems it has been found necessary to employ the differential method of thermocouple arrangement to increase the sensitivity of measurement of heat changes. The molybdenum crucible being small, it can be treated as the hot junction of the thermocouple system, the thermocouple wires being bound to the outside of the crucible. In earlier work where the wires were immersed in the slag, contamination occurred due to the slag creeping up the wires and attacking the silica insulation. The thermocouple arrangement finally adopted is shown in fig. 3. A piece of molybdenum rod of approximately the same weight as the crucible, served as the blank. Both the crucible and blank fitted into pockets in the alundum container, the couple wires passing through holes in the lid. The temperature recording thermocouple which was attached to the crucible was connected to a Tinsley Vernier Potentiometer, and the differential thermocouple to a high resistance galvanometer. The usual set up of differential thermocouple necessitates two opposed thermocouples and a separate thermocouple for recording the temperature as shown in fig. 4. Employing the former method is more economical, since for each experiment new

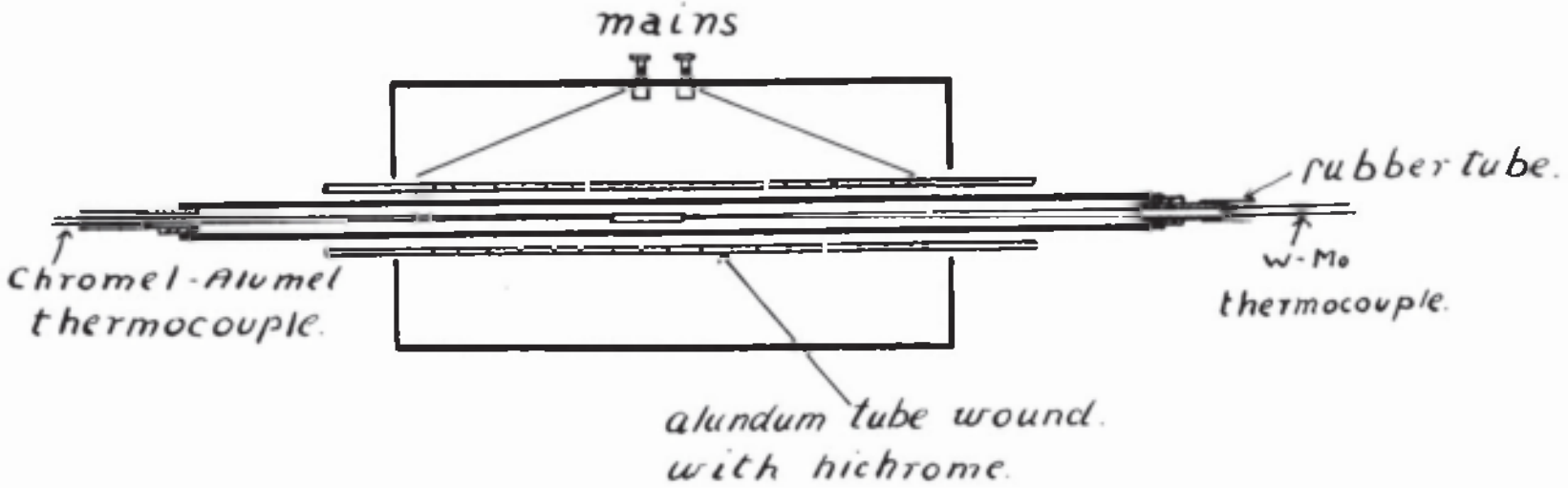
mains
rubber tube.
Chromel-Alumel
thermocouple.
W-Mo
thermocouple.
alundum tube wound
with nichrome.

fig. 5

thermocouple junctions have to be made. After heating to about 1600°C and cooling, about 6 ins. of tungsten and molybdenum wire must be removed before the new hot junctions are made. Hence, in the method employed 18" of thermocouple wire is lost against 24" in the usual method. Since molybdenum wire is less brittle than the tungsten wire, it was always twisted round the tungsten wire in making the hot junctions.

Calibration of Thermocouple.

Since each tungsten-molybdenum thermocouple has a limited life for reasons given in previous paragraph, and also since each batch of couple wires have a slightly different temperature - e.m.f. curve, a standard method of calibration was necessary. The thermocouple was calibrated in the following manner:-

1) Comparison with a standardised "Chromel-alumel" thermocouple to 900°C.

2) Determination of heating and cooling curves of pure electolytic copper which melts at 1083°C.

3) Determination of the heating and cooling curves of pure iron, the melting point of which is 1525°C and the A_4 point is at 1400°C. EPSTEIN[22] has pointed out that these temperatures are uncertain unless absolutely pure iron is obtained.

Further precautions taken and methods employed are described in a later part of this thesis.

1) The Chromel-alumel thermocouple was first standardised against the melting points of tin, lead, zinc and silver which are recognised standards on the thermodynamic scale. This standardised chromel-alumel thermocouple was employed in the calibration of subsequent thermocouples in the following way. The chromel-alumel and tungsten-molybdenum thermocouples were fixed to a small piece of molybdenum in a morganite tube (see fig. 5) . The tube was evacuated. The required temperatures were obtained by means of a nichrome wound furnace and each temperature was maintained constant for about 30 minutes before thermocouple readings were taken. The temperatures corresponding to a given e.m.f. for the tungsten-molybdenum thermocouple was obtained from the e,m.f. temperature curve for chromel-alumel. In this way, the e.m.f.-

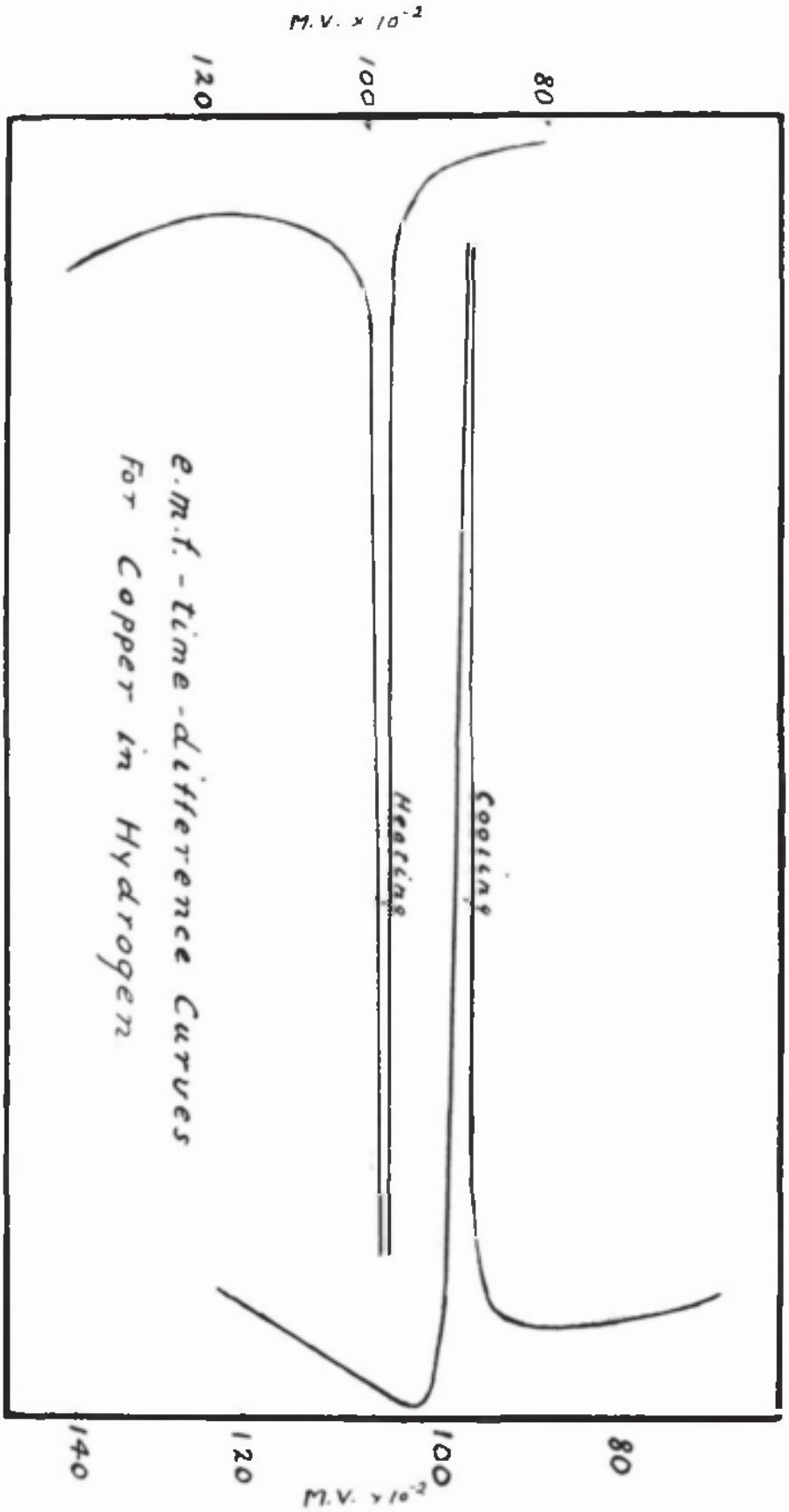
M.V. x 10⁻²
120
100
80
e.m.f. - time - difference Curves
For Copper in Hydrogen
Heating
Cooling
140
120
100
80
M.V. x 10⁻²

fig. 6.

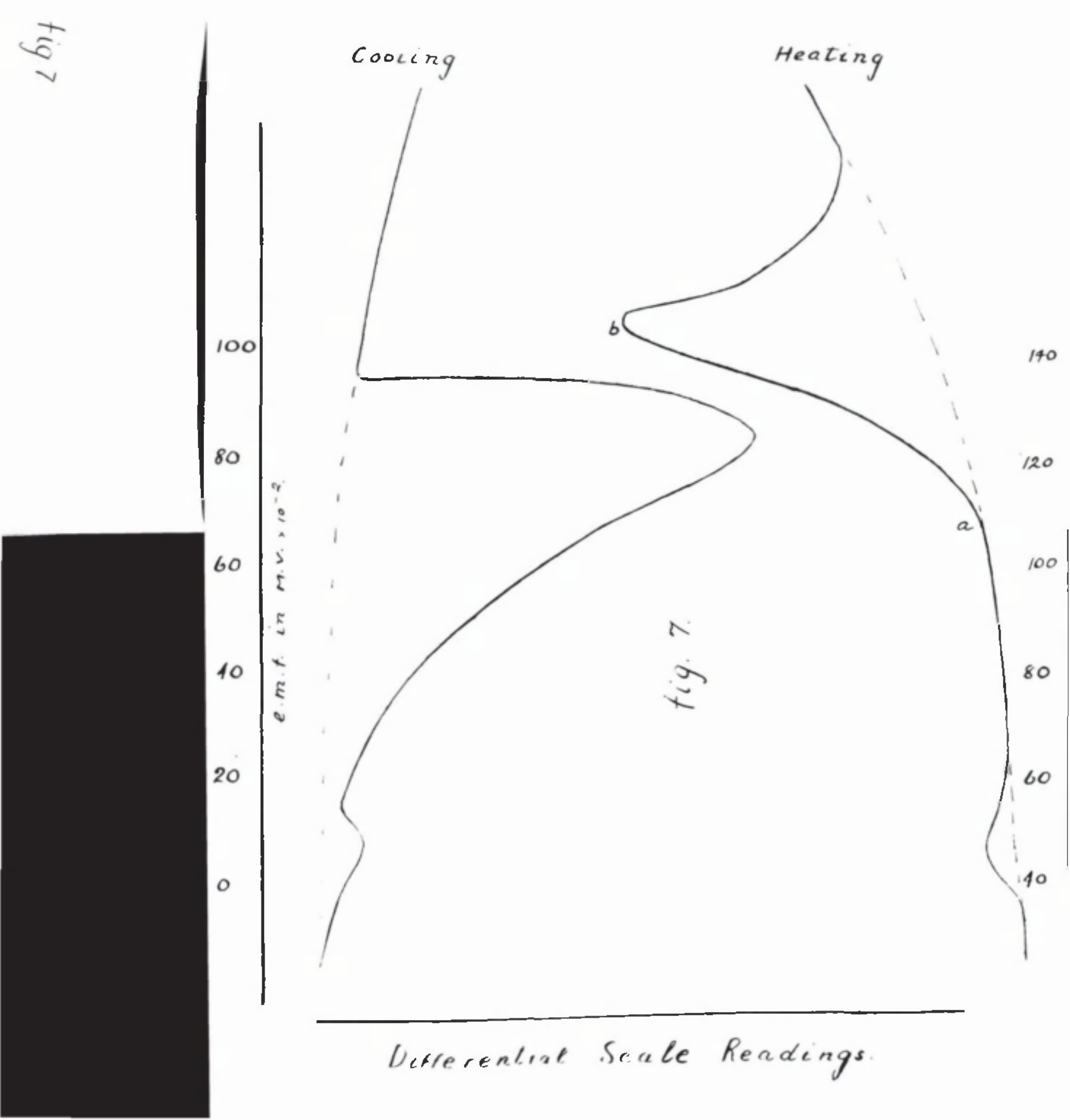
fig 7
Cooling
Heating
b
a
100
80
60
40
20
0
140
120
100
80
60
40
e.m.f. in M.V. x 10⁻².
fig. 7.
Differential Scale Readings.

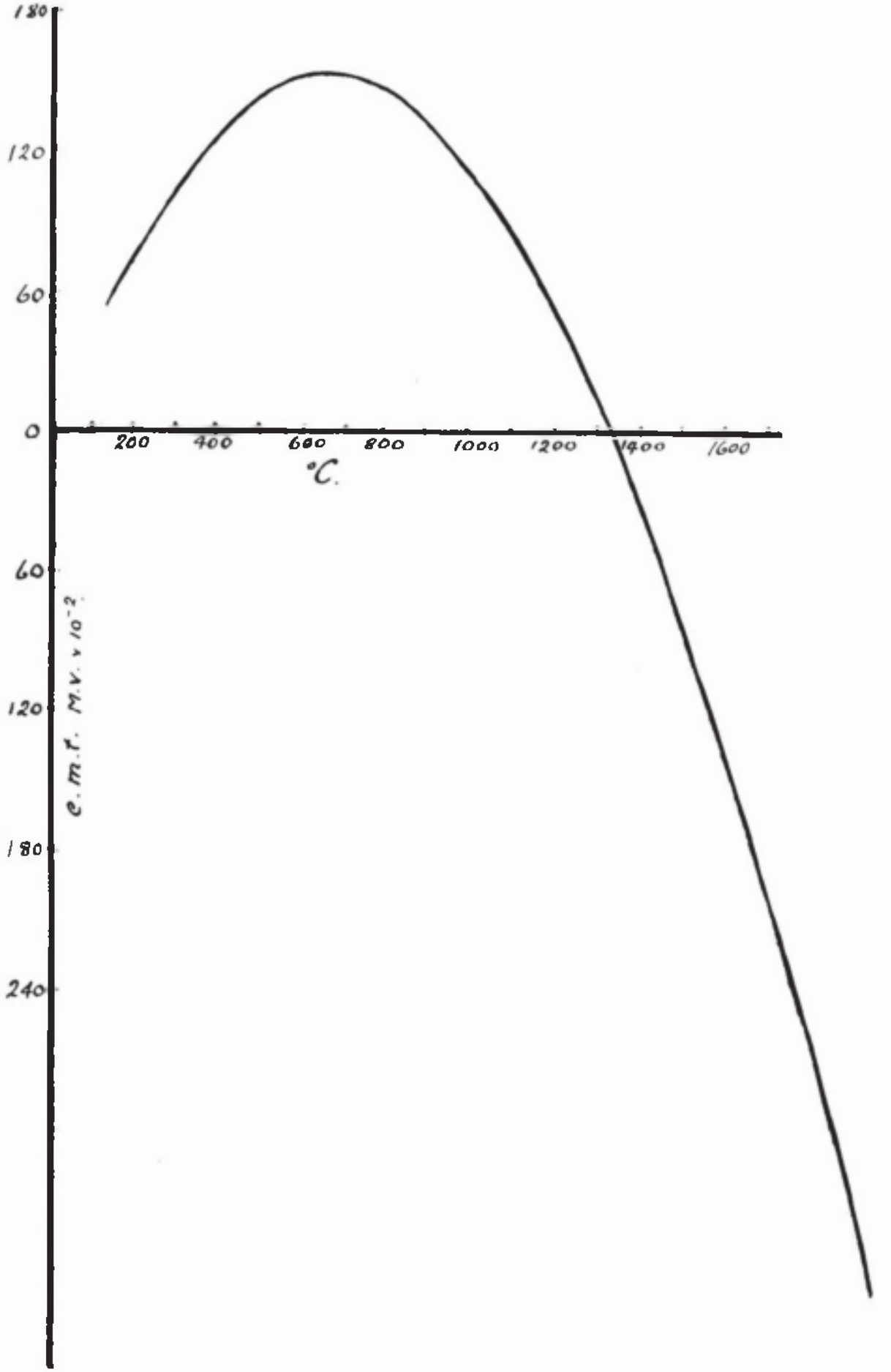
180
120
60
0
60
120
180
240
200
400
600
800
1000
1200
1400
1600
°C.
e.m.f. M.V. x 10⁻²

fig. 8.

temperature curve for tungsten-molybdenum was found to a temperature of 900°C.

2) Heating and cooling curves for pure electrolytic copper were obtained in a similar apparatus as that described for the determination of thermal curves for slags. However, since the heat changes involved are much greater for copper than for slags, a differential thermocouple system was not required. A hole was drilled in a piece of copper and the tungsten-molybdenum thermocouple protected by a fireclay sheath inserted. A salamander pot containing the copper was placed on an alundum stool in the Pythagoras tube suspended in the molybdenum wound furnace (see fig. 1). The alundum stool is so arranged that the graphite pot is in the "hot zone" of the furnace. The tube was evacuated and an atmosphere of hydrogen introduced. A reducing atmosphere must be employed in determining the melting point of pure copper since a small amount of Cu_2O gives a marked eutectic point on the heating and cooling curves. The heating and cooling curves were obtained by plotting the time interval for each increase (or decrease) of .02 m.v. against e.m.f. Typical curves are shown in fig. 6. The mean e.m.f. corresponding to 1083°C is thus found.

3) The thermal curves for pure iron were experimentally determined in an apparatus similar to that used for slags. Three differential heating and cooling curves were obtained. The technique employed is exactly as that for slags, the iron specimen replacing the molybdenum crucible. The thermocouple point protected from the molten iron by means of a silica tube was inserted into a hole drilled in the specimen. Typical curves are shown in fig. 7.

The e.m.f. -temperature curve for a tungsten-molybdenum thermocouple is shown in fig. 8. As the temperature increases, the e.m.f. increases to a maximum at about 600-700°C, decreases to zero, and then changes sign. This thermocouple is only useful for measuring temperatures from 900°C, since below 900°C due to the flat maximum on the e.m.f.-temperature curve, the thermocouple is not sufficiently sensitive, there being

only a relatively small change in e.m.f. over a wide range of temperature. However, for the present investigation, the range of temperature was from 900°C upwards. In this range, the sign of the e.m.f. changes. A uni-directional e.m.f. can only be measured by means of a Tinsley Vernier Potentiometer, hence a reversing key is fitted into the circuit of thermocouple leads and potentiometer. When the e.m.f. reaches zero the arm of the commutator is switched over, so maintaining a uni-directional e.m.f.

Molybdenum "Grid"

In earlier investigations using tungsten-molybdenum thermocouples, "grid" trouble had been experienced at temperatures above 1200°C. When an electric current was passing through the furnace, the thermocouple readings became very erratic above 1200°C, In fact, at times the galvanometer mirror became so unstable that the e.m.f. of thermocouple could not be obtained. However, if the current was switched off, the mirror became quite stable and the e.m.f. could be measured. Below 1200°C, this "grid" trouble did not exist to any marked extent. Probably at temperatures above 1200°C thermionic emission occurs, the thermions being picked up by the thermocouple. A clean piece of molybdenum sheet about 9 in. in length is bound round the Pythagoras tube, and the container with the crucible and blank is placed in the centre of this shield or grid. This prevented grid trouble.

Preparation of the materials employed.

(1) Ferrous Oxide (FeO).

The existence of three oxides of iron has been established:-

a) Fe_2O_3 - 70% Fe.

b) Fe_3O_4 - 72.36% Fe.

c) FeO - 77.73% Fe.

Ferrous oxide was prepared by decomposing recrystallised ferrous oxalate at 650°C in vacuo, raising the temperature to 1000°C and maintaining for an hour at that temperature before cooling. Ferrous oxalate in a hard baked alundum container was placed inside a 'Pythagoras' tube heated by a nichrome wound furnace. The tube was evacuated by a "Cenco-Hyvac" pump and the temperature slowly raised to 650°C. The oxalate decomposed yielding ferrous oxide, CO and CO_2. As the gases were evolved, they were removed by the pump and the completion of decomposition was denoted by the return of a vacuum. The temperature was then raised to 1000°C. The decomposition must not take place too quickly, since the pump is then incapable of removing the gases as rapidly as they are formed. During decomposition, the fall in the vacuum should not be greater than 1 cm. of mercury. It was found that when the decomposition was too rapid, a product was obtained which was highly magnetic and had a higher oxygen content than that of ferrous oxide. MATSUBARA and SCHENK[23] have shown that an equilibrium exists between FeO, Fe_3O_4, CO and CO_2 at the temperature of decomposition.

$$2Fe_3O_4 + 2CO \rightleftarrows 2CO_2 + 6FeO.$$

If CO_2 and CO are removed from the system before reaction occurs, ferrous oxide will be obtained. Matsubara and Schenk have also shown that below 575°C, ferrous oxide is unstable, undergoing dissociation into Fe and Fe_3O_4. Unless this dissociation is prevented, the resulting product although having the correct proportion of Iron and oxygen, will be magnetic; the magnetic test for purity of FeO is not then very dependable. However, this dissociation is very sluggish

and if the product is cooled very rapidly, it is suppressed, the resulting ferrous oxide being non-magnetic. The ferrous oxide so prepared was black with a slightly bluish tinge. Analysis showed a total iron content of 77.5-77.6%. WHITE, HOWAT and HAY[20] found that if the final heating to 1000°C was omitted, the product became rapidly magnetic on exposure to air. It is interesting to note that in the "Chimie Minerale", 1905, vol. 4, p. 399, it is stated that there are two modifications of FeO. The low-temperature modification is pyrophoric and when heated in nitric acid, nitrous fumes are evolved. The high-temperature modification does not decompose nitric acid and is more stable in air. It is also stated that the low-temperature modification can be converted to the high-temperature modification by heating to above 1000°C. The differential curves for FeO are reproduced in fig. 10. The thermal changes will be discussed in detail later. However, it is of interest here to discuss the point occurring at 1170°C. In the curve for non-magnetic FeO, this deflection is small. However, from a batch of ferrous oxide which was magnetic some of the magnetic material was separated by means of a magnet. The differential curve for this magnetic portion showed a more pronounced deflection at 1170°C. The presence of this low point at 1170°C and the increase in magnitude of this arrest with the presence of Fe_3O_4 tends to confirm the work of MATHEWSON, SPIRE and MILLIGAN[13], rather than the work of FOOTE and JETTE[14], the former workers reporting a eutectic between FeO and Fe_3O_4 with a melting point of 1175°C.

In analysing the product for total iron, a very sensitive test would be essential, for if we had a material containing say, 10% Fe_3O_4, the total iron content would be 77.19% as compared with 77.73% for pure FeO. It is obvious from examination of these figures that to detect a small amount of Fe_3O_4 in FeO, the analysis for total iron would require to be very carefully carried out and the method used should yield highly accurate results.

WHITE, HOWAT and HAY[20] carried out x-ray spectrographic analysis of FeO. In the prepared FeO there was evidence of one very faint line which has been identified as the α-reflection from the 440 plane of the Fe_3O_4 crystal lattice. In fused FeO, three very faint lines were observed and identified as the reflections of the α and β radiations from the 440 and the α-radiation from the 222 plane of Fe_3O_4. All this goes to show that there is a very small amount or Fe_3O_4 in the prepared material, and that this amount increases after fusion.

(2) Manganous Oxide (MnO)

Manganous oxide was prepared in a similar apparatus to that employed for preparing FeO. Manganese oxalate was decomposed by heating slowly to 750°C, the gases produced being removed by the pump. When decomposition was complete, the product was heated to 1000°C and cooled in vacuo. Since MnO is stable and is not reduced by hydrogen, it was cooled in hydrogen to prevent higher oxides being formed.

The product was an olive-green powder, which analysis showed to have 77.4% manganese. The sintered MnO, when examined under the microscope appeared as clear deep green crystals, while the same material which had been cooled from 750°C appeared opaque and cross-hatched. This latter product was pyrophoric.

X-ray analysis of the MnO showed that it had a cubic space lattice of the NaCl type. The length of the elementary cube was found to be 4.44_5 A°.U., which is in good agreement with the generally accepted figure for this material. The melting point of the MnO was found to be 1785°C.

The optical properties of the FeO and MnO have been investigated by HAY and his co-workers[20].

(3) Alumina

Previously, alumina had been prepared from the hydrate, but it was found possible to purchase a very pure form of anhydrous alumina. This material was analysed before being used in the present investigation.

Method of Experiment.

The mixtures of required composition were made up by weighing the necessary quantities of materials, which were thoroughly mixed by grinding in an agate mortar. About 2 gms. of mixture were packed into a molybdenum crucible and the lid, which was cut out of molybdenum, was jammed into the crucible top. Slags rich in FeO were found to have a tendency to 'boil over', but the fitting of a lid to the crucible prevented this occurrence. The thermocouple and differential leads were bound to the crucible and blank (as shown in fig. 4) , which were inserted into the appropriate pockets of the alundum container. The top of the container was then luted on with alundum cement. An important practical point in this arrangement is that the hot junction of the thermocouple must be fitted to the bottom of the crucible, since after fusion the slag occupies a much smaller volume than the original mixture. In some cases where thermal changes were not indicated by the differential curves, they appeared when the hot junction was placed at the bottom of the crucible. To prevent short circuiting, the thermocouple leads were insulated with silica sheathing.

The container was lowered into the 'Pythagoras' tube until it came to rest on an alundum stool, which was so arranged that when the tube was placed in position in the furnace, the container was in the hot zone. The bottom of the 'Pythagoras' tube which is the weakest part, was then below the hot zone and was, therefore, not overheated.

The molybdenum 'grid', which was bound round the 'Pythagoras' tube, must not come into contact with the furnace wall, since on expanding it is liable to stress the alundum tube. This was believed to be the cause of some furnace failures. However, if the furnace tube was too great in diameter, it was not possible to obtain a sufficient rate of heating to the high temperatures (1600°C), so it was made of size just sufficient to accomodate this expansion.

The 'Pythagoras' tube was closed with a rubber stopper through which passed three glass tubes. One of the glass tubes was connected through a mercury manometer to a

'Cenco-Hyvac' pump and through the other two tubes passed the thermocouple and differential couples. To these glass tubes were fitted pressure rubber tubes which were sealed by screw clips.

The 'Pythagoras' tube was evacuated, and, after the train gases had been passing for a few minutes, the furnace was slowly heated to about 1000°C which was a temperature suitable for beginning a heating curve.

Since, in most cases, a temperature of over 1500°C was necessary to attain the completely liquid state, nitrogen at a pressure of one atmosphere was maintained in the 'Pythagoras' tube to prevent its collapse. Small traces of oxygen in the commercial nitrogen attacked the thermocouple hot junction, and it was necessary to remove the oxygen by passing the gas over copper turnings at 900°C before it entered the tube.

The e.m.f. registered by the thermocouple was measured by a Tinsley Vernier Potentiometer. The differential leads were connected to a high resistance mirror galvanometer, whose deflection was measured by a spot of light, reflected from the mirror of the galvanometer, moving over a scale. Differential scale and time readings were noted at each 2×10^{-5} volts increase or decrease in e.m.f. Differential curves were obtained by plotting differential scale readings against temperature. Where necessary, time difference-temperature curves were plotted for additional evidence of phase changes. Three heating and two cooling curves were determined for each mixture. The first heating curve gave no data of value for the construction of the diagrams due to its lack of homogenity and the formation of compounds. The second and third heating curves were always in agreement, otherwise the experiment was repeated; this also applied to the cooling curves.

When the current supplied to the furnace was increased during the determination of a heating curve an apparent phase change appeared at this point on the differential curve. To avoid this complication, it was arranged that a

current of 32 amps. was passing through the furnace at the beginning of the determination which enabled the temperature of 1600°C to be attained without a further increase of current. However, if then the rate of heating was too great, current changes were made at different temperatures in subsequent determinations. Similarly, for the cooling curves, the current was decreased to an amount which allowed the temperature to fall to about 1000°C without further reduction of current. If the rate of cooling was then too great, the current was reduced in stages, but at different temperatures in subsequent determinations.

Deduction of the thermal equilibrium diagram $FeO-Al_2O_3$.

The phase diagram or thermal equilibrium diagram is a graphic representation of one or two or more related phases. Since the most complete information on a system is given by a set of capacity factors in number just sufficient to fully define the state, it follows that, for example, complete information would be given by a volume-energy-entropy-mass diagram. Because of its experimental convenience, however, the set of thermo-dynamic quantities ordinarily represented is one which is mathematically equivalent to the above, namely, Gibbs free energy, temperature, pressure, and chemical content. Because the free energy is defined when the temperature, pressure and composition are defined, it is usual to omit free energy and so three variables remain -- temperature, pressure and composition. These are the quantities plotted in most phase diagrams.

Since three variables are involved, three dimensional space is required for the representation of a binary system. However, invariably, binary diagrams as found in the literature are two dimensional and are usually isobaric sections taken from the whole diagram. As a further simplification it is frequently assumed that the pressure variable can be neglected and for metallic systems, the assumption is justifiable since vapour pressures are usually

small at the temperatures under consideration and this also applies to the slag systems in the present investigation.

The Phase Rule states:-

$$f = c + 2 - p$$

where f = no. of degrees of freedom
c = components
p = number of phases in equilibrium.

Neglecting the pressure variable, the number of variables is reduced by one and the phase rule is stated:-

$$f = c + 1 - p$$

The phase rule statement of the equilibria which may exist in an isobaric binary system is:-

$$f = 2 + 1 - p = 3 - p$$

when $p = 3$, $f = 0$ - invariant point. This is the only point at which the three phases are in equilibrium.

" $p = 2$, $f = 1$ - one degree of freedom.

$p = 1$, $f = 2$ If composition is fixed, then temperature is fixed.

For a pure substance

$$f = 1 + 1 - p = 2 - p.$$

Therefore, at the melting point two phases are present and hence $f = 0$. Therefore melting will occur at constant temperature.

The fact, that the compositions of the phases in equilibrium at any one temperature in a two phase region do not change, leads to the important rule for the construction of a binary isobaric diagram, that, it is necessary and sufficient to know the one-phase region boundaries. This is likewise true for ternaries.

Interpretation of Differantial Thermal Curves.

The crucible and the blank change in temperature at approximately the same rate, since they are of the same material and approximately the same mass; hence the differantial curve should be a vertical straight line provided there is no phase change. That is, the differential scale reading should remain constant. Actually, however, there is a slight drift of the zero due to small difference in mass and the presence of the mixture.

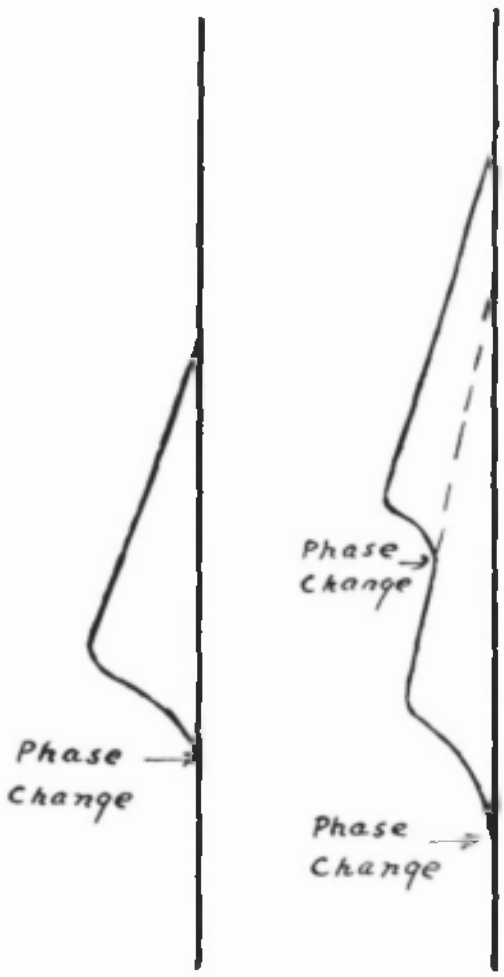

fig. 9.

When the contents of the crucible undergo a phase change, heat is either absorbed or evolved, causing a rate of change in the heating or cooling, and it will lag behind or advance in front of that of the blank. The first deviation from the normal curve indicates the commencement of this phase change. e.g. During melting of a pure substance, heat is absorbed and the temperature of the crucible falls behind that of the blank whose temperature increases steadily as the temperature or the furnace increases. Hence the differential couple will register a difference in temperature resulting in a deviation from the normal curve. When melting is completed, the temperature of the crucible begins to gain on that of the blank and the deflection decreases till the normal is reached. This is illustrated in fig. 9, which also shows a change when a second phase change occurs. It follows that the maximum deviation from the normal occurs at the conclusion of the heat absorption or evolution. This is merely a qualitative method of detecting heat changes. However, for the same phase change(e.g. eutectic) occurring in mixtures of different compositions, comparison of the deflections gives a relative measure of the amounts of heat involved.

The differential heating and cooling curves for pure iron are shown in fig. 7. Two phase changes are indicated. The phase change occurring at the lower temperature is the γ to δ change (1400°C). According to the phase rule, melting occurs at a constant temperature. Hence, with ideal rate of heating the temperature of the crucible would remain constant at the melting point and the deflection would proceed to its maximum at this temperature. On completion of melting the temperature of the crucible would start to gain on that of the blank and there would be a gradual return to the normal curve. However, it is evident that melting has commenced at a and is completed at b . There has been superheating shown by the range of temperature between a and b.

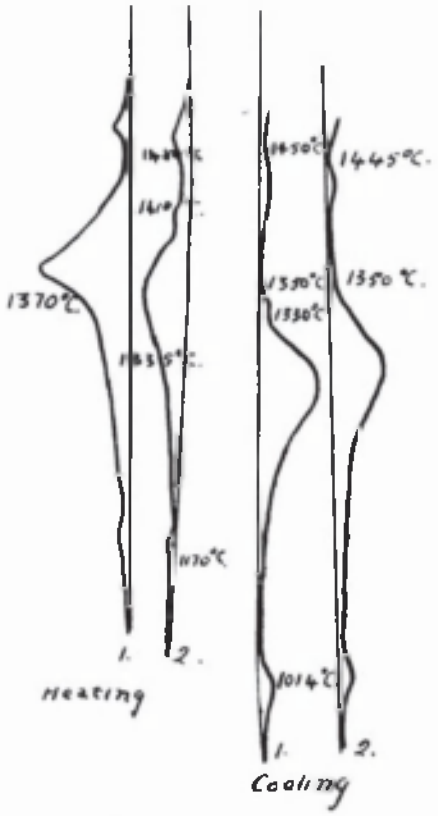

FeO ... 100%
(Non-Magnetic).

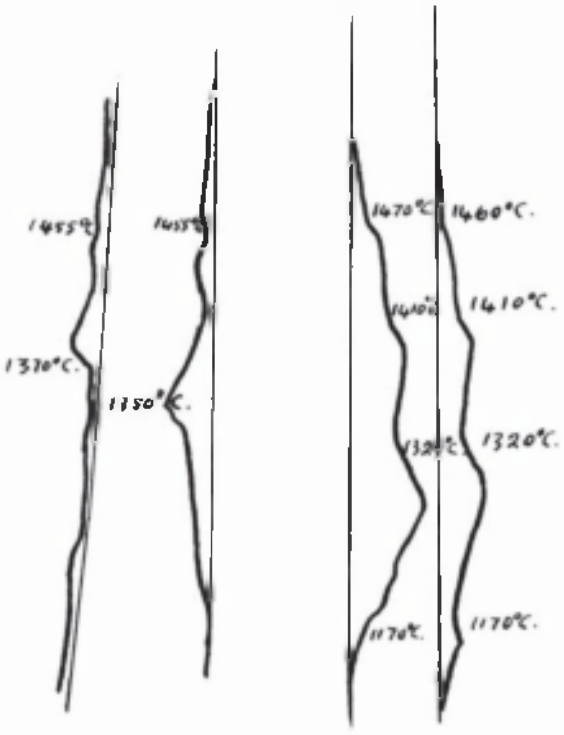

FeO ... 100%
(Magnetic).

Fig. 10.

However, with different rates of heating, although the position of b varies, a is fairly constant and is always taken as the temperature of such a phase change. Comparing the heating and cooling curves it will be observed that the beginning of melting on heating occurs at a slightly higher temperature than the beginning of crystallisation on cooling. The faster the cooling the greater is this difference up to a limit. Even with slow rates of cooling, supercooling occurs and it is very marked in the case of some slags. It is necessary for the success of the differential thermal method to employ sufficiently rapid rates of heating and cooling, otherwise temperatures of the crucible and blank are equalled by conduction of heat and the sensitivity of the apparatus is decreased.

The differential heating and cooling curves for FeO are shown in fig. 10. The heating curves show a small deflection at 1170°C which has already been discussed. There is a large deflection at 1370°C and small but definite arrests occur at 1410°C and 1480°C. FeO does not appear to have a definite melting point, but at 1370°C undergoes a peritectic transformation, in which liquid phase and a very small amount of solid solution of oxygen in iron are in equilibrium. The small arrest at 1410°C is due to the γ to δ change in the iron, and the point at 1480°C to the final solution of the iron. These thermal changes are in very ggod agreement with those found by TRITTON and HANSON[15]. No attempt was made to look for the arrest at 570°C which has been observed by various workers[4], as the molybdenum-tungsten thermocouple is not sufficiently sensitive in the region of 600°C due to the occurrence of a maximum in the e.m.f.-temperature curve. Since FeO occurs in a two component system, and three phases are in equilibrium at the peritectic transformation, temperature should remain constant until the transformation is complete. Hence, in the heating curve the deflection should begin and reach its maximum at 1370°C when on completion of the transformation there should be a gradual return to the normal. However, there has been a small degree of superheating.

As the temperature increases from 1370°C , iron goes into solution and the contents of the crucible absorb heat, the curve gradually returning to the normal. The small but marked deviation at 1480°C would not occur with an ideal rate of heating. While iron is going into solution the temperature of the crucible is gradually gaining on that of the blank. At 1480°C, the last traces of iron go into solution rapidly, causing a small arrest in the temperature of the crucible.

Phase changes which produce large thermal arrests are readily detected by heating and cooling curves. Slag systems seldom produce such arrests but in most cases the differential thermal curves are sufficiently sensitive to indicate them. There is a certain type of slag whose phase changes are difficult to detect. Slags of glassy nature belong to this type. On cooling from the liquid state, the viscosity increases so rapidly and to such an extent that crystallisation may be partially or wholly suppressed, resulting in straight line differential curves or curves showing ill-defined points. RANKIN and WRIGHT[10] obtained such curves for some slags composed of lime, silica and alumina. Thermal curves for slags with high silica content gave no evidence of phase changes. To obtain this information, the slags were annealed at various temperatures, quenched, and the optical properties examined.

Types of Deflections found in Thermal Curves for Binary Mixtures.

The type of curve for a pure one component system such as iron has been discussed and a pure undissociated compound behaves similarly.

The occurrence of a eutectic, eutectoid, peritectic or peritectoid is indicated by a deflection of the invariant type. At the composition of the eutectic etc., the deflection is at a maximum, decreasing progressively as the composition moves away from that of the eutectic etc.

In the case of solid solution, transformation from solid to liquid occurs over a range of temperature. In the heating curve, the first deviation from the normal indicates the solidus, the maximum of the deflection occurring at the

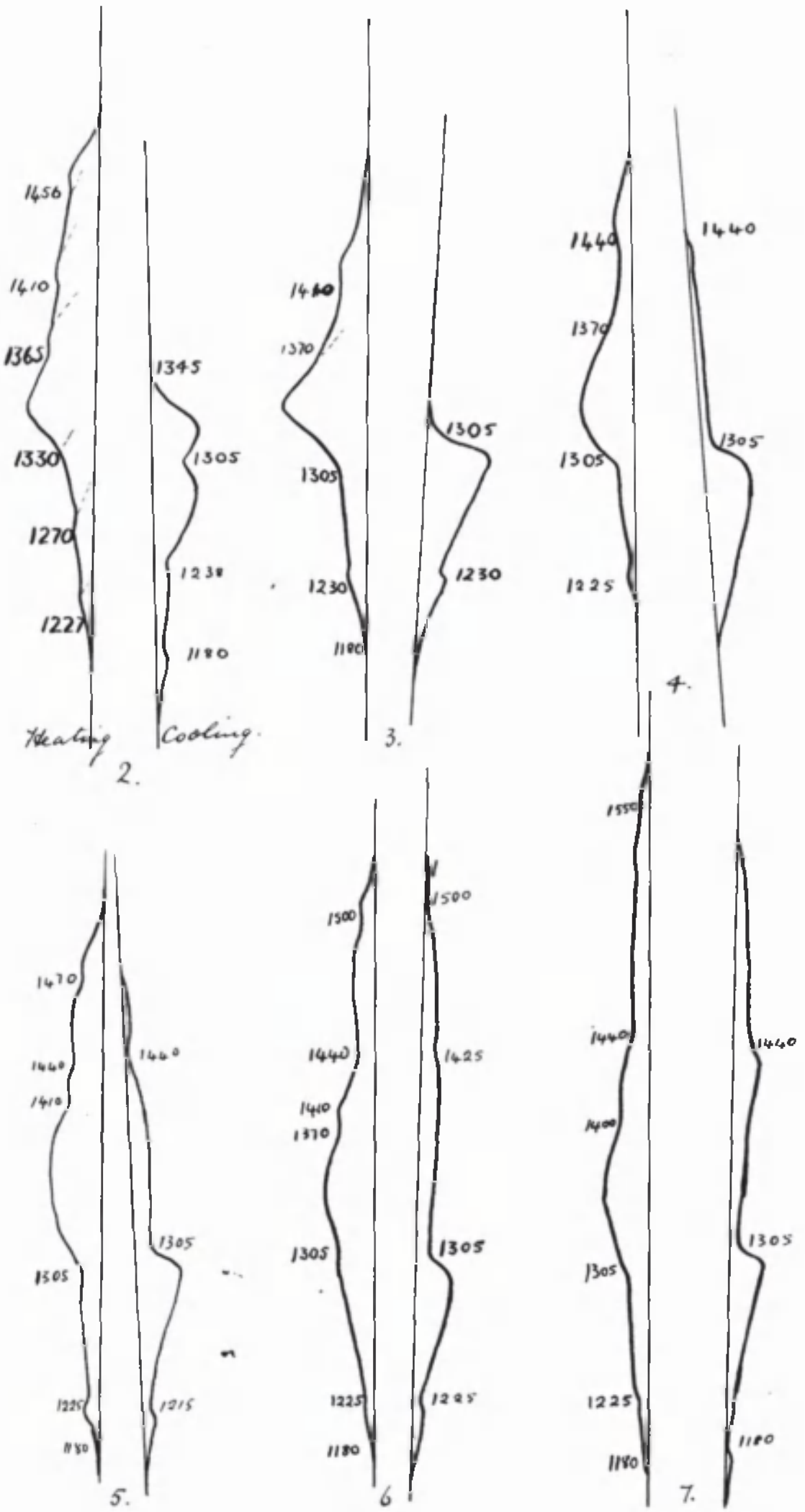
1456
1410
1365
1330
1270
1227
Heating
2.
1345
1305
1238
1180
Cooling
1440
1370
1305
1230
1180
3.
1440
1370
1305
1225
1440
1305
4.
1470
1440
1410
1305
1505
1225
1180
5.
1500
1440
1410
1370
1305
1225
1180
1500
1425
1305
1285
6
1550
1440
1400
1305
1225
1180
1440
1305
1180
7.

fig. 11.

liquidus. The first deviation from the normal in the cooling curve indicates the liquidus and the maximum, the solidus.

The thermal arrests in the heating and cooling curves corresponding to the passage from a one phase to a two phase region in the solid state are small. As in the case of FeO-MnO[20] however, such arrests are often quite definite and so it is possible to fix the limits of solubility in the solid state. Other changes in the solid state are liable to be sluggish resulting in small deflections in the thermal curves.

A transformation occurring at constant temperature only yields a deflection of the invariant type when the heat change involved is sufficient to maintain the crucible and contents at a constant temperature for the rate of heating or cooling employed.

Experimental evidence obtained for the construction of the Binary Diagram $FeO-Al_2O_3$.

The thermal evidence obtained is shown in table I.

Table I

Composition %FeO	%Al_2O_3	Thermal Curves	Temperatures of phase changes °C.
1) 100	0	fig. 10	1170, 1370, 1410, 1480.
2) 98	2	fig. 11	1227, 1270, 1330, 1360, 1305.
3) 95	5	" "	1180, 1229, 1305, 1370, 1410.
4) 90	10	" "	1170, 1225, 1305, 1370, 1390, 1440.
5) 85	15	" "	1180, 1225, 1305, 1370, 1410, 1410, 1470.
6) 80	20	" "	1180, 1225, 1305, 1370, 1410, 1440, 1500.
7) 75	25	" "	1180, 1225, 1305, 1370, 1410, 1440, 1550.
8) 60	40	After soaking at 1600°C these slags were not completely liquid. Hence, liquidus must be above 1600°C.	
9) 43	57	After soaking at 1670°C, mixture was only sintered.	

No thermal curves were obtained for slags with more than 25% Al_2O_3. Examination of the previous table shows that slags with more than 25% Al_2O_3 are not completely liquid at a temperature of 1600°C. Hence the number of slags whose thermal curves could be determined was limited by the upper temperature limit of the furnace. Unless the mixture has been completely molten, phase changes shown by the thermal curves are unreliable.

The thermal arrests at 1170°C, 1370°C and 1410°C appearing in the curves of FeO persist in the curves of the FeO-Al_2O_3 mixtures. The 1370°C peritectic of FeO is taken as the melting point. Consequently, the system in the FeO rich region is only a pseudo-binary and strictly should be considered as a ternary system of Fe, O_2, Al.

All the thermal curves with the exception of (1) and (2) show a large deflection at 1305°C. This deflection is greatest in curve (3). This is the eutectic transformation, the composition of the eutectic according to the thermal evidence, being about 95% FeO, 5% Al_2O_3. There is also a small but definite arrest at about 1225°C in all the curves except (1), and in all the curves except (1), (2) and (3) there is an arrest occurring at 1440°C. These are invariant points. The transformation at 1225°C might be eutectoid or peritectoid. The phase change at 1440°C was possibly a peritectic transformation.

All the curves for slag (2) do not show the 1305°C arrest and this slag was considered to be just within the one-phase region of FeO solid solution. The arrest at 1360°C was taken as the liquidus and 1330°C as the solidus. The small arrest at 1270°C then indicates that 2% Al_2O_3 is the limit of this one phase region at this temperature. For all the slags except (1) and (2) the highest arrest points increase in temperature with increasing Al_2O_3 content and these points were taken as lying on the liquidus.

These arrest points were plotted against composition (see fig. 12). From the above consideration of the

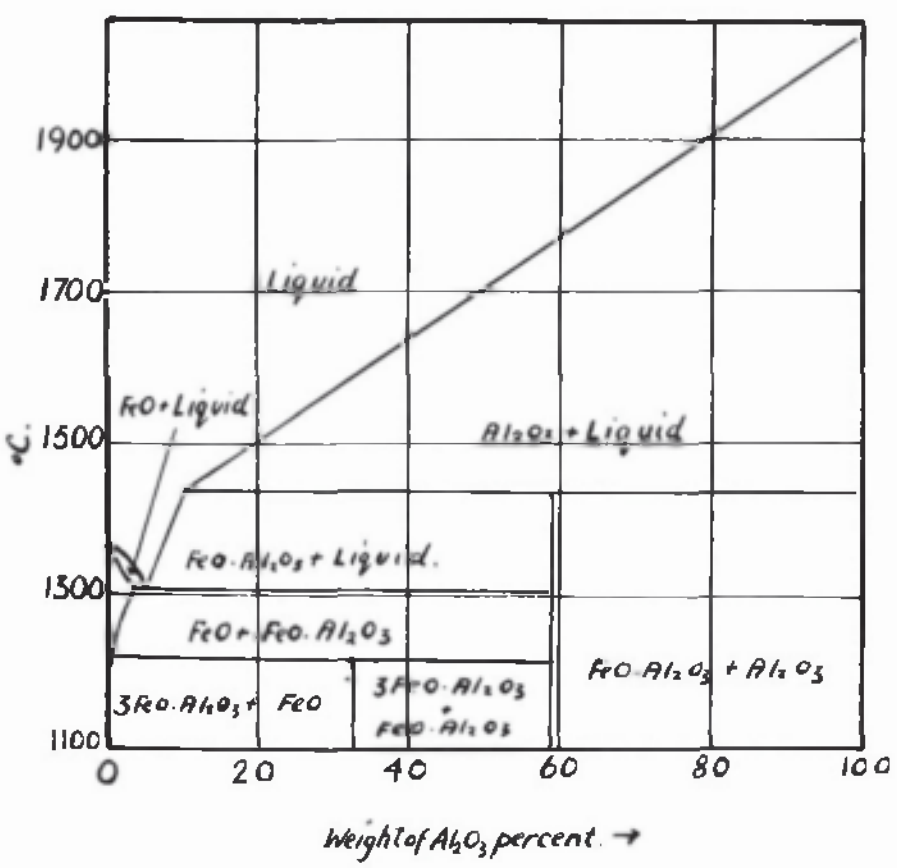
1900
1700
1500
1300
1100
°C
Liquid
FeO + Liquid
Al2O3 + Liquid
FeO·Al2O3 + Liquid.
FeO + FeO·Al2O3
3FeO·Al2O3 + FeO
3FeO·Al2O3
FeO·Al2O3
FeO·Al2O3 + Al2O3
0
20
40
60
80
100
Weight of Al2O3 percent →

fig. 12.

fig. 13.

(1) × 94

(2) × 94

(3) × 300

ETCHED WITH
1% HCl IN WATER.

(4) × 300

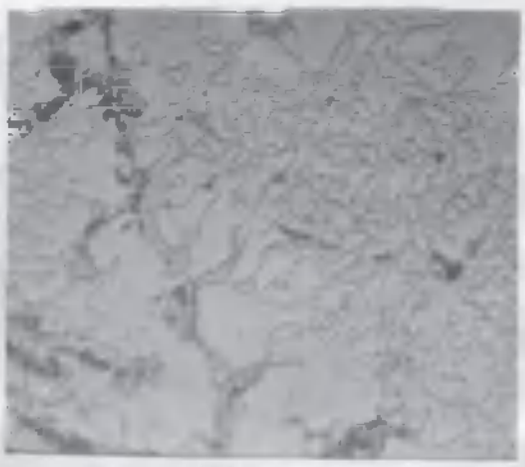

(5) × 300

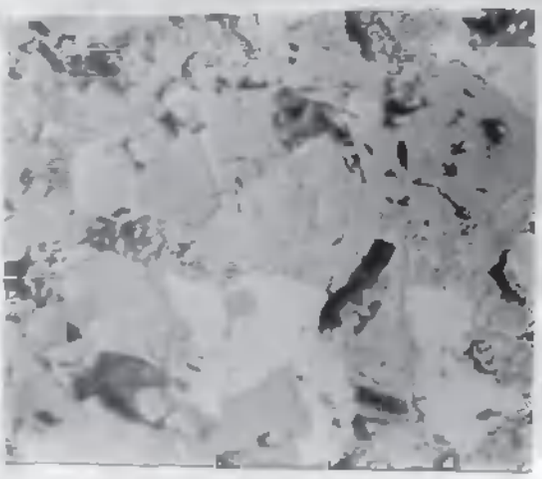

6. × 300

(7) × 300

(8) × 350

fig 13.

fig. 13.

9 × 300

ETCHED WITH 1% HCl IN WATER.

10. × 300

11. × 350

fig. 13.

thermal evidence and from the microscopic data obtained, the diagram shown in fig. 12 was constructed.

Photomicrographs which are shown in fig. 13 were prepared in the following manner. The molybdenum crucible was cut by a saw and one half levered off. The slag remained intact attached to the other half of the crucible. To produce a flat surface the slag was ground with suitably graded emery powder and water on a smooth steel plate, washed and dried, and then polished with 00 and 000 Hubert emery papers. Polishing was completed with a paste of pure Al_2O_3 and water on a 'Selvyt' cloth. The surface was etched in 1% HCl in water, dried, and then examined by a microscope using reflected light. If the surface was free from scratches, suitable fields were photographed by the Reichert Metallurgical Microscope using reflected light. Due to the soft and friable nature of FeO it was only with great care in polishing that suitable surfaces could be obtained.

Description of photomicrographs is given in Table II.

Table II

No.	Composition % FeO	Al_2O_3	Magnif.	Description
1,2	98	2	x 94	Primary FeO solid solution (half tone) with highly crystalline spinel which appears to have separated from the solid solution.
3	98	2	x 300	"
4	95	5	x 300	The strongly crystalline property of the spinel is evident causing large crystals to occur along with masses of FeO instead of the more usual eutectic structure.
5	95	5	x 300	Coarse eutectic of FeO and spinel
6,7	90	10	x 300	There is an increase in spinel which is now the primary phase. There are two distinct spinels, the dark compound appearing to have been produced from some transformation in the light spinel.

No.	Composition % FeO	Al_2O_3	Magnif.	Description
8	85	15	x 350	There is a further increase in spinel material. Note the "reaction rims" and the appearance of transformation from light to dark spinel.
9,10	80	20	x 300	Similar to 8 but with further increase in spinel material.
11	85	15	x 350	This specimen was annealed at 1150°C for five days. Annealing has caused an increase of dark spinel at the expense of some light spinel.

According to the micrographs there are two compounds, and the compositions $FeO.Al_2O_3$ and $3FeO.Al_2O_3$ have been provisionally assigned to them. Evidence that the dark spinel was formed from reaction between light spinel and FeO was proved by the annealing experiment. The invariant arrest at 1225°C was considered to correspond to this peritectoid transformation. The light spinel is $FeO.Al_2O_3$ and the dark spinel is $3FeO.Al_2O_3$. Solid solution of FeO, and $FeO.Al_2O_3$ react to give $3FeO.Al_2O_3$. Since this transformation occurs in the solid state it is liable to be sluggish and not to proceed to completion with the rate of cooling employed. Prolonged annealing at a temperature about 1200°C enables the reaction to continue.

The invariant point at 1440°C indicated in curves 4,5,6 and 7 was due to the peritectic transformation or the compound $FeO.Al_2O_3$ into FeO rich liquid and solid phase Al_2O_3.

The eutectic composition was fixed at 95% FeO, since the highest arrest on the thermal curves for slag or this composition is at 1305°C and the photomicrographs show complete eutectic. Also the magnitude of the 1305°C arrest is greatest in the thermal curves for this slag.

Evidence of decreasing solubility of $FeO.Al_2O_3$ in FeO with fall in temperature was found in photomicrographs 1,2 and 3 and the small arrest at 1270°C in the thermal curve for slag with 98% FeO.

The chief feature of the diagram is the eutectic occurring at 5% Al_2O_3. With increase of Al_2O_3 from 5-10% the

liquidus rises steeply from 1305°C to 1440°C. With further increase of Al_2O_3 the liquidus rises linearly to the melting point of pure Al_2O_3 at 2050°C.

HERTY[24] has reported a eutectic occurring at 57% Al_2O_3 with a melting point of 1480°C. To determine if the alumina rich portion of the diagram were of this form rather than that as shown in fig. 12, a mixture containing 57% Al_2O_3 and 43% FeO was heated to 1670°C, but no evidence of such a eutectic was obtained. The contents of the crucible were only slightly sintered. This agrees with the diagram in fig. 12, which shows that this mixture would contain a very small amount of eutectic and have a melting range of almost 500°C, the liquidus being about 1760°C.

The following observations were made on the melts after solidification:-

Colour: The colour varied from jet black with a bluish iridescence in the melts of high FeO content(98%, 95%) to a slate grey in melts of higher Al_2O_3 content.

Fluidity: The melts with high FeO content were very fluid, but fluidity appeared to decrease rapidly as Al_2O_3 increased.

Surface Tension: The melts appear to have a low surface tension giving a concave meniscus.

Hardness: FeO is soft and friable, but the addition of so small a quantity as 2% Al_2O_3 rendered the melt so hard that it could not be cut with a saw and filed only with difficulty. With high Al_2O_3 content, the material was so hard as to cut glass readily.

Brittleness: All melts containing Al_2O_3 were brittle and presented great difficulty in polishing for micro examination. The most satisfactory method found was that previously described.

Crystal Habit: Pronounced crystal habit was shown in melts with very low Al_2O_3 content. Whenever a 'pipe' appeared in the melt this contained bluish black triangular or hexagonal plates, in some cases piled up on each other in a manner reminiscent of the "key" pattern in cast bismuth.

Crystal Size: Melts with high FeO content were coarsely crystalline, whilst those with a high Al_2O_3 content had a much

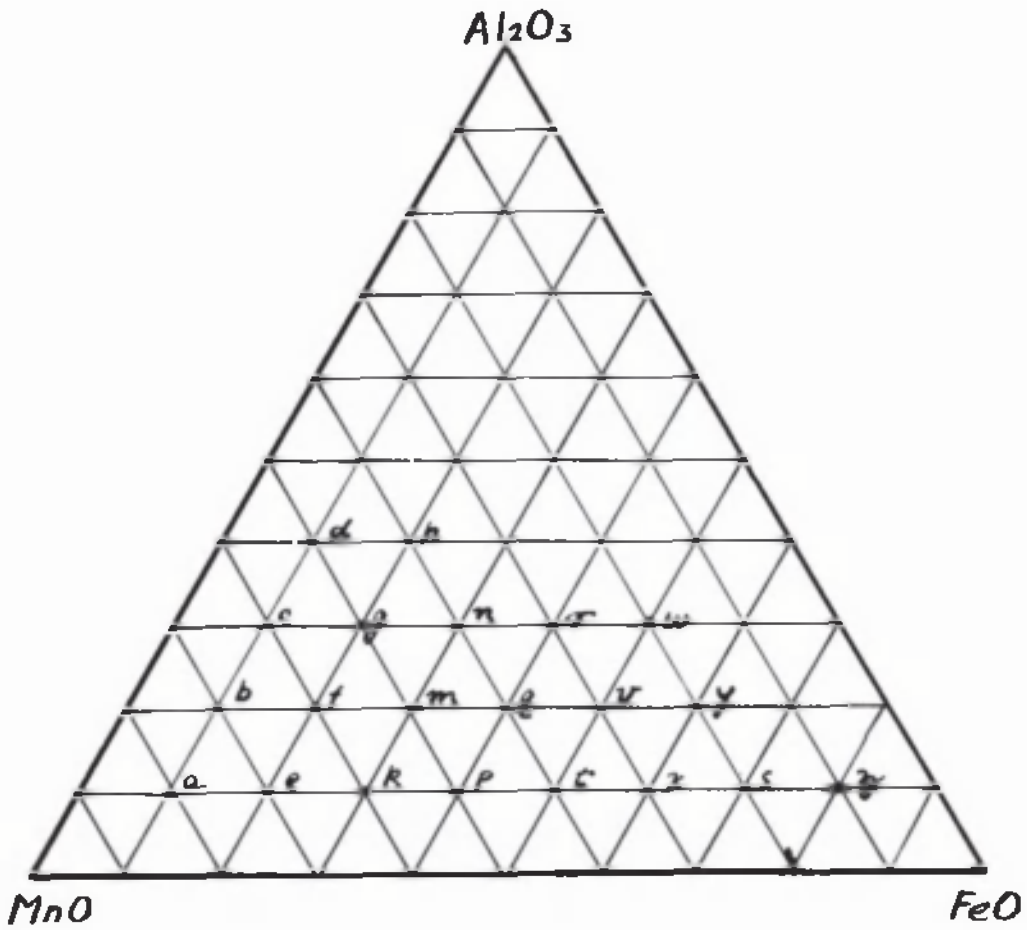

Melt	MnO	FeO	Al_2O_3
a	80	10	10
b	70	10	20
c	60	10	30
d	30	10	40
e	70	20	10
f	60	20	20
g	50	20	30
h	40	20	40
k	60	30	10
m	50	30	20

Melt	MnO	FeO	Al_2O_3
n	40	30	30
p	50	40	10
q	40	40	20
r	30	40	30
t	40	50	10
v	30	50	20
w	20	50	30
x	30	60	10
y	20	60	20
z	10	80	10

fig. 14.

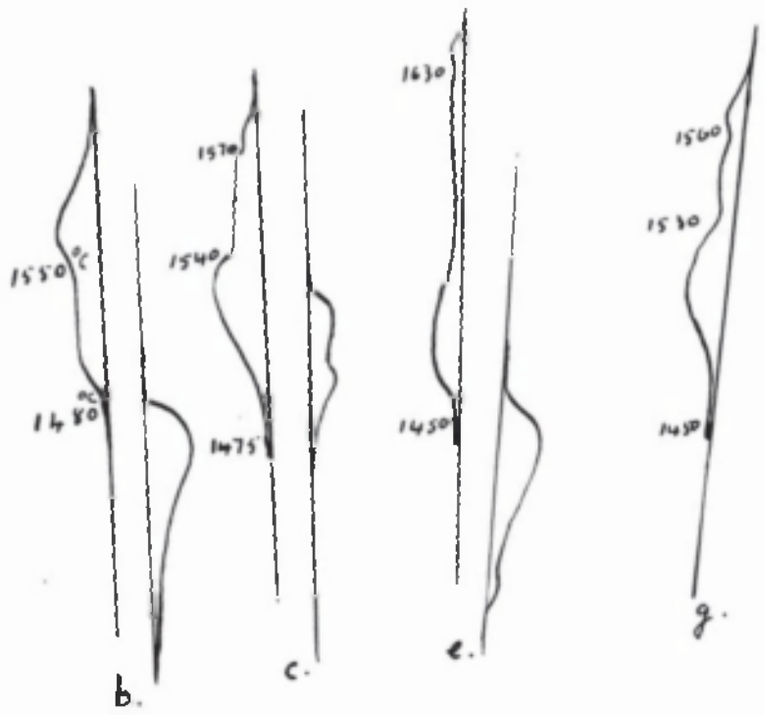
1550 °C
1480 °C
b.
1570
1540
1475
c.
1630
1450
e.
1560
1530
1450
g.

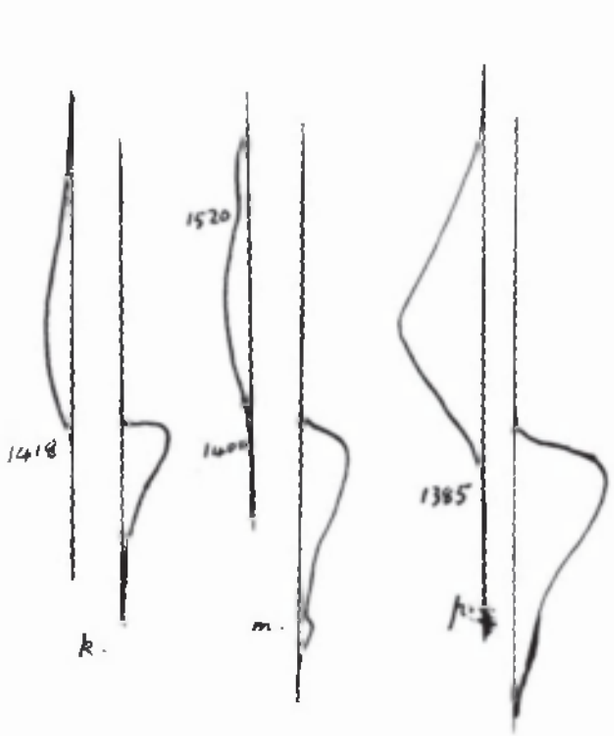
1418
k.
1520
1400
m.
1385
h.

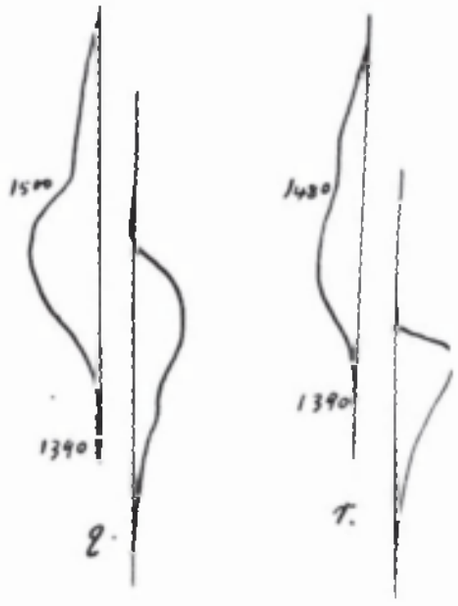
1500
1390
l.
1480
1390
r.

fig. 15

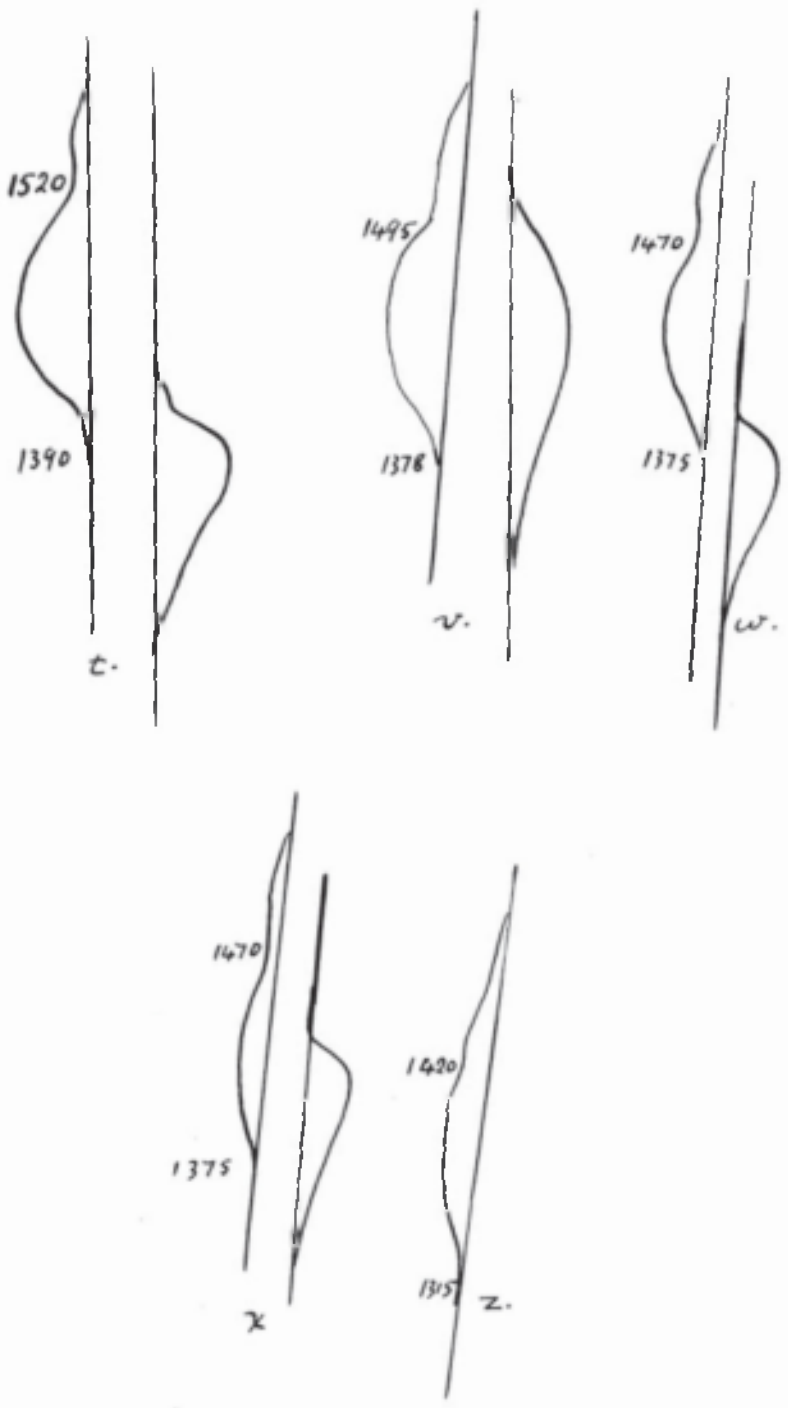

fig. 15

finer crystalline appearance. It was observed that the prolonged annealing of the melt containing 15% Al_2O_3 resulted in a very coarsely crystalline structure which was very brittle and very difficult to polish.

The Ternary System FeO-MnO-Al_2O_3.

Introduction

Until recent years, ternary systems were believed to be too complicated to make their study practicable. Information about this subject has seldom appeared in readily usable form. Most Metallography text-books give only a brief treatment of ternary systems, the best source of information being Masing's "Ternare Systemes"[25]. Recently an excellent text-book - " Principles of Phase Diagrams " [26] - has been published in which ternary thermal equilibrium diagrams are discussed in detail.

Early work on ternary systems was carried out with organic substances and only in recent times have metallic and slag systems been investigated.

The study of multi-component systems is of great importance in Metallurgy, as reflected by the number of diagrams (especially metallic systems) appearing in the literature. Much attention is now being directed to multi-component slag systems of the type occurring in blast furnace and steel furnace practice. The ternary diagram FeO-MnO-Al_2O_3 has important applications to steel refining and refractory manufacture. FeO, MnO and to a lesser extent Al_2O_3 are constituents of open hearth slags. These also occur in non-metallic inclusions in steel. The diagram yields information concerning the refractoriness of different compositions of FeO, MnO and Al_2O_3 and the behaviour of aluminous refractories in contact with FeO and MnO.

Method of Experiment.

The apparatus and method of experiment were similar to those employed in the investigation of the binary system FeO-Al_2O_3. Differential heating and cooling curves and photomicrographs were obtained for various ternary compositions. The compositions of the mixtures are shown in fig. 14 and typical differential curves in fig. 15.

Mixtures with higher alumina content are very refractory as are mixtures with higher MnO. The area of the diagram investigated was limited, since 'Pythagoras' tubes cannot withstand a temperature of over 1650°C.

RANKIN and WRIGHT[10] in their study of the lime-silica-alumina diagram obtained heating and cooling curves which were unsatisfactory for some of the slags due to their viscous nature, and petrographic examination of annealed and quenched specimens was also carried out.

However, differential curves for the FeO-MnO-Al_2O_3 slags were satisfactory and in conjunction with the photo-micrographs yielded sufficient experimental evidence for the construction of the diagram. Annealing and quenching experiments with subsequent petrographic examination is only necessary when the diagram is very complicated or when the thermal curves are unsatisfactory. For exact information regarding phase boundaries in the solid state such as limits of solubility, quenching experiments are very desirable, but these were not carried out with FeO-MnO-Al_2O_3 slags since it is difficult to quench in vacuo or controlled neutral atmosphere. Hence the limits of solubility in the solid state are only approximate, but this is of little interest from the practical point of view and so there is no need for greater accuracy than that obtained.

Interpretation of Thermal Curves.

The interpretation of the thermal curves was discussed fully for the system FeO-Al_2O_3 and a similar interpretation applies here. The summary of the thermal evidence is shown in Table III.

Table III

% Composition MnO	FeO	Al_2O_3	Temperature of phase changes °C
a)80	10	10	At 1620 was not molten
b)70	10	20	1480, 1550
c)60	10	30	1475, 1540, 1570
d)50	10	40	At 1620 was not molten
e)70	20	10	1450, 1630
f)60	20	20	1450, 1530
g)50	20	30	1460, 1530, 1560
h)40	20	40	At 1620 was not molten
k)60	30	10	1418, 1600
m)50	30	20	1400, 1520
n)40	30	30	1430, 1510
p)50	40	10	1385
q)40	40	20	1390, 1500
r)30	40	30	1390, 1480
t)40	50	10	1390, 1520
v)30	50	20	1378, 1495
w)20	50	30	1375, 1470
x)30	60	10	1375, 1470
y)20	60	20	1350, 1460
z)10	80	10	1315, 1400

Deduction of the Ternary Diagram.

The methods of representing the ternary system graphically are sufficiently different to warrant an explanation of the method to be employed.

The Phase Rule statements of the equilibria which may exist in a ternary system is summarised in the table following:-

$$f = 3 + 2 - p = 5 - p$$

p	f	Spatial Representation
1	4	A four-dimensional solid.
2	3	A three-dimensional solid.
3	2	A surface.
4	1	A space curve
5	0	A point.

The Isobaric Ternary System.

$$f = 3 + 1 - p = 4 - p.$$

p	f	Spatial Representation
1	3	A three-dimensional solid
2	2	A surface
3	1	A space curve
4	0	A point.

where,

p = no. of phases

f = degrees of freedom.

As in the binary system $FeO-Al_2O_3$, the isobaric section is considered. Because four variables - pressure, temperature and two concentrations are involved - there is no simple way to represent a ternary system graphically and even an isobaric ternary system is three-dimensional. Various methods have been proposed to represent the composition of ternary isobaric systems based on the triangle, but Roozeboom's equilateral triangle in which the length of the side is equal to 100 units has found great usage and is employed here. Temperature is usually plotted in the direction perpendicular to the composition triangle. It follows

that the composition triangle is an isothermic section of a ternary isobaric section and that all isothermic sections of such sections are horizontal. Sections at constant concentration of one component or a constant ratio of two components are vertical.

The three binary systems involved $FeO-Al_2O_3$ [20], $FeO-MnO$ [16] and $MnO-Al_2O_3$ [20] have all been previously published, but they are reproduced in fig. 16 . Spinel compounds $FeO.Al_2O_3$ and $MnO.Al_2O_3$ occur in the systems $FeO-Al_2O_3$ and $MnO-Al_2O_3$ respectively. It follows, provided no ternary compound is formed and no isomorphous series occurs, that the complete ternary system could be considered as being made up of three ternary systems. If no ternary compound is formed and an isomorphous series occurs, the complete ternary system would consist of one ternary. In the former case there would be three ternary invariant points, but in the latter there would be only one. From the thermal curves and the microscopic examination of the melts no evidence was obtained for the presence of any ternary compound. The microscope only revealed one type of spinel indicating the occurrence of an isomorphous series in which MnO replaces FeO wholly or in part in the compound $FeO.Al_2O_3$. The thermal curves indicated one ternary invariant point at a temperature about 1390°C. Since the melting point of FeO is 1370°C it is obvious that this ternary point is not a eutectic. The photomicrographs reveal that the only ternary combination occurring is FeO, spinel and MnO. All the evidence points to the ternary system $FeO-MnO-Al_2O_3$ existing as one ternary, in which an isomorphous series of spinels and one invariant point at a temperature above that of the melting point of FeO occur. In the FeO rich region the diagram is a pseudo-ternary due to the peritectic dissociation of FeO at 1370°C being considered as the melting point.

The Ternary Invariant Point

There are three kinds of non-variant equilibrium in ternary isobaric sections. Four phases such as α, β, γ and L (liquid) can participate in four different three-phase equilibria.

(a) $\alpha+\beta+\gamma$ (b) $\alpha+\beta+L$ (c) $\alpha+\gamma+L$ (d) $\beta+\gamma+L$.

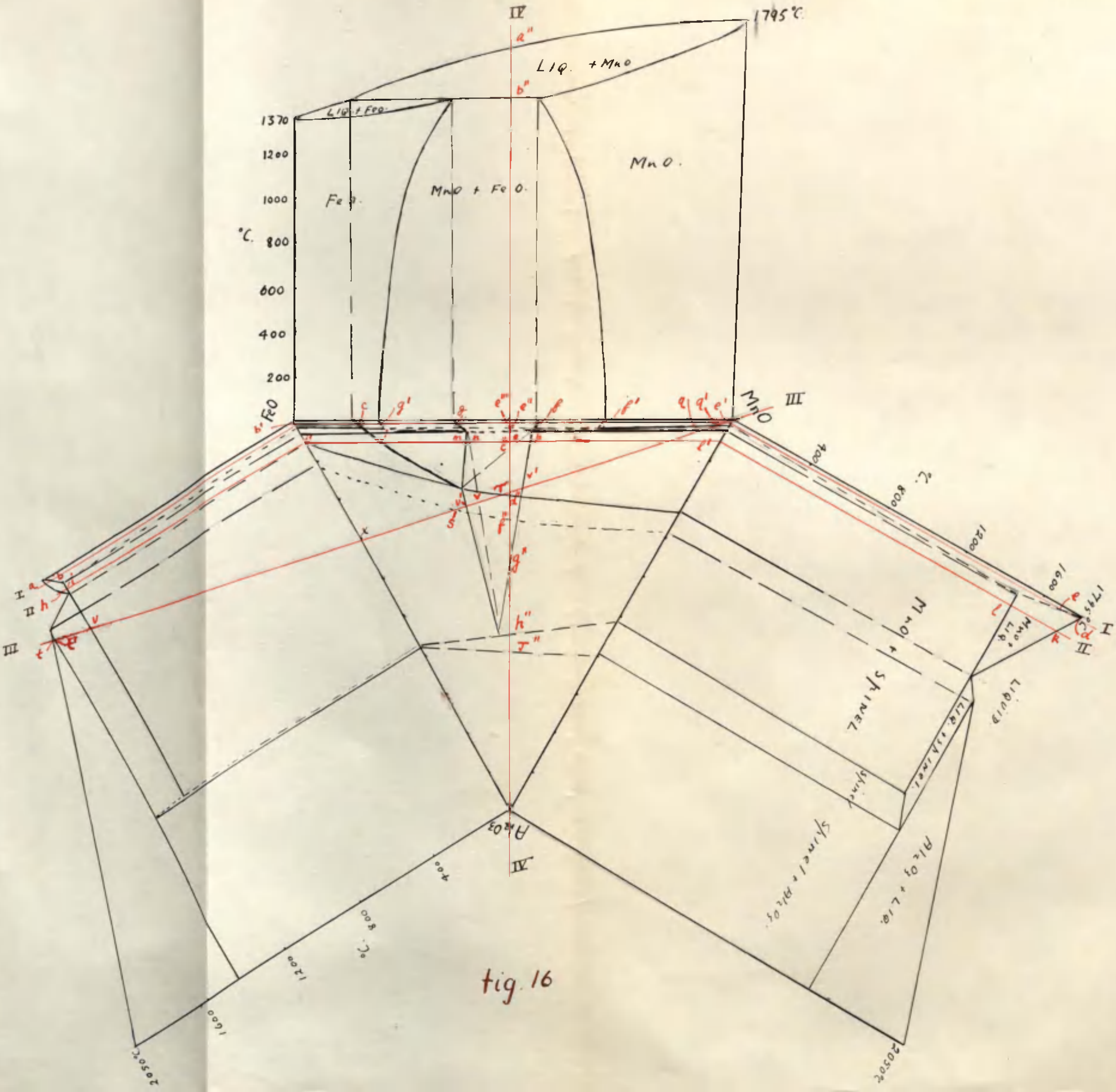

IV
1795°C
LIQ. + MnO
1370
LIQ + FeO
1200
1000
800
600
400
200
°C.
FeO
MnO + FeO
MnO
FeO
MnO
III
I
II
III
Al2O3
IV
MnO + SPINEL
LIQUID
Spinel
Spinel + Al2O3
Al2O3 + LIQ.

fig. 16

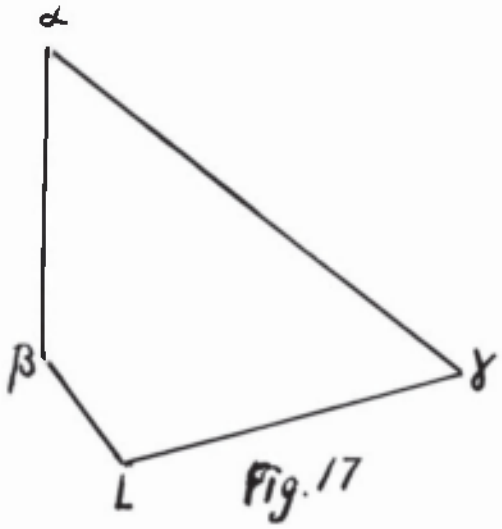

Fig. 17

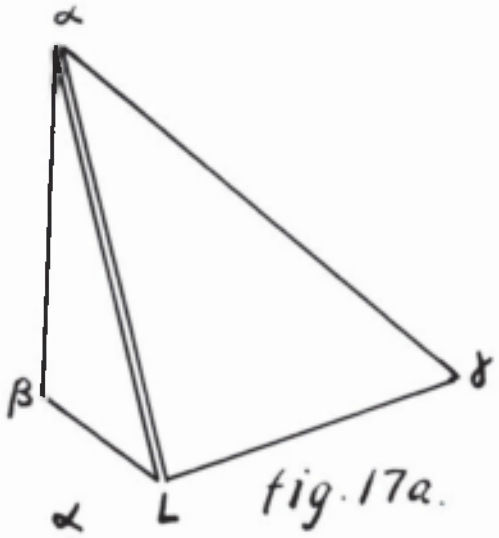

fig. 17a.

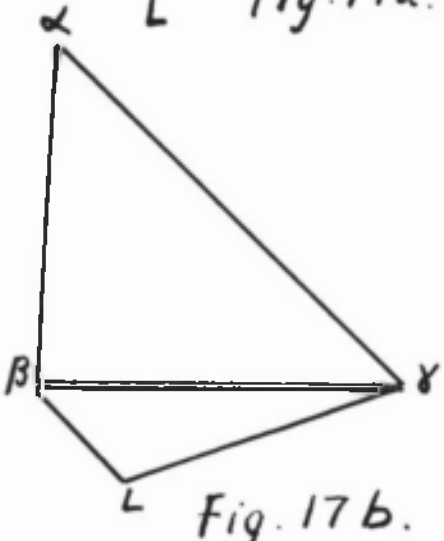

Fig. 17 b.

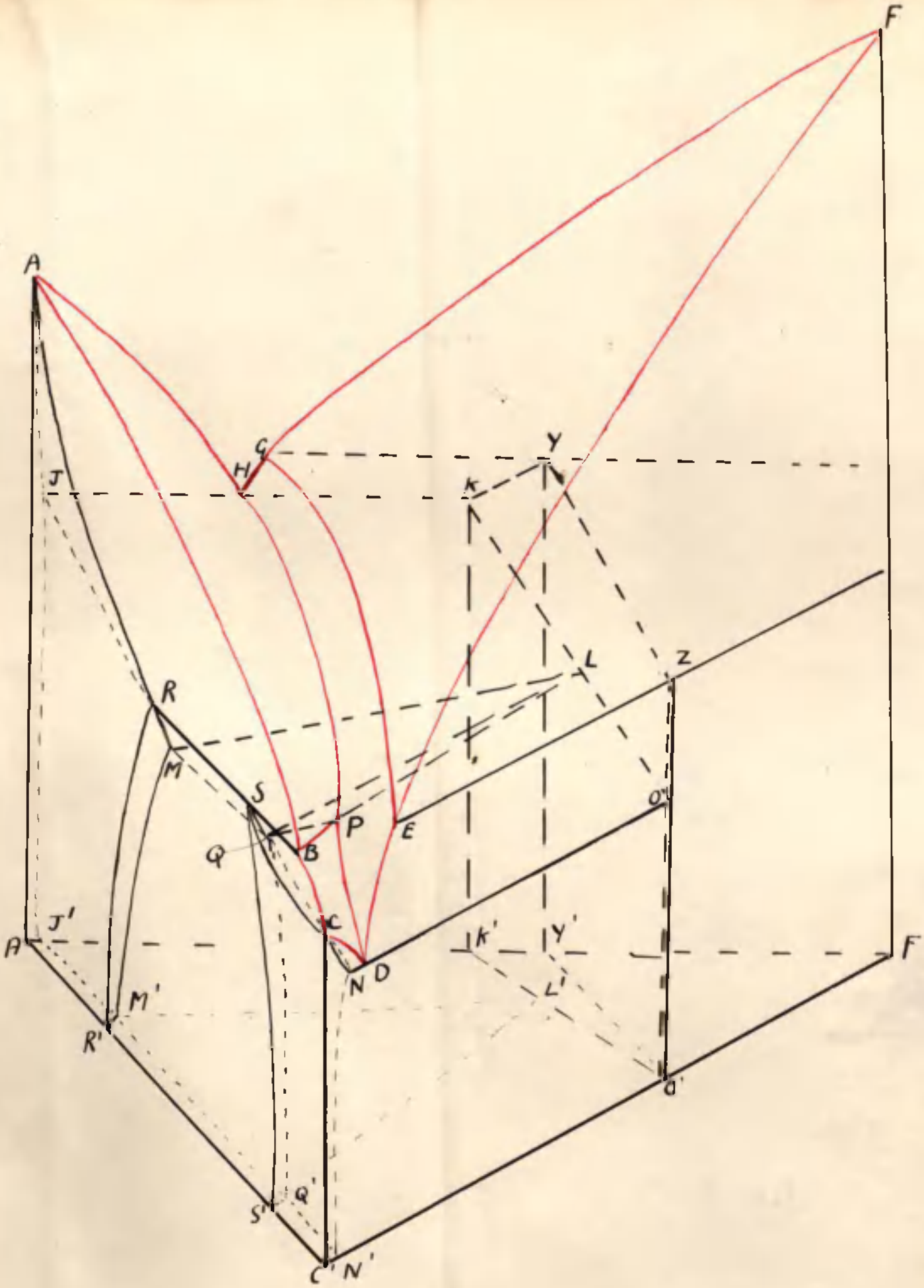

fig. 18.

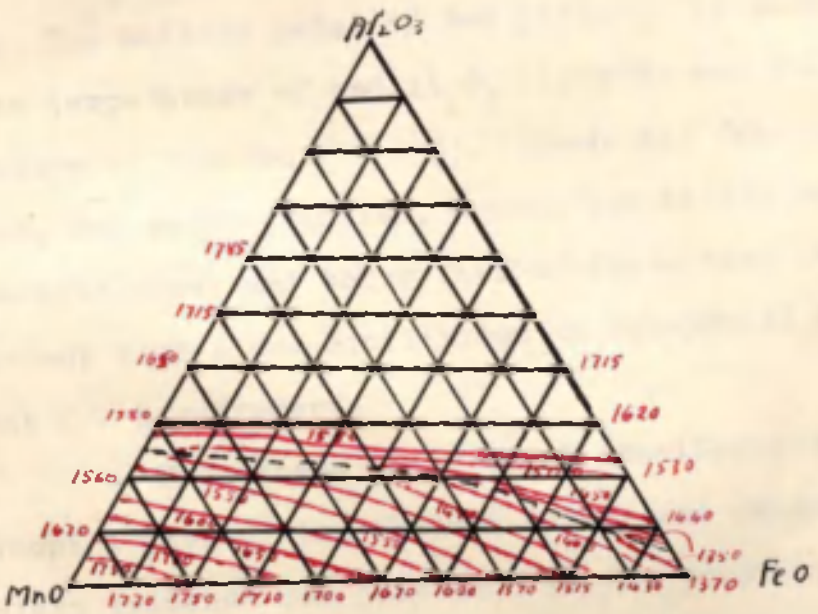
Al_2O_3
1745
1715
1650
1715
1580
1620
1560
1530
1670
1640
1250
MnO
1370
FeO

fig. 19.

Thus, each phase can participate in three different three-phase equilibria. The four three-phase equilibria may be distributed above and below the four-phase equilibrium as follows:- 3/1, 2/2, 1/3. The 3/1 arrangement can only exist if the three contiguous binary sections contain one eutectic or eutectoid each. The 1/3 arrangement is the inversion or the 3/1 arrangement and so is ternary peritectic or peritectoid equilibrium. The 2/2 arrangement is illustrated in fig. 17 and this kind of non-variant equilibrium is always represented by a quadrangle. At a temperature value slightly greater than that of the quadrangle, the quadrangle is split along the α L diagonal into $\alpha + \beta + L$ and the $\alpha + \gamma + L$ triangles as shown in fig. 17 a . At a temperature slightly less than that of the quadrangle, the split is along the $\beta\ \gamma$ diagonal into the $\alpha + \beta + \gamma$ and the $\beta + \gamma + L$ as shown in fig. 17b.

The thermal curves indicate an invariant point at 1390°C. The melting point of FeO (1370°C) is lower than the eutectic temperature of MnO-Al_2O_3 (1520°C) and the peritectic temperature of MnO-FeO (1450°C). Hence all four phases FeO solid solution, MnO solid solution, spinel and liquid can exist at temperatures above and below that of four-phase equilibrium. The non-variant four-phase equilibrium in FeO-MnO-Al_2O_3 system is then the 2/2 arrangement.

From these theoretical considerations and the experimental data of the thermal curves and photomicrographs, sufficient evidence was obtained for the construction of the ternary diagram. A wire model, which showed very clearly the various planes and their intersections, was constructed on a suitable triangular cardboard base. Unfortunately it was not possible to obtain a suitable photograph. Fig. 18 shows a diagram of the model.

<u>The Liquidus Surfaces</u> (see fig. 18)

AHPB, BCDP, GEDPH and FGE are the liquidus surfaces. HPD is the line produced by the intersection of surfaces AHPB, GEDPH and BCDP and extends from the eutectic of the binary MnO-Al_2O_3 (1520°C) to the eutectic of FeO-Al_2O_3 (1305°C). The liquidus isotherms are shown in fig. 19.

The path of HPD was fixed from the thermal evidence and the photomicrographs. Thus, a melt whose composition lies in HPD has a lower range of melting than those lying on either side. Photomicrographs 3 and 4 (see figs. 24, 25 and description of photomicrographs) show primary MnO solid solution and eutectic of MnO solid solution and spinel; 5,6 and 7 consist of 100% eutectic; 8 shows primary spinel and eutectic. Hence HPD passes through the composition 50% MnO, 30% FeO, 20% Al_2O_3.

The Ternary Invariant Point P(1390°C)

At P, liquid, spinel, FeO solid solution and MnO solid solution exist in equilibrium at a temperature just above 1390°C two three-phase equilibria are possible:-

a) Liquid, FeO solid solution and MnO solid solution
b) Liquid, FeO solid solution and spinel.

At a temperature slightly less than 1390°C two three-phase equilibria are possible:-

c) Liquid, FeO solid solution and spinel.
d) MnO solid solution, FeO solid solution and spinel.

Thermal curves for the slag of composition P exhibit the maximum invariant arrest at 1390°C with no higher liquidus point. Thermal curves for melts within the quadrangle QPLM (see fig. 18) exhibit a thermal arrest at 1390°C decreasing in magnitude and liquidus arrests increasing in temperature as the composition moves towards the $MnO-Al_2O_3$ side. Slags whose composition lie on the $FeO-Al_2O_3$ side of P begin to melt at temperatures lower than 1390°C. Photomicrographs of slags in the area M'L'Q' show three phases:- FeO, MnO solid solutions and spinel; within J'M'L'K' MnO solid solution and spinel; within N'Q'L'O' FeO solid solution and spinel. However, on examination it was difficult to distinguish between the three phases in the finely banded eutectic structure and so the thermal evidence was more reliable for fixing P. Determination of refractive indices, angle of extinction etc. would enable the number of phases in the melts and so the area PQML to be fixed.

Plane JKLM.

Since P,L and M lie on a horizontal plane, it follows that HP lies above the plane JKLM. This plane from a temperature of

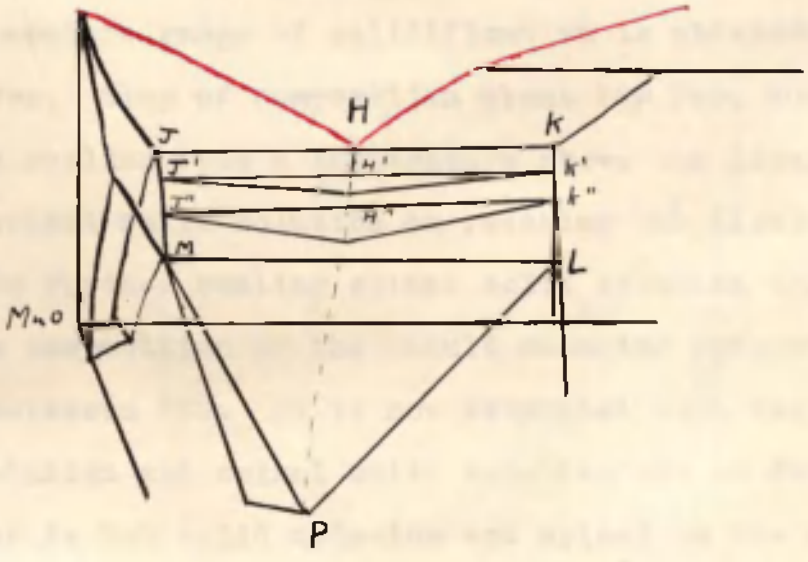

fig. 20

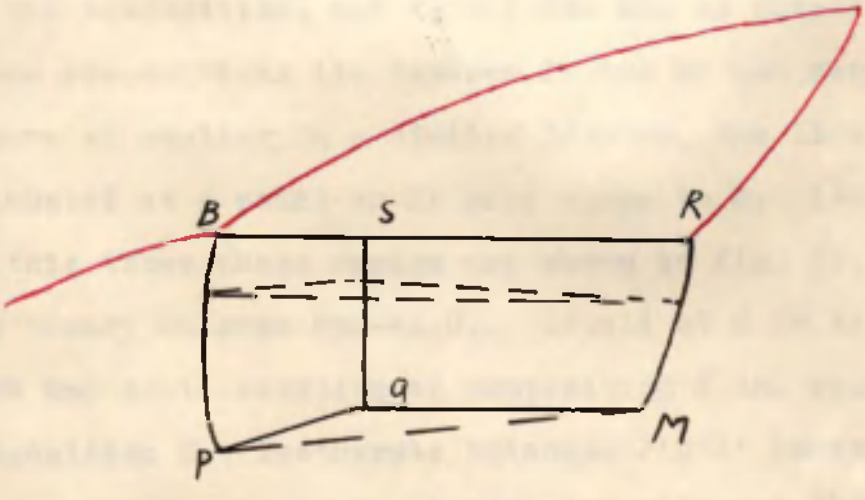

fig. 22.

1520°C along JK, slopes down to ML at a temperature of 1390°C. Consider slag of composition 70% MnO, 10% FeO, 20% Al_2O_3 on cooling from a temperature above the liquidus. On reaching the liquidus ABPH, MnO solid solution is deposited and on further cooling, MnO solid solution continues to deposit, the composition of the liquid changing progressively until it intersects HPD. The liquid is now saturated with MnO solid solution and spinel and on firther cooling deposits MnO solid solution and spinel in the form of a eutectic, the liquid being exhausted before reaching P. The temperature range of solidification is obtained from the thermal curves. Slag of composition about 10% FeO, 60% MnO, 30% Al_2O_3 on cooling from a temperature above the liquidus begins to deposit spinel solid solution on reaching the liquidus surface GHPDE, and on further cooling spinel solid solution continues to deposit, the composition of the liquid changing progressively until it intersects HPD. It is now saturated with respect to MnO solid solution and spinel solid solution and on further cooling deposits MnO solid solution and spinel in the form of a eutectic. Before reaching P the liquid is exhausted. Slags whose compositions lie within the area J'M'L'K' show either MnO or spinel as primary phase depending on which side of HPD is the composition, and spinel and MnO as eutectic. Melts whose compositions lie between JK and ML and very near ML will behave on cooling in a similar fashion, the liquid being exhausted at a point on HP very close to P. Isothermic sections of this three-phase region are shown in fig. 20. JHK lies in the binary diagram MnO-Al_2O_3. Liquid at H is in equilibrium with MnO solid solution of composition J and spinel of composition K. Isothermic triangle J'H'K' indicates that liquid of composition H' is in equilibrium with MnO solid solution of composition J' and spinel of composition K'. It can be seen from fig. 20 that the motion of the triangle generates a three-cornered space bounded by three ruled surfaces, the upper limit of the space being the straight line JHK, which is a degenerated triangle. The lower limit is the triangle MPL.

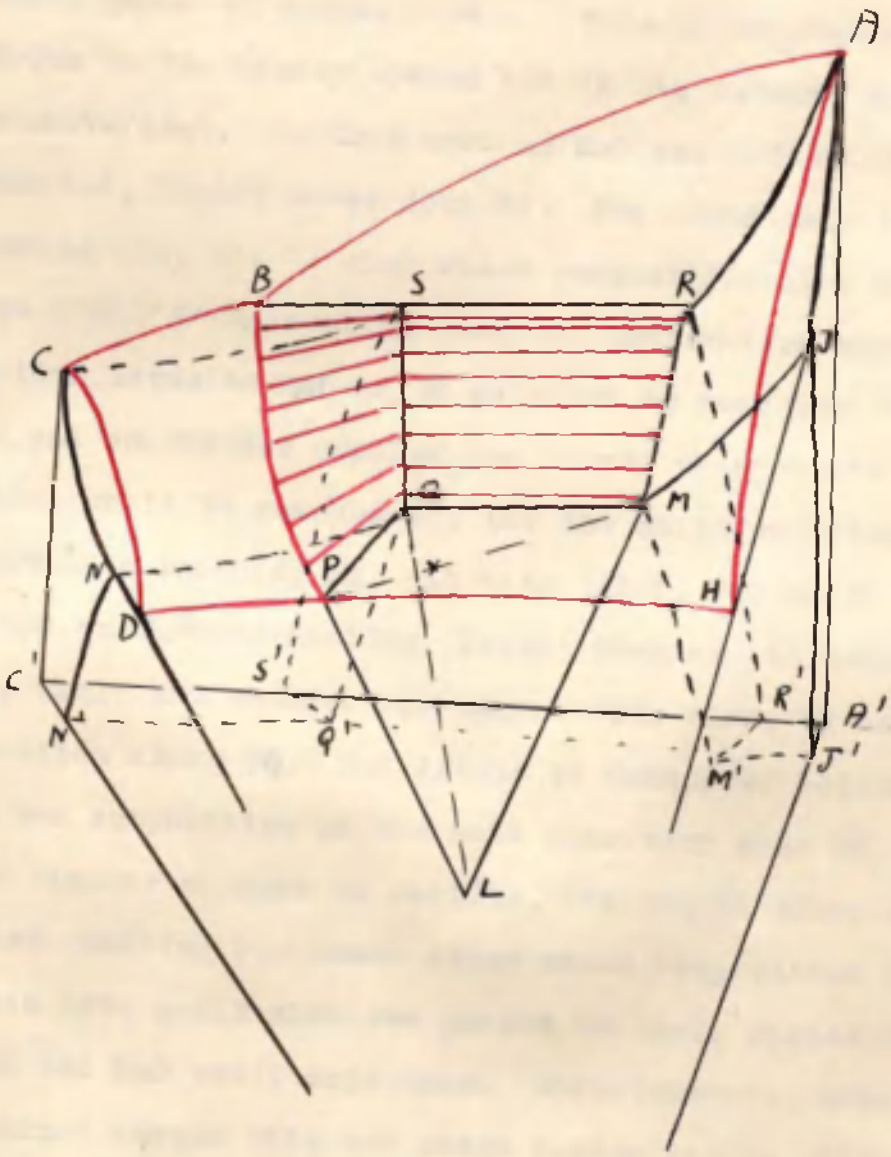

fig. 21

Region ARMJJ'M'R'A'

Melts whose compositions lie within the area A'J'M'R' yield micrographs which show only MnO solid solution. However, since no ternary melts with less than 10% Al_2O_3 were examined, the area A'J'M'R' is only arbitrarily fixed.

Region R'M'Q'S'

Fig. 21 shows clearly the type of equilibrium found in this region. In the binary system FeO-MnO, liquid of composition B is in equilibrium with solid phase of composition S and solid phase of composition R. This is non-variant equilibrium in the binary system but in the ternary system becomes univariant. In this case as MnO and FeO solid solutions are deposited, liquid moves down BP. The isothermic triangles are shown in fig. 22. A slag whose composition lies within the same area R'M'Q'S' on cooling from a temperature above that of the liquidus, deposits MnO solid solution on reaching the liquidus, and on further cooling the liquid changes its composition until it reaches BP, the MnO solid solution changing its composition reaching RM. At this point, FeO solid solution appears and on further cooling, liquid changes its composition along BP, while MnO changes its composition along RM and FeO solid solution along SQ. The liquid is exhausted before reaching P. When the composition of the melt lies very near QM, the slag undergoes similar changes on cooling, the liquid being exhausted just before reaching P. Hence slags whose composition lie within this area would show two phases in their photomicrographs, namely FeO and MnO solid solutions. Unfortunately, none of the slags examined showed this two phase region and so this region must lie somewhere between 0% and 10% Al_2O_3. Hence the region S'Q'M'R' is only arbitrarily fixed.

Region CBSS'C'N'Q'QN.

Melts whose composition lie to the MnO side of BP, on cooling from a temperature above the liquidus, first deposit MnO solid solution. On further cooling, MnO solid solution continues to deposit and the composition of the liquid changes until it reaches BP. At this point there is liquid, FeO solid solution and MnO solid solution in equilibrium. On further

cooling, the MnO disappears, more FeO is deposited and the composition of the liquid changes, moving over the surface CBPD towards PD, the liquid being exhausted before reaching DP. On the FeO side of BP, MnO solid solution is not deposited on cooling. FeO solid solution is deposited, the composition of the liquid moving over the surface CBPD towards DP the liquid being exhausted before reaching DP.

Region PQML

All melts whose compositions lie within QML yield photomicrographs which show MnO solid solution, FeO solid solution and spinel. All melts within QXM (fig. 21) undergo the following changes on cooling from a temperature above the liquidus. On reaching the liquidus, MnO solid solution is deposited and on further cooling continues to deposit, composition of the liquid moving over the surface ABPH. When the liquid composition reaches BP, FeO solid solution appears and on further cooling, composition of liquid moves along BP while the compositions of MnO and FeO move along RM and SQ. At P, spinel appears and solidification is completed at 1390°C. Slags within the area PQX undergo the same changes on cooling until P is reached. At P, spinel appears while MnO disappears at constant temperature. On further cooling, liquid changes its composition along PD while FeO and spinel are deposited in the form of a eutectic, the liquid being exhausted before reaching D, Consider melts within the region XML.

a) Melts which are between XM and PH.

On cooling, such a slag will begin to deposit MnO when the liquidus temperature is reached and on further cooling MnO will continue to deposit, the composition of the liquid changing until it reaches HP. On further cooling MnO and spinel are deposited in the form of a eutectic, the liquid altering its composition along HP until it reaches P. FeO appears at constant temperature and solidification is complete before further cooling can take place.

b) Melts lying between PH and L undergo similar changes on cooling except that spinel is the primary phase.

Melts within the region PXL behave as above on

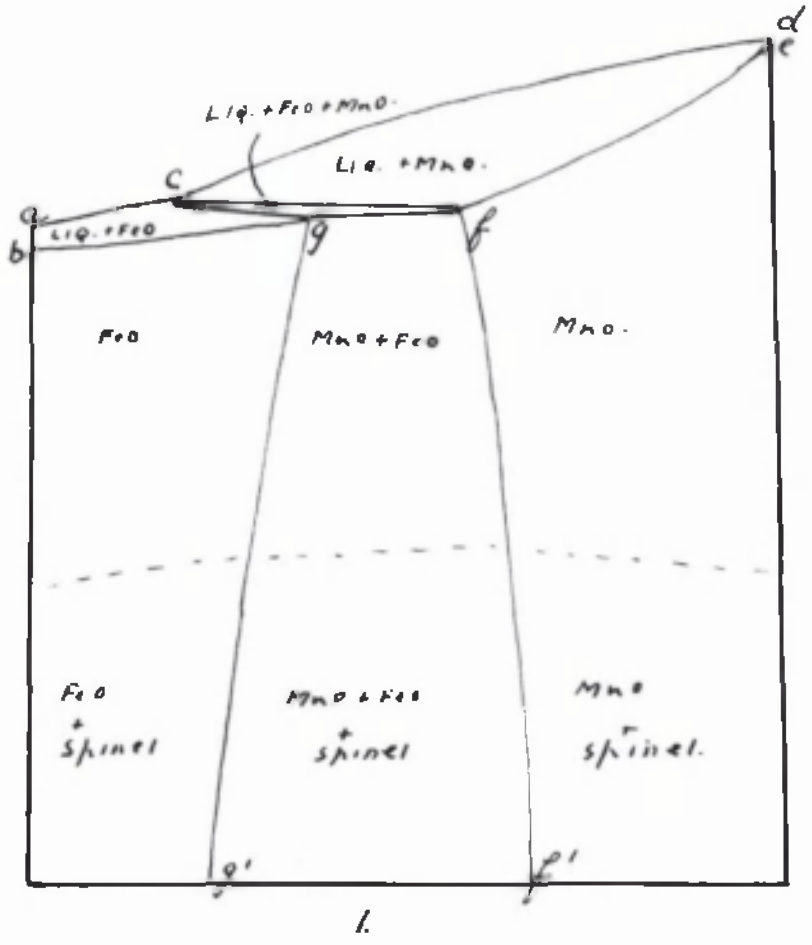
a
b
c
d
e
f
g
Liq. + FeO + MnO.
Liq. + MnO.
Liq. + FeO
FeO
MnO + FeO
MnO.
FeO + spinel
MnO + FeO + spinel
MnO + spinel
g'
f'
1.

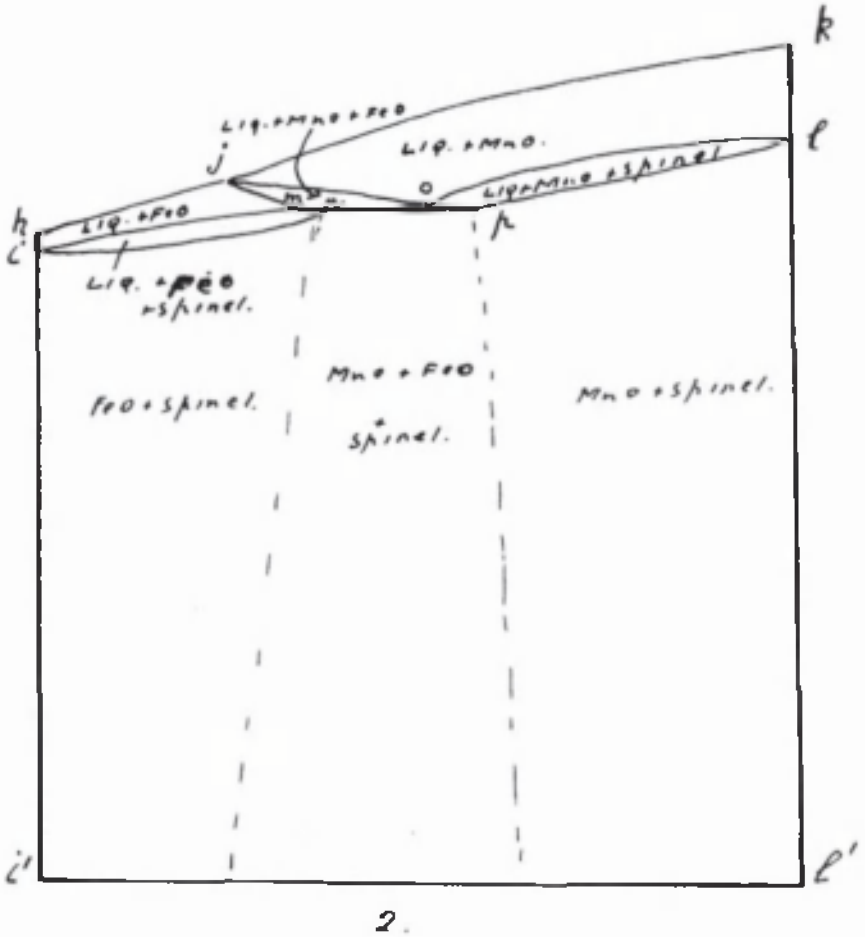
h
i
j
k
l
m
n
o
p
Liq. + MnO + FeO
Liq. + MnO.
Liq. + MnO + spinel
Liq. + FeO
Liq. + FeO + spinel
FeO + spinel.
MnO + FeO + spinel
MnO + spinel.
i'
l'
2.

Fig. 23.

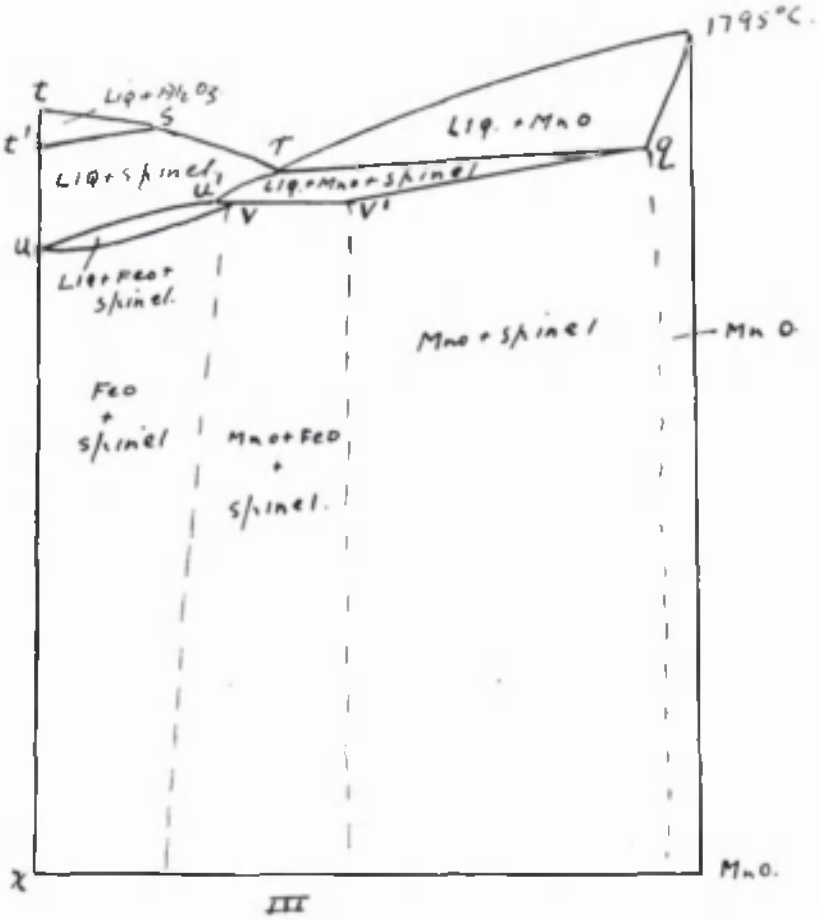
1795°C.
t
t'
u
u'
v
v'
s
T
q
x
Liq + Al2O3
Liq + spinel
Liq + MnO
Liq + MnO + spinel
Liq + FeO + spinel
MnO + spinel
MnO
FeO + spinel
MnO + FeO + spinel
MnO.
III

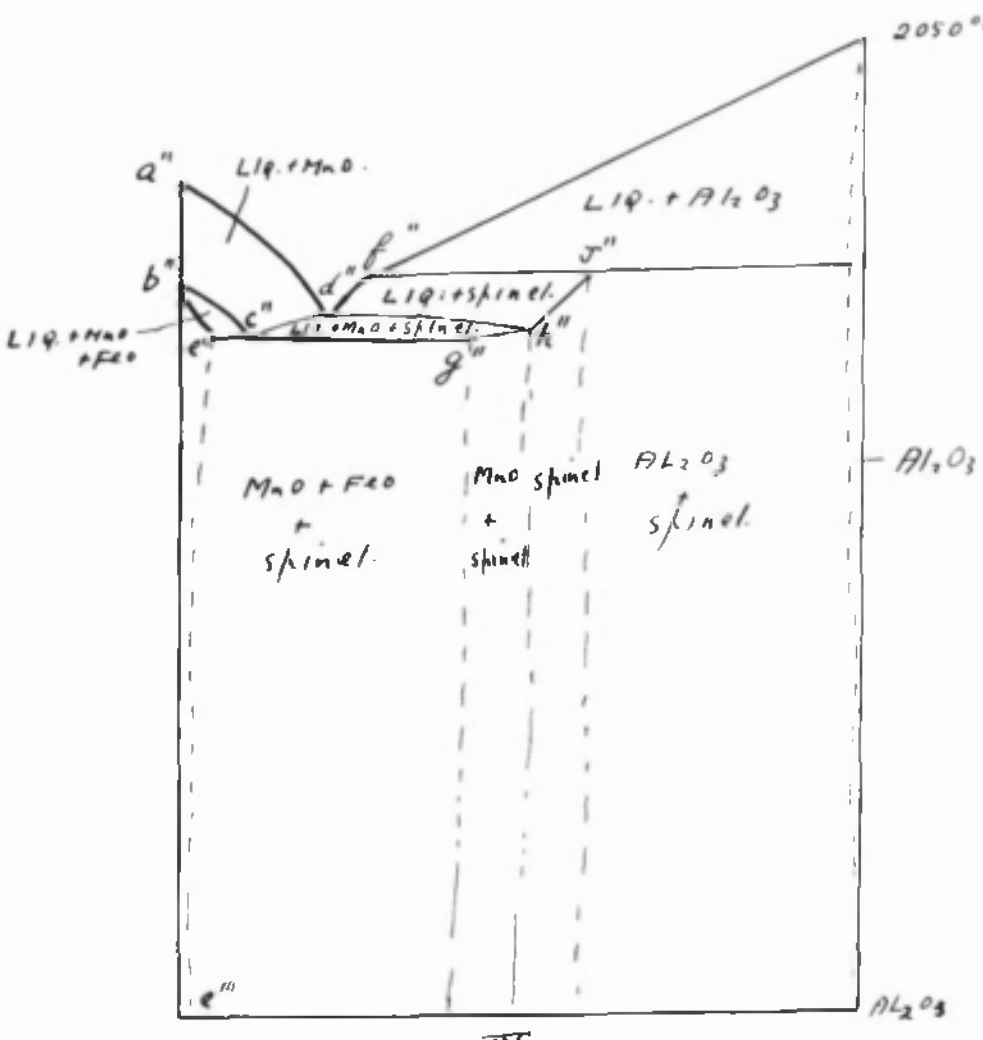
2050°C.
a"
b"
c"
d"
e"
e'''
f"
g"
h"
T"
Liq + MnO
Liq + Al2O3
Liq + spinel
Liq + MnO + spinel
Liq + MnO + FeO
MnO + FeO + spinel
MnO spinel + spinel
Al2O3 spinel
Al2O3
Al2O3
IV

fig. 23.

cooling except that at P the liquid is not exhausted. At P, FeO appears and MnO disappears at constant temperature. When all the MnO solid solution has disappeared further cooling occurs with deposition of MnO and FeO solid solutions in the form or a eutectic, the liquid changing its composition along PD. Solidification is complete at temperatures between 1390°C and 1305°C. It follows that all melts within PQL will on heating begin to form liquid at temperatures slightly below that or P (1390°C). Under ideal comditions, the differential heating curves would show a phase change below 1390°C and then the invariant change at 1390°C .

Plane NQLOD

Since P,Q and L lie on a horizontal plane, it will be easily seen (figs. 18 and 21) that DF lies above this plane. This plane slopes up from NDO at 1305°C until it intersects the quadrangle PQML along QL. All melts within this region on cooling deposit FeO solid solution or spinel as primary phase and then eutectic of FeO and spinel. The Spinel Peritectic

The Spinel Peritectic.

All melts whose compositions lie on the Al_2O_3 side of GE, on cooling from temperatures above that of liquidus FGE, deposit alumina on reaching the liquidus. On further cooling alumina continues to deposit, the liquid changing its composition until GE is reached when spinel appears. If the composition of the slag is within K'L'O'Y', the liquid is exhausted on reaching GE, the alumina disappears, only spinel remaining. If the composition of the slag is within F'Y'O', then liquid is exhausted at GE but spinel and alumina remain. This region was not investigated experimentally since slags in this region are too refractory.

The previous description of the changes which the various slags undergo on heating or cooling is summarised in the vertical sections of the diagram shown in fig. 23. Fig. 16 shows the position of the sections and the intersections.

fig. 25.

×214 (11)

(12) ×214

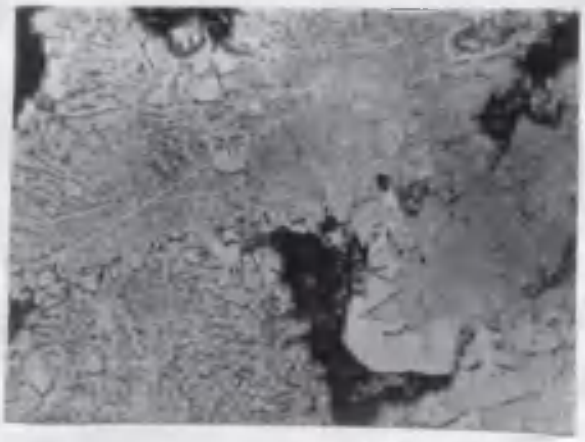

×214 (13)

(14) ×214.

×214 (15)

ETCHED WITH 1% NITRIC WATER

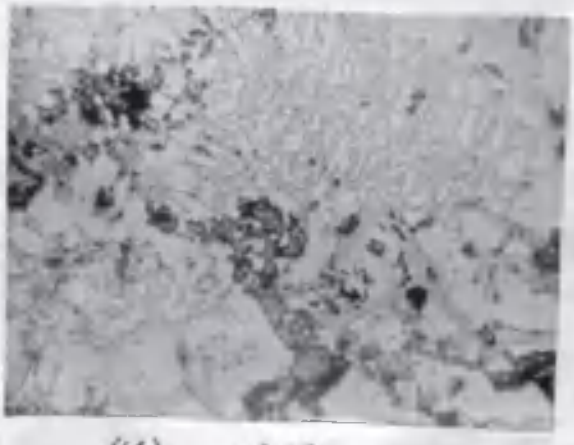

(16) ×214

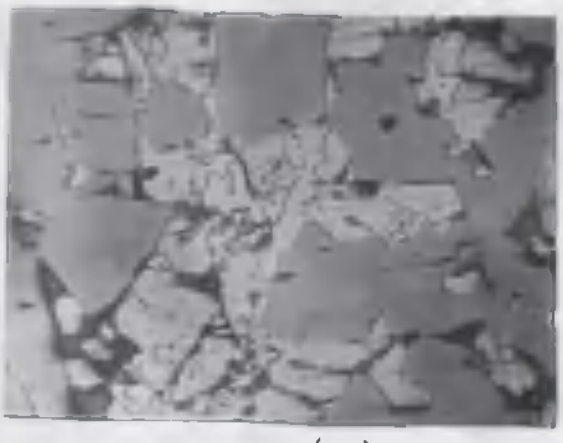

×214 (17)

(18) ×214

×214 (19)

Fig 25.

(20) ×214

fig 25.

×214 (1)

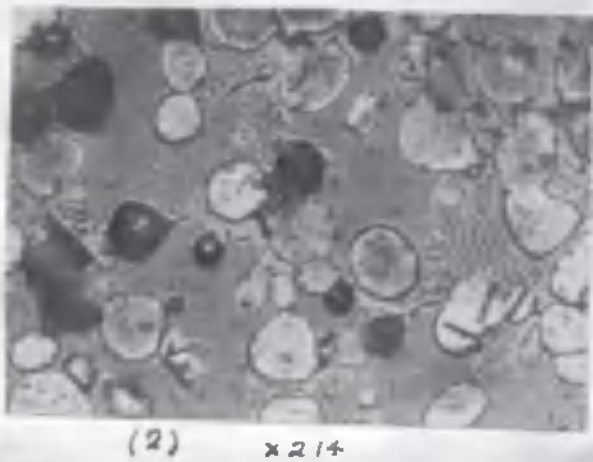

(2) ×214

×214 (3)

(4) × 214

×104 (5)

ETCHED WITH 1% HNO3 IN WATER.

(6) × 214

×214 (7)

(8) × 214

×214 (9)

(10) ×214

fig 25.

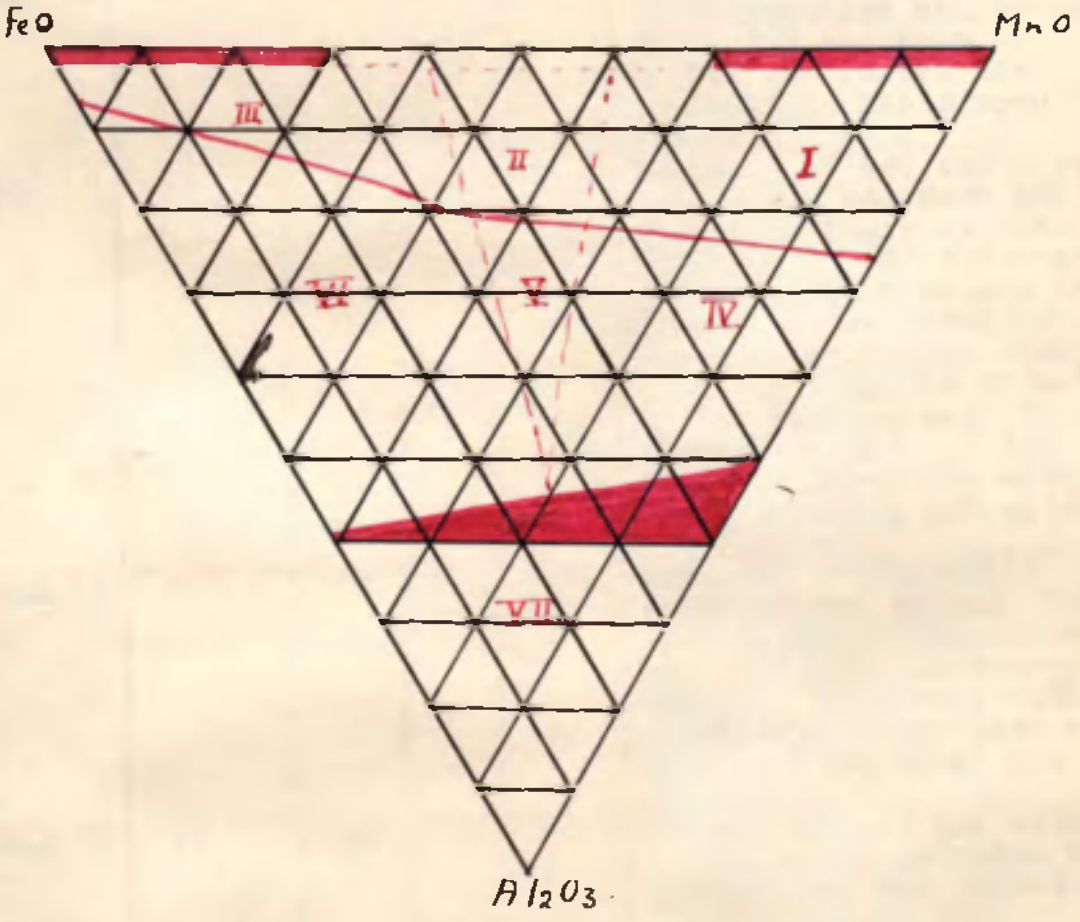

fig. 24

Description of the Photomicrographs.

No. (fig.25)	Field (fig.24)	Composition % FeO	MnO	Al_2O_3	Description.
1 and 2	I	10	70	20	Primary MnO solid solution and eutectic of MnO solid solution and spinel.
3 and 4	I	30	60	10	Primary MnO solid solution dendrites and eutectic of MnO solid solution and spinel.
5,6 and 7	I	30	50	20	MnO solid solution and spinel in the form of a eutectic.
8	IV	30	40	30	Primary spinel and eutectic of spinel and MnO solid solution.
9 and 10	II	40	50	10	Primary dendrites of MnO solid solution and eutectic of MnO solid solution, spinel and probably some FeO solid solution.
11 and 12	II	40	40	20	100% eutectic of spinel, MnO solid solution and probably FeO solid solution. The spinel has forced its crystalline habit upon the eutectic.
13 and 14	II	50	40	10	Eutectic of FeO solid solution and spinel and some MnO solid solution. There is also evidence of the 'peritectoid' reaction which occurs in the binary system FeO-Al_2O_3. The eutectic structure disappears in parts with the formation of the dark spinel. The lamellar nature of the eutectic structure with MnO solid solution and spinel has changed.
15 and 16	III	60	30	10	Eutectic of FeO solid solution and spinel. The 'Peritectoid' transformation has partially destroyed the eutectic structure with the formation of the dark spinel. The 'reaction rims' are evident in 16.
17 and 18	VI	60	20	20	Primary spinel and eutectic of FeO solid solution and spinel. The two spinels are present due to the Peritectoid transformation. Light spinel ($FeO.Al_2O_3$) is the one first formed on cooling. The dark spinel ($3FeO.Al_2O_3$) is formed in the solid. 17 shows a field of FeO solid solution and $3FeO.Al_2O_3$.
19 and 20	II	70	20	10	Primary FeO and eutectic of FeO and spinel. Again the Peritectoid transformation has occurred.

General Observations made on the Solidified Slags.

Colour:- An attempt was made to arrange the melts according to the effect of FeO or MnO on the colour, but there appeared to be no relationship. All the melts were black, some showing a blue

iridescence and others a greenish sheen.

Fluidity:- The melts appeared to be quite fluid at the temperature employed. The melts rich in Al_2O_3 (more than 20%) seem to be the most viscous of the series.

Surface Tension:- All the melts appear to have a low surface tension, showing a decided concave meniscus.

Hardness:- The melts have a hardness between 9 and 10 on Moh's Scale. These could be used as glass cutters.

Brittleness:- The melts were not as brittle as those of the $FeO-Al_2O_3$ system. When the crucibles were sectioned and the two parts eased apart the melts remained intact, but disintegration of the melts occurred in the case of $FeO-Al_2O_3$.

Crystal Habit:- Crystal habit of spinels was very pronounced in the systems $FeO-Al_2O_3$ and $MnO-Al_2O_3$. Plates of spinels were visible to the naked eye in the sectioned melts often appearing in the pipe contraction. The crystal habit was not so pronounced in the ternary melts and no plates were observed.

Liquation:- Melts rich in spinel tended to liquate, the spinel having a lower specific gravity than the eutectic.

Conclusion

The chief feature of the diagram is the low melting trough extending from the eutectic of $MnO-Al_2O_3$ at 1520°C to the eutectic of $FeO-Al_2O_3$ at 1305°C. The lowest temperature of melting occurs at the eutectic of $FeO-Al_2O_3$. As shown in fig. 19, this trough is narrow, rising steeply on either side. Inclusions in steel whose composition lies on the $MnO-Al_2O_3$ side of the diagram and in this trough, will begin to solidify at about 1500°C. On casting steel from 1600°C, such inclusions would tend to solidify quickly resulting in small, hard particles since there would be little time for coalescence with subsequent rise to the surface.

Small quantities of FeO and MnO do not seriously flux Alumina. However, FeO and MnO react with Alumina to form spinel, and mixtures of spinel, FeO and MnO are low melting. Alumina in contact with FeO and MnO will be slagged to some extent.

Part II

VISCOSITY OF SLAG SYSTEMS.

Introduction:-

The study of viscosity of slags forms an important part of the general scheme of research into the constitution and properties of slag systems, undertaken by HAY and his co-workers[20]. Viscosity is an important physical property of slags and exact knowledge of its variation with temperature and constitution is necessary to steel furnace and blast furnace practice. The importance of such knowledge becomes apparent when it is realised that little is known quantitatively about the effect of the variation of temperature or constitution on the viscosity of open hearth slags. It is now generally accepted that the success of the steel refining process depends largely upon the reactions which occur between the slag and the underlying bath of metal, and upon the transfer of heat through the slag to the metal. It is evident that the velocity of chemical reactions and the rate of heat transfer in turn, depend upon the diffusion and convection of reactants towards the slag-metal interface and of the products away from there. Also, in a fluid medium, the transfer of heat by convection is much more rapid than by conduction. Hence the speed of these processes in the slag is governed by its fluidity. In basic open hearth practice, for example, fluorspar additions are made to 'thin' the slag and speed up the reactions. However, although it is known that fluorspar lowers the viscosity of slags, the quantitative decrease is not known.

In blast furnace practice, the viscosity of the slag has a very important influence on the running of the furnace. For efficient and regular practice, the slag should be fluid at the temperature of the tuyeres zone. It is usual to produce a certain grade of iron in each furnace and to do so it is essential to run the furnace at a definite temperature since carbon reduces silica in the slag, the resulting silicon passing into the metal. If the temperature of the furnace is too high for the grade of iron desired, the resulting iron will be too high in silicon and if the temperature is too low, the iron

will have a silicon content which is too low. As FEILD and ROYSTER[11] have suggested, there is probably a definite value of viscosity of the slag which gives the best results. Since viscosity decreases with temperature and varies with composition, there will be a definite temperature at which a slag of given composition will have this value of viscosity. Hence the temperature of the tuyeres zone varies and so the grade of iron produced according to the composition of the slag employed. COLCLOUGH[27] has applied the results of RANKIN and WRIGHT[10] and McCAFFERY[12] on the constitution and viscosity of blast furnace slags respectively, to the problem of producing basic pig iron from ores of higher alumina content than those usually employed. The slag should have the two following properties:-

a) The melting point should be below the temperature of the tuyeres zone.

b) The viscosity should be as low as possible.

The study of thermal equilibrium diagrams of slag systems as described in the first part of this thesis produces information regarding the different molecular species occurring in the solid state. But dissociation may occur. Hence, for example, where there are three components such as FeO, MnO and SiO_2, the ternary diagram gives the maximum number of phases in the liquid slag. Rhodonite and Tephroite both undergo peritectic dissociations and so are dissociated to some extent in the liquid state. Fayalite melts as a pure compound, but at temperatures above the liquidus, dissociation may occur. KRINGS and SCHACKMANN[28] in an investigation into the various equilibria existing in open hearth slags obtained information about the stability of the molecular species in the liquid state. The systematic measurement of viscosity of slags in a system such as $CaO-SiO_2$ might yield some information about the stability in the liquid of the various compounds which exist in the solid. C.H. HERTY[29] inferred from his viscosity results that the compound $CaO.SiO_2$ existed at temperatures up to 1650°C., but this is denied by ENDELL[30]. McCAFFERY[12] suggested from evidence of viscosity results for the quaternary system

lime-magnesia-silica-alumina, that compounds existed at temperatures just above the liquidus, but at temperatures about 1600°C, dissociation was far advanced.

Much work has been carried out on the viscosity of glasses and in many cases it has been attempted to prove the existence of compounds in the liquid state. ENGLISH[31] inferred from viscosity results that the compound $3Na_2O.2B_2O_3 . x\ SiO_2$ existed in a glass at a temperature just above the liquidus, but dissociation proceeded as the temperature increased. STOTT[32] showed that the turning point of viscosity-composition isotherms in the Na_2O-SiO_2 system was situated in the region of the compound $Na_2O.2SiO_2$ and suggested this as evidence of the existence of this compound in the liquid. In a work on the viscosity of mixtures of $Na_2B_4O_7$ and B_2O_3, VOLARIVICH and TOLSOI[33] found that the maximum points on the liquidus corresponded to the viscosity-composition isotherm maxima.

Slag particles occurring as non-metallic inclusions in steel are detrimental. When liquid steel is cast into a mould, small globules of liquid slag are distributed throughout the steel. Assuming that these globules are spherical, the velocity of rise to the surface of the steel is given by the following equation:-

$$v = \frac{2}{9} \frac{r^2(d - d')g}{\eta}$$

where

V = velocity of rise of slag globules
r = radius of slag globules
d = density of steel
d' = density of slag
η = viscosity coefficient of steel.

It is obvious that the greater the radius of the slag globule, the greater will be the velocity of rise. The more fluid is the slag and the lower is its melting point, the greater will be the tendency to coalescence. But if the viscosity is great and the melting point high, the tendency to coalescence will be small and the resulting steel will be "dirty".

The present work was undertaken with a view to measuring systematically the viscosity of the various slag systems occurring in blast furnace and open hearth furnace

practice, since results obtained would be extremely useful practically, while their interpretation might yield some information concerning the constitution of the liquid slags.

The first problem to be tackled was the construction of a viscometer capable of measuring viscosity over a wide range and to a temperature of 1650°C. A thorough study of the various methods of measuring viscosity was made, Hatschek's 'Viscosity of Liquids' being found very useful. The literature was then searched to find which methods had been successfully applied to the measurement of viscosity of liquids at high temperatures.

Summary of the Various Methods employed in the Determination of Viscosity of Liquids.

Considering the important applications of viscosity results for open hearth slags, it seems surprising that very little work has been carried out in this field. However, there are many difficulties to be encountered and two chief factors appear to be responsible.

(1) The refractory material employed in the construction of the viscometer should resist the attack of the slag at temperatures up to 1650°C such as obtained in steel making furnaces and should not become weak at such temperatures; it should also be resistant to thermal shock. There are very few materials which approach these specifications. Platinum -10% Rhodium fulfills these requirements but it is very expensive. Molybdenum would be suitable, but it cannot be obtained in suitable form for the construction of a viscometer. Low porosity fused alumina ware was found to resist the attack of some FeO-MnO-SiO_2 slags at 1600°C but had a low resistance to thermal shock and is also very expensive. The only other material available which approached the required specifications was graphite, but it can only be used with slags which do not contain reducible oxides. Ferrous oxide and manganese oxide which are present in open hearth slags would be reduced to iron and manganese respectively in contact with graphite. For blast furnace slags containing no reducible oxides, graphite or platinum could be employed, but for open hearth slags, platinum

appears to be the only available material.

(2)

The viscosity of glasses and slags appears to vary over a wide range with change in temperature and composition. Hence the apparatus to be employed must be responsive to a wide range of viscosity.

It appears that all the methods for measuring viscosity of liquids belong to four types.

(1) Capillary tube methods.

(2) Concentric cylindar methods.

(3) Falling Sphere or methods depending on the movement of a sphere through the liquid, governed by Stoke's Law.

(4) Logarithmic Decrement Method.

Since Poiseulle developed the theory for viscous flow of a liquid through a capillary tube, the capillary viscometer in various forms has been most commonly used for measuring the coefficients of viscosity of liquids at ordinary temperatures. A concentric cylinder method was devised by MARGULES[33], and values of absolute viscosity of liquids obtained by COUETTE[34] and HATSCHEK[35] using this method, agree with those obtained by capillary methods. LADENBURG[36] introduced a modified formula for the calculation of viscosity from experimental observations made in the falling sphere viscometer. Stoke's Law only holds for a cylinder of infinite dimensions, Ladenburg's corrections being for the effects produced on the fall of the sphere through the liquid by the diameter and length of the experimental cylinder employed. Absolute viscosities of liquids obtained by the falling sphere method using Ladenburg's corrected formula agree with those obtained by previous methods. However, this method is more usually employed in measuring high values of viscosity and is not usually employed in measuring a viscosity coefficient less than about 8 Poise. Logarithmic decrement methods have been successfully employed to measure the viscosity coefficients of fluid liquids.

It would appear from the literature that glass at such temperatures as 1300°C or 1400°C is viscous compared with ordinary liquids, but as the temperature falls, its viscosity

increases rapidly and reaches exceedingly high values. The viscosity of blast furnace slags also appears to increase very rapidly as the temperature falls from 1650°C. Hence any apparatus used for the study of the viscosity of fused silicates must be capable of use over a very wide range. For this reason the ordinary capillary method or logarithmic decrement method is not satisfactory for a complete study of the viscosity variation with temperature. In any case, suitable materials for the construction of a capillary viscometer for high temperature measurements are not readily available.

The only methods which appear to be of use for measurement of viscosity at temperatures up to 1650°C are the falling sphere method and a concentric cylinder method. A logarithmic decrement would be useful for measuring low values of viscosity at high temperatures.

Viscosity of tar and pitch mixtures was determined by SCHOTTENER[37] by allowing spheres attached to a wire to fall through the liquid under test. Ladenburg's corrected formula was used in calculating the results which agreed with those found by other methods.

GREINER[38], determining the rate of fall of a platinum sphere, compared the viscosities of a few simple silicates with the viscosity of sodium orthosilicate up to 1200°C.

ARNDT and GESSLER[39] measured the viscosities of glasses up to 1100°C by a falling sphere method. The apparatus consisted of a cylindrical platinum vessel, capped with hemispherical ends, attached to a platinum wire, which was in turn attached to a thin cord passing over a free running pulley wheel. A scalepan carrying weights to control the rate of fall of the vessel through the liquid was attached to the free end of this cord. DOELTER[40] and STALEY[41] measured viscosities of synthetic silicates and various vitreous borates respectively using a similar apparatus.

ENGLISH[31], using a somewhat similar apparatus, obtained inconsistent results for glass owing to the fact that, no matter how fine the thread or wire supporting the sphere, there was always a drag caused by the passage of the thread

through the liquid, this drag varying continuously as the depth of the sphere in the liquid increased.

TROUTON and ANDREWS[42] employed a falling sphere method for measuring the viscosity of pitch-like substances, but eliminated the errors caused by the viscous resistance to the movement of the wire and to the friction losses in the pulley, by allowing the sphere to fall perfectly freely through the pitch, determining its position by x-ray photographs taken at definite time intervals. This method of following the sphere's passage through the liquid is impractical at temperatures above 1200°C owing to the necessary bulky nature of the furnace which has to maintain the high temperatures, and to the fact, that a platinum sphere falling freely through a slag at 1650°C would attain a fairly high velocity.

ENDELL[43] using a similar method to that of ENGLISH, modified the apparatus by fitting the sphere to the end of a platinum cylinder. To the other end of the cylinder was attached a wire passing over a free running pulley. This wire carried a scale pan and weights to control the rate of fall of the vessel through the liquid. Only the ball and part of the cylinder were immersed in the liquid. Fixed to the scale pan was a pointer which in moving over a scale indicated the passage of the vessel through the liquid. Using a modified expression of Ladenburg's formula and from the dimensions of the cylinder and ball, initial immersion, final immersion, velocity of fall and density of the liquid, the coefficient of viscosity was calculated. The viscosities of a number of glasses were thus investigated. The error due to the variable viscous resistance to the wire was thus eliminated, but an error, which was greatest in measuring low coefficients of viscosity, persisted owing to friction losses at the pulley.

Objections to the use of a falling sphere viscometer for measuring the viscosity of slags at high temperatures are summarised below:-

(1) For low coefficients of viscosity, about 2 or 3 poise, the passage of the platinum sphere falling freely through

the liquid does not obey Stoke's Law.

(2) There is an error owing to friction losses at the pulley, which increases in magnitude as the viscosity coefficient of the liquid decreases.

(3) An error is introduced owing to the variable resistance to the connecting wire in its passage through the liquid.

(4) When obeying Stoke's Law, a sphere falls through a liquid at constant velocity. However, it has to fall some distance before this constant velocity is attained. For liquids at ordinary temperatures, the sphere is usually allowed to fall about 5 cms. through the liquid, before measuring the velocity; the length of the cylinder being about 30 cms. For high temperature work, a smaller cylinder is used. The maximum length of cylinder permissible with the molybdenum furnace to be employed is three to four inches, since only a uniform temperature hot zone of this length can be obtained. Such a cylinder is too small for accurate results. Even with a different type of furnace, it would be difficult to maintain a longer cylinder of slag at a uniform temperature of 1600°C throughout.

(5) It is not possible to follow the passage of a sphere falling freely through liquid slag at high temperatures, because of the necessarily bulky nature of the furnace.

(6) For each determination of viscosity coefficient, the density of the liquid has to be measured.

The theory of the falling sphere viscometer is discussed in detail in the chapter dealing with the calibration of the apparatus employed in this investigation.

Since Margules in 1881 devised the concentric cylinder method for measuring the viscosity coefficients of liquids, investigations have been made into the viscosity of glasses and slags using various forms of this apparatus. There are two procedures. In one, the space between the two co-axial cylinders is filled with the liquid to be tested, and the coefficient of viscosity is measured from the torque of the inner cylinder caused by the outer cylinder which is fixed; the rate of

revolution of the inner cylinder driven by a known couple being determined. ENGLISH[31], GEHLOFF and THOMAS[44] and PROCTOR and DOUGLAS[45] measured the viscosity of glasses by this method. SAITO and MATSUKAWA[46] measured the viscosity of molten light alloys, copper alloys and cast irons, MATSUKAWA[47] later modifying the apparatus to make it suitable for measuring the viscosity of open hearth and cupola furnace slags.

The method of rotating the outer cylinder and measuring the torque produced on the inner cylinder was successfully used by HATSCHEK[35] and COUETTE[34] in measuring the viscosity of liquids at ordinary temperatures, and by FEILD and ROYSTER[11] and later McCAFFERY[12] in measuring the viscosity of blast furnace slags up to 1650°C.

The concentric cylinder method for measuring viscosity of fused silicates at high temperatures has the following advantages:-

(1) It is responsive to a wide range of viscosity.

(2) Materials for its construction are available.

(3) Since a cylinder of slag three inches in length is sufficient, a uniform high temperature can be maintained throughout the slag.

It has the following disadvantages:-

(1) When the outer cylinder is to be rotated at a constant speed, some complicated driving mechanism is required. An open end at the bottom of the furnace is necessary to allow the passage of the connecting rod from the driving mechanism to the cylinder. Access of air might occur through this open end with disastrous results to the molybdenum winding.

(2) Although the method of rotating the inner cylinder can be used with a furnace closed at the bottom, great care has to be taken in the construction and setting up of the apparatus.

(3) Since slags containing FeO and MnO oxidise in air at high temperatures, it is intended to measure their viscosity in controlled atmosphere. A concentric cylinder method does not appear to be very suitable for controlled atmosphere work.

Using an oscillating disc method, FAWSITT[48] measured viscosity of liquids at high temperatures.

GUYE and VASILEFF[49] by measuring the damping of the swing of a body immersed in glass and supported by a torsion member, determined the viscosity of the glass at high

temperatures. It was not possible to employ this method with extremely viscous liquids such as glass at temperatures below 1300°C.

OBERHOFFER and WIMMER[50] investigated the influence of temperature and composition on the viscosity of iron using a logarithmic decrement method.

THIELMANN and WIMMER[51] and later ESSER, GREIS and BUNGARDT[52] measured the viscosity of liquid pig iron. The damping of a pendulum vibrating in the liquid pig iron, contained in graphite crucibles which had been soaked in colloidal silica and fired to 1750°C, was measured.

STOTT[53] calculated the viscosity of molten metals from the damping of a disc oscillating in the liquid.

ENDELL[30] by measuring the logarithmic decrement of a platinum sphere oscillating in the liquid obtained viscosity results for some slags.

Hatschek, in "Viscosity of Liquids", refers to other logarithmic decrement methods, but these do not appear to have been successful with liquids at ordinary temperatures and have not been used for high temperature viscosity determinations.

It appears that all logarithmic decrement methods of measuring viscosity of liquids at high temperatures employ a circular disc or cylinder oscillating in the liquid. Such a method has the following advantages:-

(1) Materials for its construction are available.

(2) Since a cylinder of liquid three inches in length is sufficient, a uniform high temperature can be maintained throughout the slag.

(3) Low coefficients of viscosity such as those of molten metals can be measured accurately. Hence it should be possible to measure low coefficients of viscosity of fluid slags at temperatures about 1650°C.

(4) It was considered possible to measure the viscosity of slags in controlled atmosphere.

(5) It can be used with a furnace closed at the bottom.

It has the following disadvantage :-

(1) It is not responsive to a wide range of viscosity. Hence it is not suitable for a complete study of the viscosity variation with temperature for glasses or blast furnace slags.

Selection of a suitable method for measuring the Viscosity of fused Silicates at high Temperatures.

It would appear from consideration of the preceding discussion that the two most suitable methods available for the work in hand are (1) Concentric cylinder method in which the inner cylinder is rotated and (2) Logarithmic decrement method. As shown by the work of PROCTOR and DOUGLAS[45] on the viscosity of glass, high coefficients of viscosity can be accurately measured by the first method. However, some doubt seems to exist as to the lower limit of viscosity which can be measured accurately. From the results given by McCAFFERY[12] it would appear that the lower limit of viscosity coefficient of blast furnace slags at 1650°C is about 2 poises. MATSUKAWA[47] gives viscosity results for open hearth furnace slags as obtained by the first method. The outer cylinder containing the slag is fixed, the inner cylinder immersed in the slag being rotated at a constant speed by a constant couple. Provided that the assumptions made in devising the concentric cylinder theory hold, the viscosity coefficient is directly proportional to the time of rotation as measured in this apparatus. Matsukawa has expressed his viscosity coefficients as times of rotation in comparing the viscosities of various slags, but since his results are not expressed in absolute units(poise), the actual viscosities of the slags investigated are not known. Hence it is not possible to compare his results with those of other workers. Unfortunately, other data on viscosity of open hearth slags is not available, but it is known qualitatively, that at temperatures of 1650°C, open hearth slags are more fluid than blast furnace slags.

Since it is not possible to measure the high coefficients of viscosity which obtain in blast furnace slags and glass at low temperatures by a logarithmic decrement method, it was decided to construct a concentric cylinder apparatus in which the inner cylinder is rotated. Viscosity measurements on some glasses which had been made by other investigators were repaated and the technique developed before attempting to measure the viscosity of blast furnace slags to

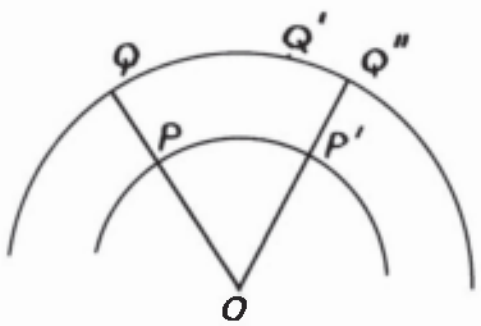

fig. 26.

temperatures about 1650°C. It was also decided that, if the concentric cylinder apparatus could not be made suitable for measuring the lower viscosities which obtain in blast furnace and open hearth furnace slags at 1650°C, a logarithmic decrement method would be devised.

Theoretical Considerations of the Concentric Cylinder Method.

Before designing and constructing the apparatus, the theory of the concentric cylinder method of measuring viscosity was considered.

The coefficient of viscosity (η) is defined as the force required per unit area to maintain unit gradient of velocity, or, the force required per unit area to maintain unit difference of velocity between two parallel planes in the liquid unit distance apart. It is usually expressed in dynes, cms., secs., the unit being called a Poise.

Consider a liquid contained between two vertical coaxial cylinders. When the inner cylinder is rotated by a constant couple, the liquid assumes a stationary state and tends to communicate it to the outer cylinder. When the outer cylinder is fixed, a certain torque is produced on the inner cylinder.

Let L = length of inner cylinder in contact with the liquid
r_1 = radius of inner cylinder
r_2 = radius of outer cylinder
ω = angular velocity of inner cylinder
$T = \frac{2\pi}{\omega}$ = time of rotation of inner cylinder
G = couple applied to inner cylinder

When the inner cylinder is rotated in the liquid coaxially with the outer cylinder by couple G, the liquid is set in motion, and when a stationary condition has been reached, each circle of radius r revolves with constant angular velocity For any such circle, the condition that no acceleration takes place is that the moment maintaining rotation is equal to the moment due to viscous resistance, which is the product of the area, viscosity coefficient, velocity gradient and radius.

In fig. 26, P and Q represent points on two of the concentric circles in which the liquid moves, lying on the same

radius. After a time t, the point P has come to P^1 and Q to Q^1. Radius through P^1 cuts the outer circle at Q^{11}.

The velocity gradient at P $= \frac{Q'Q''}{t\ P'Q''}$

Let ω = ang. velocity on circle containing P

$\omega - \Delta\omega$ = " " " " " "

Then $\frac{QQ''}{t\ OQ'} = -\Delta\omega$ i.e. $\frac{Q'Q''}{t} = -OQ'\Delta\omega$.

Let $OP = r$, and $OQ = r+\Delta r$

$\therefore P'Q'' = \Delta r$.

Velocity gradient at P $= \frac{-OQ'\Delta\omega}{P'Q''}$

$= -(r+\Delta r)\frac{\Delta\omega}{\Delta r}$

$= -r\frac{d\omega}{dr}$ when Δr is very small.

Moment due to viscous resistance $= -2\pi r L\eta . r\frac{d\omega}{dr} . r$

$= -2\pi L\eta r^3\frac{d\omega}{dr}$.

Since r may be any value, this expression must be a constant for the apparatus and equal to the moment maintaining rotation.

Integrating,

$$G\frac{dr}{r^3} = -2\pi L\eta\, d\omega$$

$$-G/r^2 = -4\pi L\eta\omega + C.$$

Since the inner cylinder rotates with constant angular velocity while the outer cylinder is prevented from rotating, the following conditions exist at the bounderies :-

when $r = r_1$, $\omega = W$

" $r = r_2$, $\omega = 0$. $\therefore C = -\frac{G}{r_2^2}$

$$\therefore G = 4\pi L\eta W\frac{r_1^2 r_2^2}{(r_2^2 - r_1^2)}$$

$$\therefore \eta = \frac{G(r_2^2 - r_1^2)}{4\pi L r_1^2 r_2^2 W} = \frac{GT(r_2^2 - r_1^2)}{8\pi^2 L r_1^2 r_2^2}$$

In this type of apparatus, the inner cylinder is usually carried by a spindle working in fixed bearings. The couple G is produced by a mass M carried by a thread wound round a drum of radius R fixed to the spindle

$$\therefore G = gMR.$$

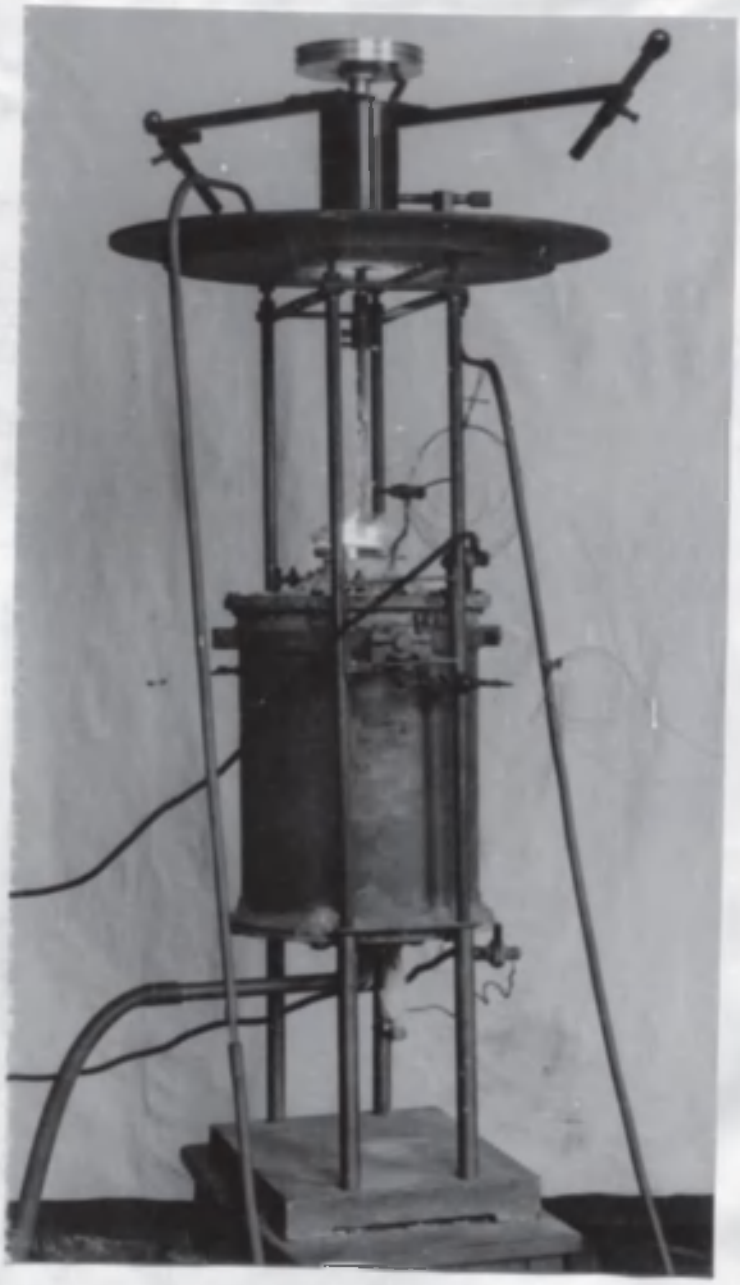

fig. 27.

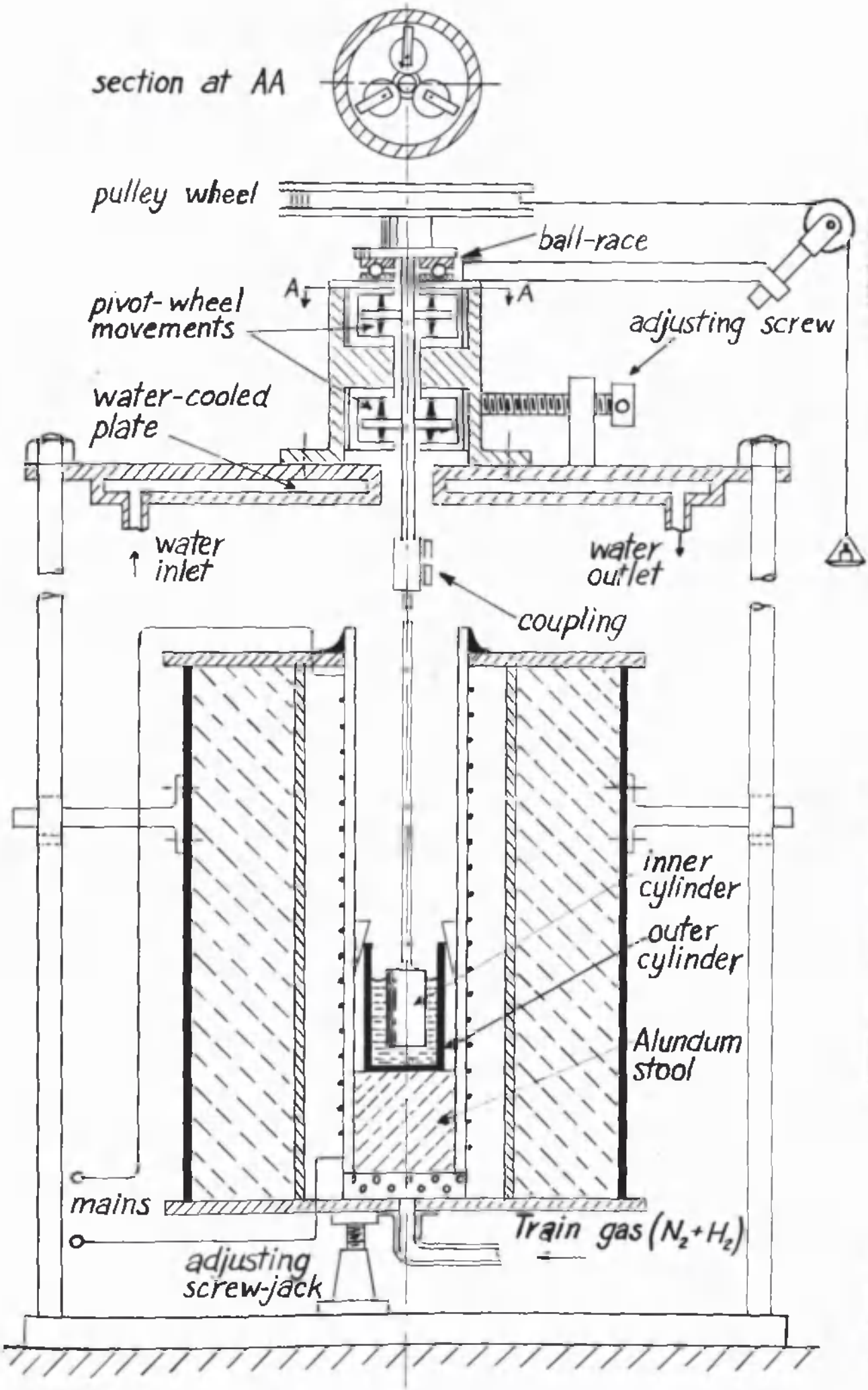
section at AA
pulley wheel
ball-race
A
A
pivot-wheel movements
adjusting screw
water-cooled plate
water inlet
water outlet
coupling
inner cylinder
outer cylinder
Alundum stool
mains
Train gas (N_2+H_2)
adjusting screw-jack

fig. 28.

$$\therefore \eta = \frac{g M R T (r_2^2 - r_1^2)}{8 \pi^2 L r_1^2 r_2^2} \qquad \text{----------(1)}$$

$$= \frac{K' M T}{L} \qquad \text{----------(2)}$$

Equations (1) and (2) apply to infinite cylinders and do not allow for the dragging effect between the ends of the cylinders. If the distance between the ends of the cylinders be kept constant, the couple required to maintain a given angular velocity is proportional to $L + \ell$ where ℓ is the correction for the end effect.

$$\therefore \eta = \frac{K' M T}{L + \ell} \qquad \text{----------(3)}$$

There is also a friction loss at the spindle bearings and applying a correction

$$\therefore \eta = \frac{K'(M - \beta) T}{L + \ell} \qquad \text{----------(4)}$$

It is possible to eliminate the end effect by calculation, by exposing different lengths of the inner cylinder to the viscous drag. This necessitates at least two experimental observations for each viscosity coefficient determination. It is much more suitable for high temperature work that the distance between the ends of the cylinders, the level of the liquid in the container and the dimensions of the cylinders be the same for each viscosity determination, when equation (4) can be expressed in the form

$$\eta = K(M - \beta) T \qquad \text{----------(5)}$$

The value of K can be found experimentally by calibrating the apparatus with liquids of known viscosity.

Design and Construction of the Apparatus for High Temperature Measurements.

Fig. 27 shows a photograph of the assembled apparatus, and fig. 28 a diagram. The essential features of the apparatus are

1. The rotating member
2. Cylindrical container.
3. Water-cooled plate supporting the bush of the rotating member.

4. Stand supporting the water-cooled plate and also carrying the furnace.

5. Molybdenum wire wound furnace.

6. Cracking train for the production of the inert atmosphere surrounding the furnace winding.

7. Thermocouple for measuring temperatures of slags.

It is necessary for success that the inner cylinder be vertically co-axial with the outer cylinder and should rotate about this axis. The friction loss should be constant and as small as possible. To meet the first requirement, a special brass bush was constructed so that the spindle should rotate about its own axis. Special balance movements were fitted at the top and bottom of the bush. Each movement consisted of two parallel brass plates held apart by three vertical brass pillars. Pivoted between those plates were three alarm balance wheels at equal intervals around the spindle. These movements were fitted into recesses in the brass bush, and a cover plate fitted over the top and bottom of the bush. When adjusted, the hardened faces of the balance wheels just touched the silver steel spindle and maintained it in correct alignment. The second condition was met by a ball-bearing at the top of the bush where a silver steel plate with a groove to take the ball race, was fitted. A similar silver steel plate with a groove was fitted to the bottom of the aluminium-silicon pulley wheel. This groove formed the upper half of the track for the ball race. When the spindle was fitted into the bush the pulley rested on the ball race whilst the spindle was maintained in correct alignment by the free running pivoted balance wheels.

The refractory rod carrying the inner cylinder was coupled to the spindle by means of a special brass coupling shown in fig. 28. A locking screw fixed one end of the coupling to the spindle; the other end held the refractory rod by six screws. These screws were arranged in two sets of three, one set above the other, and in each set the screws were placed at equal intervals round the coupling. By means of these screws it was possible to adjust accurately the alignment of the refractory rod so that its axis coincided with the prolongation of the axis of the spindle. It was essential that the refractory rod be rigid

at low and high temperatures, and that its coefficient of expansion be very low. When the refractory rod and cylinder were fixed in correct alignment with the spindle, the cylinder rotated about its own axis. The cylinder was rotated by a falling weight attached to a light thread wound round the pulley wheel and passing over a pivoted wheel adjustable in height as shown in fig. 28. The pulley wheel had two diameters, 6 in. and 1 in. The outer cylinder was placed on top of an alundum stool so as to be in the hot zone of the furnace. The position of this zone was found by searching the furnace with a thermocouple. The container was fixed rigidly in the furnace by means of alundum wedges to prevent movement when the inner cylinder was rotating in the liquid being investigated.

The water-cooled plate, a hollow casting made of Admiralty Gun Metal, was necessary to prevent heat from the furnace reaching the bush and so causing expansion of the bearings with subsequent alteration of the friction factor. In its centre there was a hole ¾ in. in diameter, through which passed the spindle. Concentric with the hole on the upper surface was a highly circular surface, 6 in. in diameter. On this rested the bush, the base of which also had a highly machined surface. Three holes equally spaced round the bottom flange of the bush formed a slack fit with three studs on the water-cooled plate. Two centring screws, mounted on brackets fixed to the plate, permitted the adjustment of the bush and rotating member until the inner cylinder was concentric with the outer cylinder. When correctly adjusted, the bush was locked on the studs with locking screws.

The stand which supported the water-cooled plate had a steel base plate, 18 ins. × 12 ins. × 12 ins. Fixed to this base plate were four vertical steel rods, ¾ in. in diameter by 3½ ft. in length, connected by tie rods at top and bottom for rigidity. These rods also acted as slide rods for the brackets supporting the furnace which could be raised or lowered as required and fixed by means of a locking device. At the top of the rods were adjusting screws on which rested the water-cooled

plate. It was possible by means of these screws to level the plate.

Figs. 27 and 28 show the molybdenum furnace employed in viscosity measurements up to 1650°C. This furnace and cracking train were similar in design and operation to those described in a previous part of this thesis.

For investigation of viscosity of glasses and enamels up to temperatures of 1200°C, a Kanthal wire-wound furnace was employed.

The cylinders should have the following properties:-

(1) The liquid under test must wet the cylinders, since the method is based upon the fact that the force required to cause slip or shear between concentric layers of liquid is a true measure of viscosity. Unless the adhesive force between the inner cylinder and the liquid is greater than the cohesive force between concentric layers of liquid, slip will not take place between those layers but between the slag and the cylinder, resulting in erratic and inaccurate measurements.

(2) The cylinders must conform to the standard dimensions for which the calibration constant was found.

(3) They should retain their shape and strength at high temperatures.

(4) The coefficient of expansion of the cylinders should be small.

(5) They should have a high resistance to attack by the fused silicate.

(6) They should not contaminate the liquid under test.

Platinum - 10% Rhodium cylinders are the most desirable, but they are very expensive.

It was found that hard baked alundum cylinders were suitable for glass and enamels, while graphite fulfilled the specifications for blast furnace slags. Dimensions of the alundum cylinders were as follow:-

Outer cylinder

Internal diameter	4 cms.
Internal height	7.6 cms.
Wall thickness	0.5 cm.

Inner cylinder

Length	7 cms.
Diameter	1.6 cms.

The alundum rods for connecting the inner cylinder to the spindle were 20 ins. in length by ¼ in. in diameter. A plastic mixture of alundum and water was moulded round pieces of wood 1/8 in. in diameter by 2 ft. long. After drying, the alundum was

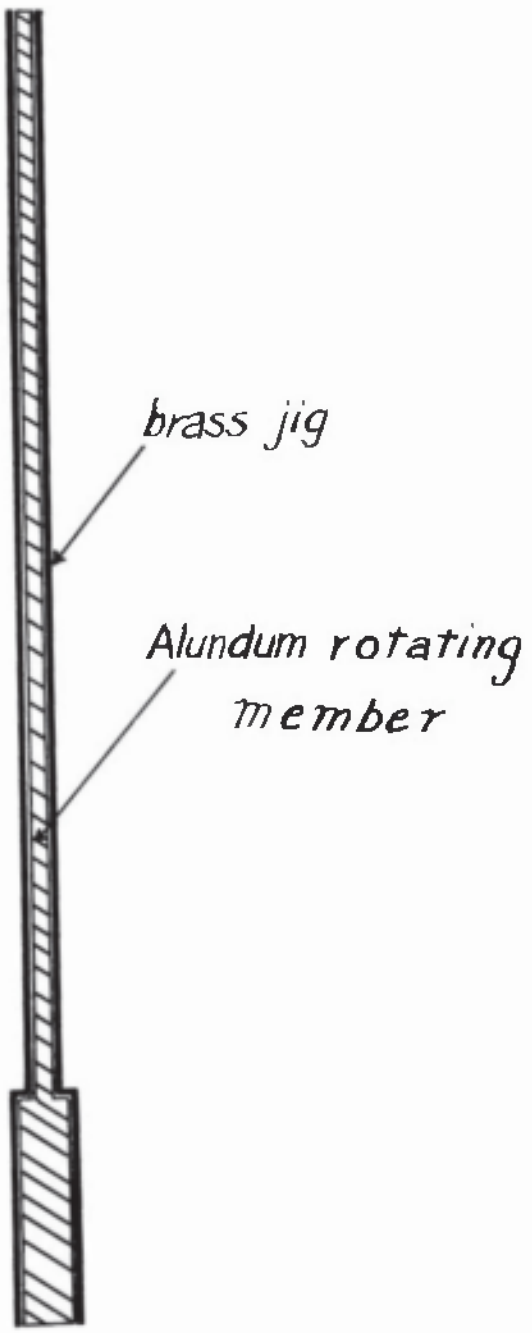

fig. 29.

smoothed into a cylindrical rod by emery paper. By burning out the wooden core at 900°C, hollow cylindrical rods which had just sufficient strength to permit of grinding, were obtained. Using a specially designed tubular grinder with a slotted grinding edge, a hollow rod 20 in. long by ⅛ in. in diameter was obtained.

The inner cylinders were made in the following manner. Alundum was moulded into a cylinder and dried before rubbing down with emery paper to a cylinder of diameter slightly greater than that required in the finished state. After firing at 900°C, it was ground down on the lathe to the exact size of 1.6 cm. diameter by 7 cms. long.

At one end of the cylinder a hole was drilled in the centre and the alundum rod was cemented into this hole. These were joined in a jig (see fig. 29) to ensure that the axis of the rod and cylinder coincided. When the alundum cement had set, the rotating member was fired at 1650°C. It was then tested in the lathe, only being employed in the viscometer when free from eccentricity.

The alundum pots were hand-moulded. A hollow steel tube closed at one end, was covered with a few layers of wet brown paper, so that the diameter was a shade under 4 cms. A plastic mixture of alundum and water was moulded over the tube, allowed to dry and then was ground to give a cylinder with a wall thickness of 0.5 cm. On firing at 600°C, the paper was burned to ash and the alundum pot could be removed from the steel tube. After facing off the open end to give an internal height of 7.6 cm. the pot was fired at 1650°C. Pots could be made in this way to within .05 cm. of the correct diameter, those outwith this range being discarded. The dimensions of the graphite cylinders used for investigating viscosity of synthetic slags composed of two or more constituents like CaO, SiO_2 and Al_2O_3 were as follow:-

Inner cylinder		Outer cylinder	
Diameter	3 cm.	Int. diameter	5 cm.
Length	7 cm.	Int. height	7.6 cm.
		Wall thickness	0.5 cm.

Electrographitic carbon with a very low ash content can be obtained in the form of solid cylindrical rods of suitable dimensions.

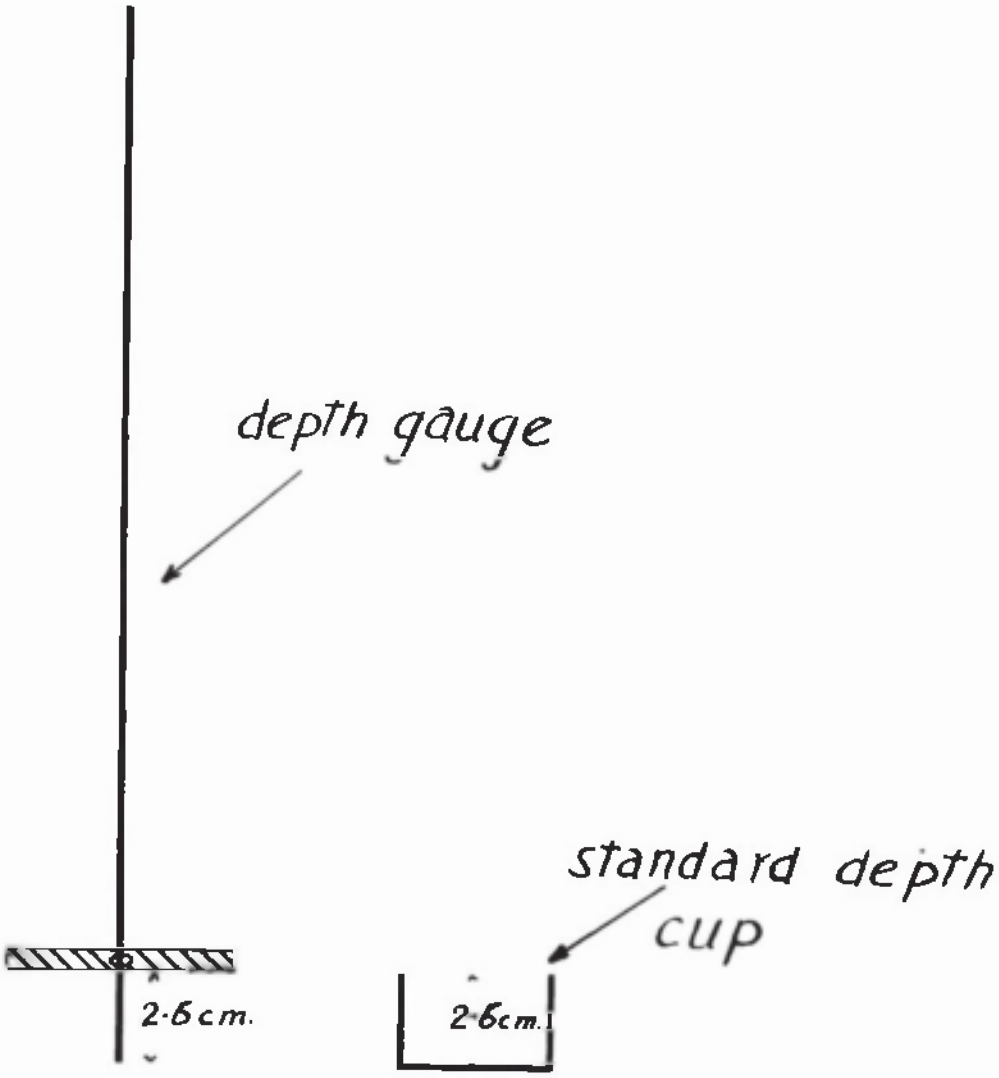

fig. 30

A suitable length of rod was turned on the lathe to a diameter of 3 cm. and the ends faced off to give a cylinder 7 cm. long. At one end a central hole ½ in. in diameter was drilled and tapped. A graphite rod 20 in. long by ½ in. diameter was screwed at one end. This rod was screwed into the cylinder and cemented with alundum to prevent it unscrewing. Before using in the viscometer, this rotating member was tested for eccentricity in the lathe. It was found in practice that this rod tended to burn away at the point where it emerged from the furnace. To prevent this, alundum was coated over this part of the rod.

The outer cylinders were made as follows:-A suitable length was cut from a graphite rod of about 6 cm. diameter and the ends faced off in the lathe. A hole ¾ in. in diameter was drilled down the centre of the rod to a depth of 7.6 cm. and then turned to 5 cm. diameter. In this way outer cylinders could be made to correct dimensions within one-thousandth of an inch.

To ensure that the same depth of liquid was employed in each viscosity determination as in the calibration, a depth gauge (fig. 30) was devised. This consisted of a rigid wire of monel metal, 20 in. x 1/8 in., which made a sliding fit into a transverse hole in a block of monel 2½ in. long. In the calibration of the apparatus for glass and enamels, liquid was placed in the pot to a depth of 2.6 cm. from the top. A steel cup 2.6 cm. deep was employed as a standard. To obtain the correct setting on the depth gauge, the monel block was set on the top of the cup. The wire was pushed through the block until it touched the bottom of the cup, when the block was locked in position. The gauge was then inserted into the outer cylinder with the block resting on top of it, the level of the liquid being adjusted by making additions until the liquid just touched the wire. Different depths were employed with other forms of this viscometer and with the logarithmic decrement viscometer. For each depth a standard depth gauge of the above type was used.

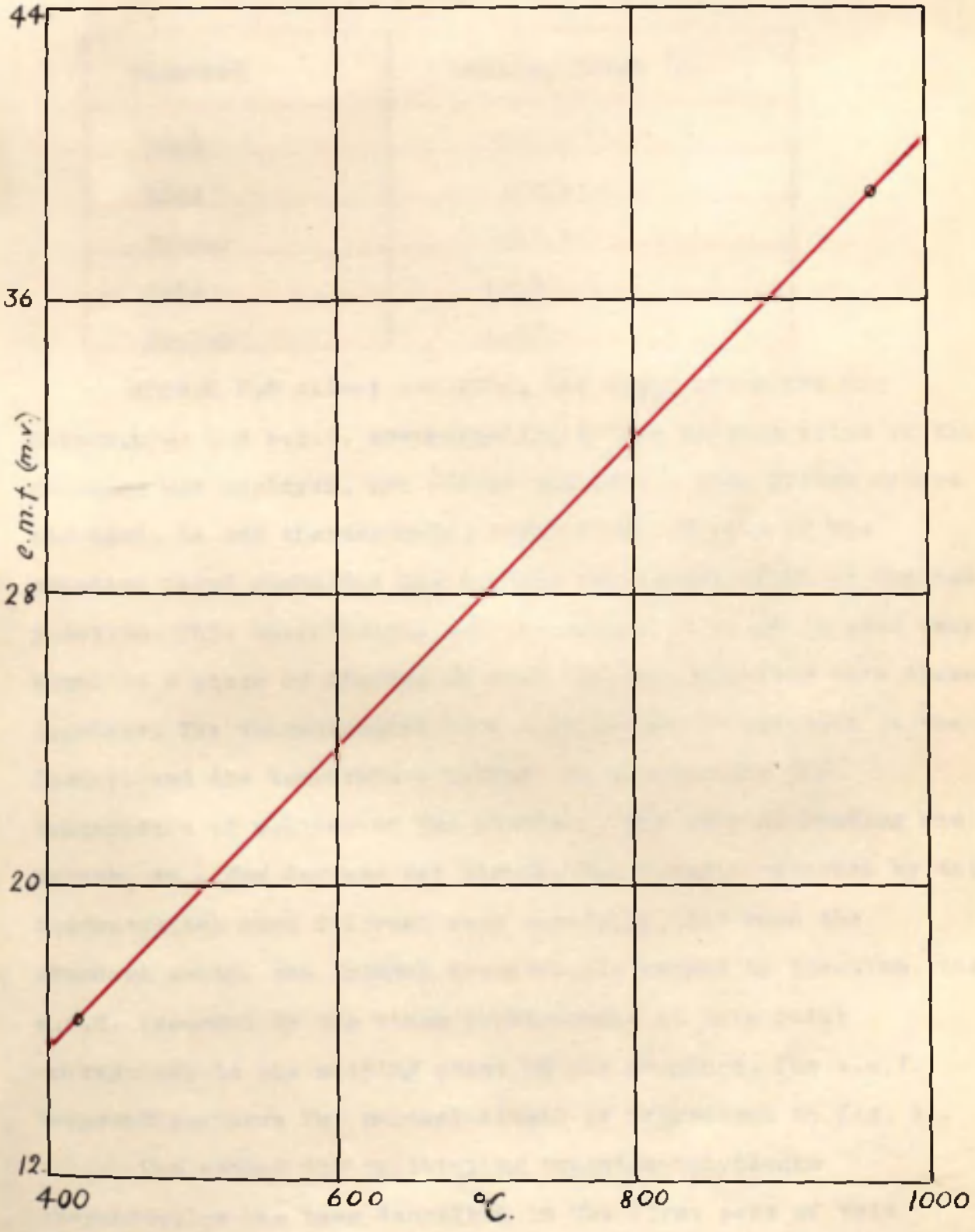

Fig. 31.

Calibration of Thermocouples.

Temperatures up to 1000°C were recorded by a chromel-alumel thermocouple and above 1000°C by a tungsten-molybdenum thermocouple. Information about the thermodynamic scale of temperatures and its standards was found in E. Griffiths' "Methods of Measuring Temperature" and International Critical Tables. Standards used for calibrating the chromel-alumel thermocouple are shown in table V.

Table V

Standard	Melting Point °C.
Lead	327.4
Zinc	419.4
Silver	961.7
Gold	1064
Copper	1083

Except for silver and gold, the usual procedure for determining the e.m.f. corresponding to the melting point of the standard was employed. For silver and gold a wire bridge method was used. In one thermocouple, about 1 cm. of wire of the standard metal connected the chromel and alumel wires at the hot junction. This thermocouple and the couple to be calibrated were bound to a piece of alundum so that the hot junctions were close together. The thermocouples were then placed in position in the furnace and the temperature raised. On approaching the temperature of melting of the standard, the rate of heating was reduced to a few degrees per minute. The e.m.f's recorded by the thermocouples were followed very carefully, for when the standard melts, the bridged thermocouple ceases to function. The e.m.f. recorded by the other thermocouple at this point corresponds to the melting point of the standard. The e.m.f. temperature curve for chromel-alumel is reproduced in fig. 31.

The method for calibrating tungsten-molybdenum thermocouples has been described in the first part of this thesis. However, further precautions in the calibration for the work on viscosity were taken. It is evident from the

viscosity-temperature curves of $CaO-SiO_2-Al_2O_3$ slags that temperature is very critical, even a change of 10C° in some cases making a large difference in viscosity. Since each tungsten-molybdenum thermocouple has a limited life and each batch of thermocouple wires has a different e.m.f.-temperature curve, standards were selected from the thermodynamic scale against which all tungsten-molybdenum thermocouples were calibrated. The standards are shown in table VI.

Table VI

Standard	Melting Point °C
Silver	961.7
Gold	1064
Copper	1083
Nickel	1452
Calcium bisilicate	1536
Palladium	1550

When a thermocouple was almost finished, the new thermocouple besides being calibrated against these standards, was also calibrated against the old thermocouple.

The e.m.fs. corresponding to the melting points of silver, gold, palladium and nickel were obtained by the wire bridge method. A small angular piece of calcium bisilicate suspended in the hot zone of the furnace was observed to melt very sharply and the corresponding e.m.f. of the tungsten-molybdenum was obtained. Employing a standard Pt-Pt-Rh couple, the melting point was found in a number of such experiments to be 1536°C.

Calibration of the apparatus for the Measurement of Viscosities of Molten Glasses and Enamels.

In order to determine the value of K in the equation $\eta = K(M-f)T$, it was necessary to employ a series of liquids of known viscosity. For each value of viscosity various loads were used, and corresponding values of T measured. From the above equation it follows that, when the viscosity and

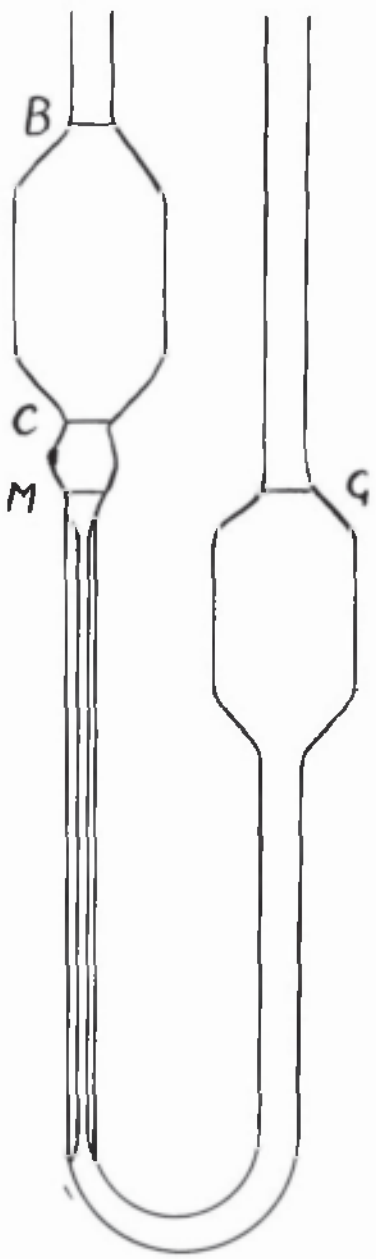

fig. 32.

f remain constant, the plot of M against 1/T should give a straight line, intersecting the load axis at a value equivalent to f. For this investigation, the two liquids chosen were Lyle's Golden Syrup and Corn Syrup, since these liquids have viscosities similar to that of molten glass.

Since these liquids at various temperatures gave a wide range of viscosity values, it was possible to test the constancy of K.

The first step was to determine the viscosity-temperature curves of the syrups. Since syrup is very viscous compared with ordinary liquids, the determination of its viscosity cannot be carried out in the ordinary way, by comparison of its time of flow with that of water in an Ostwald viscometer. A Falling Sphere method was used for syrups and to confirm the accuracy of this method, the viscosities of castor oil and glycerine were measured at various temperatures by the capillary viscometer method and the results compared with those obtained by the falling sphere method.

Capillary Method.

The capillary viscometers used were numbers 1, 2 and 3 of the B.S.I. Specification no. 188. Fig. 32 shows a diagram of this type of viscometer.

The viscometer was immersed in an electrically controlled thermostat bath, the top level of the liquid in the viscometer being at least 1 cm. below the level of the water in the bath. Temperature control was within 1/10 C^{o}. The viscometer was filled with the liquid up to the marks M and G. Liquid was sucked to 1 cm. above B and then allowed to flow freely from B to C and timed by means of a stop-watch to 1/5th. sec. Three readings concordant to 1% were obtained and the mean taken for each viscosity determination. Time readings should not be less than 100 secs.

It can be shown that

$$K = \frac{\nu}{t} = \frac{\eta}{dt}$$

where K = calibration constant
ν = kinematic viscosity in centistokes (cs)

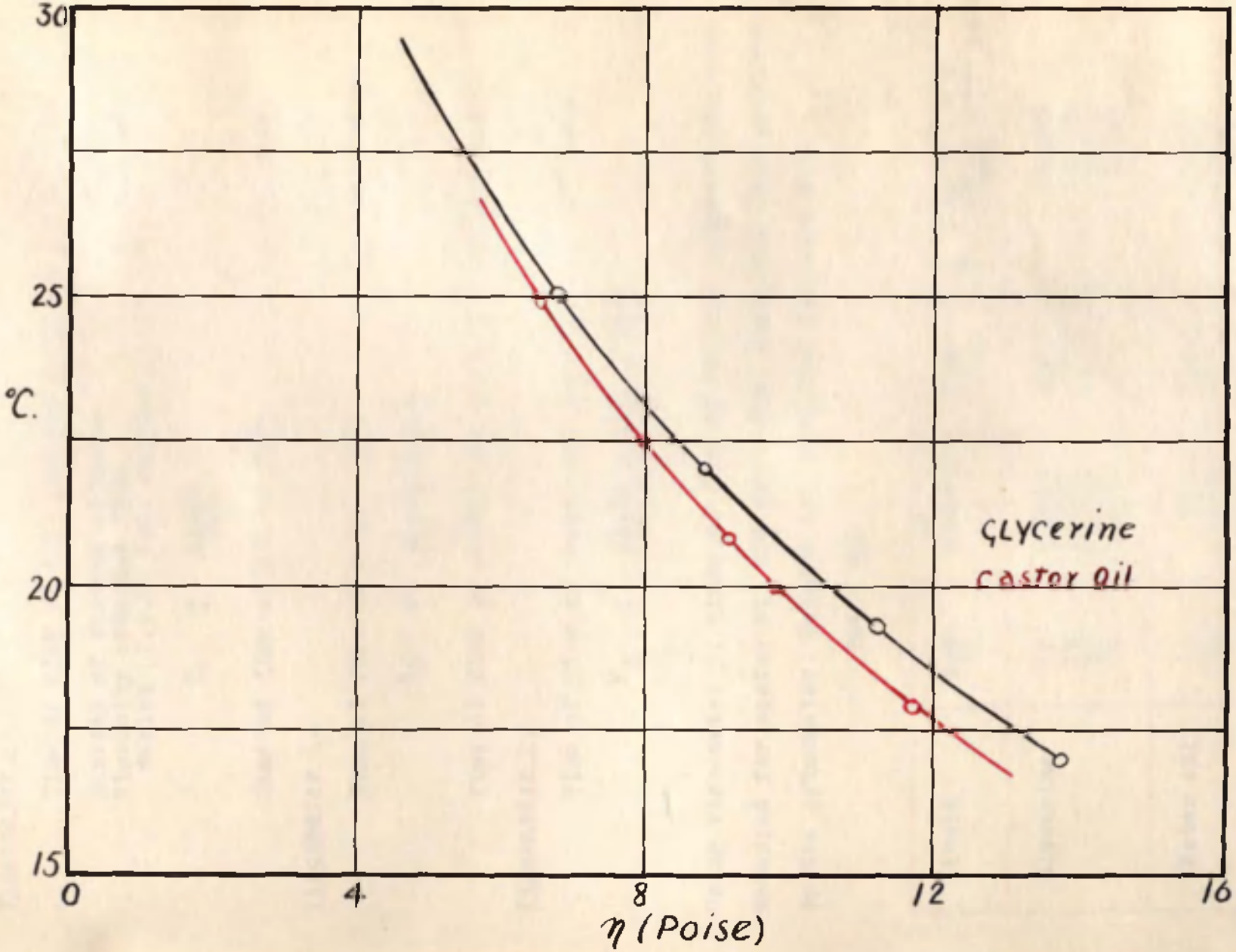

fig. 33.

t = time of flow in secs.
d = density
η = dynamic viscosity in centipoises (cp.)

The calibration constants of the viscometers were obtained as follows:-

Viscometer 1.

Time of flow of '60' sucrose solution at 25°C. = 180 secs.
Density of sucrose solution = 1.2836
Viscosity obtained from tables (I.P.T. 3rd. edition 1935) = 33.86 cs.

$$K_1 = \frac{33.86}{180}$$

Time of flow of oil at 25°C = 435 secs.

Viscometer 2.

Time of flow of oil at 25°C = 219.4 secs.

$$K_2 = \frac{33.86 \times 435}{180 \times 219.4}$$

Time of flow of castor oil at 25°C = 1838 secs.

Viscometer 3.

Time of flow of castor oil at 25°C = 441 secs.

$$K_3 = \frac{33.86 \times 435}{180 \times 219.4} \times \frac{1838}{441}$$

Using viscometer 3, times of flow at various temperatures were measured for castor oil and glycerine. Densities were measured by the pyknometer. Results are tabulated in Table VII.

Table VII

Liquid	Temp. °C.	Density	Time secs.	$\eta = \frac{K_3 \times t \times d}{100}$ poise
Glycerine	17	1.2594	684.2	13.599
	19.4	1.2580	555.8	11.036
	22	1.2565	440	8.726
	25	1.2549	341	6.755
Castor oil	18	.9617	777.4	11.62
	20	.9606	653	9.75
	20.9	.9601	609.4	9.10
	22.6	.9592	532.6	7.94
	25	.9579	441.0	6.57

The viscosity-temperature curves for glycerine and castor oil are shown in fig. 33.

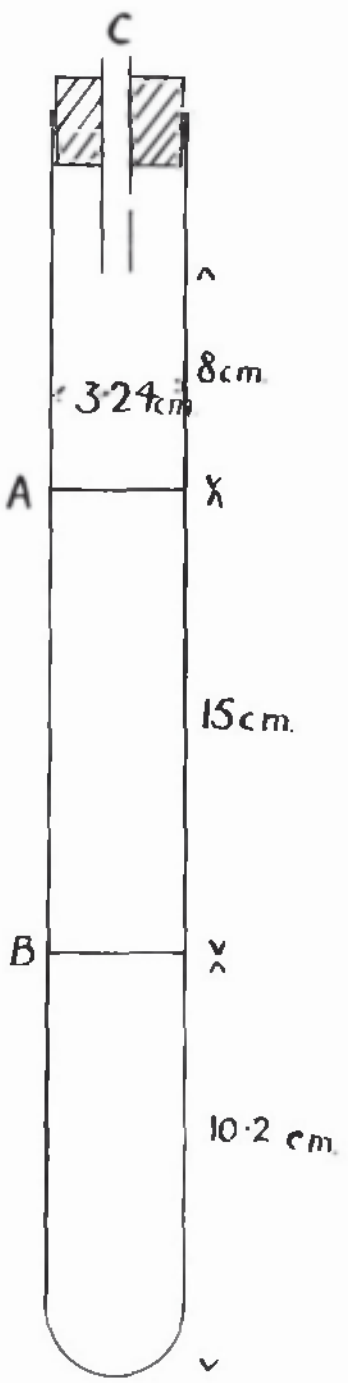

fig. 34.

Falling Sphere Method

According to Stoke's Law, a sphere falling freely through a liquid of infinite dimensions assumes a constant velocity expressed by the following equation

$$V = \frac{2 r^2 g (d-d^1)}{9 \eta}$$

LADENBURG[36] correcting for the effects produced by the dimensions of the cylinder of liquid obtained the expression

$$\eta = \frac{2 r^2 g (d-d')}{9 V (1 + 2.4 r/R)(1 + 3.4 r/L)}$$

where η = coefficient of viscosity (poise)
r = radius of sphere in cm.
d = density of sphere
d^1 = density of liquid
V = velocity of sphere cm./sec.
R = radius of cylinder
L = length of cylinder
g = 981.56 cm/sec^2.

The above equation holds provided

1) Velocity of fall is small. According to Rayleigh, velocity is small when $\frac{r d V}{\eta} < 1$. It is usual to choose a value of V and to adjust r to suit. Arnold introduced the idea of critical radius expressing it as

$$r_c \text{ (critical radius)} = \eta / d V$$

When $r < .6 r_c$ there is no deviation from Stoke's Law.

2) No slip occurs between liquid and surface of the sphere

Two practical considerations limit the application of this method to liquids of high viscosity. (1) The most readily obtainable exact spheres are steel balls used for ball bearings, with a density about 7.6, and (2) the maximum velocity of fall at which the passage through the two marks can be accurately timed, which is generally put at 1 cm./sec. The smallest current size is .15 cm. diameter.

Suppose density of liquid = 1 gm/c.c.
and velocity of fall = 1 cm./sec.

$$\therefore \eta = \frac{2 \times .075^2 \times 981.56 \times 6.6}{9}$$

$$= 8.1 \text{ poises}$$

A diagram of the apparatus employed is shown in fig.34. The liquid was contained in a long glass tube fitted with a stopper through which passed a glass tube just wide enough to allow the passage of a steel ball. This ensured that the falling sphere passed down the vertical axis of the tube. To maintain the liquid

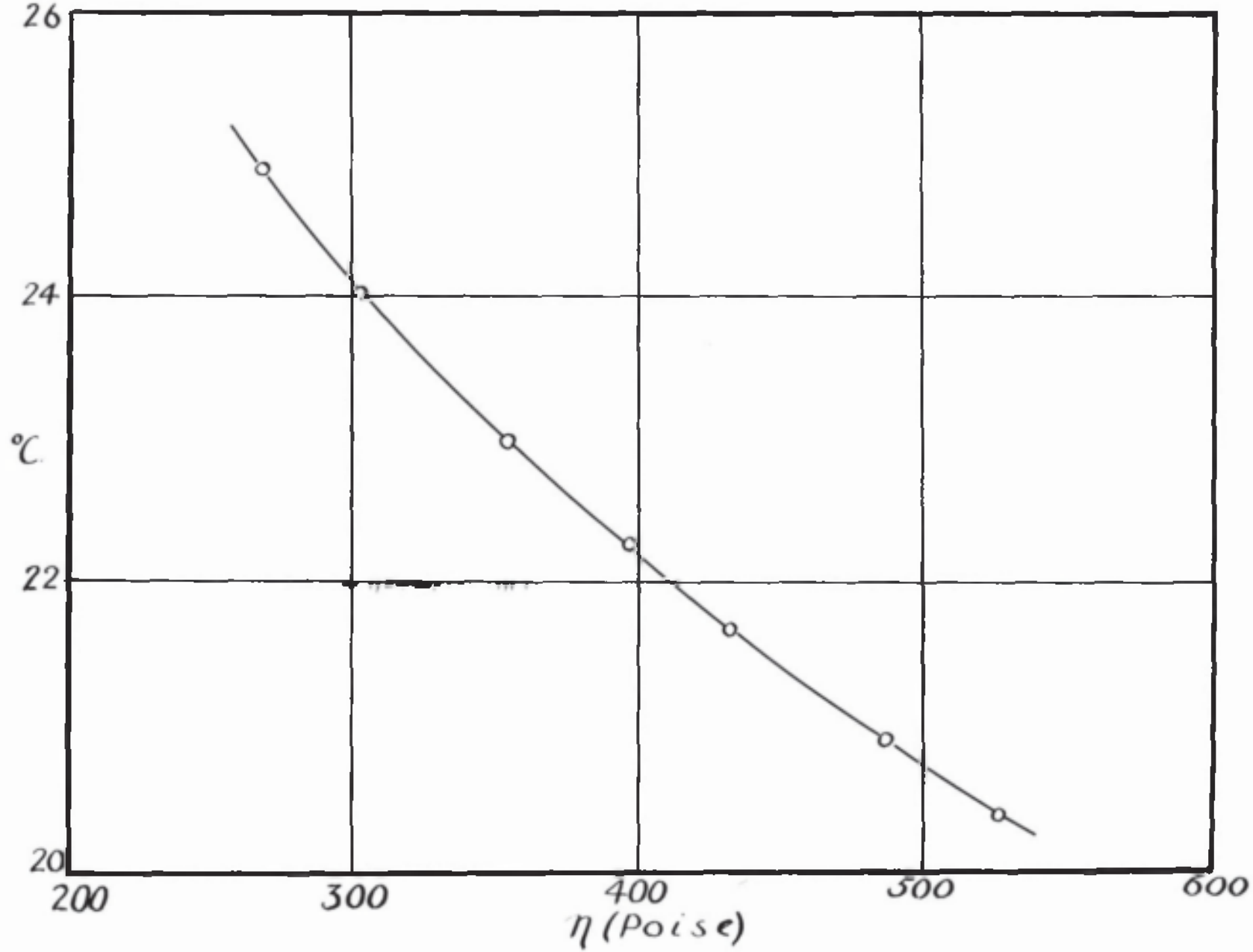

fig 35.

fig. 36

fig 37

in the tube at the desired temperature, the tube was placed vertically in a thermostat bath so that the level of the water in the bath was 2 cm. above the level of the liquid in the tube. Before measuring the velocity of the fall of the sphere through the liquid, temperature was maintained constant for at least half an hour. The sphere was dropped at C, and the time for it to pass from A to B was measured to 1/5th. sec. by means or a stop-watch.

Density of sphere.

Radius of sphere (r) = .0790 cm.
Weight of sphere = .0162 gm.

$\frac{4}{3}\pi r^3 d$ = .0162

$\therefore$ d $= \frac{.0162 \times 3 \times 7}{4 \times 22 \times (.0790)^3}$

= 7.84

Results obtained for castor oil agree with those obtained by the capillary method and are shown in table VIII.

Table VIII

Liquid	Temp. °C	Density	Time of fall in secs.	Viscosity coeff. (η) (poise) Falling Sphere	Capillary
Castor oil	18	.9617	21	11.62	11.62
"	20	.9606	17.6	9.76	9.75

Results obtained for Lyle's Golden Syrup, Syrup solution and Corn syrup are shown in table IX and the viscosity-temperature curves in figs. 35, 36, and 37 respectively.

Table IX

Liquid	Temp. °C	Time of Fall secs.	Density	η (Poise)
Lyle's Golden Syrup	20.45	1017.8	1.4165	527.1
	20.95	941.6	1.4160	487.6
	21.7	836.0	1.4159	433.0
	22.3	767.8	1.4154	397.6
	23.0	684.6	1.4150	354.6
	24.05	583.2	1.4145	302.1
	24.9	519.6	1.4140	269.1

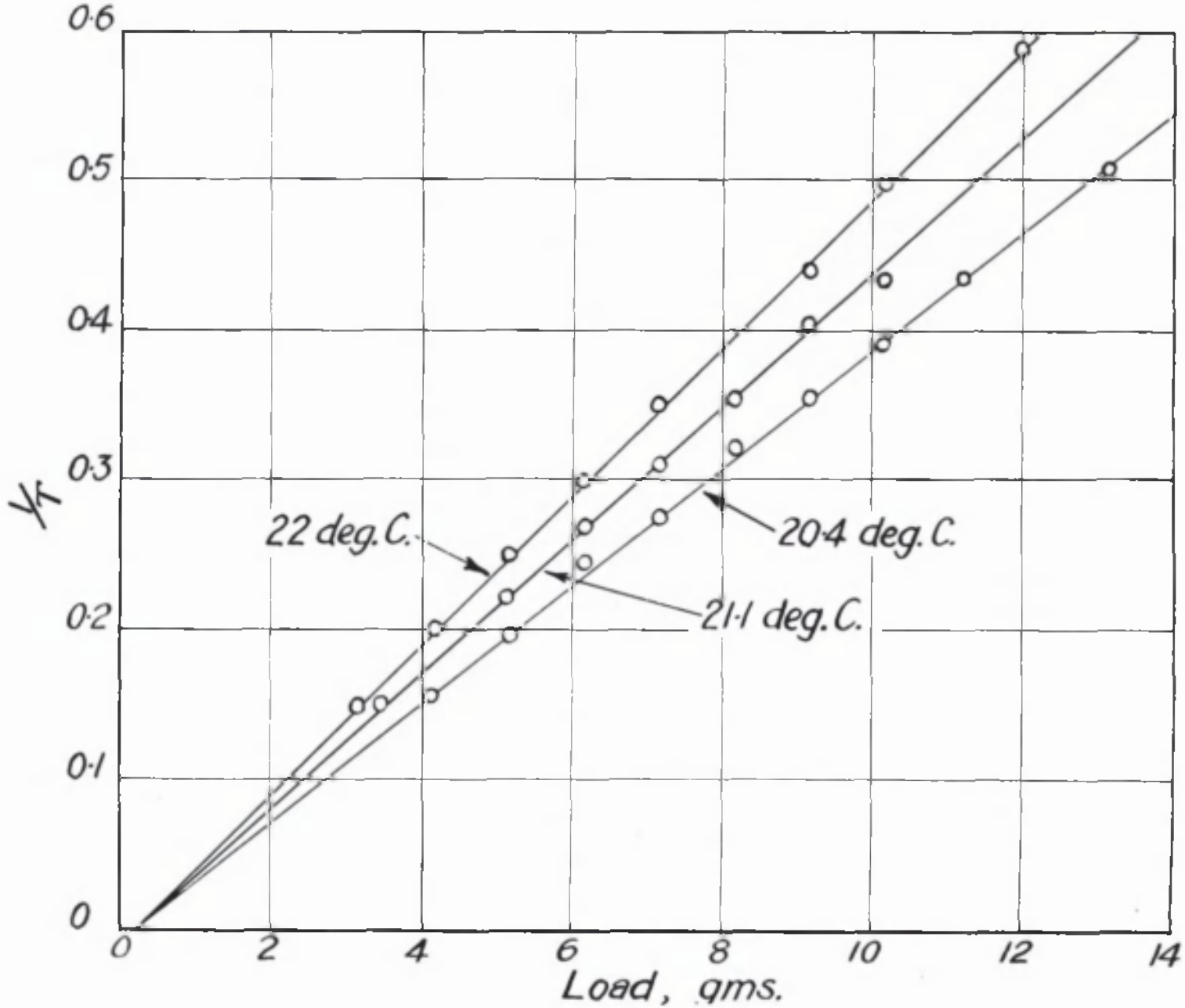
0·6
0·5
0·4
0·3
0·2
0·1
0
Y/T
22 deg.C.
20·4 deg.C.
21·1 deg.C.
0
2
4
6
8
10
12
14
Load, gms.

fig. 38.

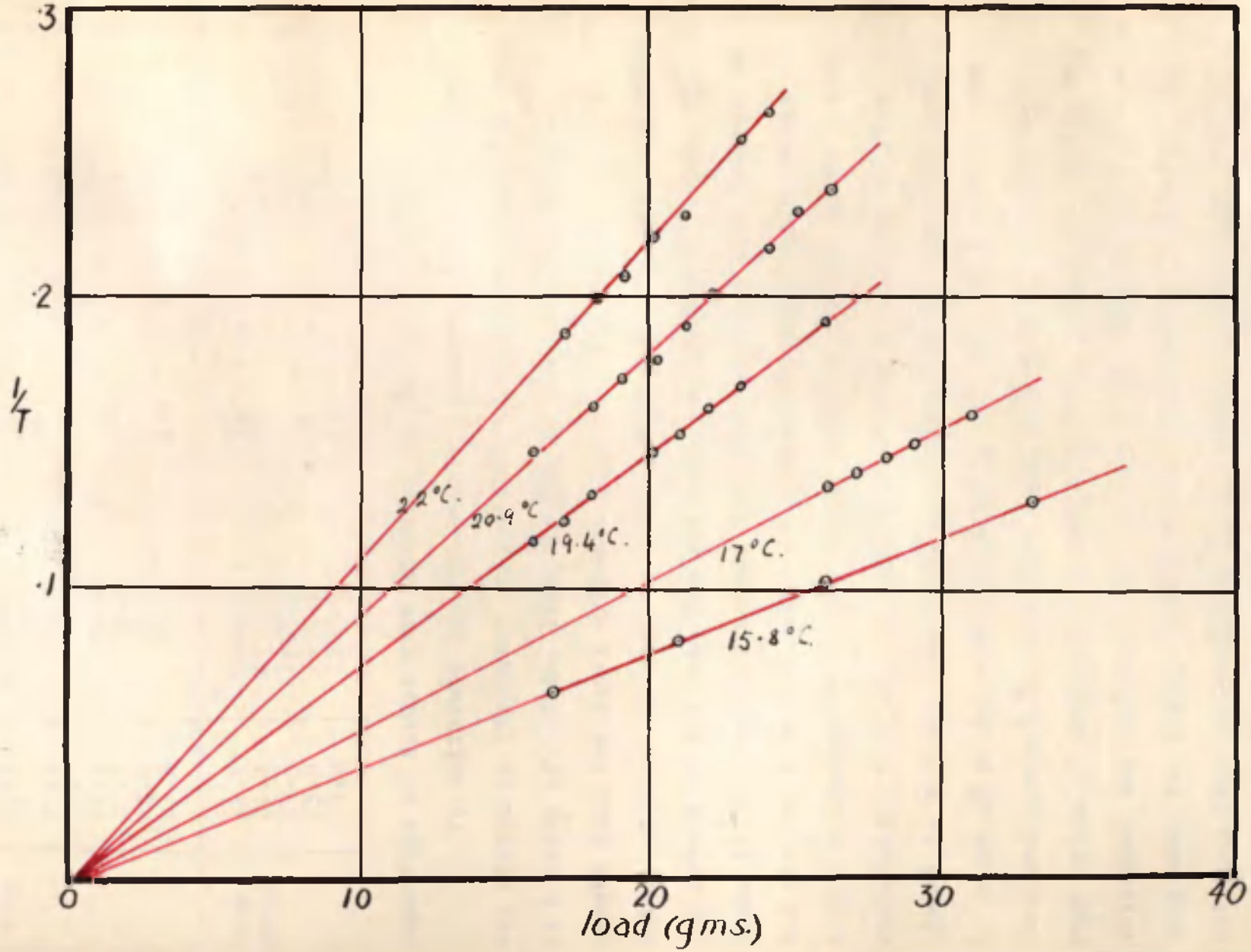

Fig. 39.

Liquid	Temp. C	Time of Fall secs.	Density	η (Poise)
Syrup sol.	20.0	136.0	1.4045	70,65
	20.5	126.2		65.56
	21.0	118.2	1.4039	61.41
	21.4	113.0		58.70
	22.1	103.7		53.90
	22.4	99.4		51.64
	22.9	94.0	1.4029	48.83
	24.0	82.6		42.90
	25.2	72.0	1.4021	37.40
Corn syrup	16.1	9900.0	1.44	5111
	20.4	4752.0	1.44	2453
	21.4	3967.0	1.44	2048
	23.0	3076.0	1.44	1588
	24.0	2598.0	1.44	1341

Densities of syrups were measured by the saccharimeter.

To calibrate the concentric cylinder apparatus syrup was placed in the outer cylindrical pot (4cm. dia. and 7.6 cm.) to a depth of 2.8 cm. from the top of the pot. The pot was raised till the inner cylinder (1.6 cm. dia. and 7 cm. long) which had been adjusted to rotate about its own axis, rested on the bottom of the pot. The pot was then lowered by .6 cm. By means of the centring screws the inner cylinder was centred in the pot. To keep the syrup at a constant temperature, water from a thermostat bath was pumped through a brass water jacket surrounding the pot. At each temperature various loads were placed in the pan, and times of rotation noted for each load by means of a stop watch reading to .01 sec. By plotting load in grams against $\frac{1}{T}$, straight line curves were obtained for each value of viscosity as shown in figs. 38 and 39. These all intersect the load axis at the same point showing that f remains constant. The factor (M-f)T in the equation $\eta = K(M-f)T$, is obtained from the gradient of the straight line curve for the particular viscosity coefficient, which is obtained from the viscosity-temperature curve. Hence K can be calculated. The results are shown in table X from which the mean value of K was found to be 20.8.

Table X

Lyle's Golden Syrup

Temperature 20.4°C.

Load (gms)	T(secs.)	$\frac{1}{T}$	(M-f)T	$K = \frac{77}{(M-f)T}$
4.1	6.5	.154		
5.1	5.05	.197		
6.1	4.1	.244		
7.1	3.6	.277		
8.1	3.1	.322		
9.1	2.8	.357	25.5	$K = \frac{530}{25.5}$
10.1	2.56	.39		
11.1	2.3	.435		
13.1	1.95	.51		$= 20.8$
16.1	1.55	.64		
18.1	1.4	.71		

Temperature 21.1°C.

5.1	4.5	.22		
6.1	3.7	.27		
7.1	3.2	.31		
8.1	2.8	.357		
9.1	2.45	.408	22.7	$K = \frac{475}{22.7}$
10.1	2.3	.435		
11.1	2.1	.46		
12.1	1.8	.55		$= 20.9$
16.1	1.55	.64		

Temperature 22°C.

3.1	6.7	.15		
4.1	5.0	.20		
5.1	4.0	.25		
6.1	3.3	.30		
7.1	2.85	.35	20.2	$K = \frac{420}{20.2}$
8.1	2.5	.40		
9.1	2.25	.44		
10.1	2.03	.49		$= 20.8$
11.1	1.8	.55		
13.1	1.6	.62		

Corn Syrup

Temperature 17°C

26.1	7.35	.136		
27.1	7.15	.140		
28.1	6.85	.146	195	$K = \frac{4169}{195}$
29.1	6.70	.150		
30.1	6.40	.156		$= 21.3$
31.1	6.20	.161		

Temperature 19.4°C

21.1	6.50	.154		
22.1	6.15	.163		
23.1	5.85	.171		
24.1	5.60	.178	140	$K = \frac{2884}{140}$
26.1	5.16	.193		
16.1	8.60	.116		
17.1	8.10	.123		$= 20,6$
18.1	7.50	.133		
20.1	6.75	.148		

Table X (cont,)

Temperature 15.8°C

Load (gms.)	T(secs.)	$\frac{1}{T}$	(M-f)T	$K = \frac{\eta}{(M-f)T}$
21.1	12.25	.082		
26.1	9.85	.101		
31.1	8.20	.122	250	$K = \frac{5248}{250}$
36.1	7.10	.140		
41.1	6.15	.162		
46.1	5.50	.181		$= 20.9$
51.1	4.85	.206		

Temperature 20.9°C

21.1	5.25	.190		
26.1	4.20	.238		
16.1	6.80	.147		
18.1	6.10	.164	110	$K = \frac{2240}{110}$
19.1	5.75	.174		
20.1	5.65	.177		
22.1	4.90	.204		$= 20.4$
24.1	4.55	.219		
25.1	4.30	.232		

Temperature 22°C

21.1	4.40	.227		
16.1	5.70	.175		
17.1	5.30	.189		
18.1	5.00	.200	90	$K = \frac{1862}{90}$
19.1	4.80	.208		
20.1	4.50	.222		
23.1	3.90	.256		$= 20.7$
24.1	3.75	.266		

The calibration factor K for the apparatus remained constant over a range from 400 to 5000 poise. PROCTER and DOUGLAS[45] found that the calibration factor for their apparatus remained constant for higher values of viscosity coefficients. They discussed results obtained by Washburn who found that the calibration factor varied with viscosity. Washburn, however, calibrated with sodium silicate water glass, and, probably skin formation on the surface of the glass upset his results.

Investigation into the Various Errors and their Magnitude in the Concentric Cylinder Method of Measuring Viscosity.

1. Relative Positions of the Outer and Inner Cylinders.

The apparatus was set up as before with Lyle's Golden Syrup at 20.4°C. The straight line curve yielding (M-f)T had already been obtained from the apparatus in its most accurate setting. The inner cylinder was immersed to the correct depth, and rotating about its own axis, but was set eccentric with the outer cylinder. The value of (M-f)T was obtained as before,

fig. 40

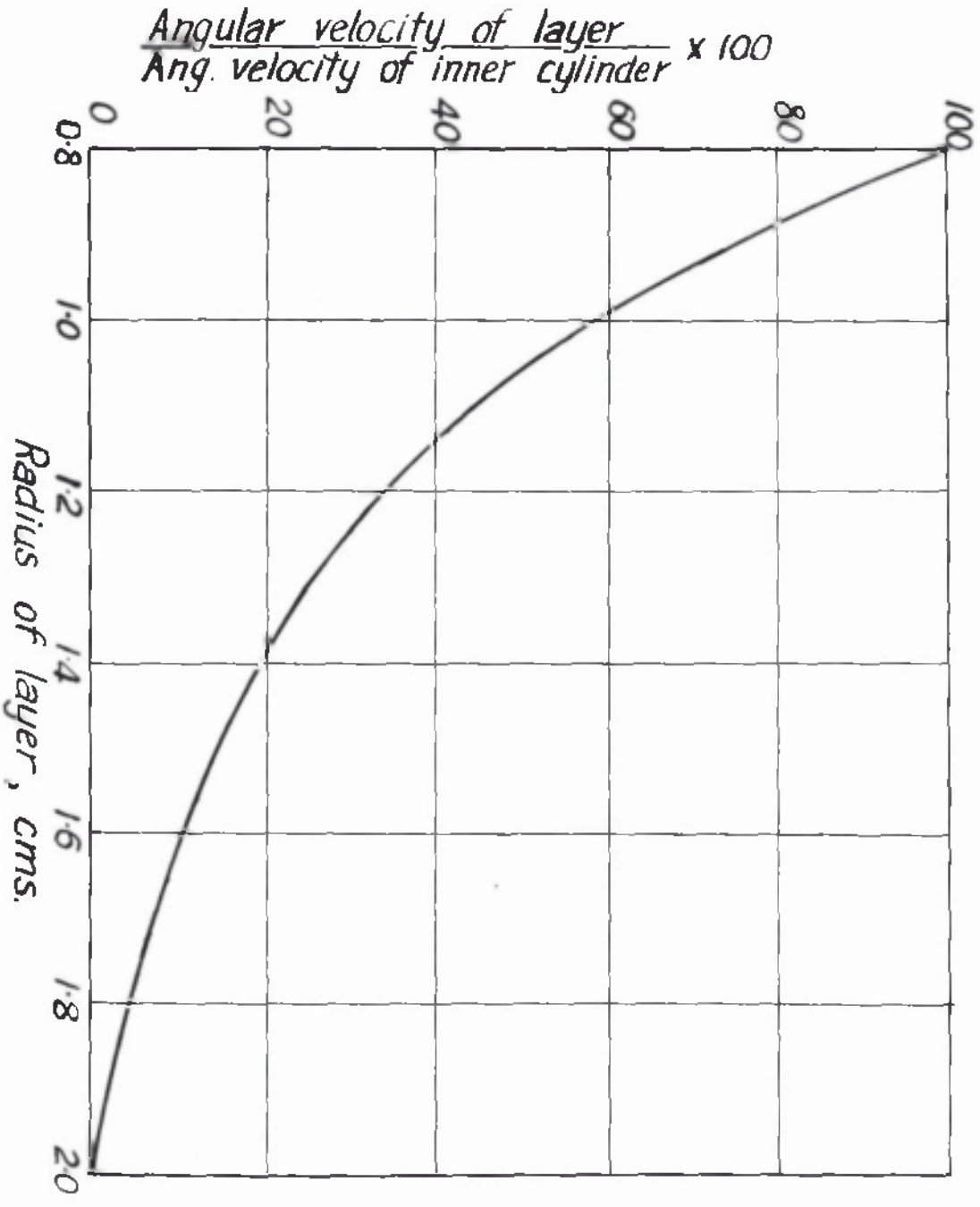
Angular velocity of layer / Ang. velocity of inner cylinder x 100
0
20
40
60
80
100
0·8
1·0
1·2
1·4
1·6
1·8
2·0
Radius of layer, cms.

fig. 41

and the differenee in the two values yielded a measure or the error.

Next the inner cylinder was set concentric with the outer cylinder, and rotating about its own axis, but was immersed too much. The value of (M-f)T obtained was compared with that of (M-f)T for the correct setting, and the percentage error worked out.

Thus, when the inner cylinder was set .4 cm. eccentric with the outer cylinder, the value of (M-f)T was 26.5. Hence the percentage error due to .4 cm. eccentricity is 4%. Since the accuracy of setting for the high temperature work is about .1 cm., the percentage error is about 1%.

When the inner cylinder was over immersed by .4 cm., the value of (M-f)T was 27, the error being about 6%. Since the immersion at high temperatures can be carried out to within .02 cm. the error is about .3%

The error due to the cylinder not rotating about its own axis was as follows:-

		% error
(M-f)T for accurate setting	25.5	0
" " .05 cm. eccentricity	26.2	2.75
" " .1 cm. "	27.0	5.9
" " .15 cm. "	30.2	18.4
" " .2 cm. "	34.8	36.4

The percentage error plotted against eccentricity is shown in fig. 40. This is the most serious source of error. However, with the previously described method of setting up the inner cylinder, eccentricity was not greater than .01 cm. Hence the error is less than .5% at high temperatures as seen from curve in fig. 40

2. Variation in the diameters of the Cylinders

Equation (1) may be written in the form

$$\frac{1}{T} = \frac{MgR}{8\pi^2 L\eta}\left(1/r_n^2 - \frac{1}{r_2^2}\right) \qquad \text{----------(6)}$$

where $1/T$ = angular velocity
r_n = radius of any given layer.

Fig. 41 gives the angular velocity of the liquid at any point between the cylinders as a percentage of that of the inner cylinder calculated by means of equation (6).

$$\% \text{ angular velocity of layer} = \frac{1/r_n^2 - 1/r_2^2}{1/r_1^2 - 1/r_2^2} \times 100$$

Examination of the curve in fig. 41 shows that an error of .005 cm. in the radius of the inner cylinder produces an error of 1% ; but since the inner cylinders were turned on the lathe, the accuracy was within .0015 cm. and so the error was about ± 0.3%. For the outer cylinder an error of .0015 cm. does not affect the accuracy.

3. Temperature Measurement.

Examination of the curve in fig. 41 shows that the velocity of the liquid at a distance of .1 cm. from the inner cylinder was about 24% less than the velocity of the inner cylinder, whereas the change in velocity over the same distance adjacent to the outer cylinder gave a change of velocity of about 2%. Hence for a given change in viscosity coefficient, the change of angular velocity is much greater for small values of r_n than for large. Therefore, the temperature of the inner layers was measured rather than the mean temperature of the liquid.

4. Level of liquid in container.

From equation (1) it follows that

$$1/T = K_1/L$$

Let correct L = 5 cm.

$$1/T = \frac{K_1}{5}$$

Let L_1 = 5.02 cm.

$$1/T_1 = \frac{K_1}{5.02}$$

% error due to .02 cm. error in the level of the liquid

$$= \pm \frac{K_1/5 - K_1/5.02}{K_1/5} \times 100 = \pm 0.4\ \%$$

5. Load could be measured to any required accuracy.

6. Speed of Rotation.

The theory for the concentric cylinder method of determining the viscosity coefficient of a liquid only holds when viscous flow is assumed. With speed of rotation of the inner cylinder exceeding a certain value, turbulent motion sets in, and equation $\eta = K(M-f)T$ is no longer valid. When load is plotted against 1/T, the straight line curve obtained

indicates true viscous flow, but, as soon as a certain load is exceeded, the occurrence of turbulent motion is shown by a departure from the straight line curve. However, the value of (M-f)T was in all cases calculated from the straight part of this curve.

7. Friction.

Provided the apparatus was kept clean and free from dust, the friction force remained small and constant. This is shown by the straight line curves obtained by plotting load against 1/T to the same point on the load axis.

8. Expansion of Cylinders.

Since the calibration factor was obtained with the cylinders at room temperature, an error is introduced at high temperatures due to the expansion of the cylinders. The radius of the inner cylinder at 1200°C can be calculated from the following equation:-

$$l_t = l_o(1+\alpha 1200)$$

where l_t = radius in cm. at 1200°C
l_o = radius in cm. at room temperature
α = mean coefficient of expansion of alundum.

$$l_t = .8(1+ 8\times10^{-6} \times 1200)$$

$$= .8077$$

Increase in radius of inner cylinder = .0077 cm.
Similarly, increase in radius of outer cylinder = .019 cm.

Error introduced in viscosity determinations at 1200°C = ±2.3 %

Errors are summarised as follow:-

	% error
Eccentricity of cylinder and pot	± 1
Immersion of inner cylinder	± 0.3
Eccentricity of inner cylinder	± 0.5
Dimensions of inner cylinder	± 0.3
Level of liquid in pot	± 0.4
Error due to expansion of cylinders at 1200°C	± 2.3

The error due to expansion of the cylinders does not affect the reproducibility of the results when the cylinders for a particular value of calibration constant always consist of the same material. The reproducibility of results is within ±2.5%.

Determination of the Viscosity-Temperature Curves for Two Silicate Glasses and Comparison of Results with those of other Workers.

Since the ultimate aim of this research was to measure the viscosity of synthetic slags of the open hearth and blast furnace type at temperatures up to 1650°C., it was considered desirable to experiment with glass up to temperatures of about 1200°C., for which the results of investigation by various workers were fairly well established. Hence, a check on the accuracy of the method would be obtained, and, at the same time, the technique developed before attempting to obtain results at 1650°C.

The following glasses were selected:-

	SiO_2	Na_2O	CaO	MgO	Fe_2O_3	Al_2O_3	
1)	73	19.4	6.9	.2		.4	per cent
2)	74.05	25.34	.21	-	.14	.24	per cent

Preparation of Glass

1) The following mixture was placed in a salamander pot and heated in a gas fired furnace up to 1400°C.

219	gm.	SiO_2
99.39	"	Na_2CO_3
35.96	"	$CaCO_3$
.6	"	MgO
1.2	"	Al_2O_3
.54	"	FeO

After melting, the glass was cast into slabs, crushed and powdered. This process was repeated twice, when the glass was ready for the viscosity determinations.

2) This glass was prepared in a similar fashion.

The materials used in the preparation of the glass had been previously analysed and found to be pure.

Determination of the Viscosity of Glass.

The apparatus employed was the same as described previously except that the furnace employed had a Kanthal wound element which avoided the necessity of an inert atmosphere. The cylindrical pot and the inner cylinder were of the hard-baked alundum type.

Relevant data are as follow:-

Internal diameter of pot---- 4.0 cm.
Internal height of pot------ 7.6 cm.
Diameter of cylinder-------- 1.6 cm.
Length of cylinder---------- 7.0 cm.

Height of glass in pot--------- 4.8 cm.
before immersion of
cylinder.

Depth of glass from top
of pot---------- 2.8 cm.

Calibration Constant----------20.8

The pot contained crushed glass, which on melting, would give less than the required height of 4.8 cm. It was placed in the furnace, resting on an alundum stool in the hot zone of the furnace, being held in position by alundum wedges. The temperature of the furnace was then raised to 1200°C., and the level of the glass checked by the depth gauge. Glass in the form of short rods was added and allowed to melt completely before a further check was made. After the correct level of glass had been obtained, the inner cylinder and rod were coupled to the spindle and adjusted in alignment with the axis thereof. The free running of the rotating system was then checked and proved to be satisfactory by taking the times of rotation in air under the action of small loads. The furnace was raised until the inner cylinder rested on the bottom of the outer pot when the furnace was lowered by .6 cm. By means of the centering screws, the inner cylinder was made concentric with the outer cylinder. The furnace top was almost completely closed by an alundum collar which just allowed the alundum rod freedom of rotation. A uniform temperature could thus be attained in the hot zone of the furnace.

Temperature Measurement. Two chromel-alumel thermocouples were used. One passed down the inside of the alundum rod into the cylinder, while the other was attached to the outside of the outer pot. It was possible, therefore, to measure the uniformity of temperature throughout the glass and to measure the temperature of the inner layers of the glass accurately.

The temperature was maintained constant at 1200°C for about two hours to ensure the complete removal of bubbles from the glass, after which a series of readings was begun. Before each reading, the furnace temperature was kept constant, until the whole of the glass had reached a uniform temperature as

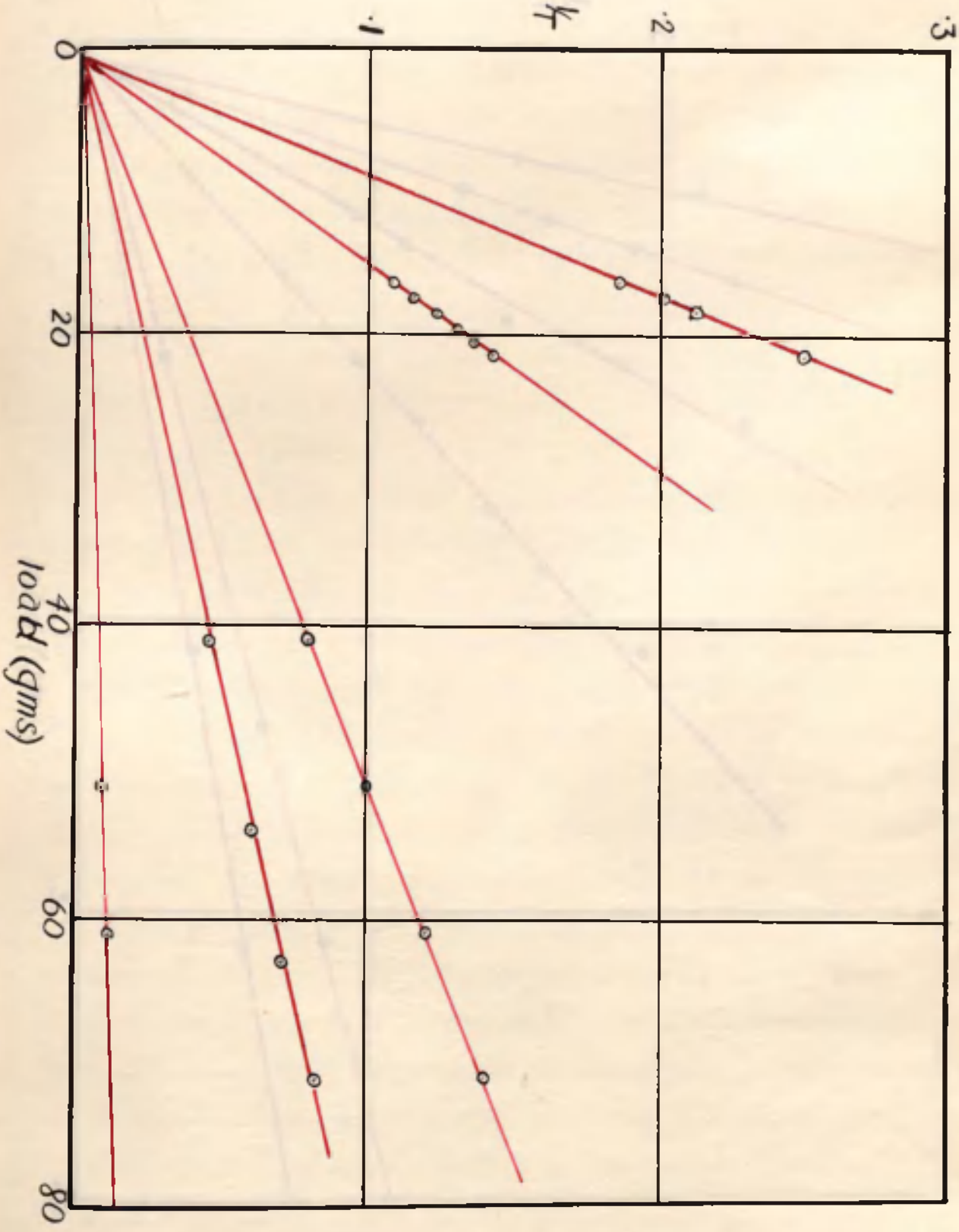

fig. 42.

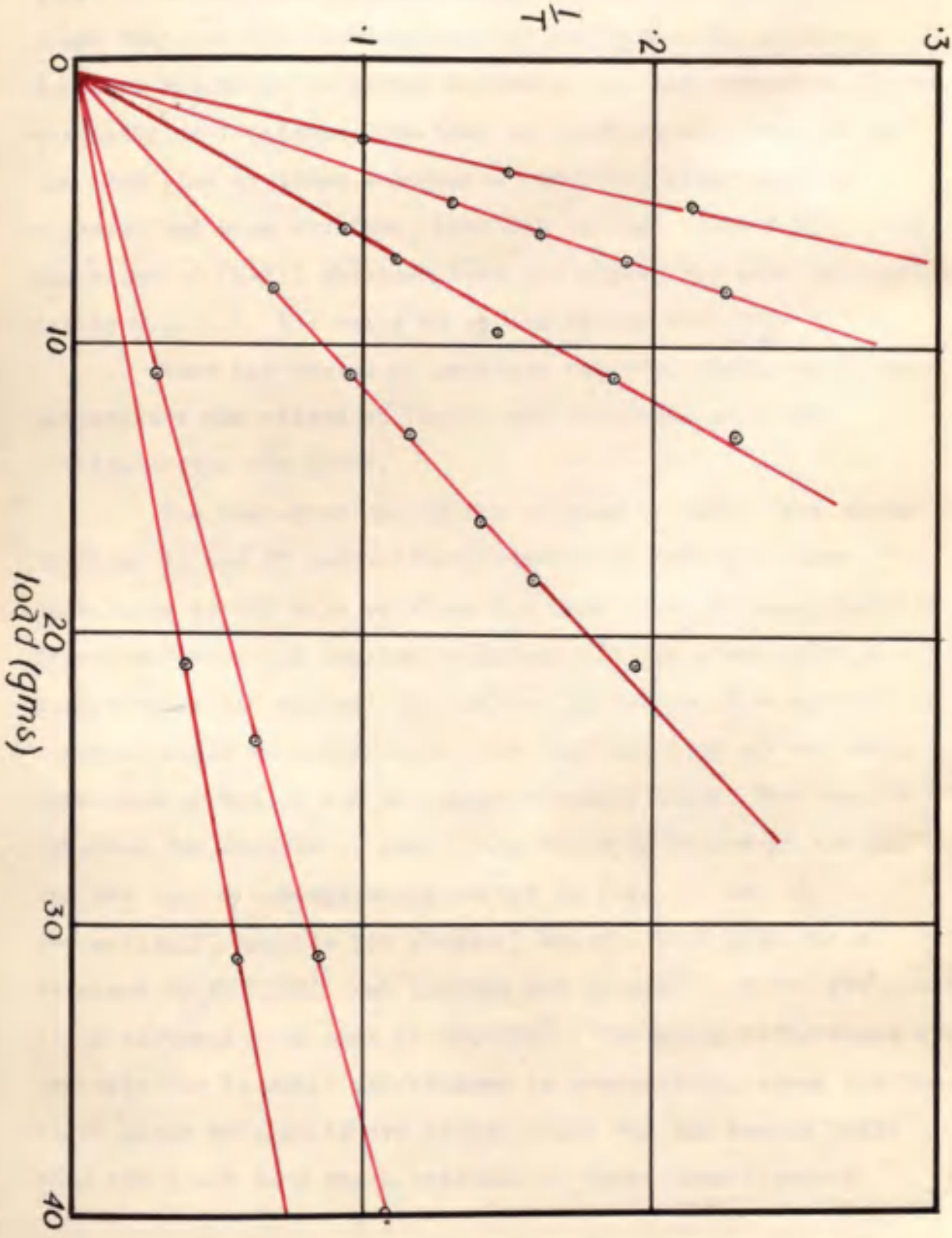

fig. 43.

indicated by similar readings of the two thermocouples. The times of rotation of the inner cylinder under different loads were measured to .01 second for each temperature. By measuring times of successive rotations under a constant load, it was found that one rotation was usually sufficient to produce a constant velocity. At higher temperatures, and therefore, lower viscosity coefficients, the time of rotation was recorded as the mean time of three successive rotations after constant velocity had been attained. Lead was plotted against 1/T, and the value of (M-f)T obtained from the curve, for each temperature. Taking K = 20.8, the value of η was calculated.

When the series of readings was completed, the furnace temperature was raised to 1200°C and the inner cylinder withdrawn from the glass.

The load-time graphs for glasses 1) and 2) are shown in figs. 42 and 43 respectively. These are straight lines converging to the same point on the load axis, showing that the friction factor had remained constant. If the glass at high temperatures did not wet the alundum cylinders, the calibration constant would no longer hold. But the load-time graphs would have been irregular and no longer straight lines. The results obtained for glasses 1) and 2) are shown in tables XI and XII and the log. η -temperature curves in figs. 44 and 45 respectively. Results for glass 1) are compared with those obtained by ENGLISH[31] and PROCTER and DOUGLAS[45]. Curve for glass 2) is compared with that by ENGLISH[31]. The small differences are probably due to small differences in composition, since for the first glass my results are higher while for the second glass they are lower than those obtained by these investigators.

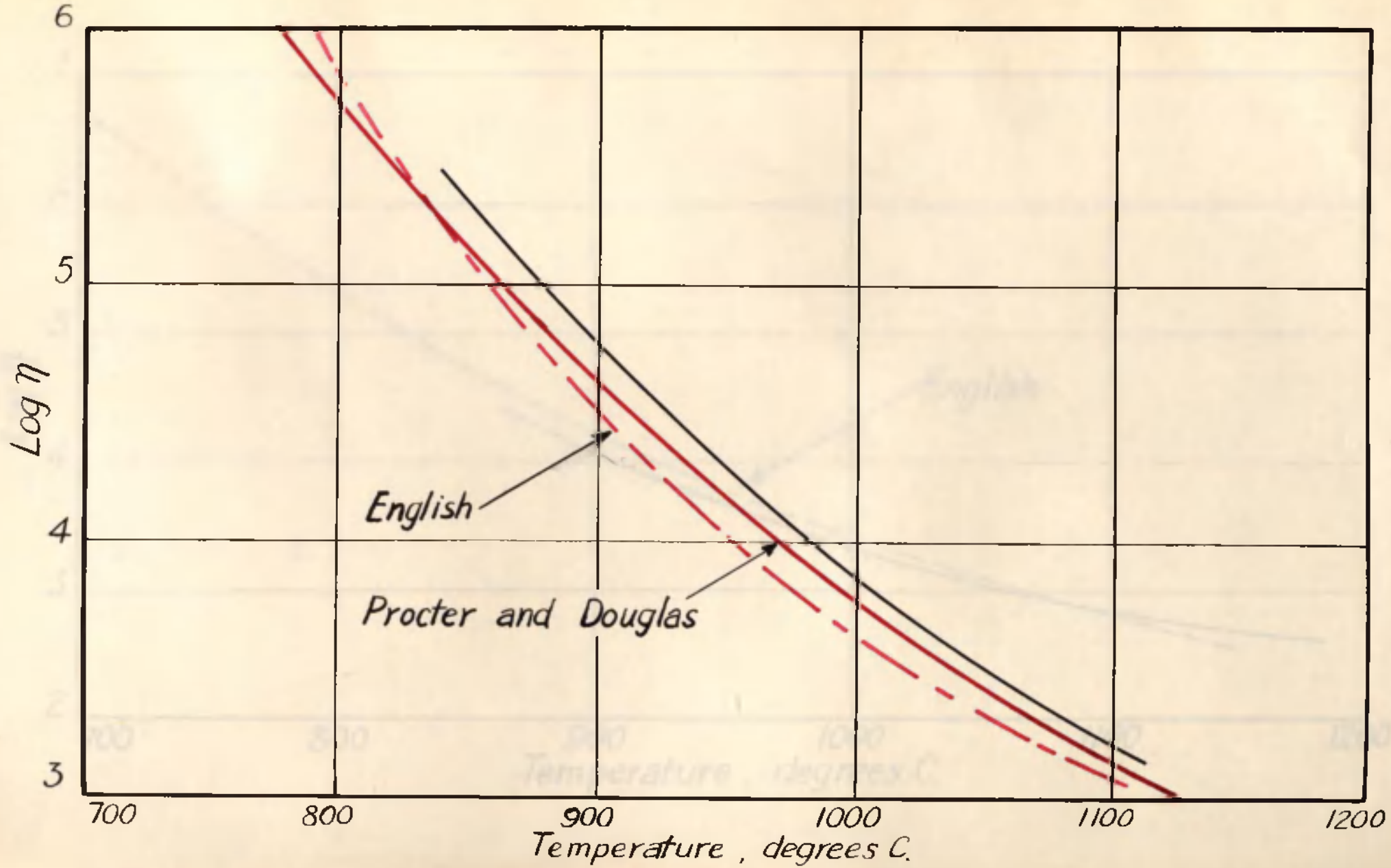
6
5
4
3
Log η
English
Procter and Douglas
700
800
900
1000
1100
1200
Temperature , degrees C.

fig. 44.

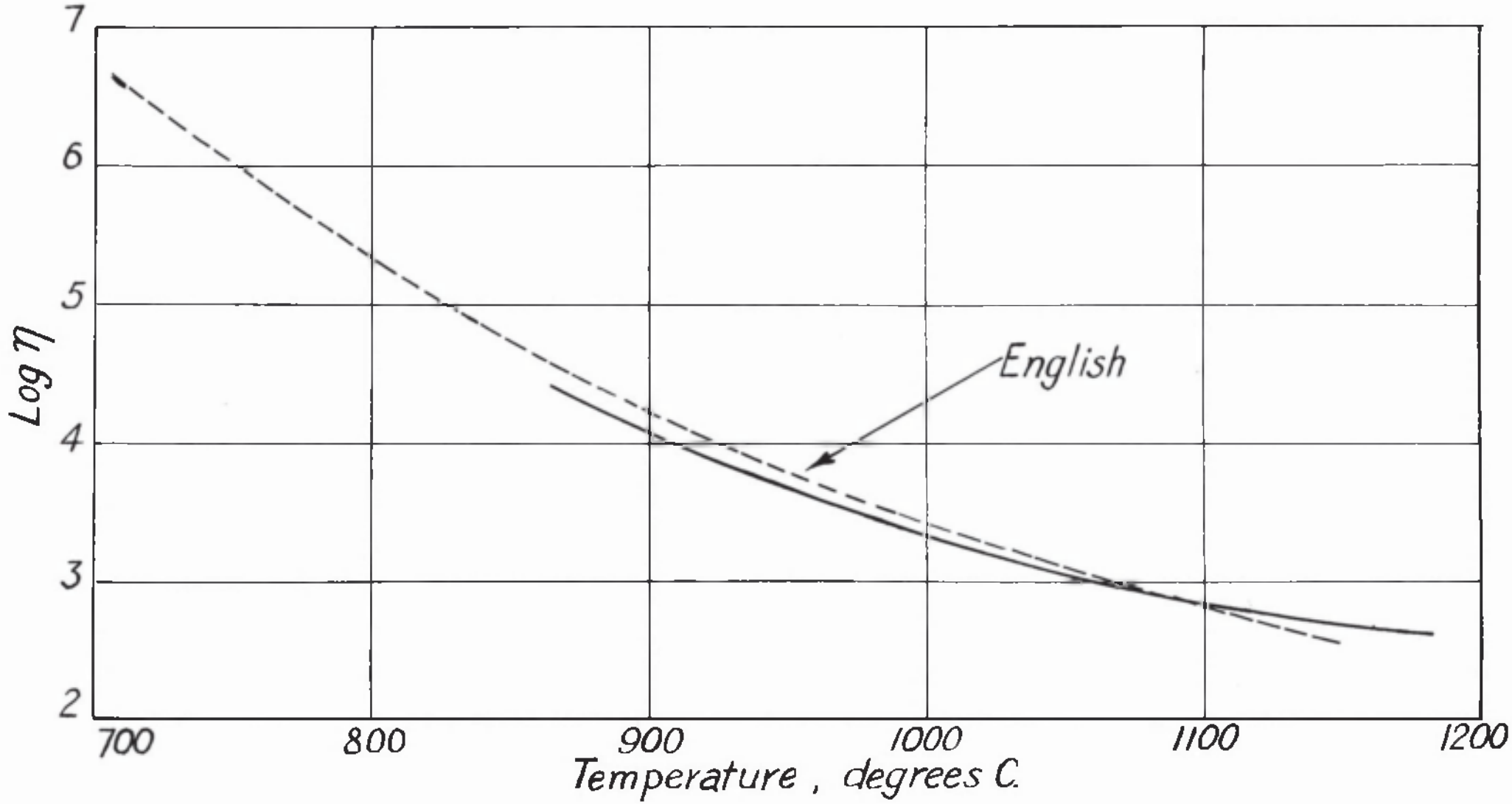
7
6
5
4
3
2
Log η
English
700
800
900
1000
1100
1200
Temperature , degrees C.

fig. 45.

Table XI

Temp. °C.	Load (gms)	T(secs)	$\frac{1}{T}$	(M-f)T	(Poise)	$\log_{10}\eta$
1100	16.1 17.1 18.1 21.1	5.3 4.95 4.7 4.0	.188 .202 .213 .25	84	1.747×10^3	3.242
1050	16.1 17.1 18.1 19.1 21.1	9.2 8.6 8.0 7.6 6.95	.108 .116 .125 .131 .144	145	3.016×10^3	3.479
980	41.1 51.1 61.1 71.1	12.5 10.0 8.4 7.1	.08 .10 .12 .14	508	1.056×10^4	4.023
950	41.1 54.1 63.1 71.1 101.1	22.0 16.5 14.3 12.6 8.8	.045 .081 .07 .079 .113	896	1.863×10^4	4.270
860	51.1 61.1 101.1	135.0 112.7 68.0	.0074 .009 .015	6865	1.427×10^5	5.154

Table XII

1130	3.1 4.1 5.1 7.1	9.90 6.50 4.60 3.05	.101 .15 .215 .325	25	5.20×10^2	2.716
1085	5.1 6.1 7.1 8.1 10.1	7.65 6.15 5.20 4.45 3.50	.131 .162 .192 .225 .298	35.8	7.44×10^2	2.871
1050	6.1 7.1 9.1 11.1 13.1	10.50 8.80 6.75 5.30 4.35	.095 .113 .148 .188 .230	59.3	1.233×10^3	3.091
990	8.1 11.1 13.1 16.1 18.1 21.1	14.00 10.35 8.60 6.95 6.20 5.15	.07 .046 .116 .14 .16 .19	108	2.246×10^3	3.351
920	11.1 31.1 41.1 51.1	34.30 11.80 8.90 7.10	.03 .085 .112 .140	365	7.592×10^3	3.880
900	21.1 31.1 51.1 61.1	24.00 16.20 9.75 8.10	.041 .062 .102 .123	500	1.04×10^4	4.017
880	61.1	12.40		750	1.56×10^4	4.193

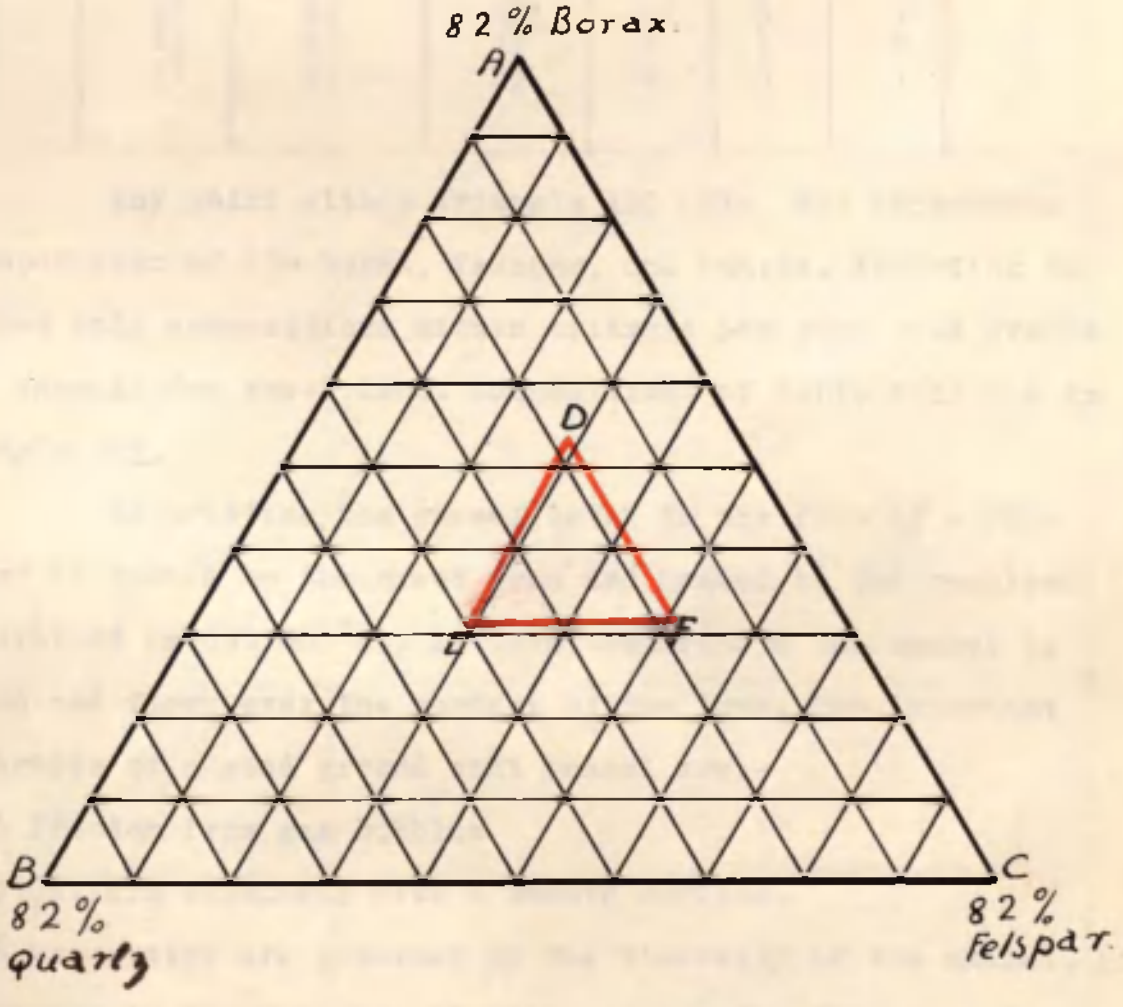

fig. 46.

The Effect of Composition on the Viscosity of Ground Coat Enamels.

The ground coat enamels employed in the dry process of enamelling iron are of a glassy nature. In composition they are somewhat similar to glass. Andrews in his book "Enamels" gives some recipes for ground coats in the dry process of enamelling sheet iron. These are shown in table XIII.

Table XIII
Percentage Composition

Enamel	Borax	Felspar	Quartz	$NaNO_3$	CaF_2	Na_2O	$CoO + MnO_2$
1	37	25	20	4	5	7	2
2	37	30	15	4	5	7	2
3	32	25	25	4	5	7	2
4	32	30	20	4	5	7	2
5	32	35	15	4	5	7	2
6	27	30	25	4	5	7	2
7	27	35	20	4	5	7	2

Any point within triangle ABC (fig. 46) represents a composition of 82% borax, felspar, and quartz. According to Andrews only compositions within triangle DEF give good ground coat enamels for sheet iron. Compositions of table XIII lie in triangle DEF.

In practice, the enamel batch in the form of a fine powder is dusted on the sheet iron and heated to the required temperature (about 800°C). At this temperature the enamel is molten and flows over the surface of the iron. Two important properties of a good ground coat enamel are:-

a) Freedom from gas bubbles

b) Uniform thickness with a smooth surface.

These properties are governed by the viscosity of the enamel. If the enamel is too viscous, it will not readily flow over the sheet iron and on cooling a ground coat with a wavy surface will be obtained. According to Stoke's Law, the rate of rise of a gas bubble through a liquid is inversely proportional to the coefficient of viscosity of the liquid. An enamel which is too viscous at the temperature of firing will tend to retain its gas bubbles. Where the bubbles burst at the surface, irregularities are produced and a smooth surface can only be obtained when the enamel flows readily.

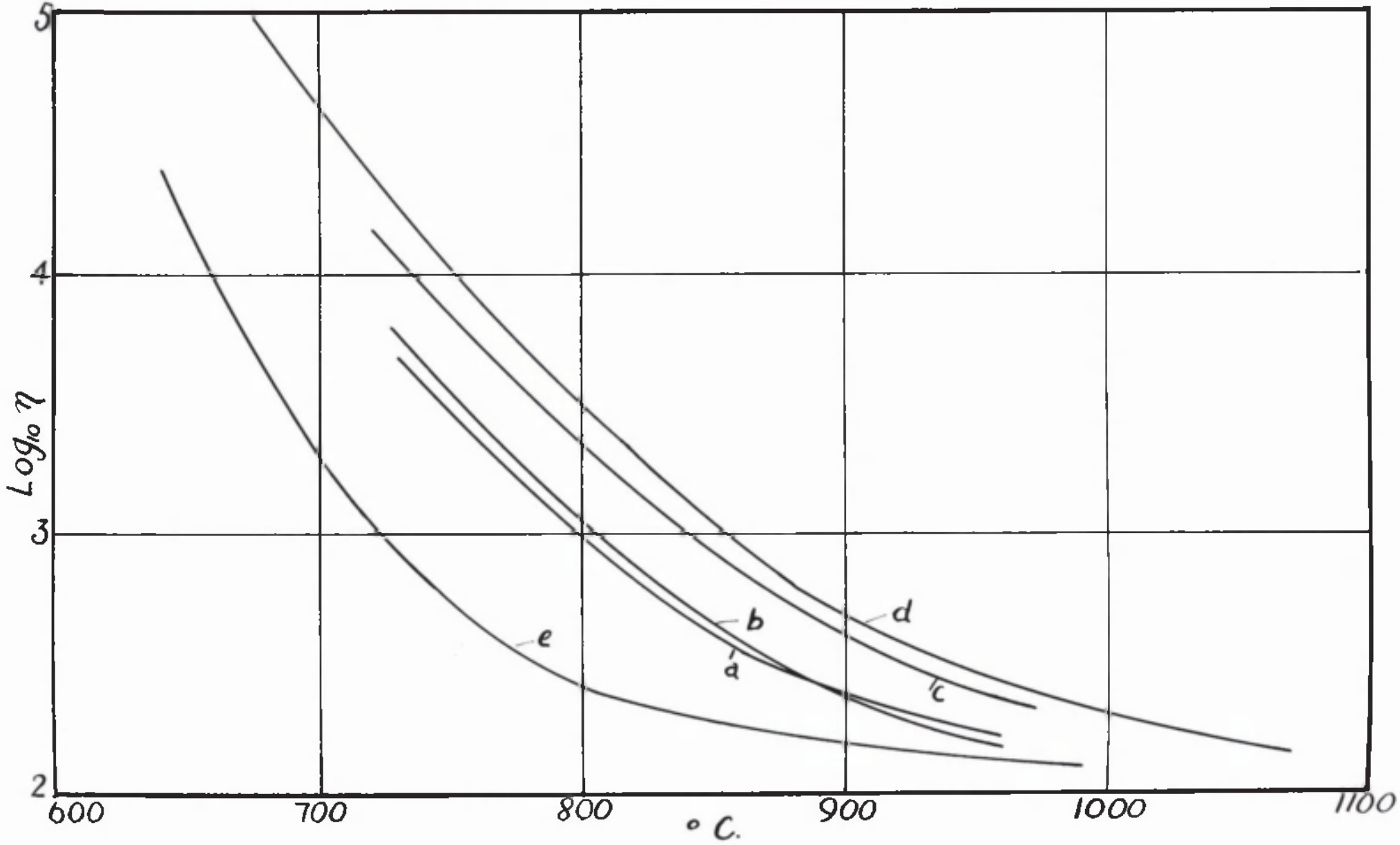

fig. 47.

However, when the enamel is not sufficiently viscous it flows too easily and devitrification may also occur.

Quantitative data on the effect of composition on the viscosity of ground coat enamels are not available and since such information would be useful to the industry, an investigation was undertaken. At the same time more experience of the method would be acquired before proceeding to the work on slags at higher temperatures. The compositions of the enamels investigated are given in table XIV.

Table XIV

Enamel	Percentage Composition							
	Borax	Felspar	Quartz	$NaNO_3$	CaF_2	Na_2O	$CoO + MnO_2$	Fe_2O_3
(a)	37	25	20	4	5	7	2	-
(b)	37	30	15	4	5	7	2	-
(c)	32	25	25	4	5	7	2	-
(d)	27	30	25	4	5	7	2	-
(e)	47	15	20	4	5	7	2	-
(f)	25.7	28.5	23.8	3.8	4.8	6.6	1.8	5

Preparation enamel.

The mixture of the constituents in the correct proportion (see table XIV) was placed in a salamander pot and heated in a gas fired furnace to 1000°C. After melting, the enamel was cast into slabs, crushed and powdered.

Determination of viscosity of enamel.

The viscosity-temperatures for these enamels were obtained with the same technique and apparatus as for glass. New cylinders were employed for each enamel. Results are given in table XV and $\log\eta$-temperature curves in fig. 47.

Table XV.

Enamel	Viscosity-Temperature Results		
	°C	(M-f)T	η (Poise)
a	960	8.4	175
	905	12	249.6
	880	13.6	284
	845	21	437
	820	36.5	759
	795	55	1144
	755	127	2641
b	960	8	166.4
	905	11	229
	880	15	312
	820	37.7	784
	795	60	1248
	755	144	2995
	730	335	6968
c	960	11.5	239
	905	20.4	424
	880	25.3	526
	835	61	1269
	795	99	2059
d	1070	7	145.6
	1040	8.4	174.7
	970	12.6	262
	880	28.3	589
	825	90	1872
	820	98	2038
	785	197	4097
	750	496	1.031×10^4
	700	1989	4.137×10^4
	670	6328	1.316×10^5
	640	13260	2.758×10^5
e	980	6.2	129
	940	7.2	150
	905	7.7	160
	865	8.4	175
	800	12.8	266
	705	86.2	1793
	690	155	3224
	665	366	7612
f	990	13.7	285
	885	30	624
	855	52.3	1088
	820	98.2	2042
	770	255	5304
	725	1170	2.434×10^4

Discussion of Results.

The feature of the logη-temperature curves is that with decreasing borax there is an increase in viscosity coefficient at all temperatures in the range examined. The logη - temperature curves of enamels a) and b) are very similar. Enamel b) has 5% more felspar and 5% less quartz than a), but since felspar has the composition $KoO.Al_2O_3.6SiO_2$, the difference in molecular compostion is small. It would appear that for a constant borax, and hence constant quartz + felspar content, small variations of felspar and quartz have little effect on the viscosity. The relative viscosities of the enamels at 800°C are shown in table XVI.

Table XVI

Enamel	$\frac{\eta \text{ of enamel at } 800^\circ C.}{\eta \text{ of enamel a at } 800^\circ C}$
a	1
c	2.24
d	3.16
e	.266

It is obvious that unless there is close control of the composition of the enamel batch, marked variations in the viscosity of the enamel would occur.

Enamel e) was made up by adding 5 gm. Fe_2O_3 to 100 gms. enamel d). In the range examined enamels d) and e) have the same viscosity-temperature curves.

The enamel in contact with iron may dissolve some iron oxide. However, 5% Fe_2O_3 does not appear to affect the viscosity.

The Apparatus for measuring the Viscosity Coefficients of Slags at High Temperatures.

When the work was begun on $CaO-SiO_2$ mixtures, it was soon evident that these slags were too fluid at temperatures about 1600°C to have their viscosity coefficients accurately measured by the concentric cylinder apparatus as used for glass. Using cylinders of fused alumina, an $MnO-SiO_2$ slag was also found to be very fluid even at 1200°C. Hence the first step was to consider how to modify the apparatus to measure lower coefficients of viscosity.

English, in a contribution to a paper by PROCTER and DOUGLAS[45], has suggested that the lowest viscosity coefficient which can be measured accurately in a concentric cylinder apparatus of this type is 1000 Poise. In the apparatus for glass, K was 20.8. Hence, for a liquid say with a viscosity coefficient of 10 Poise, (M-f)T would be .48. Even with a small load, the angular velocity of the inner cylinder would not be proportional to the load because of turbulent motion. The load-$\frac{1}{T}$ graph would be irregular. Also the error due to small variations in the friction factor f would be very great. However, it is obvious that by decreasing K the value of (M-f)T is increased for a given value of viscosity coefficient. Hence, by decreasing K, the lower limit of viscosity coefficient which can be determined is decreased.

From a study of the equations

$$\eta = \frac{g M R T (r_2^2 - r_1^2)}{8 \pi^2 L r_1^2 r_2^2} \qquad \text{----------(1)}$$

$$= K(M-f)T \qquad \text{----------(2)}$$

it follows that there are four methods of lowering K:-

1. By increasing r_1 and r_2
2. By decreasing $(r_2 - r_1)$
3. By increasing L
4. By decreasing R

It can be shown that by taking cylinders of large diameters- say outer cylinder 11 cms. and inner cylinder 9 cms., the value of K becomes very small. The value of (M-f)T would be greatly increased for any given viscosity coefficient. Hence, for small viscosity coefficients, the smaller K is the greater (M-f)T, and hence, for a given load the greater is T. Since T is greater, it can be measured with greater accuracy and the possibility of turbulent motion is reduced. COUETTE[34] employed cylinders of large diameter in his concentric cylinder apparatus when successfully measuring the low coefficients of viscosity of water at various temperatures. In the apparatus herein described, the diameters of the cylinders were limited by the diameter of the furnace tube.

To give a temperature of 1650°C the greatest possible diameter was 3 inches and hence the greatest possible diameter of the outer cylinder was about 6 cms. The depth of immersion was limited by the length of the hot zone of the furnace, which was about 4 inches. The most suitable depth, therefore, was that already employed. The diameter of the pulley wheel could be made any suitable size.

Experimental Determination of the Calibration Constants for Various Cylinders of Suitable Dimensions.

(a) Outer cylinder — Inner cylinder

Internal Dia. = 4 cm. — Diameter = 2.4 cm.
Internal ht. = 7.6 cm. — Height = 7 cm.
Depth of immersion of inner cylinder = 5 cm.
Distance between ends of cylinders = .6 cm.
Diameter of pulley wheel = 6 ins.

Liquid	Temp. °C	(Poise)	(M-f)T	$K = \frac{\eta}{(M-f)T}$
Syrup	21.0	487.7	84.7	5.75
"	23.2	354.6	61.7	5.75
"	24.0	325.5	56.6	5.75

(b) Outer cylinder — Inner cylinder

Internal dia. = 6 cm. — Diameter = 5 cm.
Internal ht. = 7.6 cm. — Height = 7 cm.
Depth of immersion of inner cylinder = 5 cm.
Distance between ends of cylinders = .6 cm.
Diameter of pulley wheel = 6 ins.

Liquid	Temp. °C	(Poise)	(M-f)T	$K = \frac{\eta}{(M-f)T}$
Glycerine	20.0	10.4	17.5	.594
"	21.5	9.0	15.9	.566
"	18.5	11.8	19.2	.610
Syrup sol.	20.0	71.0	125.3	.566
" "	21.0	61.5	111.4	.552
" "	22.0	54.5	97.7	.557
" "	23.0	48.5	90.0	.540

(c) Outer cylinder — Inner cylinder

Internal dia. = 5 cm. — Diameter = 3 cm.
Internal ht. = 7.6 cm. — Height = 7 cm.
Height of liquid in pot before immersion of inner cylinder = 4.2 cm.
Distance between ends of cylinders = .6 cm.
Diameter of pulley wheel = 1 in.

Liquid	Temp. °C	(Poise)	(M-f)T	$K = \frac{\eta}{(M-f)T}$
Castor Oil	17	12.60	35.4	.355
Glycerine	15	16.10	46.3	.347
Syrup sol.	25.2	37.40	110.0	.340
Syrup sol.	22.9	48.83	141.5	.345
Syrup sol.	21.0	61.41	179.0	.343
Syrup sol.	20.0	70.65	204.7	.345

Mean K = .345

The calibrations were carried out as for the apparatus used for measuring the viscosity of glass. Brass cylinders were used for (a) and (b) and graphite cylinders for (c).

With cylinders as in (b) and pulley wheel 1 inch in diameter, low viscosity coefficients could be measured. However, since small variations in the relative positions of the cylinders would introduce large errors, these dimensions are not suitable for high temperature work.

The apparatus as for (c) appeared to be most suitable. With the accuracy of adjustment, the experimental error is small as shown by the fact that K remains constant from 12 poise to 70 poise. The outer cylinder just fitted into the furnace tube. As previously described, these cylinders could be accurately turned on the lathe from electrographite carbon rods of low ash content. It was, therefore, decided to experiment with a blast furnace slag to find if this apparatus would be suitable for measuring the viscosity of synthetic blast furnace slags.

Determination of the Viscosity-Temperature Curve for a Blast Furnace Slag.

% Composition of Slag

CaC	SiO_2	Al_2O_3	Fe_2O_3	MnO	MgO	S
46.58	30.3	18.5	-	.85	2.64	1.44

Experimental Details.

Relevant data are as follow:-

Internal diameter of graphite pot---------- 5 cm.
Internal height of pot---------- 7.6 cm.
Diameter of graphite cylinder---------- 3.0 cm.
Length of cylinder---------- 7.0 cm.
Height of slag in pot before immersion of cylinder-------- 4.2 cm.
Distance between ends of cylinders---------- 0.6 cm.

The pot contained powdered slag which, on melting, would give less than the required height of 4.2 cm. It was placed in the molybdenum furnace, resting on an alundum stool in the hot zone of the furnace, being held in position by alundum wedges. The temperature of the furnace was then raised to about 1600°C., and small pieces of slag added until the correct depth of slag was obtained as shown by the depth gauge.The inner cylinder and rod were then coupled to the spindle and adjusted in alignment. The furnace was then raised until the inner cylinder rested on the bottom of the pot when the furnace was lowered by .6 cm. The inner cylinder was made concentric with the outer cylinder by means of the centering screws. The furnace top was then almost completely closed by an alundum collar which just allowed the graphite connecting rod freedom of rotation. A uniform temperature could thus be attained in the hot zone of the furnace.

Temperature was measured by a tungsten-molybdenum thermocouple whose hot junction was just above the surface of the slag. The temperature was kept constant at 1600°C for about two hours, after which a series of readings was begun. Before each reading the temperature of the slag was kept constant for 15 to 30 mins.

The times of rotation of the inner cylinder under different loads were measured to .01 second by means of a stop-watch for each temperature. For each load, times of successive rotations were measured, the time of rotation being noted after constant velocity had been attained. For the lower viscosity coefficients, the time of rotation was recorded as the mean time of three successive rotations. Load was plotted against $\frac{1}{T}$, and the value of (M-f)T obtained from the straight line curve. Taking K = .345, the value of η was calculated.

When the series of readings was completed at about 1400°C, the temperature was raised to 1600°C before the inner cylinder was withdrawn from the slag.

The load-reciprocal time graphs were straight lines converging to the same point on the load axis for all

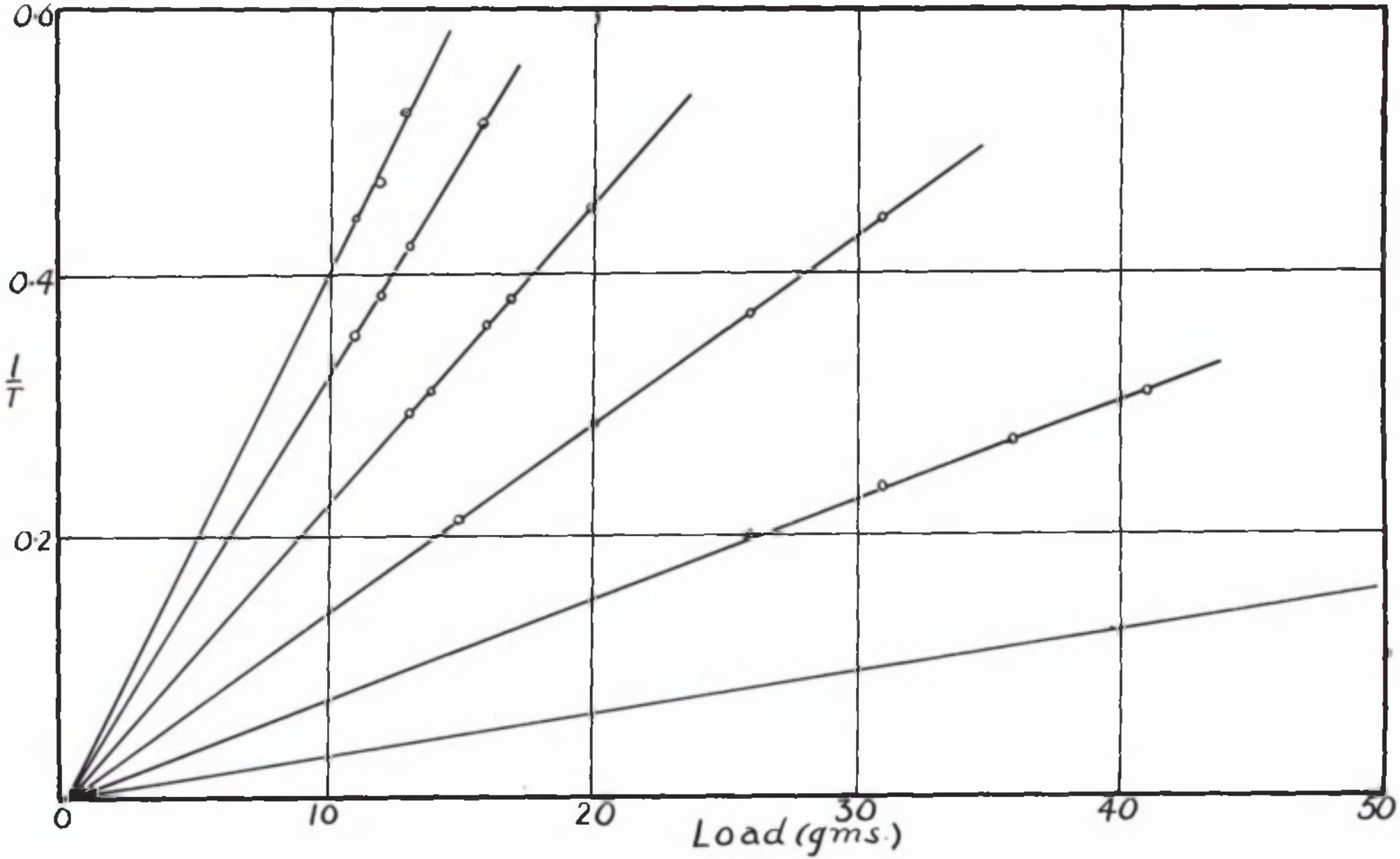

fig. 48.

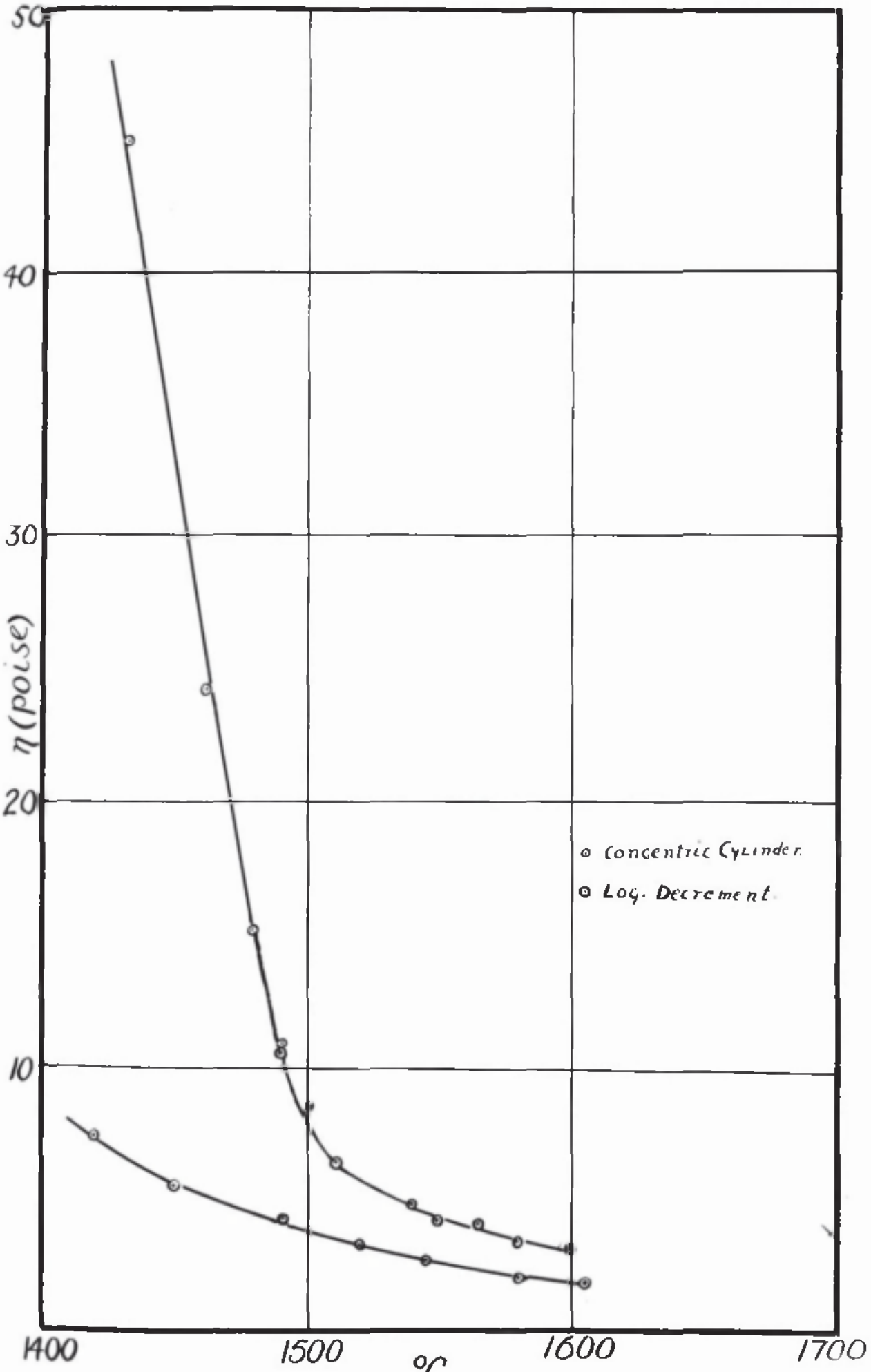
50
40
30
20
10
η (poise)
o Concentric Cylinder
o Log. Decrement
1400
1500
1600
1700
°C.

fig. 49

readings up to 1500°C. At higher temperatures the viscosity coefficients are less than 8 poise and the load-$\frac{1}{T}$ graphs were irregular. Hence the lower limit of viscosity coefficients which could be accurately determined with this apparatus was about 8 poise. The results obtained are shown in table XVII. The load-$\frac{1}{T}$ graphs and viscosity-temperature curve are shown in figs. 48 and 49 respectively. Results obtained by the logarithmic decrement method to be described are plotted in fig. 49. Examination of these curves provide further evidence that 8 poise is the lower limit of the concentric cylinder method. For viscosity coefficients greater than 8 poise these two methods give identical results, but below 8 poise the results obtained by the concentric cylinder method are higher than those obtained by the logarithmic decrement method.

Table XVII

Temp. °C	(M-f)T	η = .345(M-f)T (Poise)
1530	21.4	7.4
1500	24.6	8.5
1490	31.0	10.7
1480	44.0	15.2
1460	70.0	24.2
1430	130.0	45.0
1400	310.0	107.0

The Logarithmic Decrement Method.

The lower limit achieved by making alterations in the apparatus was only about 8 poise, and hence, it was decided to apply a logarithmic decrement method in an attempt to measure lower viscosities which occur in slags. The apparatus should be capable of measuring viscosity coefficients from less than 1 poise to about 15 poise so that the range would overlap with that of the concentric cylinder method. It was also desired that the method employed would not require many changes in the furnace etc. as used in the concentric cylinder method.

Two types of logarithmic decrement methods have been used:-

1) The viscosity coefficient is calculated from the logarithmic decrement of a horizontal circular disc suspended by its middle point and undergoing torsional oscillations in its own plane in the liquid.

2) The viscosity coefficient is calculated from the logarithmic decrement of a pendulum vibrating in the liquid.

It was considered that in the furnace to be employed the torsional oscillation type would be most suitable. This method has not been used to any great extent for ordinary viscosity determinations. According to FAWSITT[48] this is due to the following facts:-

1) The disc used has to be fairly large, (usually 15-20 cm.) involving the use of large quantities of liquid.

2) Calculation of viscosity from experimental observations is much more involved than in the case of the capillary method.

3) Error in observation produces a much greater error in the calculated value of .

It has been shown that

$$\lambda - \lambda_0 = c_1\sqrt{d\eta} + c_2\eta + c_3\eta d \qquad \text{----------(6}$$

where λ and λ_0 are the logarithmic decrements of the disc in the liquid and air respectively; c_1, c_2 and c_3 are apparatus constants and d is the density of the liquid.

In adapting this method to high temperatures the following difficulties have to be encountered:-

1) It is not practicable to keep large amounts of liquid at high temperatures.

2) The solid whose oscillations are to be damped cannot be made too small otherwise the sensitivity of the apparatus is decreased.

3) For liquids with high density, such as molten metals, the apparatus must be made to sink to the proper depth.

Using discs of different materials but of the same size, FAWSITT[48] measured the viscosity of a number of liquids. For each liquid, the different discs gave identical results. This proved the absence of slip. He, and later, STOTT[53] successfully measured the viscosities of various metals.

However, for liquids 50 times more viscous than water, i.e. about .5 poise equation (6 no longer holds. Hence, the apparatus as used by FAWSITT[48] cannot be used for blast furnace slags.

Since graphite outer and inner cylinders could be accurately made, and, since these had been found to be satisfactory in use with blast furnace slags, it was decided to devise a logarithmic decrement method applicable to an

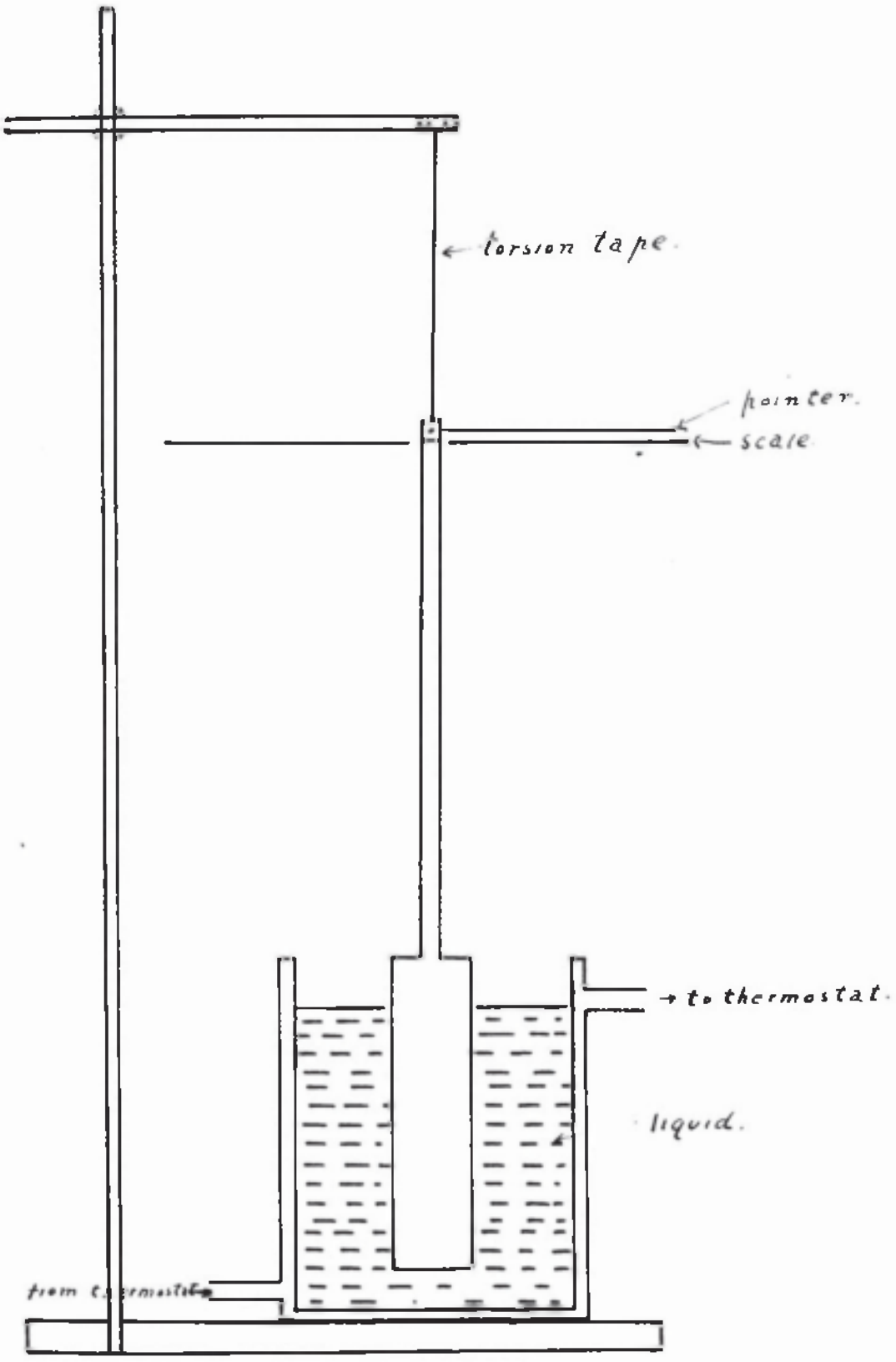
torsion tape
pointer
scale
to thermostat
liquid
from thermostat

fig. 50.

oscillating cylinder instead of to a disc.

Experiments at room temperatures were carried out with the apparatus shown in fig. 50. A brass cylinder, suspended by a phosphor bronze torsion tape, was immersed to a given depth in a suitable liquid contained in a cylindrical water-jacketed brass pot. Through the water-jacket was pumped water thermostatically controlled to 0.1 C°. A pointer fixed to the cylinder and moving over a graduated circular scale allowed torsional oscillations to be followed. The decrement of the amplitude could, therefore, be measured, and from this, a measure of the viscosity obtained as follows:-

Let I = Moment of inertia about the axis of rotation of the oscillating cylinder.

a = amplitude of oscillation.

D = torque per unit twist.

Da = applied torque

η = coefficient of viscosity of liquid in c.g.s. units

K = apparatus constant (depending on dimensions of cylinders, depth of immersion and end effect.)

$K\eta$ = damping constant.

When the cylinder oscillates in air, there is no damping and the simple harmonic motion can be expressed by the following equation

$$I\frac{d^2a}{dt^2} + Da = 0 \qquad \text{----------(7)}$$

When immersed in the liquid, damping occurs and the equation for damped oscillations is

$$I\frac{d^2a}{dt^2} + K\eta\frac{da}{dt} + Da = 0 \qquad \text{----------(8)}$$

Solution of equation (8)

$$\frac{d^2a}{dt^2} + \frac{K\eta}{I}\frac{da}{dt} + \frac{D}{I}a = 0$$

Let $a = Ae^{mt}$ be a solution.

$$\therefore \frac{da}{dt} = mAe^{mt} \text{ and } \frac{d^2a}{dt^2} = m^2Ae^{mt}$$

$$\therefore m^2Ae^{mt} + \frac{K\eta}{I}mAe^{mt} + \frac{D}{I}Ae^{mt} = 0$$

$$\therefore m^2 + K\eta/I + \frac{D}{I} = 0$$

Completing the square,

$$m = -\frac{1}{2}K\eta/I \pm \sqrt{-\frac{D}{I} + \frac{1}{4}(K\eta/I)^2}$$

Let $\alpha = -\frac{1}{2}K\eta/I$

$$\beta = \sqrt{D/I - \frac{1}{4}(K\eta/I)^2}$$

$$\therefore m = \alpha \pm i\beta$$

$$\therefore a = Ce^{-k\eta t/2I} \cos\left(\sqrt{D/I - \tfrac{1}{4}(k\eta/I)^2}\, t + \alpha\right) \qquad \text{----------(9)}$$

(T) Period of oscillation

$$= \frac{2\pi}{\sqrt{D/I - \frac{1}{4}(k\eta/I)^2}} \qquad \text{----------(10)}$$

Noting that $t = 0$, when $a = a_0$, and

$t = T$, when $a = a_1$, it follows that

$$a_0 = C\cos\alpha \quad \text{and} \quad a_1 = Ce^{-\frac{k\eta\pi}{\sqrt{DI - 1/4(k\eta)^2}}} \cos\alpha$$

$$\therefore a_0/a_1 = p = e^{\frac{k\eta\pi}{\sqrt{DI - 1/4(k\eta)^2}}}$$

$$\therefore \log_e p = \frac{k\eta\pi}{\sqrt{DI - 1/4(k\eta)^2}} \qquad \text{----------(11)}$$

Solving for η gives

$$\eta = \frac{\sqrt{DI}\,\log_e p}{k\pi\sqrt{\left[1 + \frac{(\log_e p)^2}{4\pi^2}\right]}} \qquad \text{----------(12)}$$

$$= \frac{\sqrt{DI}\,\log_e p}{k\pi} \qquad \text{----------(13)}$$

when $\log_e p$ is small.

In deriving equation (13) it was assumed that the damping was due to the viscosity of the liquid. But part of the damping might be due to loss of energy consequent on a simple movement of translation being imparted to the liquid.

$-\frac{da}{dt}$ (decrease in amplitude due to viscosity) $= k_1 a.$

$-\frac{da}{dt}$ (due to motion of liquid) $= k_2 a^2.$

$$\therefore -\frac{da}{dt} = k_1 a + k_2 a^2$$

when k_2 and a are small,

$$-\frac{da}{dt} = k_1 a$$

$$\therefore k_1 = 1/t \log \frac{a_0}{a_t} \qquad \text{----------(14)}$$

∴ logarithmic decrement for successive oscillations is constant

When the velocity of movement of the liquid is considerable, the last term cannot be neglected and the integral has the form

$$k_1 = \frac{1}{t}\log a_0/a_t - 1/t \log \frac{k_1 + k_2 a_0}{k_1 + k_2 a_t} \qquad \text{----------(15)}$$

In this case the logarithmic decrement is not constant for any one series of observations, but varies with amplitude. The energy of motion communicated to the liquid has to be kept to a minimum so that the logarithmic decrement is independent of amplitude.

The centre of gravity of the oscillating cylinder should be kept as low as possible, otherwise it will not oscillate about its vertical axis and the path of any particle of the cylinder becomes an ellipse instead of a circle thus making the motion correspond to equation 15 instead of to 14.

Results obtained by the apparatus should show that for a given range of viscosity, the viscosity is directly proportional to $\log_e \beta$. This range will be limited by the facts when β is too large, the approx. no longer holds, and that when β is too small (about unity) the oscillation is practically undamped. Hence in the latter case the amplitude must be kept small to avoid turbulent motion, and this increases the error in scale reading.

Logarithmic decrements were measured in liquids whose viscosities had been measured in the capillary viscometer as previously described. Table XVIII gives the results obtained using brass cylinders, the last column showing that the viscosity is proportional to the logarithmic decrement over the range of viscosity from 0.25 to 3.0 poise.

Table XVIII.

Liquid	Temp. C	Viscosity (poise)	Decrement p	$\log_{10} p$	$\log_e p/\eta$
Lubricating Oil	25.0	0.1187	1.16	0.0645	0.54
Lubricating Oil	25.0	0.7884	1.70	0.2304	0.29
Glycerine Sol.	24.8	1.398	2.34	0.3692	0.27
Glycerine Sol.	31.0	2.108	3.70	0.5682	0.27
Glycerine Sol.	28.4	2.529	4.70	0.6721	0.27
Glycerine Sol.	24.5	3.437	7.30	0.8633	0.25

It was found that the logarithmic decrement for successive oscillations was constant and independent of the amplitude.

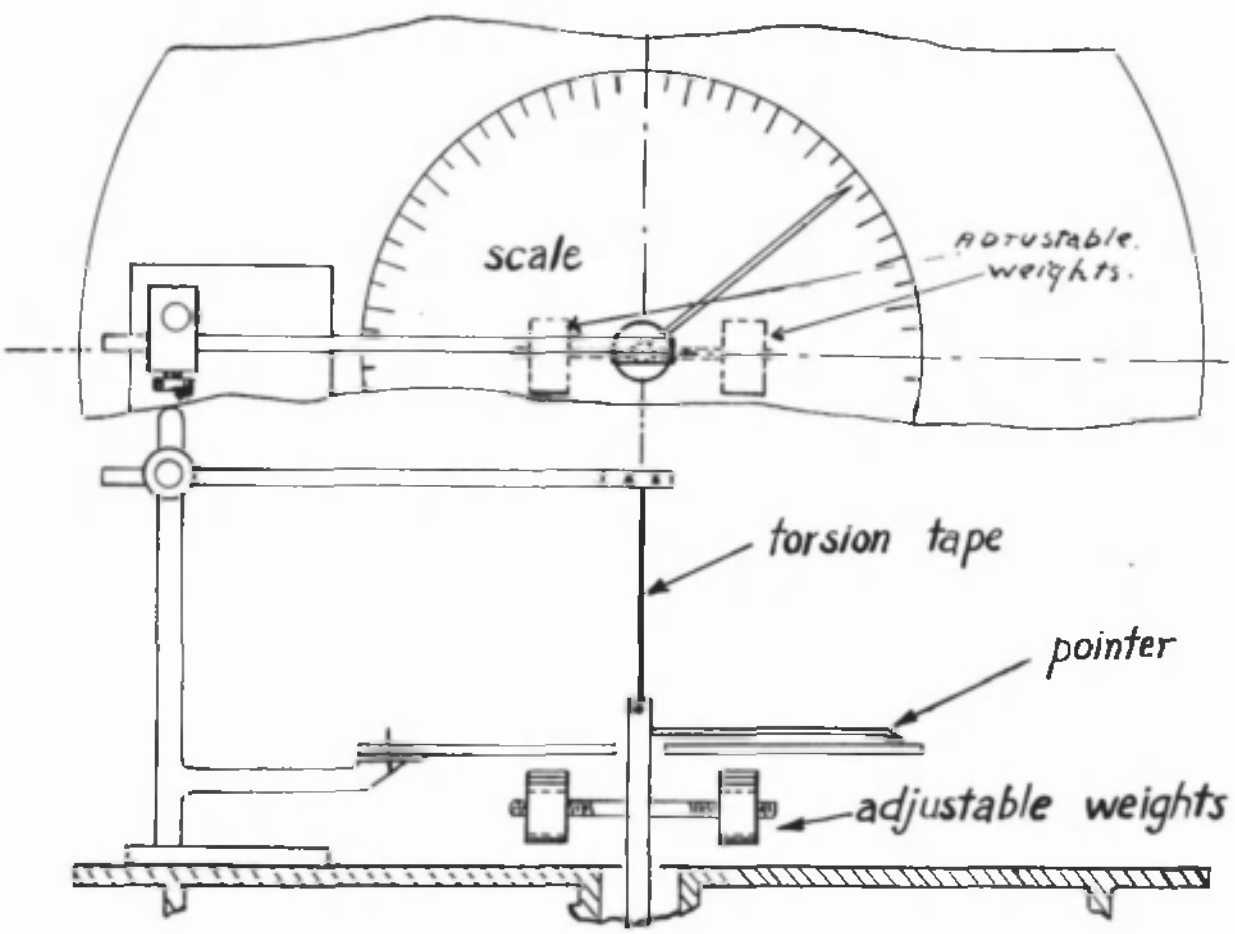
scale
adjustable weights
torsion tape
pointer
adjustable weights

fig 51

Knowing the values of K, I and D, it would be possible to calculate the range of viscosity from equation (13) for a range of decrement (p) from 1.25 to 5. Hence an apparatus could be constructed to measure viscosity over the desired range. But although I and D can be evaluated, it is not easy to calculate K. By designing an apparatus similar to the above with respect to K, the required range can be obtained by altering the value of DI according to equation (13) as follows:-

Lower limit of brass cylinder apparatus	=	.25 poise
Moment of inertia of oscillating brass cylinder (I)	=	218 gms/cm^2
Torque of torsion tape	=	D
Moment of inertia required	=	I_1
Torque of torsion tape required	=	D_1
Lower limit say	=	1 poise

From equation (13) $\sqrt{D_1 I_1} / \sqrt{DI} = 1/.25$

$\therefore .0625 D_1 I_1 = DI$

when $D = D_1$

$I_1 = 3500$ gms./cm^2

From equation (10) it follows that when D is increased, the period of oscillation is decreased. When I is increased, the period is increased. When the period is too small, turbulent motion occurs and the assumptions made in deriving equation (13) no longer hold. It was, therefore, decided to construct an apparatus in which both I and D could be varied so that a suitable period of oscillation could be obtained for each range of viscosity.

Fig. 51 shows the apparatus designed. A phosphor bronze torsion tape was held at the top by means of a clamp which could be adjusted vertically and horizontally, and was fixed at its lower end to the oscillating body. This consisted of a brass tube $\frac{5}{16}$ in. in diameter and ¼ in. bore by 20 cm. long, having two side arms of brass tubing $\frac{3}{16}$ in. in diameter, $\frac{1}{8}$ in. bore by 5 cm. long. On each side arm there was a similar sliding cylindrical weight of 100 gm. Coupled to this tube by means of a duralumin coupling was a graphite rod ⅜ in. in diameter by 20 cm. long on the end of which was screwed the graphite inner cylinder. The apparatus was so fitted up that the prolongation of the vertical

axis of the torsion tape passed down the centre of the vertical brass tube, graphite rod and cylinder. A pointer was fixed to the top of the vertical brass tube. When the body was oscillating, this pointer moved over a horizontal circular scale. In this way the decrement could be measured. The scale was 12 in. in diameter and its circumference was divided into 80 equal parts. It could be adjusted horizontally and vertically. The water cooled plate, molybdenum furnace and stand were the same as those used for the concentric cylinder apparatus.

Calibration of the Torsion Oscillation Apparatus.

The graphite pot, 5 cm. internal diameter and 7.6 cm. internal height, was filled to a depth of 4.8 cm. with a standard liquid and placed inside a water jacket, through which was pumped water from a thermostat bath, thereby maintaining the liquid at a temperature within 0.1 C^{o}. The torsion tape supporting the oscillating body was clamped in position, and the scale adjusted to zero position. The pot with the water jacket was then raised until the inner cylinder just rested on the bottom of the pot, when it was lowered by 0.6 cm. The inner cylinder 2 cm. in diameter and 7 cm. in height, was then immersed 5 cm. in the liquid. The oscillating body was adjusted so that the inner cylinder was concentric with the outer cylinder, and oscillated co-axially with the torsion tape. Oscillations were then set up, and the decrement obtained from two successive readings on the same side of the zero.

Let a_0, a_1 and a_2 lying on the same side of the zero be the amplitudes of the first, second and third oscillations respectively. Then the decrement is a_0/a_1 or a_1/a_2.

As viscosity approached the upper limit of the range of the apparatus, the first amplitude was made large, for this reduces the percentage error in the scale reading, and, since the viscosity was high, there was no error introduced due to turbulent motion. But, as the viscosity approached the lower limit of the range, the amplitude of the first oscillation was made small to prevent turbulent motion. When

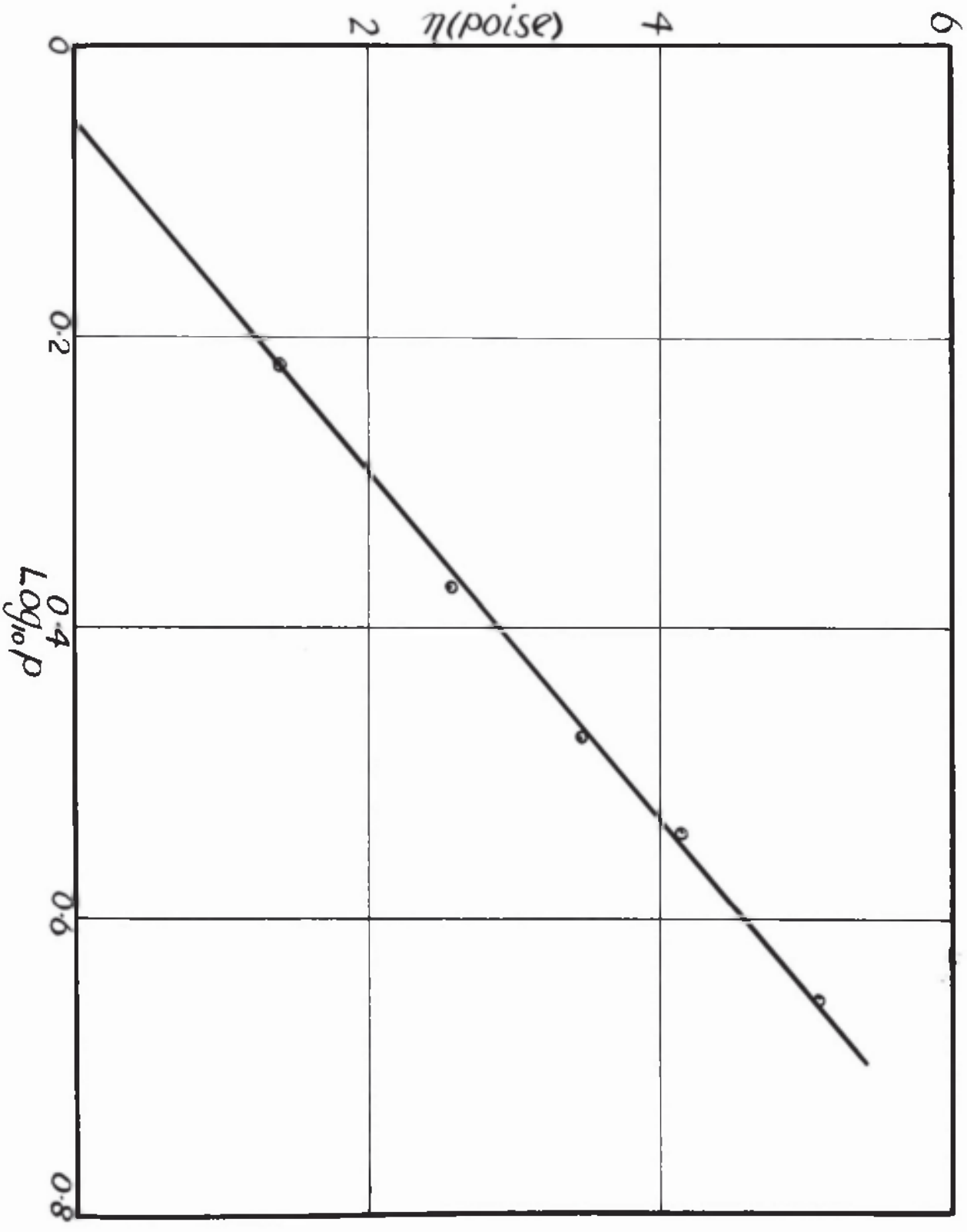

fig. 52.

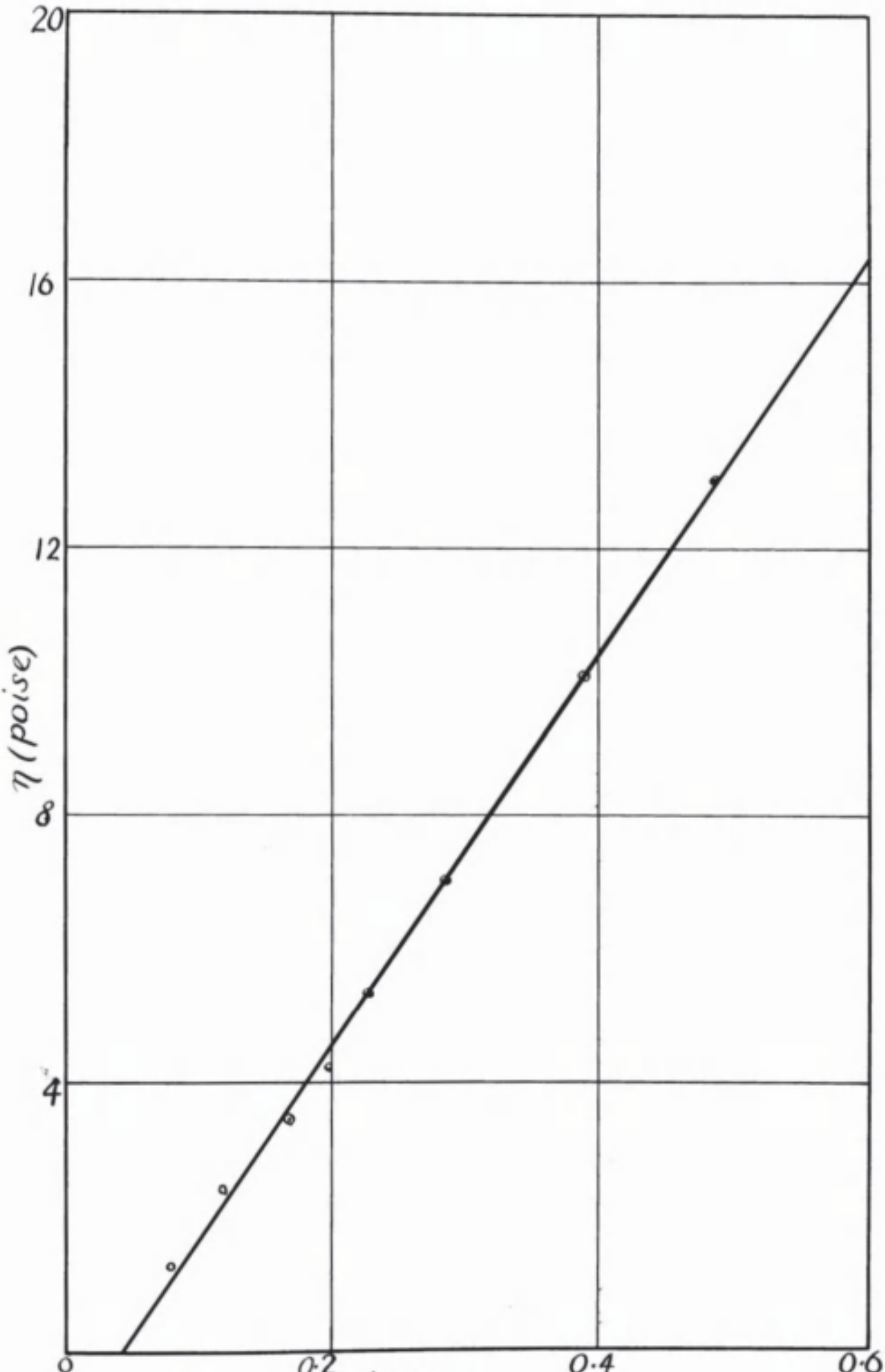

fig. 53.

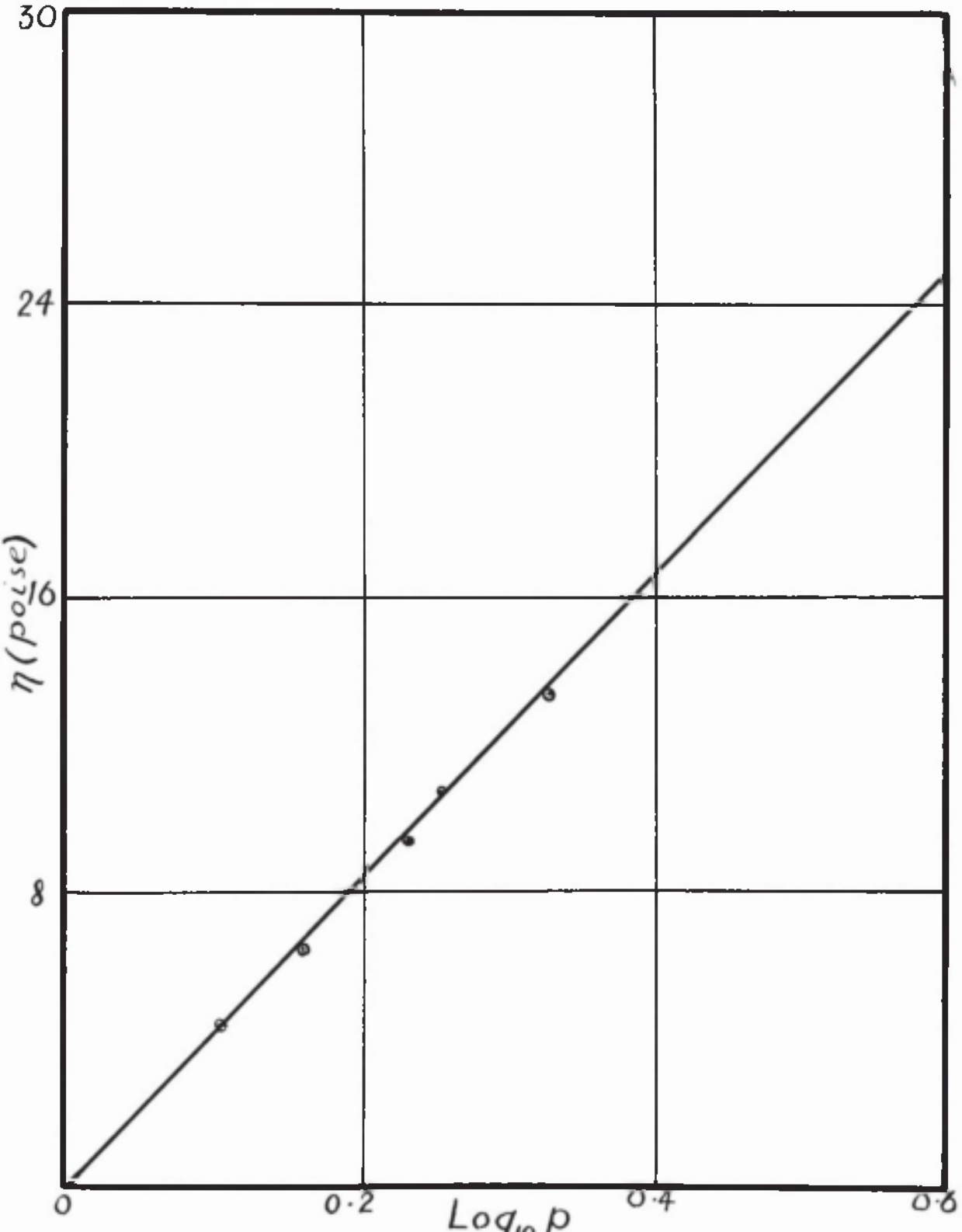

fig. 54.

amplitudes were small, the experimental error was reduced by calculating the decrement from $p = \sqrt[n]{a_0/a_n}$ where a_n is the amplitude of the $n^{th.}$ oscillation. This was done for a given series of liquids of known viscosity. The results are given in tables XIX, XX and XXI and the calibration curves are shown in figs. 52, 53 and 54. The viscosity-logarithmic decrement curves are straight lines. When, however, the value of the decrement p exceeded 5, there was a deviation from the straight line of over 3 per cent, as can be seen from a consideration of equations (12) and (13).

When the same torsion tape and the same value of K was employed it was calculated that a moment of inertia (I) of about 3500 gm./cm^2 would be necessary to give a lower limit of 1 poise.

When the weights were at a distance of about 1 cm. from the axis of oscillation, the moment of inertia was calculated to be about 510 gm/cm^2. The range of viscosity was found to be from .5 to about 5 poise. When the weights were at a distance of 5 cm. from the axis of oscillation, the moment of inertia was calculated to be about 5300 gm./cm^2; the range of viscosity was found to be from about 1.6 to 16 poise.

From examination of the calibration curves in figs. 52, 53 and 54 it can be seen that viscosity can be measured from 0.5 to 30 poise with the apparatus in its present form.

Table XIX

Torsion tape 1

Weights at a distance of 1 cm. from axis of oscillation.

Liquid	Temp. °C	η (Poise)	Decrement (p)	$\log_{10}$ p
Glycerine sol.	24.8	1.398	1.64, 1.66, 1.65 Mean = 1.65	.2175
Glycerine sol.	28.6	2.529	2.37, 2.35, 2.36 Mean = 2.36	.3729
Glycerine sol.	24.5	3.437	2.95, 3.04, 2.95, 2.93 Mean = 2.97	.4728
Glycerine	27.7	5.25	4.52, 4.47 Mean = 4.5	.6532
Glycerine	29.8	4.10	3.47, 3.41, 3.41 Mean = 3.43	.5353

Table XX

Torsion tape 1

Weights at a distance of 5 cm. from axis of oscillation

Liquid	Temp. °C	η (Poise)	Decrement (p)	$Log_{10} p$
Glycerine sol.	24.8	1.398	1.18,1.19,1.18,1.18 Mean = 1.18	.0719
Glycerine sol.	28.6	2.529	1.29,1.3,1.28 Mean = 1.29	.1106
Glycerine sol.	24.5	3.437	1.44,1.47,1.48,1.44 Mean = 1.46	.1644
Glycerine	29.8	4.10	1.58,1.57 Mean = 1.575	.1973
Glycerine	27.7	5.25	1.69,1.69,1.69 Mean = 1.69	.2279
Glycerine	24.5	7.00	1.94,1.94,1.92,1.92 Mean = 1.93	.2856
Glycerine	20.5	9.90	2.44,2.44,2.45,2.44 Mean = 2.44	.3874
Glycerine	17.5	13.00	3.05,3.11,3.07 Mean = 3.08	.4886

Table XXI

Torsion tape II

Weights at a distance of 5 cm. from the axis of oscillation

Glycerine sol.	21.0	4.50	1.28,1.27,1.3 Mean = 1.28	.1072
Castor oil	20.4	9.40	1.71,1.70,1.72 Mean = 1.71	.2304
Glycerine	19.3	10.80	1.8,1.8 Mean = 1.8	.2553
Castor oil	25.0	6.57	1.45,1.45 Mean = 1.45	.1614
Glycerine	17.0	15.60	2.1,2.18,2.14 Mean = 2.14	.3304

Investigation into the Various Sources of Error.

The following are the possible sources of error:-

1. Variation in dimensions of cylinders.
2. Variation in depth of immersion.
3. Eccentricity of pot and cylinder.
4. Eccentricity in oscillation.
5. Variation in properties of torsion tapes.
6. Occurrence of "slip".
7. Turbulent motion.
8. Error in measuring viscosity of standard liquids.
9. Error in scale reading.
10. Temperature measurement.
11. Expansion of cylinders with increase in temperature.

Since the cylinders were turned on the lathe from solid graphite rods, they were identical in size within one thousandth part of an inch. Hence, although, new cylinders were employed for each slag viscosity determination, no error was introduced due to variation in dimensions. Experiments showed that with the accuracy of setting the error in depth of immersion was negligible. Experiments were carried out in which the inner

cylinder was first set concentric with the pot, and the decrement measured. Then it was set eccentric with the pot and the decrement measured. With the accuracy of setting possible the error is negligible. If the inner cylinder does not oscillate about its own axis, which is the prolongation of the axis of the torsion tape, an error is introduced. For any one series of observations the logarithmic decrement is not constant , but varies with amplitude. However, it was found experimentally that the logarithmic decrement was independent of amplitude. The elastic properties of the torsion tapes were found to be constant by calibrating the apparatus from time to time. For work at high temperatures, the tape was shielded from the heat of the furnace by means of the water cooled plate .

In deriving equation (13) it was assumed that the liquid wets the cylinders. Unless the adhesive force between the cylinder and liquid is greater than the cohesive force between concentric layers of liquid, slip will not take place between those layers but between the liquid and the cylinder. With cylinders of different materials, consistent results were obtained. If'slip' occurred, it would be of a different degree for each material and inconsistent results would be expected.

It was also assumed in deriving equation (13) that true viscous flow occurred. If turbulent motion occurred, results would be erratic and the viscosity-logarithmic decrement curves would not be straight lines. As explained previously, the apparatus was designed to have a sufficiently slow period of oscillation so as to prevent turbulent motion. Care was also taken during the experiments to avoid turbulent motion. When the viscosity was low and the decrement approached unity, small oscillations were set up; thus, for a given viscosity, the smaller the amplitude, the smaller the velocity, and so the possibility of turbulent motion reduced.

The percentage error is determined in two parts.

1) Estimation of the error in the standard η -$\log_{\infty}$p curves.

2) Estimation of the error in measuring the viscosity at high temperatures.

1) In the calibration of the apparatus, the standard liquid was maintained at the required temperature within $\pm$ 0.1C°. The previously described method of measuring the viscosity coefficients of the standard liquid led to an error of less than $\pm$ 2%. These two latter sources of error together led to an error of about $\pm$ 2%.

The greatest error in measuring the decrement p occurs at small values of p. The lowest observed value of p was 1.25 where $p = \sqrt[n]{a_0/a_n}$ as previously explained. There was an error of about $\pm$ 4% in the ratio a_0/a_n since error in measuring a was about $\pm$ 2%.

When n = 4, the error in p = $\pm$ ¼ x 4% = $\pm$ 1%

Since η is proportional to $\log_e p$, an error of $\pm$ 1% in p yields an error for η equal to $\pm \frac{1}{\log_e 1.25}$ = $\pm$ 4.4%

By increasing the diameter of the scale, the accuracy of reading could be increased. But this is not necessary since the reproducibility of the low decrements is just about $\pm$ 4%.

2) In measuring the viscosity of a slag at high temperatures a small error probably less than 2% is introduced due to the expansion of the graphite cylinders. An error of $\pm$ 4.4% occurs in measuring the logarithmic decrement. With the method employed in calibrating the tungsten-molybdenum thermocouple a temperature of 1600°C is accurate to within $\pm$ 10°C, while the reproducibility is within $\pm$ 5°C.

The reproducibility of viscosity measurements is, therefore, within $\pm$ 10% and this was found to be so by repeating measurements on the same slag.

Determination of the Viscosity-Temperature Curve for a Blast Furnace Slag.

% Composition of slag.

CaO	SiO_2	Al_2O_3	Fe_2O_3	MnO	MgO	S
46.58	30.3	18.5	-	.85	2.64	1.44

The viscosity-temperature curve to a value of viscosity of 8 poise had already been measured by the concentric cylinder method. The logarithmic decrement method was employed to measure the viscosity below 8 poise.

Experimental Details

The graphite pot contained powdered slag, which, on melting, would give less than the required depth of 4.8 cm. It was placed in the molybdenum furnace, resting on an alundum stool in the hot zone of the furnace, being held in position by alundum wedges. The temperature of the furnace was then raised to about 1600°C., and small pieces of slag added until the correct depth of slag was obtained as shown by the depth gauge. The torsion tape supporting the oscillating body was clamped in position, and the scale adjusted to the zero. The furnace was then raised until the inner cylinder just rested on the bottom of the pot, when it was lowered by .6 cm. The oscillating body was then adjusted so that the inner cylinder was concentric with the outer cylinder, and oscillated about its own axis. The furnace top was then almost completely closed by an alundum collar which just allowed the graphite connecting rod freedom of oscillation.

The temperature measurement and control were the same as before.

The decrements for a series of temperatures from 1600°C to about 1500°C were measured and the corresponding viscosity coefficients obtained from the standard viscosity-$\log_{10}$p curve.

When the series of readings was completed at 1500°C, the temperature of the furnace was raised to 1600°C before the inner cylinder was withdrawn from the slag.

This experiment was repeated with new cylinders, the reproducibility of the results being found to be well within $\pm$ 10%.

The results are given in table XXII and the η - temperature curve in fig. 49.

Table XXII

Torsion tape 1

Weights at a distance of 5 cm. from axis of oscillation

Temp. °C	Decrement (p)	$Log_{10}p$	η (Poise)
1600	1.42,1.44,1.40 Mean = 1.42	.152	3.0
1580	1.45,1.43,1.44 Mean = 1.44	.158	3.3
1565	1.53,1.53,1.53 Mean = 1.53	.184	4.0
1550	1.55,1.56,1.57 Mean = 1.56	.193	4.2
1540	1.63,1.60,1.62 Mean = 1.62	.209	4.8
1510	1.83,1.82,1.80 Mean = 1.82	.260	6.2
1490	2.54, 2.54 Mean = 2.54	.405	10.5

The Effect of Fluorspar on the Viscosity of the Blast Furnace Slag.

The apparatus was set up as before with the sample of blast furnace slag. After reaching a temperature of 1600°C, the fluorspar addition was made and after the slag had been maintained at 1600°C for over an hour, the viscosity readings were obtained as before.

The fluorspar addition was 3.7 gm./ 100 gm. slag. The results are given in table XXIII and the viscosity-temperature curve in fig. 49.

Table XXIII

Torsion tape 1

Temp. °C	Decrement (p) (a)Wts. at 1 cm.	(b)Wts. at 5 cm.	$Log_{10}p$ (a)	(b)	η (Poise)
1605	1.83	1.26	.262	.100	1.65
1580	1.90	-	.2788	-	1.9
1545	2.32	1.37	.3655	.1367	2.6
1520	-	1.43	-	.155	3.2
1490	-	1.55	-	.190	4.2
1450	-	1.71	-	.233	5.4
1420	-	1.98	-	.297	7.3

The temperature of the slag was again raised to 1600°C., and a second set of readings were commenced after an hour. This was to allow the fluorspar to become thoroughly mixed with the slag and to allow any reactions which may be taking place between the slag and the spar to go to completion. However, it was found that the second set of readings were the same as the first.

The Viscosity of Synthetic Slags of the Blast Furnace Type.

The chief constituents of blast furnace slags are CaO, SiO_2, Al_2O_3 and MgO. For direct applications to blast furnace practice, the synthetic slags investigated should have compositions similar to those which obtain in the furnace. McCaffery has investigated quaternary slags of such composition.

However, the viscosities of slags in the systems $CaO-SiO_2$, $CaO-Al_2O_3$ and $CaO-SiO_2-Al_2O_3$ are of theoretical importance since evidence of the existence of compounds in the liquid state may be obtained. In the system $CaO-SiO_2$, conflicting viscosity results have been obtained by HERTY[29] and ENDELL[30], the former reporting the existence of the compound $CaO-SiO_2$ while the latter found no such evidence. In the system $CaO-Al_2O_3$, there is a sharp maximum in the liquidus at the compound $5CaO.3Al_2O_3$.

It was, therefore, decided to investigate the viscosities of slags in these systems to find if the results would yield evidence as to the constitution in the liquid state.

The results for $CaO-SiO_2$ and $CaO-SiO_2-Al_2O_3$ slags would show the effect of constitution on the viscosity of blast furnace slags.

Viscosity of $CaO-SiO_2$ Slags.

The slags were prepared from pure $CaCO_3$ and SiO_2 sand. These were mixed in the required proportions and placed in a graphite pot. The mixture was heated in a Carbon Gramular furnace to about 1600°C and cast into an iron mould. The slag was crushed, remelted and cast. In this way a homogeneous slag was obtained. Analysis before and after the viscosity determination showed no change in the composition of the slag.

It was found that the viscosities of the slags in the range of temperature and composition examined were below the lower limit of the concentric cylinder apparatus. The logarithmic decrement method was, therefore, used throughout. The experimental procedure was the same as that described for the blast furnace slag. The results are shown in table XXIV

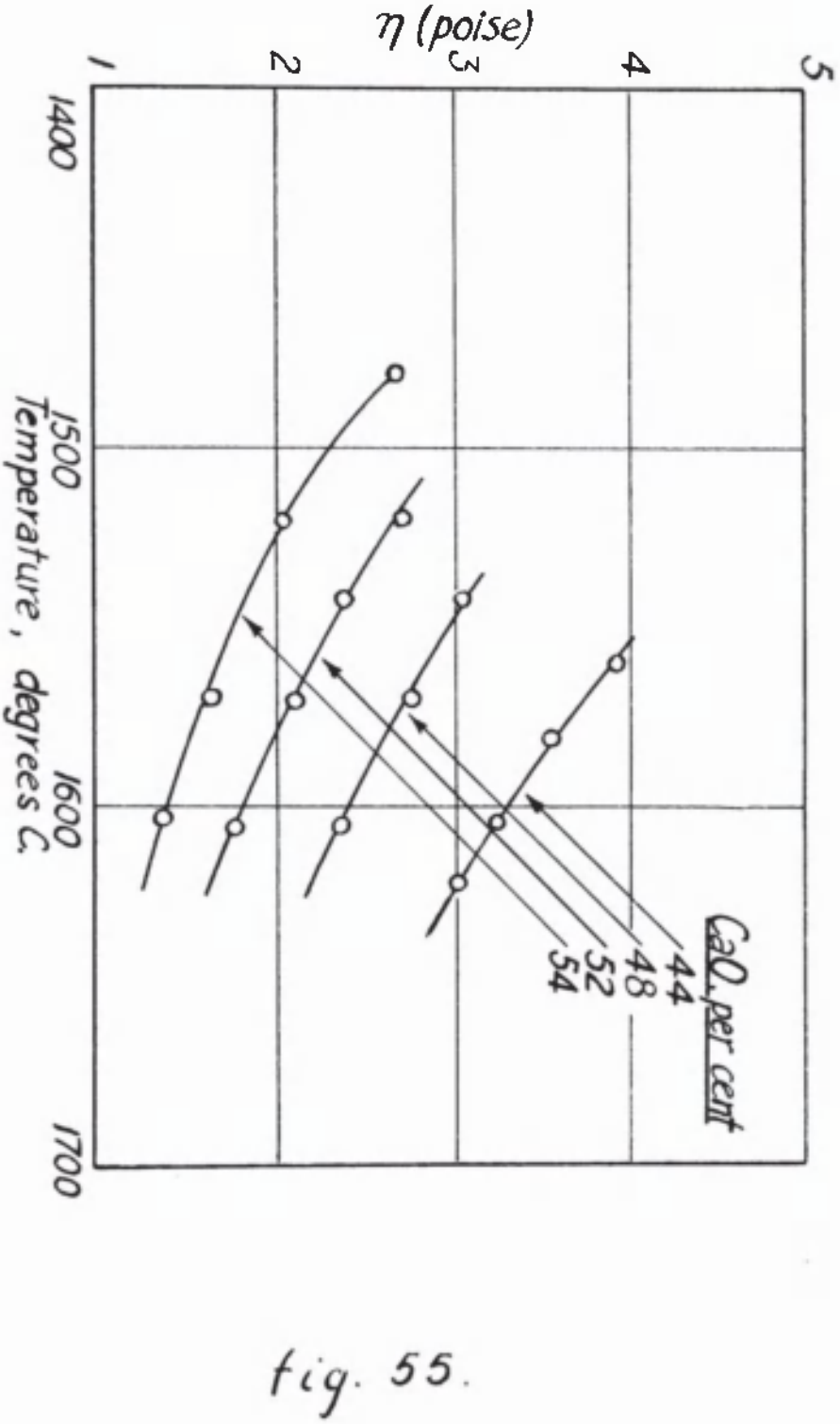
η (poise)
1
2
3
4
5
1400
1500
1600
1700
Temperature, degrees C.
CaO, per cent
44
48
52
54

fig. 55.

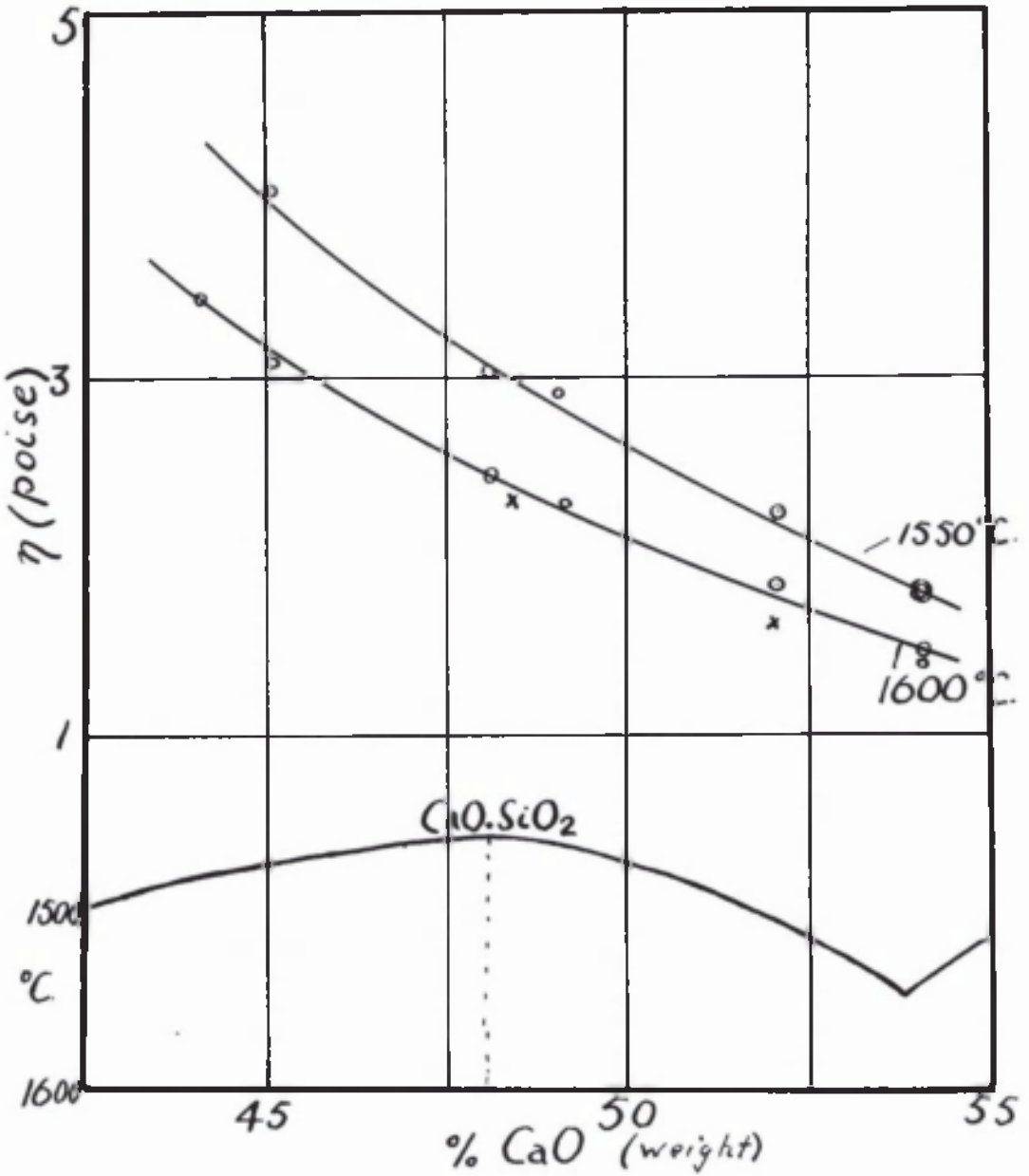
5
3
1
η (poise)
1550°C.
1600°C.
CaO.SiO2
1500
°C.
1600
45
50
55
% CaO (weight)
o Endell.
x M'Caffery.

fig. 56.

and the viscosity-temperature curves in fig.55.

Table XXIV

Torsion tape 1

Weights at a distance of 1 cm.

% Composition CaO	% Composition SiO_2	Temp. °C	Decrement (p)	$\log_{10} p$	η (poise)
52	48	1605	1.87	.2718	1.80
		1570	2.04	.3096	2.15
		1540	2.18	.3385	2.40
		1520	2.42	.3838	2.75
54	46	1605	1.65	.2175	1.40
		1570	1.80	.2553	1.70
		1540	1.88	.2742	1.85
		1520	1.95	.2900	2.00
		1480	2.37	.3747	2.70
48	52	1605	2.18	.3385	2.40
		1570	2.48	.3945	2.82
		1542	2.61	.4166	3.05
44	56	1620	2.66	.4249	3.10
		1605	2.80	.4472	3.30
		1580	3.05	.4857	3.60
		1560	3.40	.5315	4.00

Fig. 56 shows the viscosity-composition isotherms and the liquidus of the $CaO-SiO_2$ system. The latter was obtained in the I.C.T. Points obtained by ENDELL[30] and McCAFFERY[12] are also shown in fig. 56. These agree very closely with my results.

Endell employed a logarithmic decrement method similar in theory to that employed here. However, instead of graphite cylinders, Endell had a platinum sphere oscillating in the slag contained in a platinum pot. McCaffery has very few determinations in the $CaO-SiO_2$ system, most of his slags containing MgO. In a concentric cylinder apparatus in which the outer cylinder was rotated at constant speed, McCaffery measured the viscosity from the torque produced on the inner cylinder. The cylinders were made of graphite.

The Viscosity of $CaO-Al_2O_3$ Slags.

These slags were prepared in the same way as the $CaO-SiO_2$ slags. Pure $CaCO_3$ and anhydrous Al_2O_3 were used.

In all the slags, the viscosity increased very rapidly with decreasing temperature. The viscosities at high temperatures

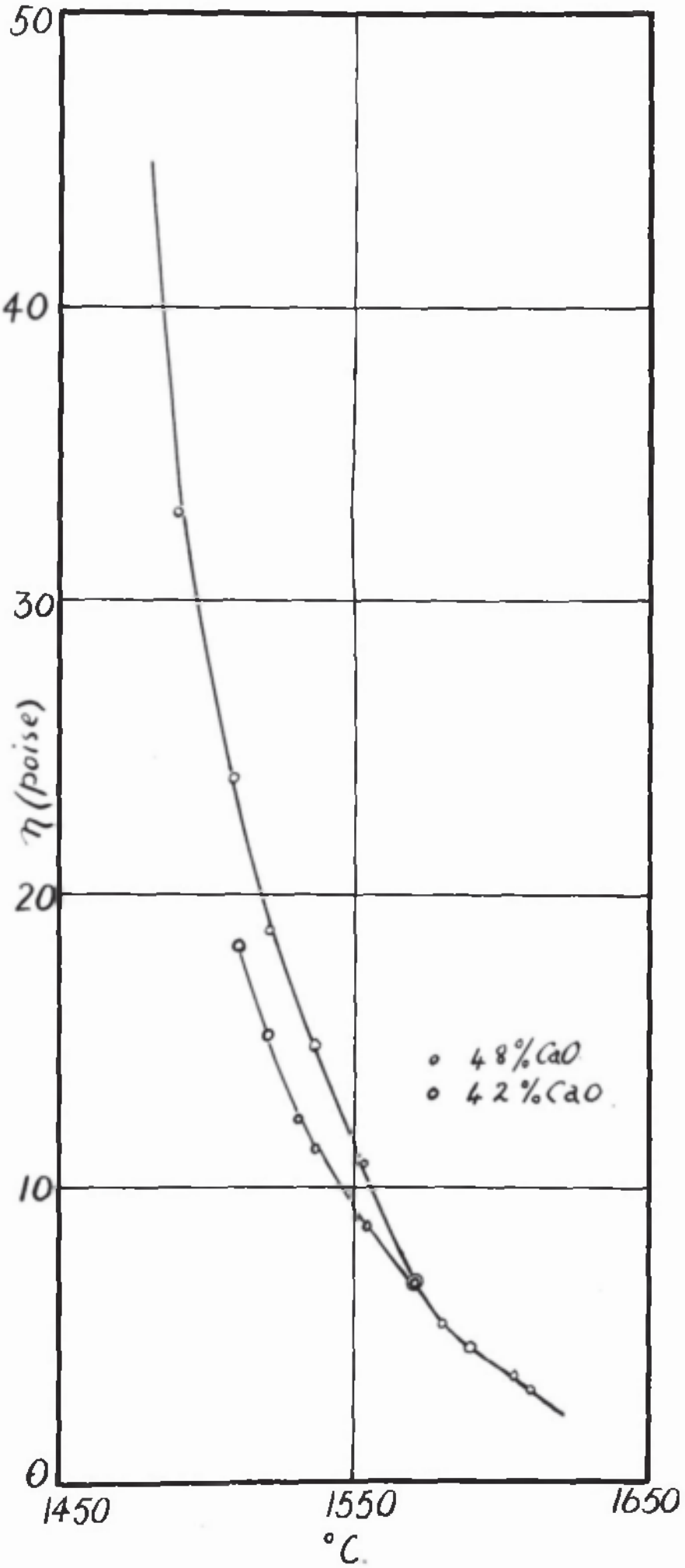

fig. 57.

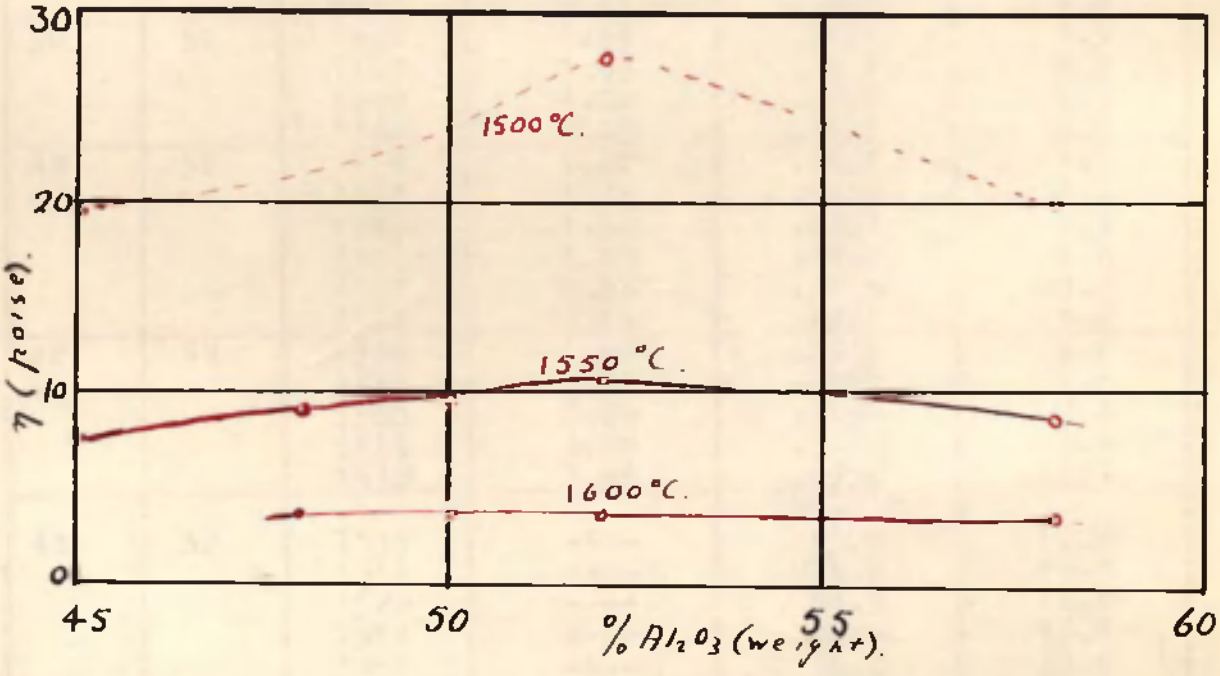
30
20
10
0
η (poise).
1500 °C.
1550 °C.
1600 °C.
45
50
55
60
% Al2O3 (weight).

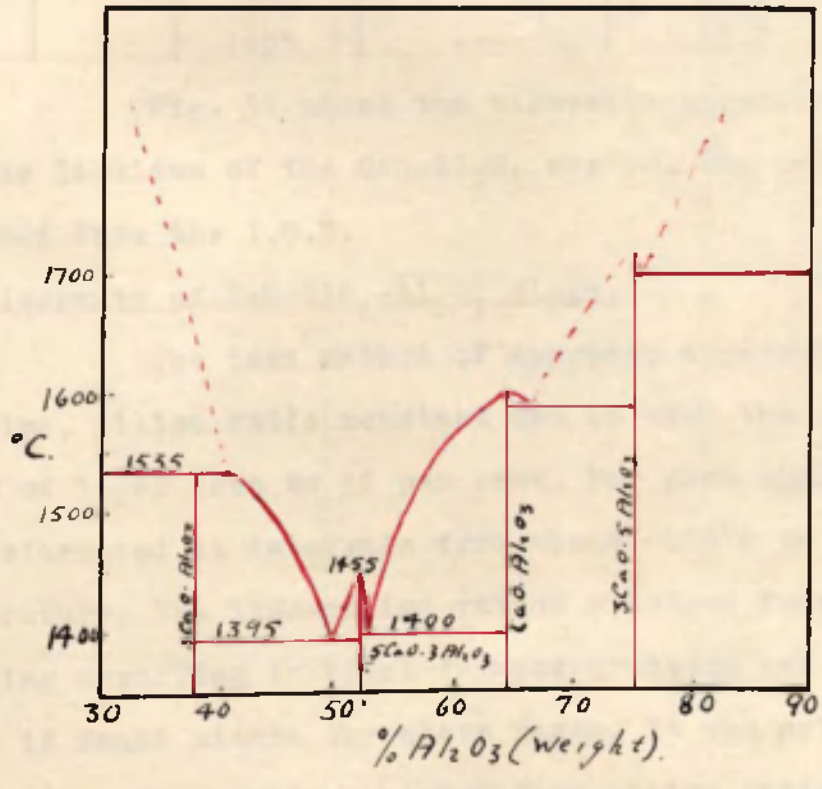
1700
1600
°C.
1555
1500
1455
1400
1395
1400
3CaO.Al2O3
CaO.Al2O3
3CaO.5Al2O3
5CaO.3Al2O3
30
40
50
60
70
80
90
% Al2O3 (weight).

fig. 58

were obtained using the logarithmic decrement method, while at the lower temperatures the concentric cylinder method was used.

The results are shown in table XXV and typical curves in fig. 57.

Table XXV

% Composition CaO	Al_2O_3	Temp. °C	Decrement (p)	$Log_{10} p$	η (poise)
52	48	1605	1.47	.1673	3.5
		1590	1.58	.1987	4.4
		1580	1.78	.2504	6.0
		1570	2.10	.3222	8.0
		1555	2.25	.3522	9.0
50	50	1630	1.33	.1239	2.3
		1605	1.47	.1673	3.5
		1580	1.68	.2253	5.3
		1560	2.25	.3522	9.0
48	52	1610	1.40	.1461	3.0
		1605	1.47	.1673	3.5
		1580	1.68	.2253	5.3
		1570	1.90	.2788	6.8
		1555	2.58	.4116	10.8
		1536	3.54	.549	14.8
42	58	1590	1.60	.2041	4.6
		1570	1.90	.2788	6.8
		1560	2.06	.3139	7.8
		1555	2.20	.3424	8.8
		1530	2.95	.4698	12.4
				(M-f)T	
48	52	1555	----	35.5	12.2
		1536	----	46.0	15.8
		1520	----	54.0	18.6
		1510	----	70.0	24.0
		1490	----	96.0	33.0
		1480	----	155.0	53.5
42	58	1536	----	33.0	11.4
		1520	----	44.0	15.2
		1510	----	53.0	18.3
55	45	1555	----	22.3	7.7
		1536	----	34.0	11.7
		1520	----	37.0	12.8
		1485	----	82.0	28.2

Fig. 58 shows the viscosity-composition isotherms and the liquidus of the $CaO-Al_2O_3$ system. The latter was obtained from the I.C.T.

The Viscosity of $CaO-SiO_2-Al_2O_3$ Slags.

The best method of approach appeared to be to keep the lime, silica ratio constant and to vary the alumina in steps of 5 per cent to 35 per cent. For each slag the viscosity was determined at intervals from about 1600°C to the liquidus temperature. The lime-silica ratios extended from .428 to 1.3, and slag occurring in blast furnace practice has a composition which is found within the above range. It was not possible to investigate slags with a higher lime-silica ratio owing to the

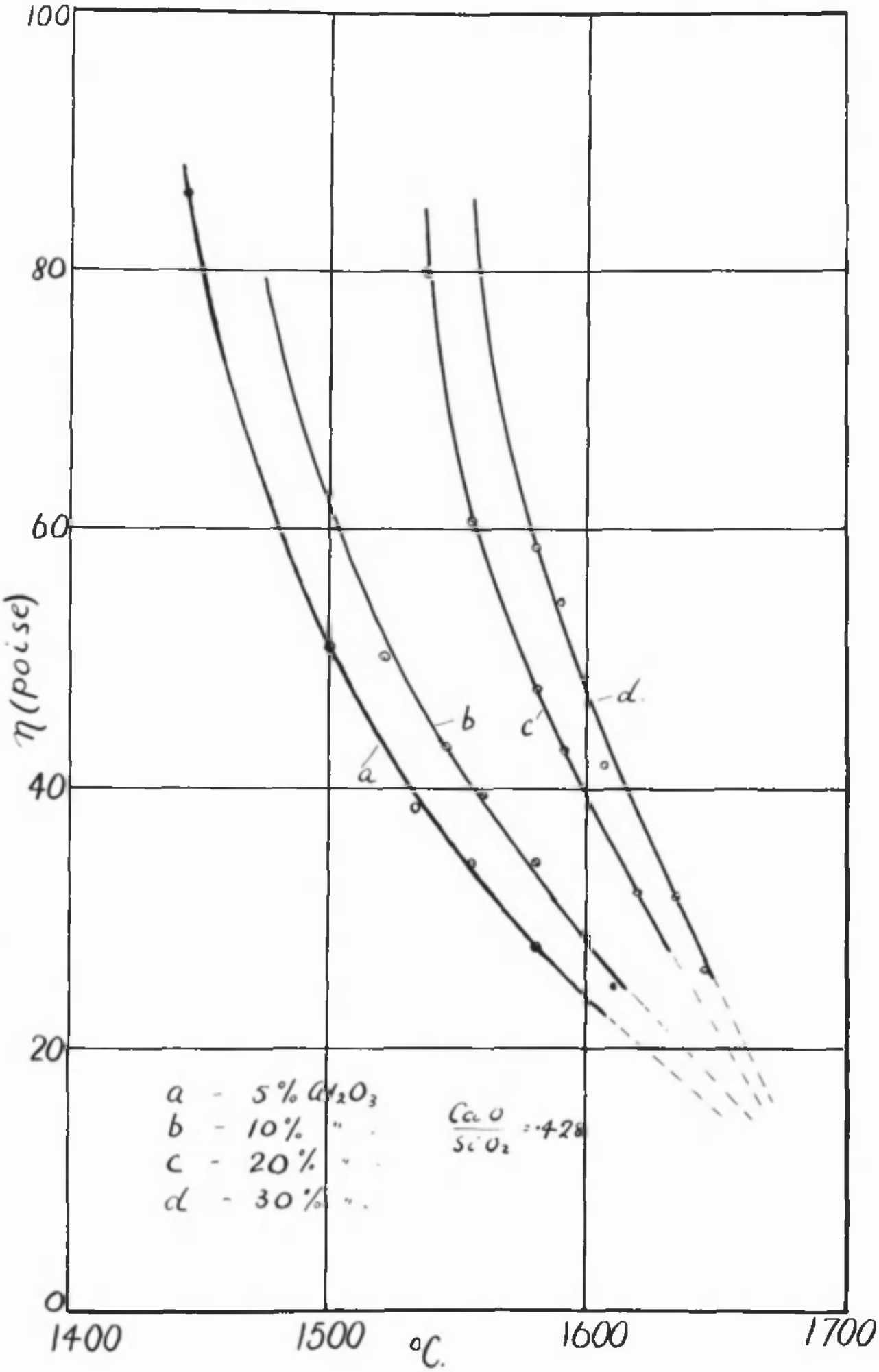
100
80
60
40
20
0
η (Poise)
1400
1500
°C.
1600
1700
a
b
c
d
a - 5% Al_2O_3
b - 10% "
c - 20% "
d - 30% "
$\frac{CaO}{SiO_2}$ = ·428

fig. 59.

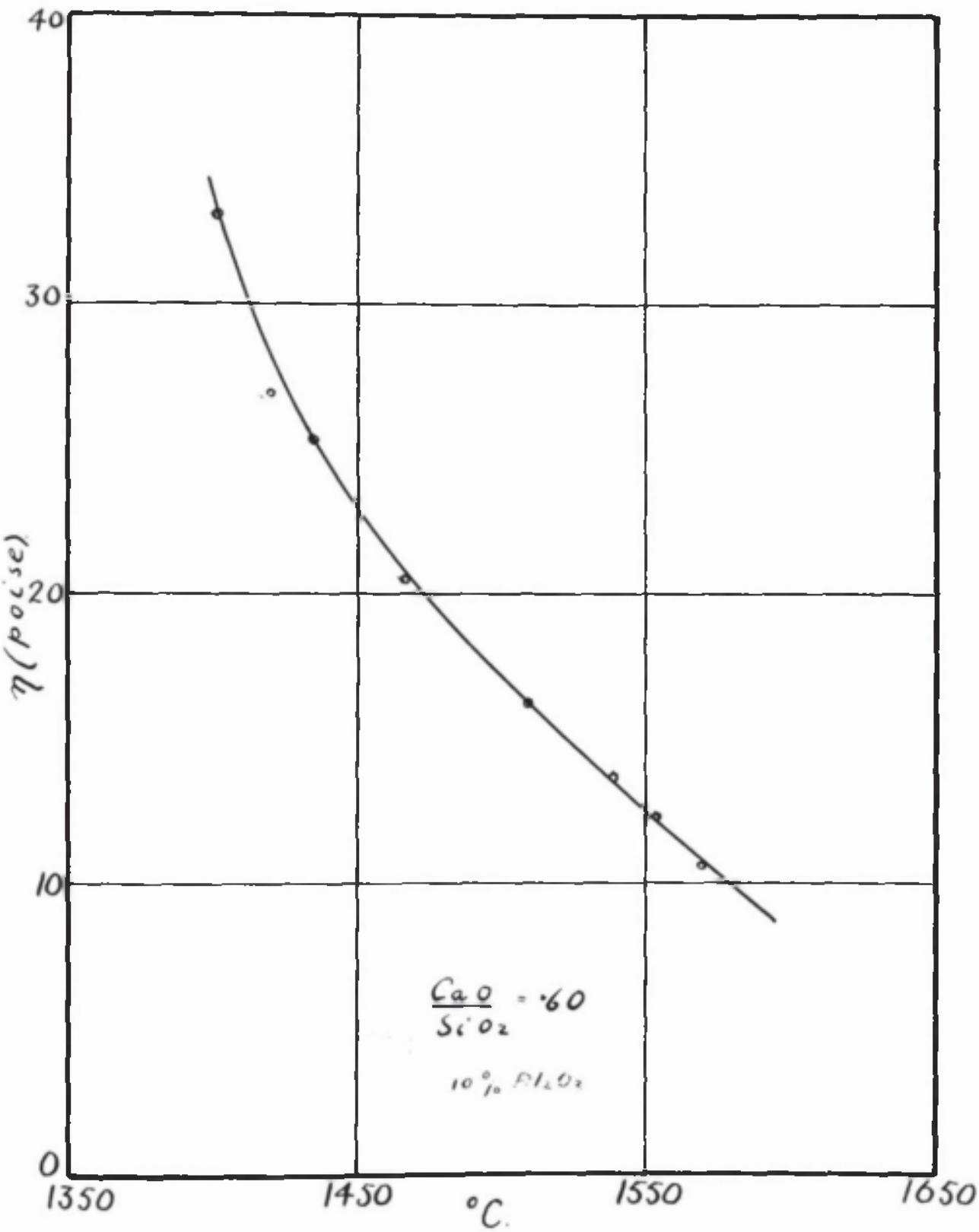

fig 60.

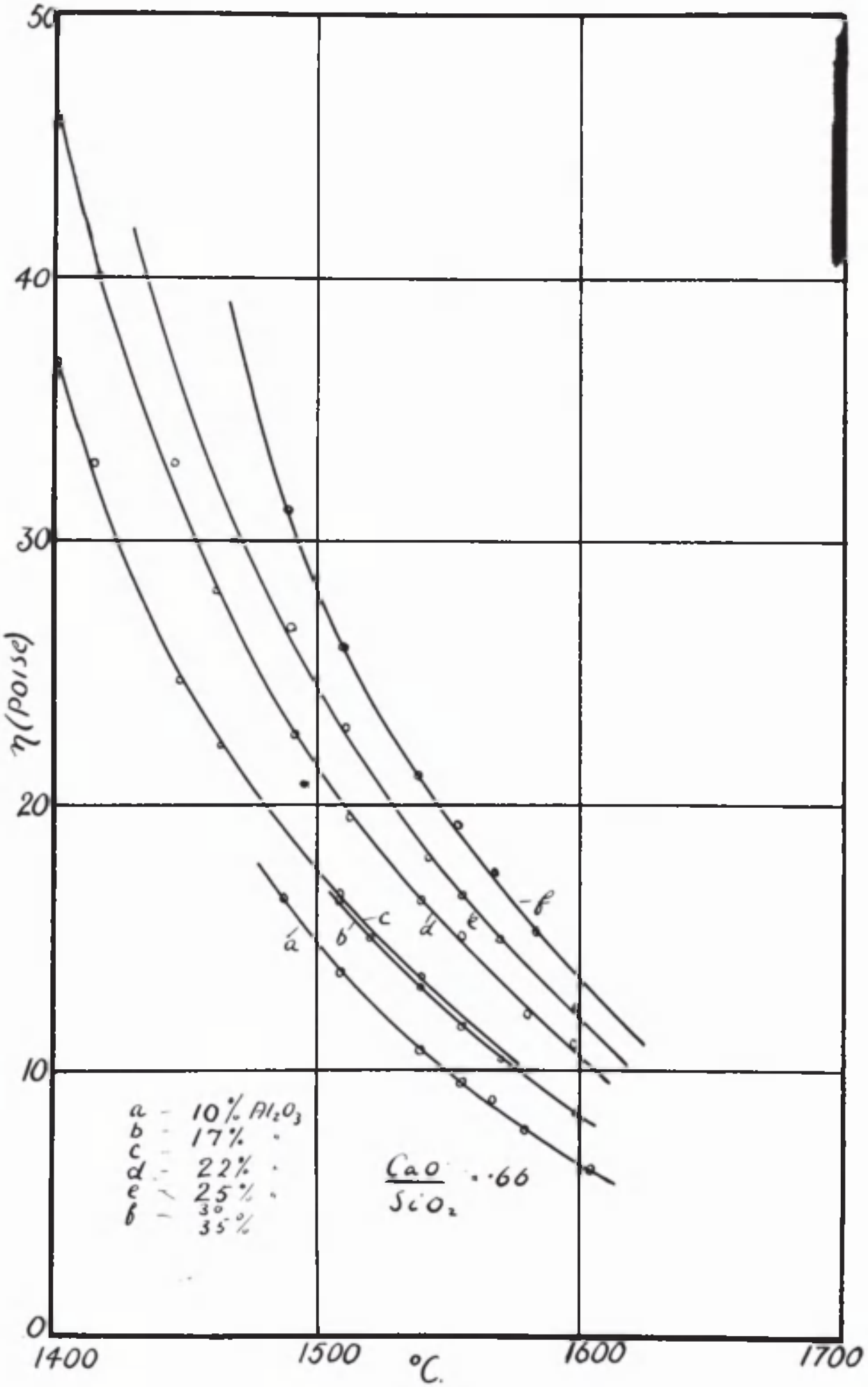
50
40
30
20
10
0
η (poise)
1400
1500
1600
1700
°C.
a
b
c
d
e
f
a - 10% Al2O3
b - 17% "
c - 22% "
d - 25% "
e - 30 35%
CaO / SiO2 .66

fig. 61.

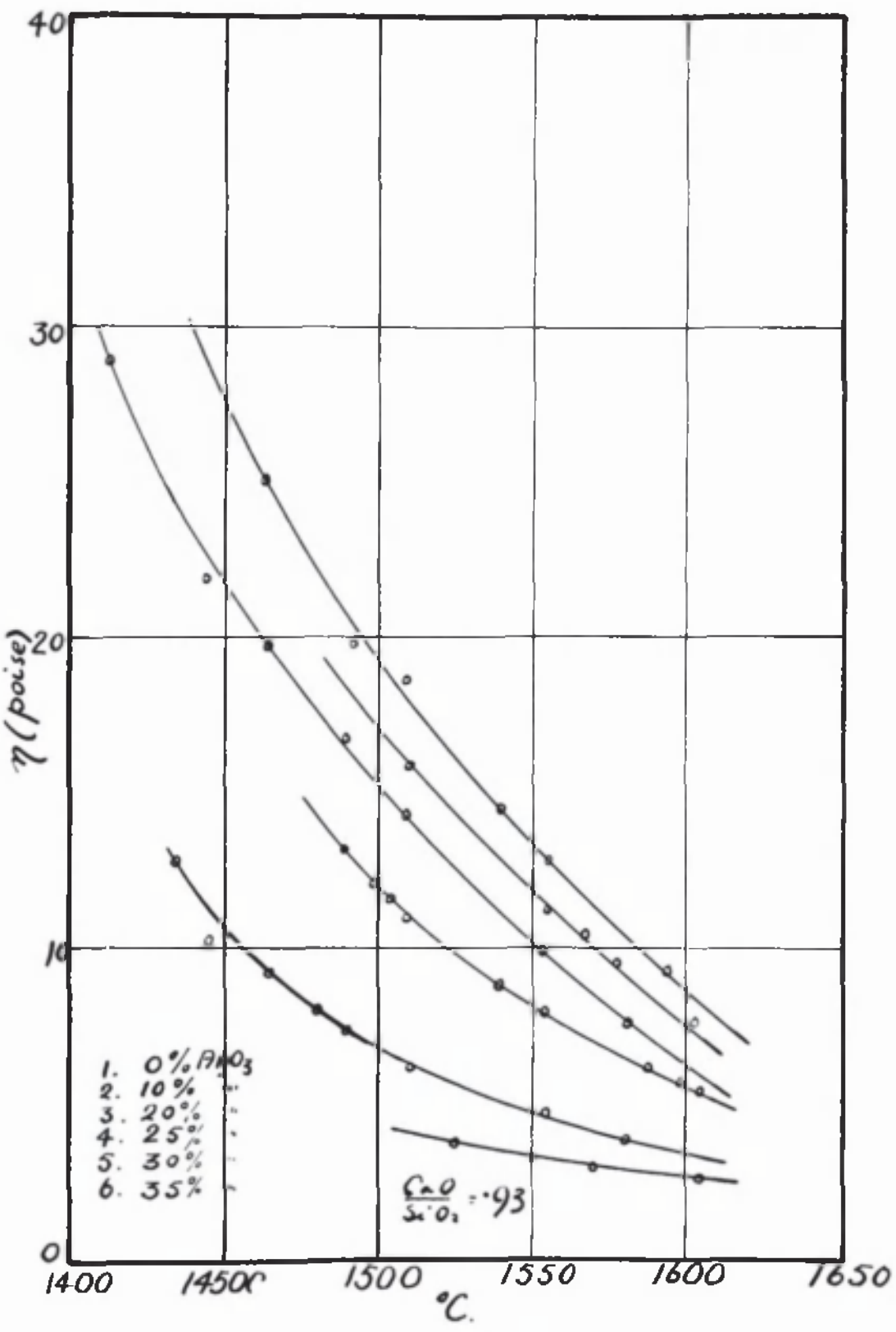
40
30
20
10
0
η (poise)
1400
1450
1500
1550
1600
1650
°C.
1. 0% Al2O3
2. 10%
3. 20%
4. 25%
5. 30%
6. 35%
CaO / SiO2 = ·93

fig. 62.

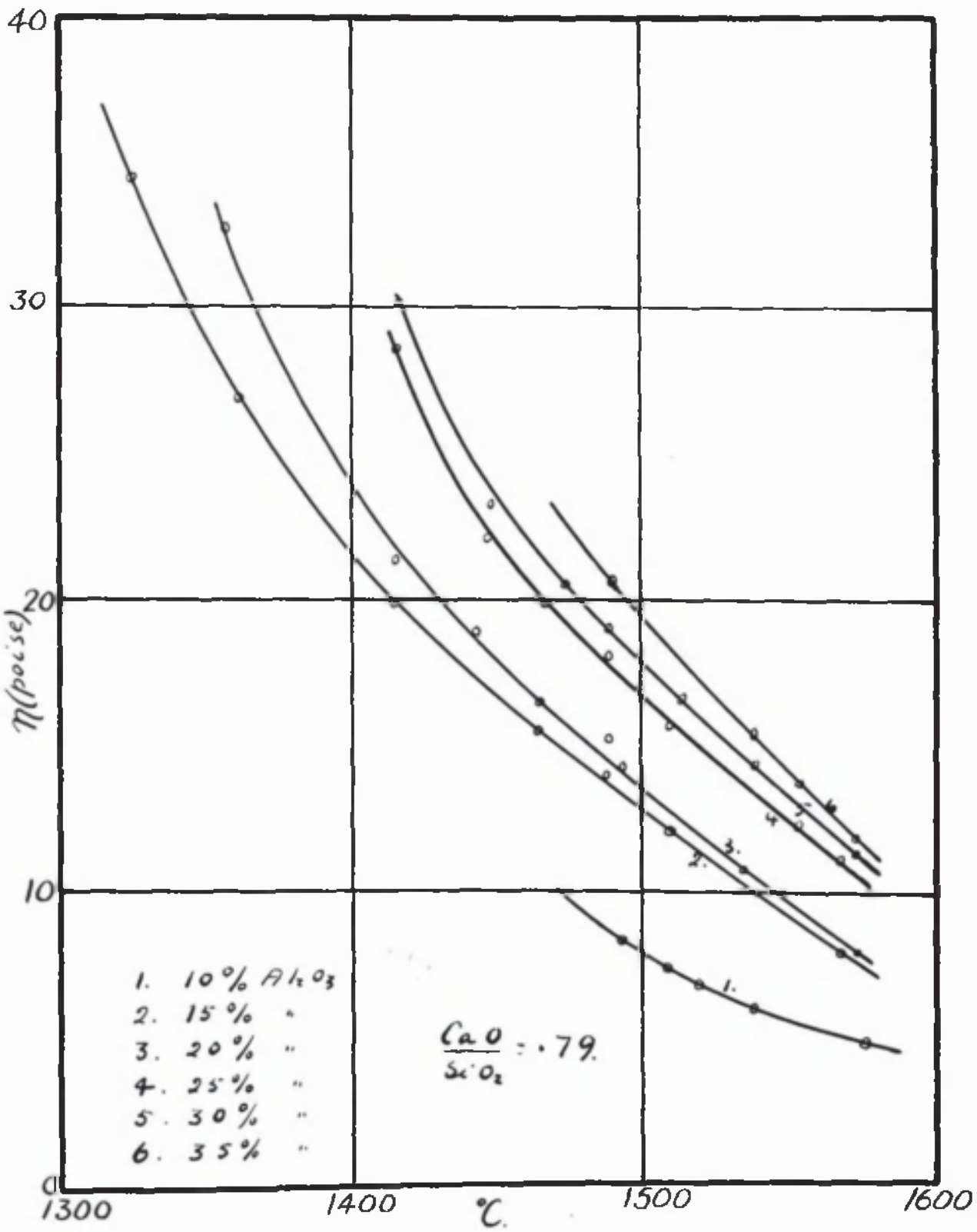
40
30
20
10
0
η (poise)
1300
1400
1500
1600
°C.
1. 10% Al2O3
2. 15% "
3. 20% "
4. 25% "
5. 30% "
6. 35% "
CaO / SiO2 = .79.

Fig. 63.

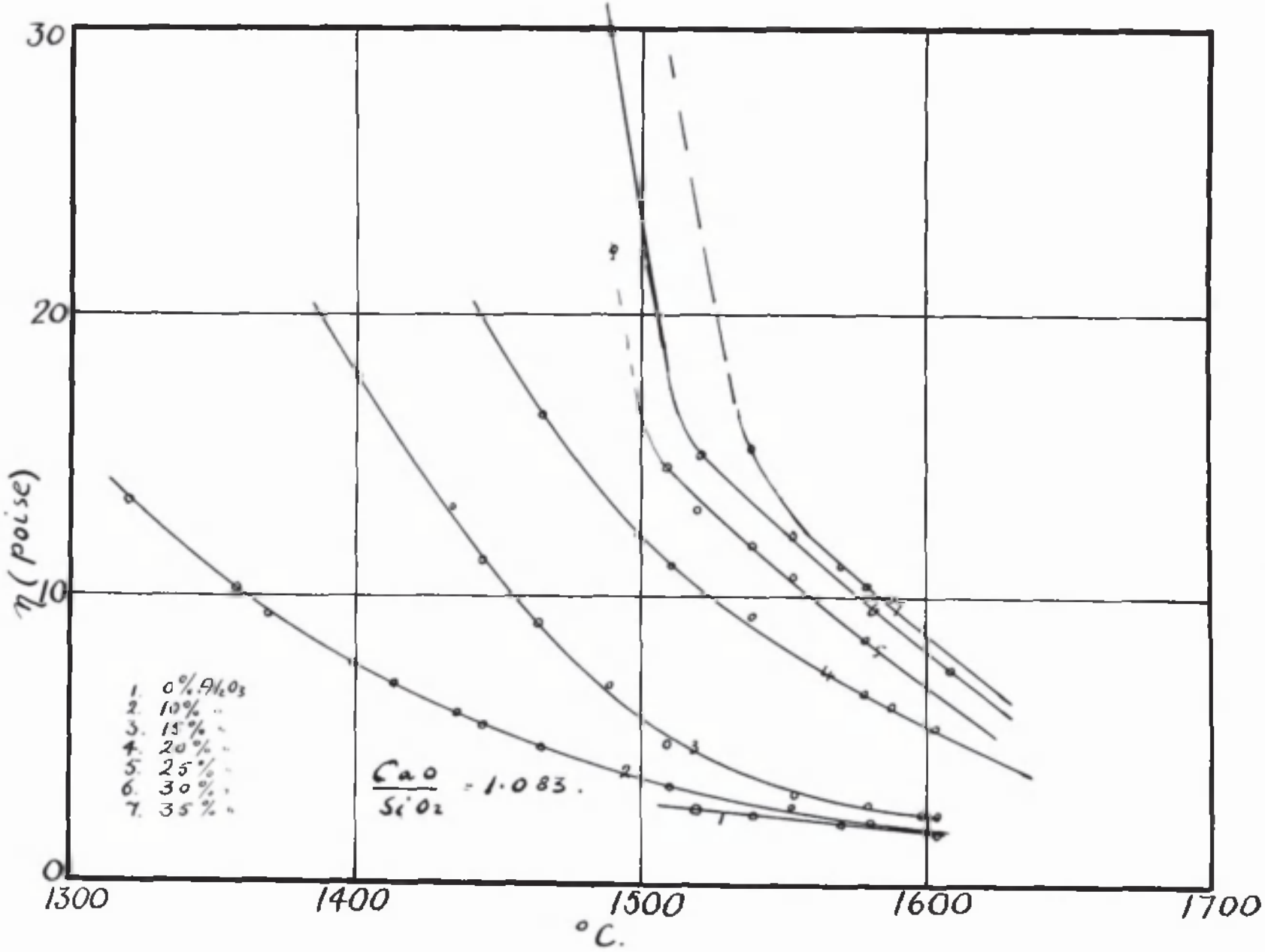
30
20
10
0
η (poise)
1300
1400
1500
1600
1700
°C.
1. 0% Al2O3
2. 10% "
3. 15% "
4. 20% "
5. 25% "
6. 30% "
7. 35% "
CaO / SiO2 = 1·083.

fig. 64.

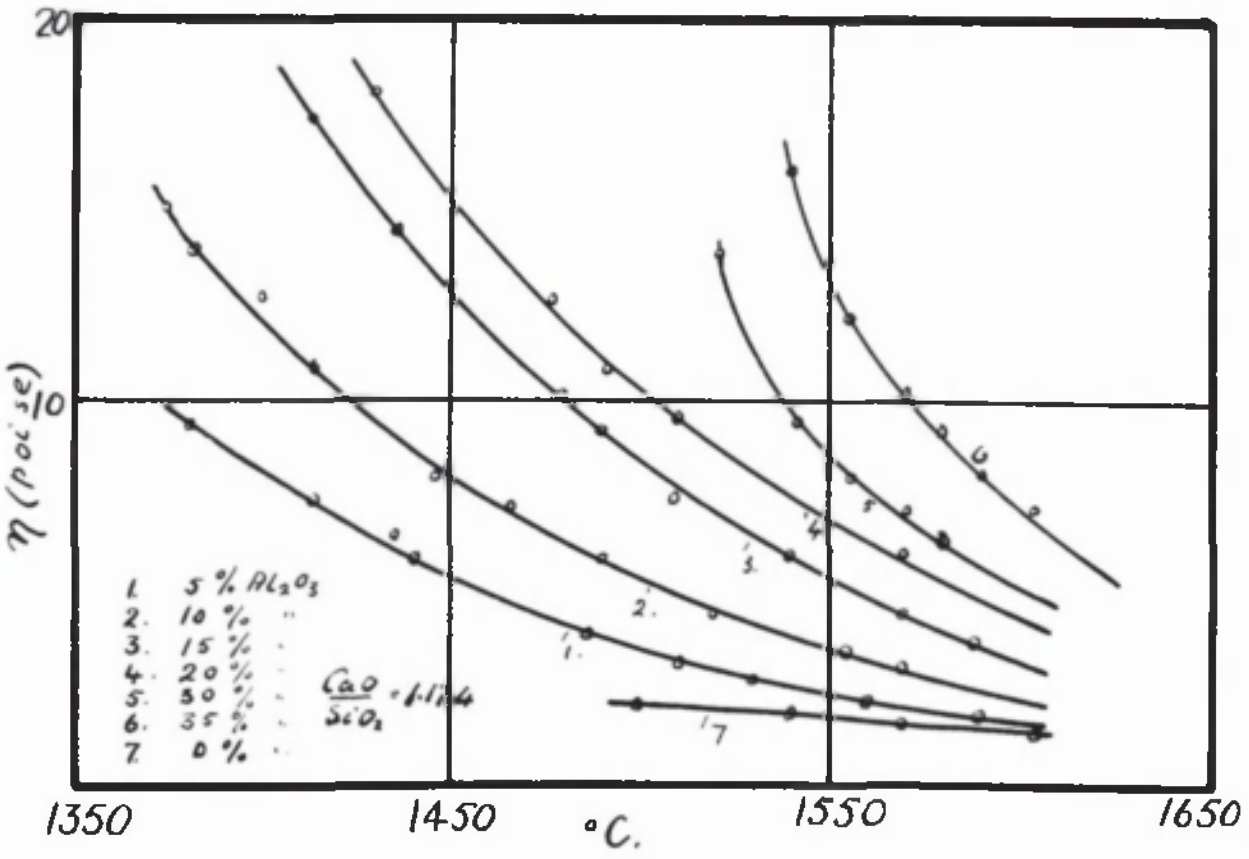
20
10
η (Poise)
1. 5 % Al_2O_3
2. 10 % "
3. 15 % "
4. 20 % "
5. 30 % "
6. 35 % "
7. 0 % "
$\frac{CaO}{SiO_2}$ = 1.114
1350
1450
°C.
1550
1650

fig. 65

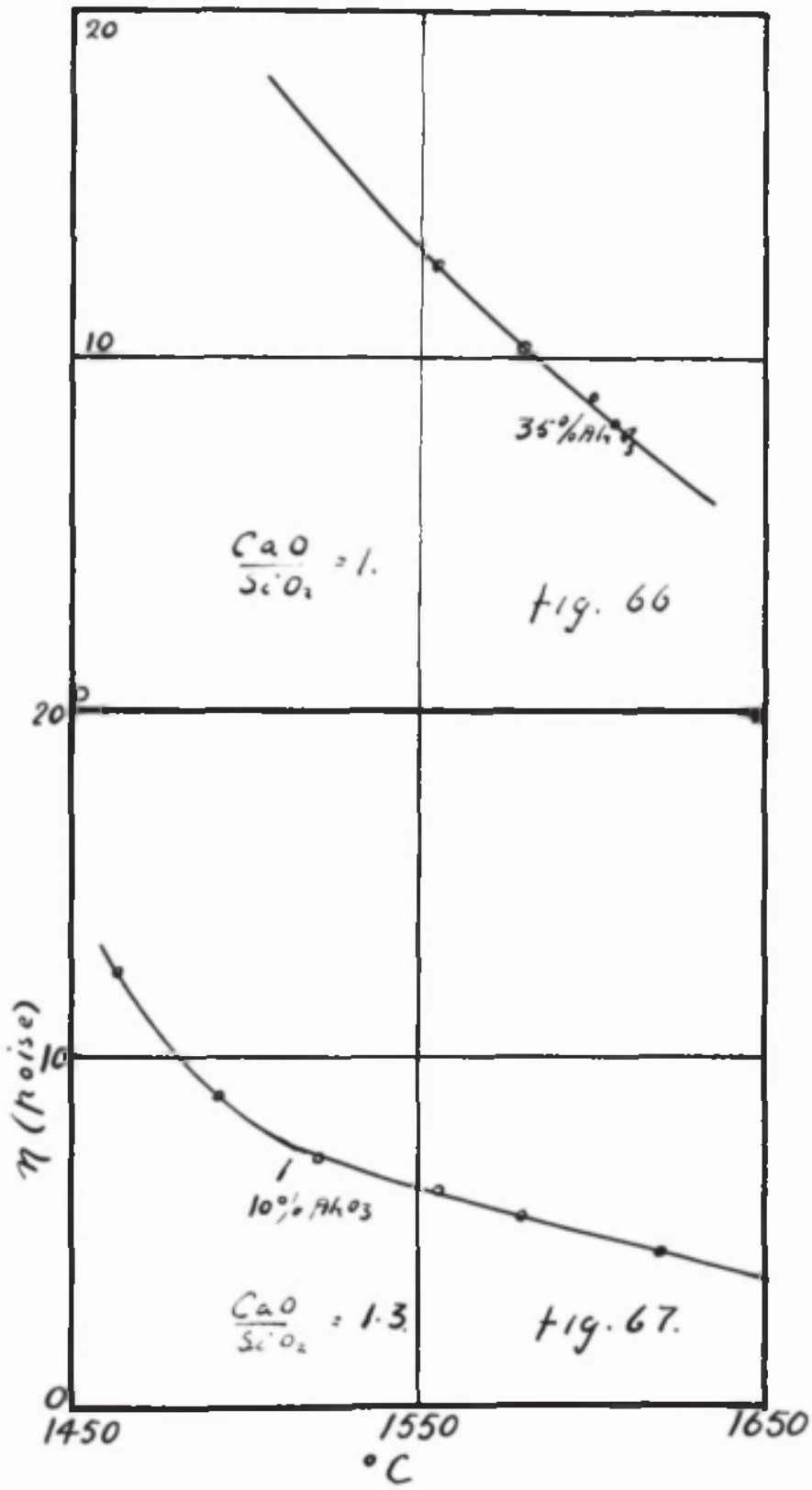
20
10
35% Al2O3
CaO / SiO2 = 1.
fig. 66
20
10
η (noise)
1
10% Al2O3
CaO / SiO2 = 1.3
fig. 67.
0
1450
1550
1650
°C

rapidly increasing temperature of the liquidus.

The slags were prepared from pure $CaCO_3$, anhydrous Al_2O_3 and SiO_2. Analysis of the slags before and after the viscosity experiments showed that no alteration in the compositions occurred. It was found necessary to employ both the concentric cylinder and the logarithmic decrement methods. The experimental procedure was the same as that described for the blast furnace slag.

The results are shown in tables XXVI-XXIV and the viscosity-temperature curves in figs. 59-67.

Table XXVI

$\frac{CaO}{SiO_2}$ = .428

% Composition CaO	SiO_2	Al_2O_3	Temp. °C	(M-f)T	η (poise)
28.5	66.5	5.0	1610	72	24.9
			1580	80	27.6
			1555	100	34.5
			1530	111	38.3
			1500	147	50.7
			1445	248	85.6
27	63	10	1600	82	28.3
			1580	100	34.5
			1560	114	39.3
			1545	125	43.1
			1520	145	50.0
25.5	59.5	15	1620	67	23.1
			1580	104	35.9
24	56	20	1620	93	32.0
			1580	138	47.6
			1555	175	60.3
			1536	231	80.0
22.5	52.5	25	1635	88	30.3
			1590	124	42.8
21	49	30	1645	75	25.9
			1635	92	31.7
			1605	121	41.7
			1590	157	54.2
			1580	170	58.6
19.48	45.52	35	1645	75	25.9
			1635	92	31.7
			1605	121	41.7
			1590	157	54.2

Table XXVII

$\frac{CaO}{SiO_2}$ = .60

33.75	56.25	10	1570	31	10.7
			1555	35	12.4
			1540	40	13.8
			1510	47	16.2
			1490	49.5	17.0
			1465	59.0	20.4
			1435	73.5	25.4
			1415	78	26.9
			1400	96	33.1

Table XXVIII

$\frac{CaO}{SiO_2} = .66$

% Composition CaO	SiO_2	Al_2O_3	Temp. °C	$Log_{10}p$	η (poise)
35.8	54.2	10	1605	.260	6.2
			1580	.301	7.4
			1570	.342	8.7
			1555	.365	9.4
			1540	.404	10.4
			1510	.512	13.4
			1490	.605	16.4
33	50	17	1600	.340	8.6
			1580	.377	9.7
			1570	.399	10.4
			1555	.444	11.7
			1540	.484	12.8
			1520	.555	15.0
			1510	.602	16.3
				(M-f)T	
31	47	22	1580	27.3	9.4
			1560	33	11.4
			1540	39	13.5
			1510	49	16.9
			1490	52	18.0
			1460	64	22.0
			1445	71	24.5
			1415	95.4	32.9
			1400	106	36.6
29.9	45.1	25	1600	33.6	11.6
			1580	35	12.0
			1570	42	14.5
			1555	44.6	15.4
			1540	48	16.6
			1510	57.3	19.5
			1490	65.7	22.7
			1460	82	28.3
			1445	96	33.1
			1414	115.6	39.9
			1400	134	46.2
27	41	32	1600	36.6	12.6
			1580	38	13.1
			1570	43.3	14.9
			1555	48	16.6
			1540	52	18.0
			1510	67	23.1
			1490	78	26.9
			1460	87	30.0
25.9	39.1	35	1585	43.6	15
			1570	50	17.3
			1555	55	19
			1540	61	21
			1510	75	25.9
			1490	90	31

Table XXIX

$\frac{CaO}{SiO_2} = .79$

% Composition CaO	SiO_2	Al_2O_3	Temp. °C	$Log_{10}\eta$	(M-f)T	η (poise)
39.8	50.2	10	1570	.212		4.8
			1540	.2455		5.8
			1520	.2742		6.6
			1510	.2900		7.1
			1495	.3222		8.1
37.5	47.5	15	1570	.3075	--	7.6
			1510		34.2	11.9
			1490		41.0	14.1
			1465		44.0	15.2
			1445		52.0	17.9
			1414		56.3	19.4
			1358		77.5	26.7
			1324		99.5	34.3
			1316		143.0	49.3
35.3	44.7	20	1575	.3075		7.6
			1536	.3979		10.4
			1495	.5300		14.2
			1540		29.5	10.2
			1510		36	12.4
			1490		44	15.2
			1465		47	16.2
			1445		55	19.0
			1414		61	21.0
			1358		95	32.8
			1315		127	43.8
33.1	41.9	25	1570		32.6	11.2
			1555		36	12.4
			1540		41.6	14.4
			1510		45	15.5
			1490		53	18.3
			1465		56.6	19.5
			1445		63.6	21.9
			1414		83	28.6
30.9	39.1	30	1575		32.4	11.2
			1540		41	14.1
			1510		44.2	15.3
			1490		54	18.6
			1475		59	20.4
			1445		66.7	23.0
			1414		87	30.0
28.7	36.3	35	1575		35.5	11.9
			1555		39.0	13.5
			1490		59.4	20.5
			1465		76.4	26.4
			1442		88.0	30.4

$\frac{CaO}{SiO_2}$ = .93 Table XXX

% Composition CaO	SiO_2	Al_2O_3	Temp. °C	$Log_{10}p$	(M-f)T	η (poise)
43.36	46.64	10	1580	.1761		3.8
			1555	.1987		4.4
			1540	.2175		5.0
			1510	.2553		6.1
			1490	.2945		7.3
			1480	.3324		8.4
			1465	.3579		9.1
			1445	.3979		10.3
			1435	.4900		13.0
38.54	41.46	20	1605	.2304		5.4
			1600	.2455		5.8
			1583	.2577		6.2
			1555	.3160		7.9
			1538	.3424		8.7
			1510	.4150		10.8
			1500	.4533	37.2	12.4
			1490		39.0	13.5
36.1	38.9	25	1580	.2967		7.3
			1555	.3802		9.8
			1510	.5340	42	14.4
			1490		49	16.9
			1465		58	20.0
			1445		63.4	21.9
			1414		84	29.0
33.7	36.3	30	1605	.3096		7.6
			1600	.3424		8.7
			1580	.3747		9.6
			1570	.4065		10.5
			1555	.4249		11.2
			1510	.5843		15.8
31.3	33.7	35	1580		30.4	10.5
			1555		36.4	12.6
			1540		41	14.1
			1510		54	18,6
			1490		56.2	19.4
			1465		73.0	25.2

Table XXXI

$\frac{CaO}{SiO_2}$ = 1

% Composition CaO	SiO_2	Al_2O_3	Temp. °C	$Log_{10}p$	η(poise)
32.5	32.5	35	1605	.3222	8.1
			1600	.3598	9.2
			1580	.4031	10.4
			1550	.4871	13.0

Table XXXII

$\frac{CaO}{SiO_2} = 1.083$

% Composition CaO	SiO_2	Al_2O_3	Temp. °C	$Log_{10}p$	(M-f)T	η (poise)
46.8	43.2	10	1605	.2718		1.8
			1580	.3160		2.2
			1555	.1461		2.9
			1510	.1644		3.5
			1465	.2068		4.7
			1445	.2380		5.6
			1435	.2553		6.1
			1414	.2878		7.0
			1400	.3118		7.8
			1370	.3692		9.4
			1360	.3979		10.3
			1320	.5024		13.4
44.2	40.8	15	1605	.3385		2.4
			1600	.3502		2.5
			1580	.3711		2.8
			1555	.1523		3.1
			1510	.2122		4.9
			1490	.2923		7.2
			1465	.3541		9.0
			1445	.4314		11.3
			1435	.5051		13.4
			1400	.6628		18.2
41.6	38.4	20	1605	.2380		5.6
			1590	.2672		6.4
			1580	.2788		6.8
			1540		28.0	9.6
			1510		32.0	11.0
			1500		36.1	12.5
			1465		46.6	16.0
39	36	25	1580	.2095		8.6
			1555	.2648		11.0
			1540	.2945		12.0
			1520	.3181		13.0
			1510	.3560		14.6
			1490	.5647		22.4
36.4	33.6	30	1610	.1847		7.6
			1580	.2095		8.6
			1550	.3010		12.3
			1520	.3655		15.0
			1510	.4669		19.0
			1490	.7443		31.0
33.8	31.2	35	1600	.2122		8.8
			1580	.2601		10.8
			1570	.2765		11.4
			1540	.3729		15.4

Table XXXIII

$\frac{CaO}{SiO_2} = 1.174$

% Composition CaO	SiO_2	Al_2O_3	Temp. °C	$Log_{10} p$	η (poise)
51.3	43.7	5	1585	.2718	1.8
			1559	.3010	2.1
			1530	.3617	2.6
			1510	.4249	3.1
			1480	.5185	3.9
			1442	.2480	5.9
			1435	.2788	6.8
			1414	.3010	7.4
			1390	.3617	9.2
			1378	.5024	13.4
48.6	41.4	10	1570	.1614	3.4
			1555	.1761	3.8
			1520	.1987	4.4.
			1490	.2504	6.0
			1445	.3222	8.0
			1414	.4314	11.2
47.8	40.8	11.3	1580	.1584	3.2
			1570	.1703	3.6
			1555	.1847	4.0
			1520	.2068	4.7
			1490	.2480	5.8
			1465	.2945	7.2
			1445	.3160	7.9
			1435	.3579	9.1
			1414	.4314	11.2
			1400	.4843	12.9
			1390	.5211	14.0
			1378	.5658	15.3
45.9	39.1	15	1590	.1703	3.6
			1570	.1959	4.4
			1540	.2504	6.0
			1508	.3054	7.6
			1490	.3560	9.1
			1480	.3979	10.3
			1445	.4314	11.2
			1435	.5441	14.6
			1414	.6405	17.6
43.2	36.8	20	1584	.1492	6.0
			1570	.1553	6.3
			1510	.2380	9.8
			1490	.2648	11.0
			1460	.3424	14.0
			1442	.3802	15.6
			1431	.4518	18.6
40.5	34.5	25	1585	.2122	8.8
			1570	.2405	9.9
			1540	.3385	13.8
			1520	.3711	15.3
37.8	32.2	30	1610	.1367	5.5
			1582	.1584	6.4
			1570	.1790	7.4
			1555	.1903	7.8
			1540	.2253	9.3
			1520	.3424	14.2
35.1	29.9	35	1605	.1875	7.7
			1590	.2000	8.2
			1580	.2304	9.4
			1570	.2601	10.8
			1555	.2900	12.2
			1540	.3927	16.2

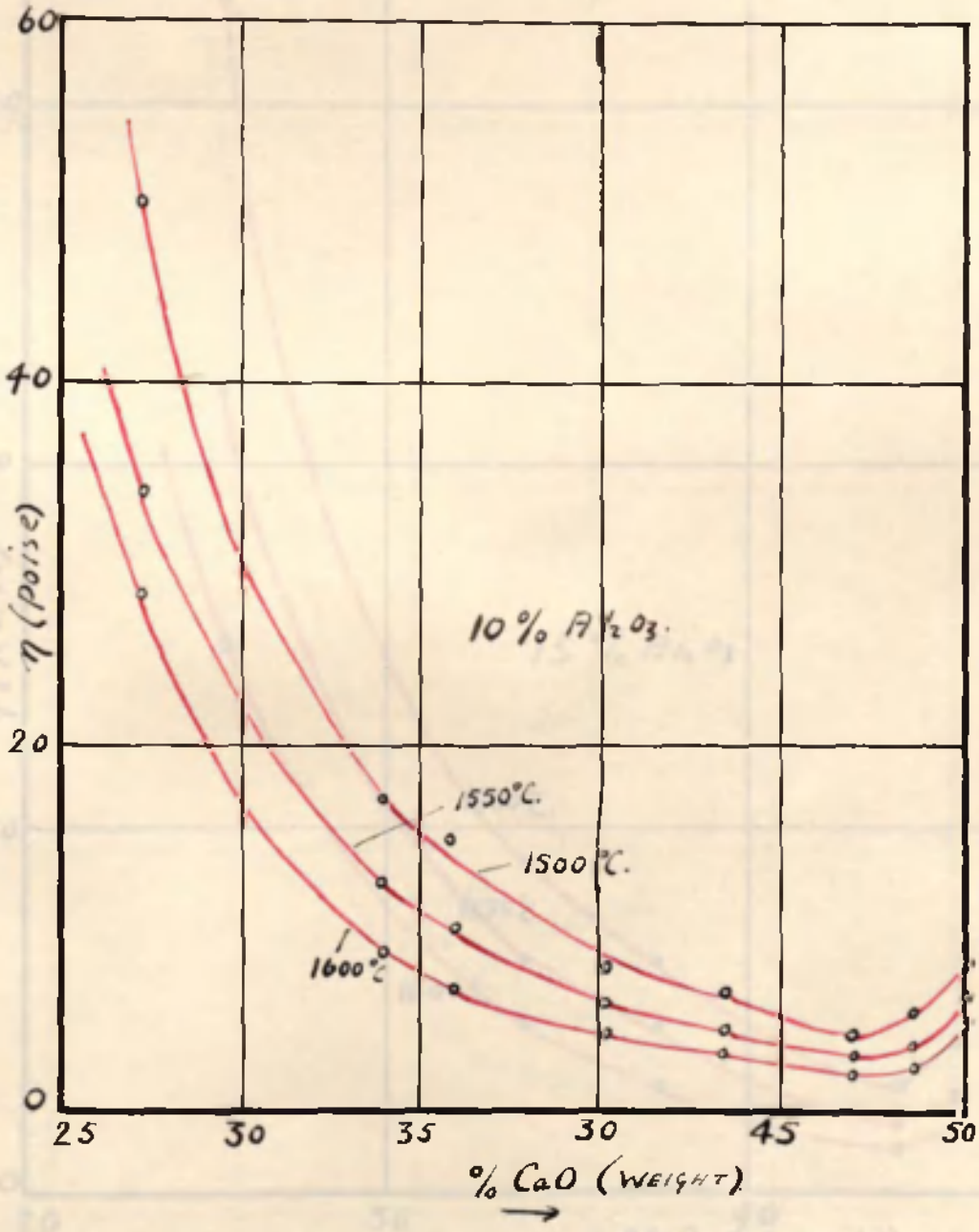
60
40
20
0
η (poise)
10% Al2O3.
1550°C.
1500°C.
1600°C.
25
30
35
30
45
50
% CaO (WEIGHT)

fig. 68.

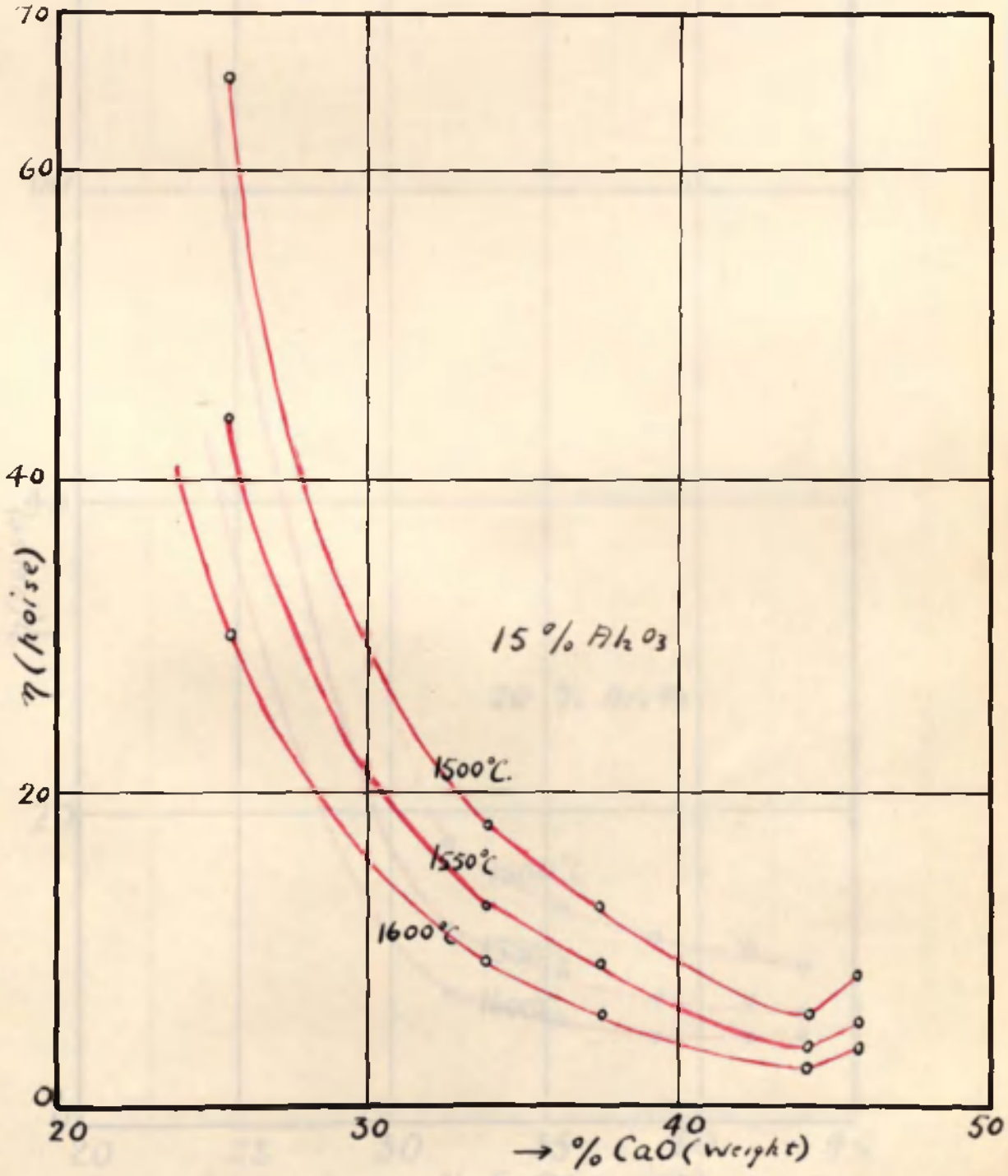
70
60
40
20
0
η (poise)
15 % Al2O3
1500°C.
1550°C
1600°C
20
30
40
50
→ % CaO (weight)

fig. 69.

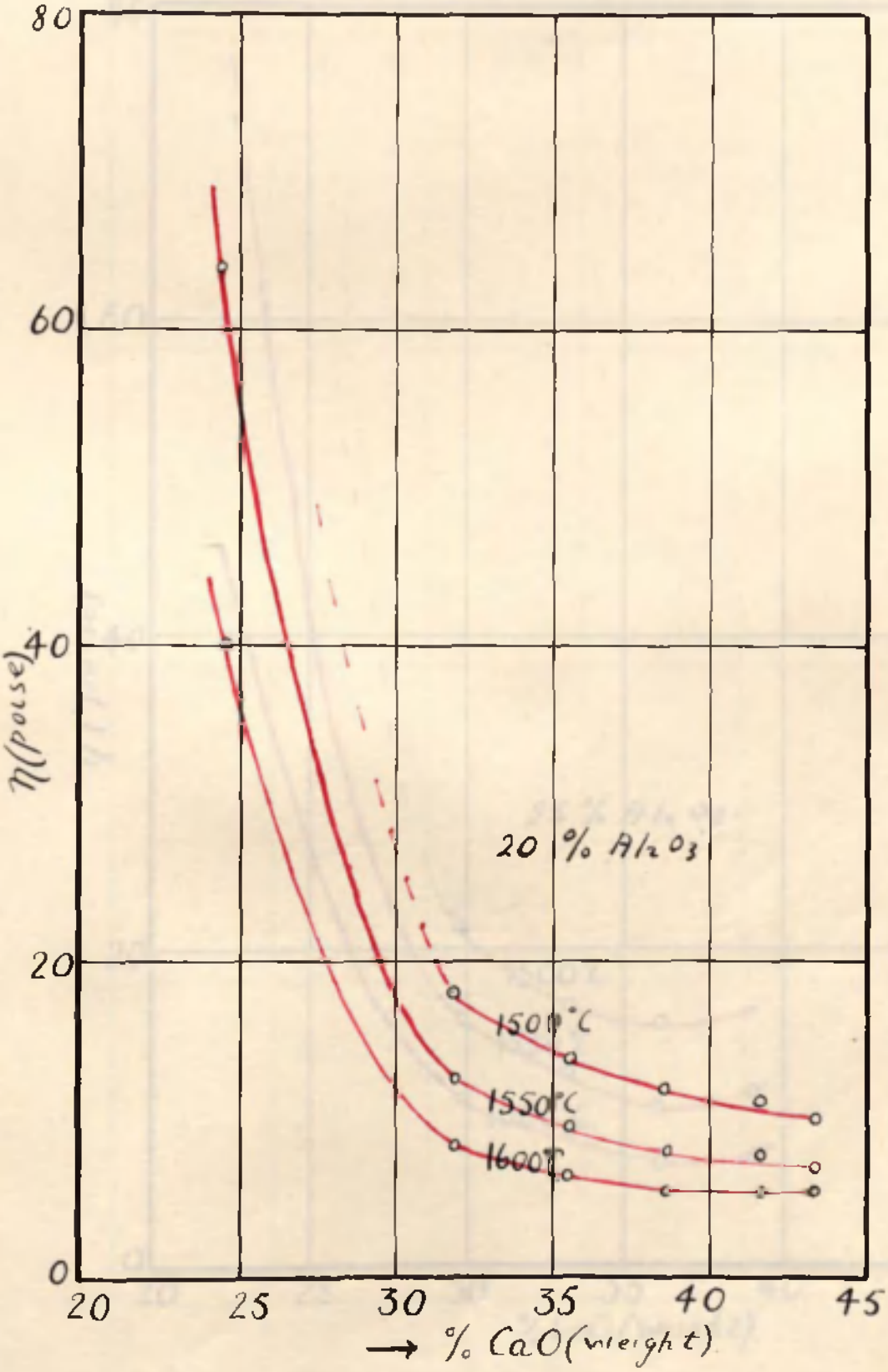
80
60
40
20
0
η(Poise)
20 % Al2O3
1500°C
1550°C
1600°C
20
25
30
35
40
45
→ % CaO (weight)

fig. 70.

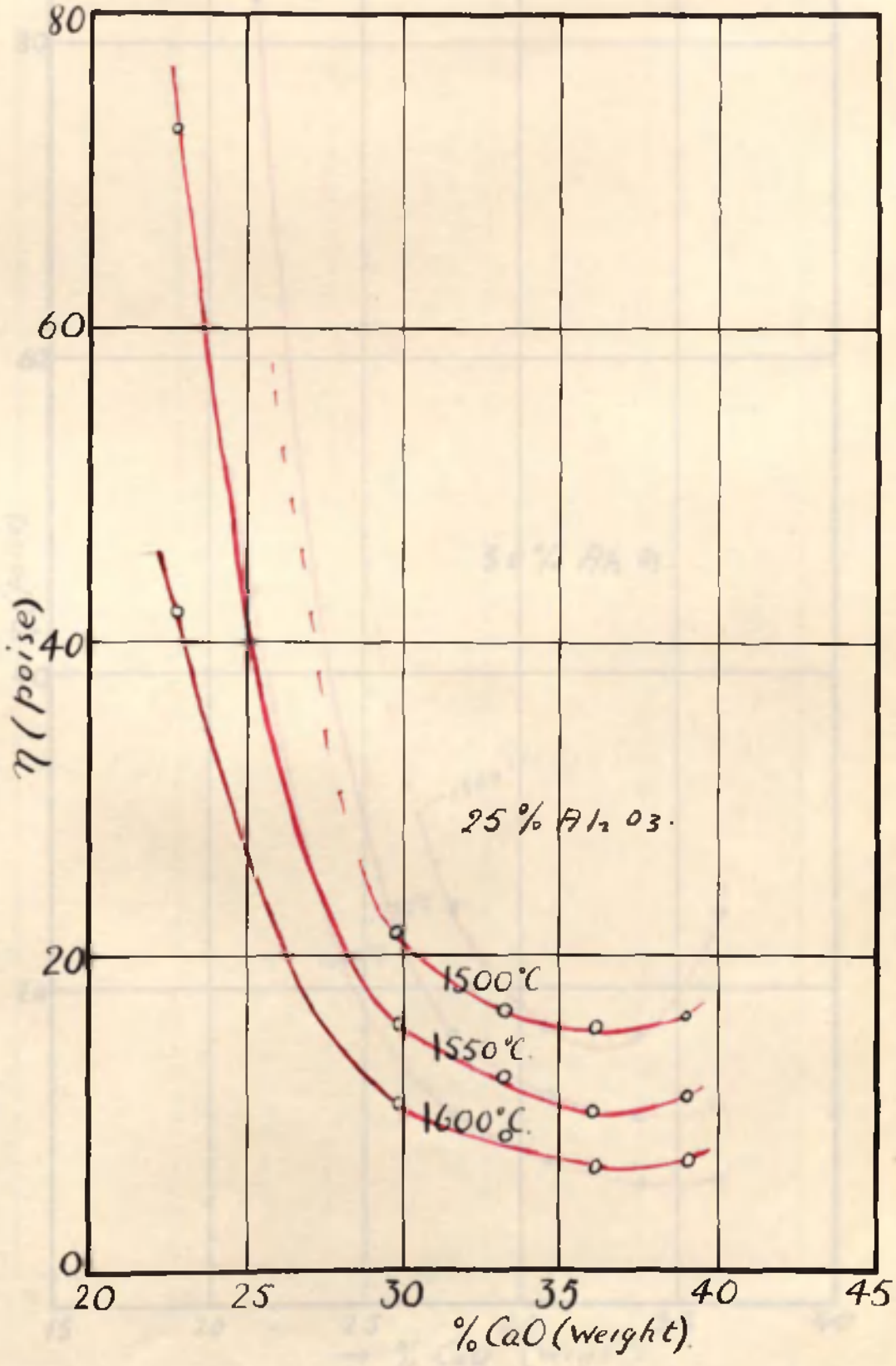
80
60
40
20
0
η (poise)
25 % Al2 O3.
1500°C
1550°C
1600°C
20
25
30
35
40
45
% CaO (weight)

fig. 71.

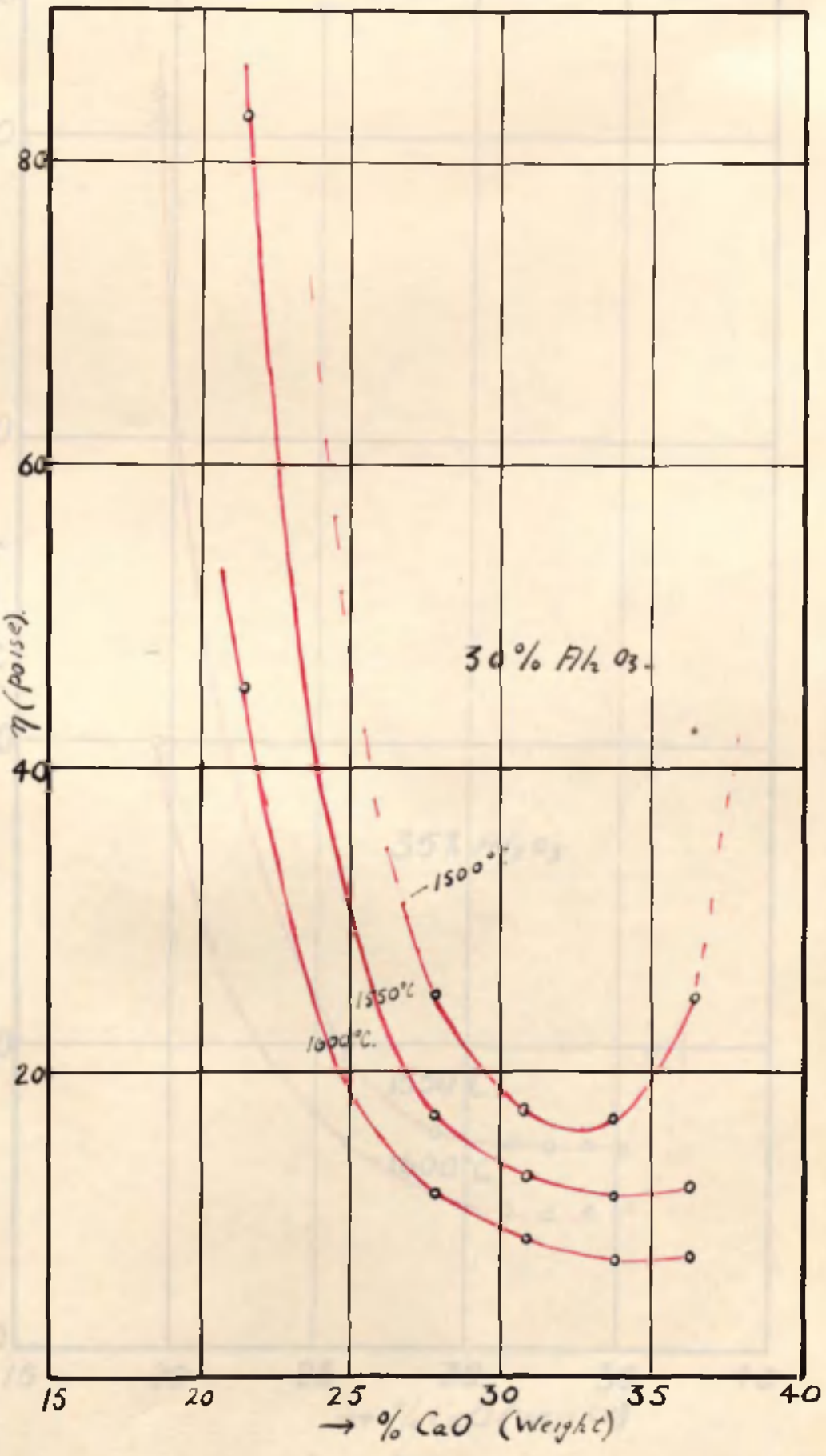
80
60
40
20
η (poise).
30 % Al2 O3.
1500°C.
1350°C.
1000°C.
15
20
25
30
35
40
→ % CaO (Weight)

fig. 72.

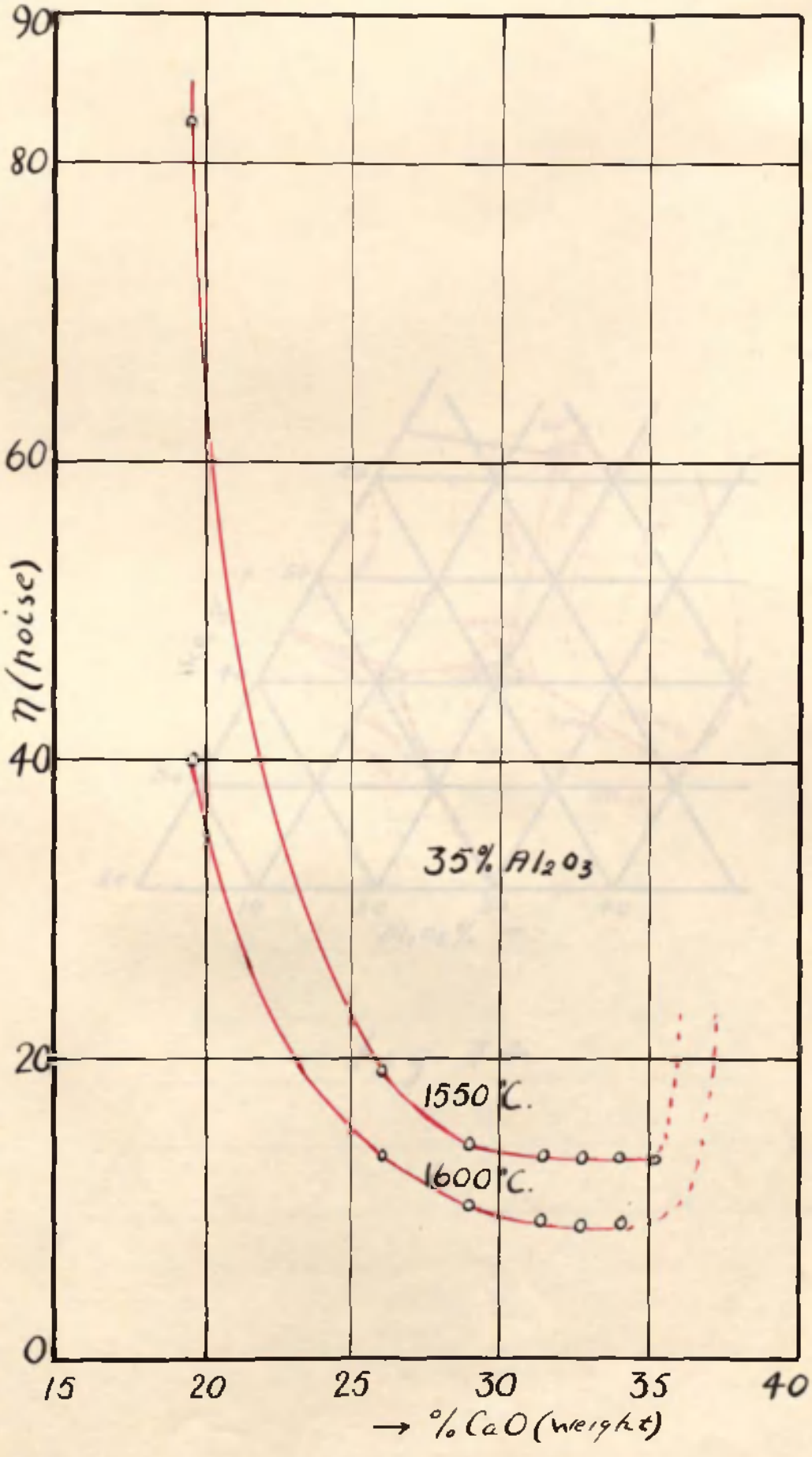
90
80
60
40
20
0
η (noise)
35% Al2O3
1550°C.
1600°C.
15
20
25
30
35
40
→ % CaO (weight)

fig. 73.

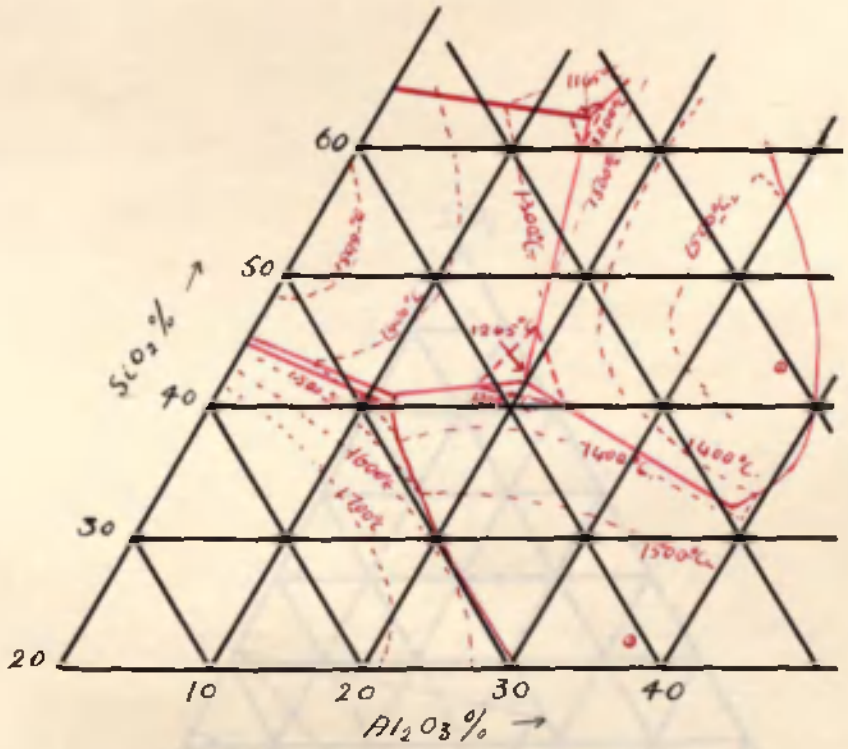

fig. 74

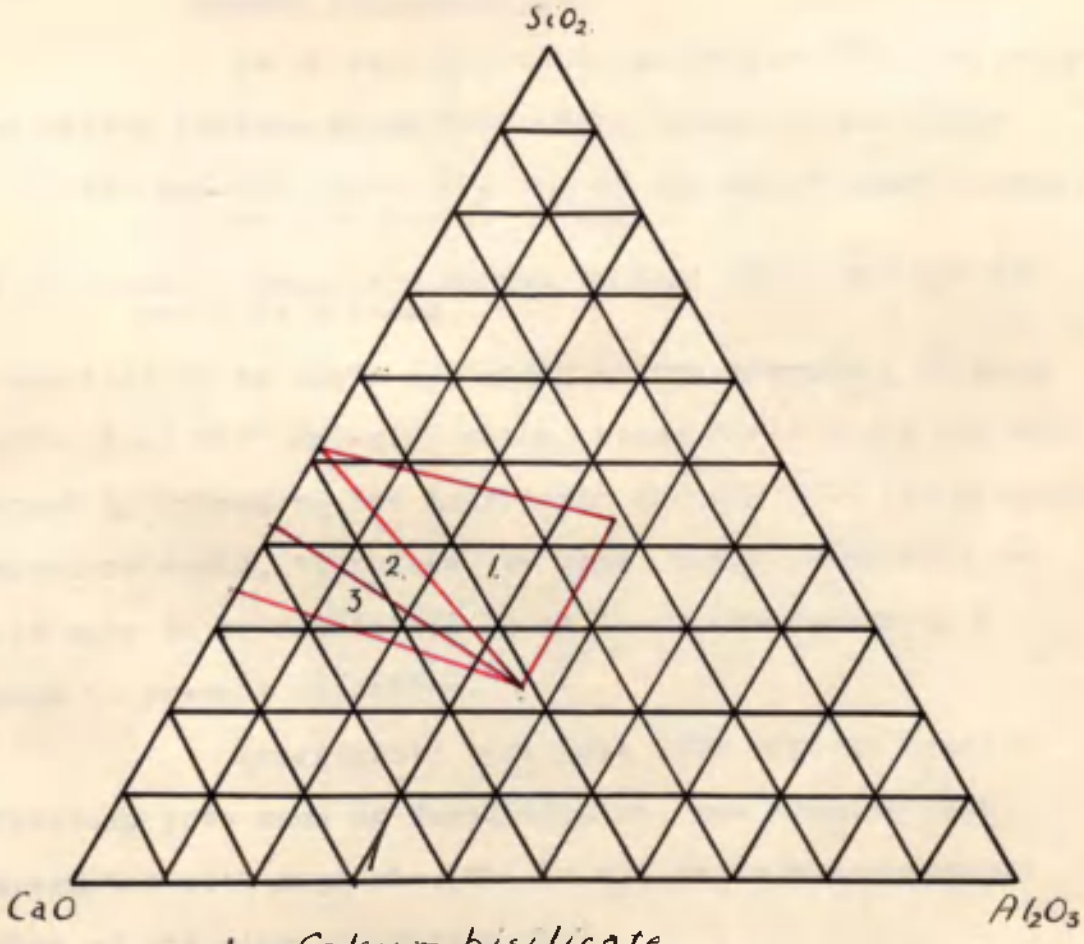

1. Calcium bisilicate.
   Gehlinite.
   Anorthite.
2. Calcium bisilicate.
   " sesquisilicate.
   Gehlinite.
3. Calcium Sesquisilicate.
   " orthosilicate.
   Gehlinite.

fig. 75.

Table XXXIV

$\frac{CaO}{SiO_2} = 1.3$

% Composition CaO	SiO_2	Al_2O_3	Temp. C	$Log_{10}P$	η (poise)
50.9	39.1	10	1620	.1139	4.5
			1580	.1367	5.5
			1555	.1523	6.2
			1520	.1703	7.0
			1490	.2122	8.8
			1460	.3010	12.6
36.8	28.2	35	1655	.2878	12.0
			1645	.3139	13.0
			1635	.3560	14.8

The viscosity-composition isotherms are shown in figs.68-73. Part of the ternary diagram $CaO-SiO_2-Al_2O_3$ is reproduced in fig. 74. Fig. 75 shows the combinations of compounds and the range of compositions covered by these combinations.

The Method for Measuring the Viscosity of Slags of the Open Hearth Furnace Type.

It is more difficult to measure the viscosity of open hearth furnace slags than blast furnace slags since

1) FeO and MnO, which are two of the chief constituents, oxidise when heated in air,

and 2) Graphite cylinders cannot be used since FeO and MnO would be reduced.

It was decided to begin the study of the viscosity of open hearth slags with $MnO-SiO_2$ slags, since these slags are not reduced by hydrogen. The molybdenum furnace with its hydrogen atmosphere could, therefore, be used. Slags containing FeO would have to be maintained in an inert atmosphere or a vacuum to prevent oxidation.

Experiments were made with various types of refractory pots such as fused alumina, and alundum pots impregnated with magnesia, but in all cases the corrosive action of the slag was very marked.

An alundum pot lined with a thin walled platinum cylinder was tried out, but on melting a mixture of MnO and SiO_2, a hole appeared in the bottom of the cylinder.

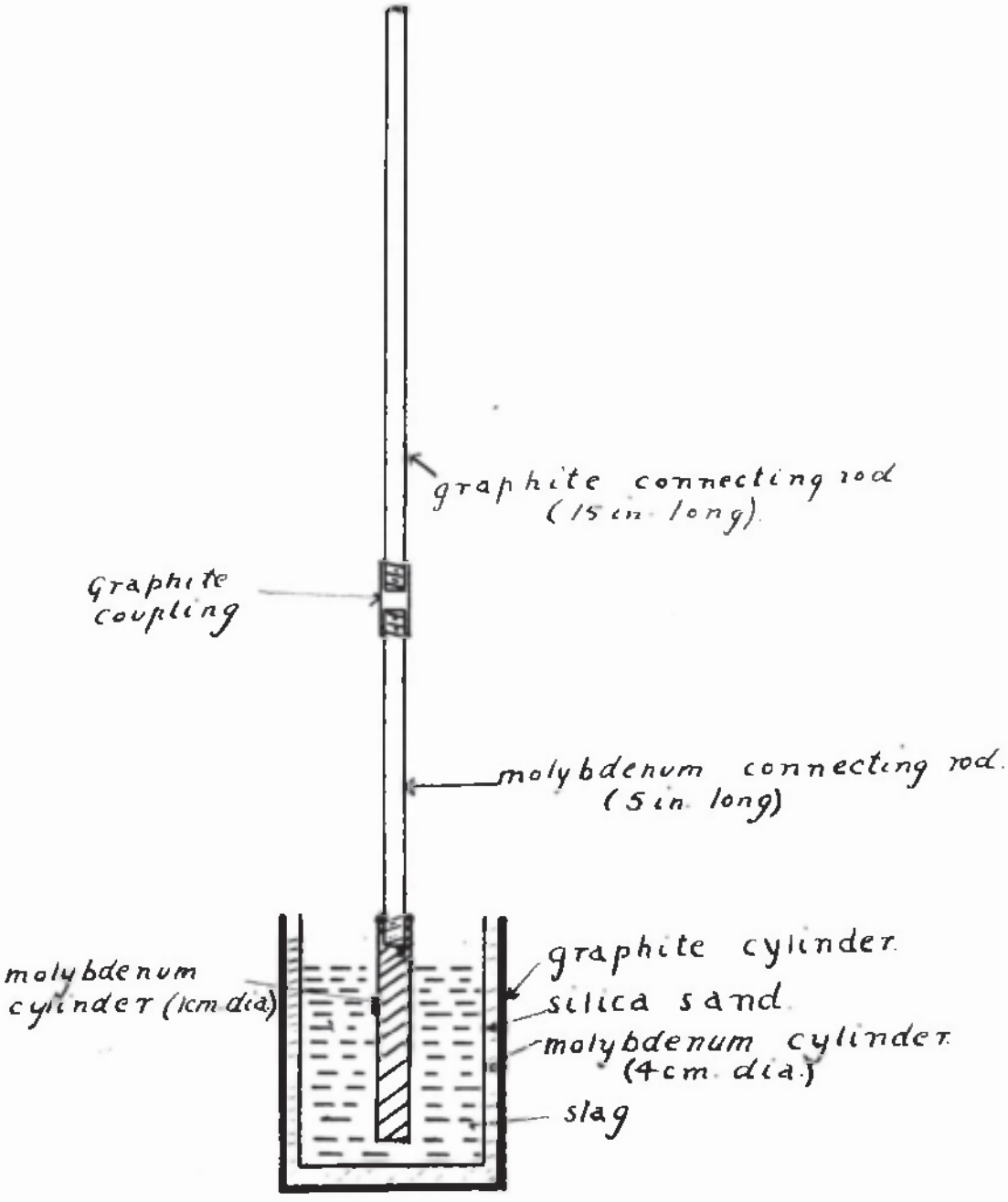
graphite connecting rod
(15 in. long)
Graphite
coupling
molybdenum connecting rod
(5 in. long)
molybdenum
cylinder (1cm dia.)
graphite cylinder
silica sand
molybdenum cylinder
(4cm. dia.)
slag

fig. 76

It was, therefore, decided to experiment with molybdenum. Molybdenum sheet can be made into a cylindrical pot and the overlaps spot welded in an atmosphere of hydrogen. However, special apparatus is required and such pots cannot be obtained in this country. For our experiments, molybdenum sheet was shaped into a cylinder, 4 cm. internal diameter, and the overlaps held with molybdenum rivets. For the high temperature experiments, this cylinder was placed inside a graphite cylinder and silica sand was packed between the graphite and the molybdenum. This is shown in fig. 76. At the high temperatures, the molybdenum pot was firmly held in the sand; the overlap was consequently prevented from opening and the slag did not leak through the pot. Analysis of the slags before and after the experiment showed that no contamination had occurred.

The greatest diameter of solid cylindrical molybdenum rod obtainable was 1 cm. A length of this rod was used as the inner cylinder. The arrangement of the oscillating inner cylinder is shown in fig. 76.

Calibration of the apparatus.

The calibration was carried out in the same way as for the previous apparatus. Results are shown in tables 35-38 and the calibration curves in figs. 77-80.

Table XXXV

Torsion tape III

Distance of weights from axis of oscillation - 1 cm.

Liquid	Temp. °C	η (poise)	Decrement (p)	$\log_{10} p$
Sugar sol.	19	.600	2.16	.3345
" "	25	.439	1.86	.2695
" "	30	.338	1.66	.2200
Lubricating oil	25	.788	2.61	.4166
" "	25	.119	1.27	.1038

Table XXXVI

Torsion tape IV

Distance of weights from axis of oscillation - 1 cm.

Liquid	Temp. °C	η (poise)	Decrement (p)	$\log_{10} p$
Sugar sol.	25	.439	1.32	.1206
Lubricating oil	25	.788	1.45	.1614
Glycerine sol	26.2	2.29	3.28	.5159
" "	28.4	1.65	2.5	.3979

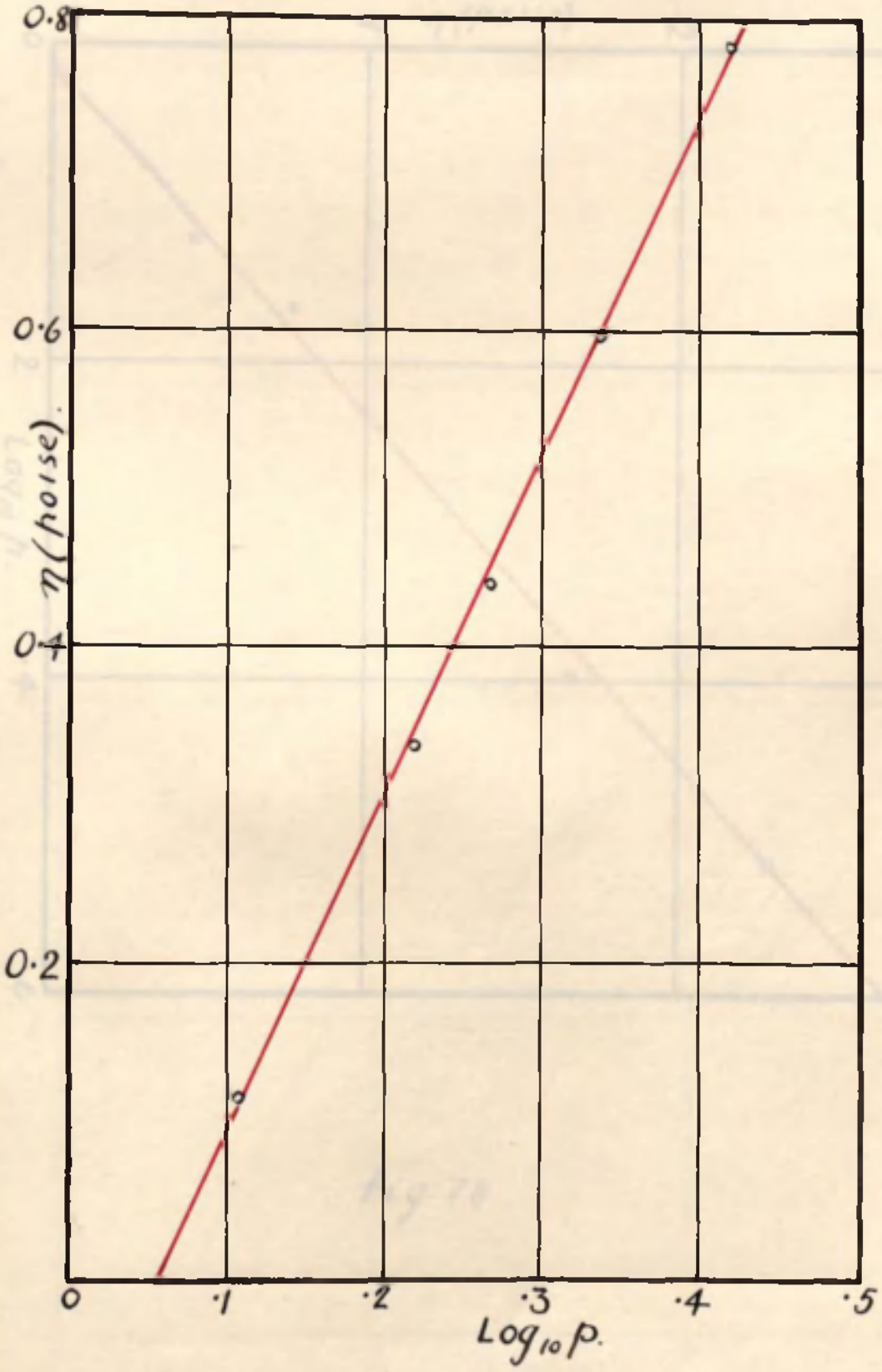

fig. 77.

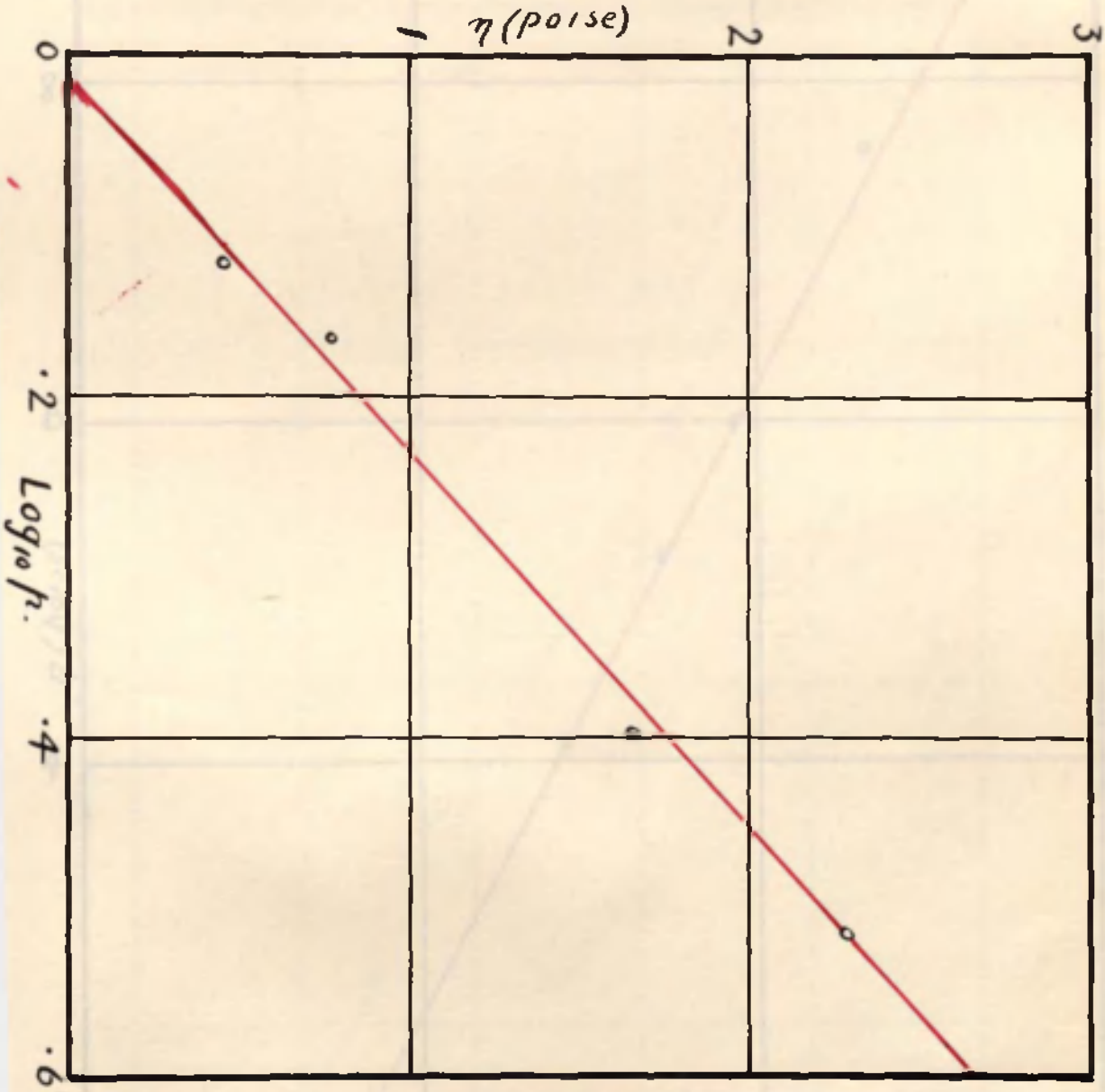

fig. 78.

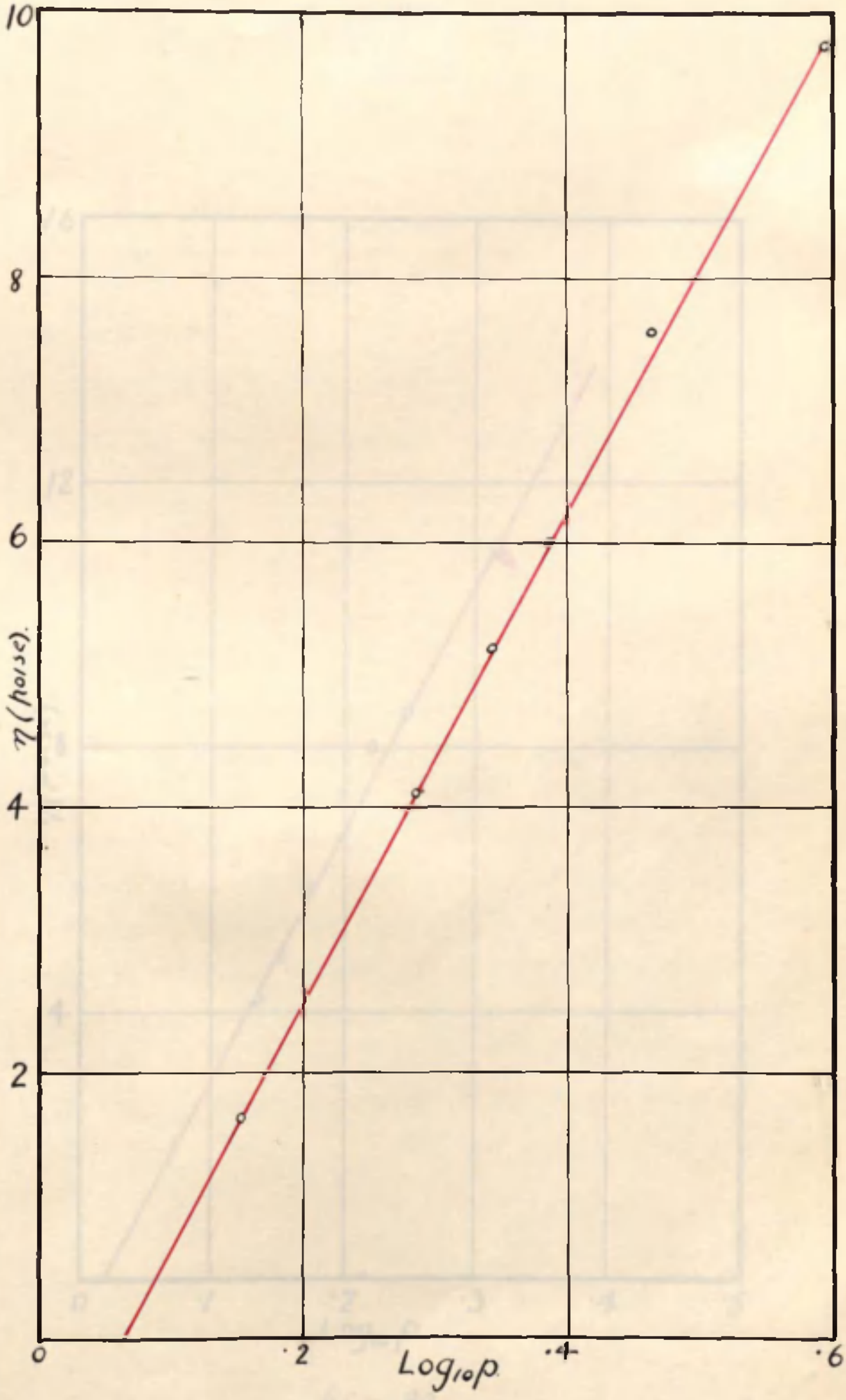

fig. 79.

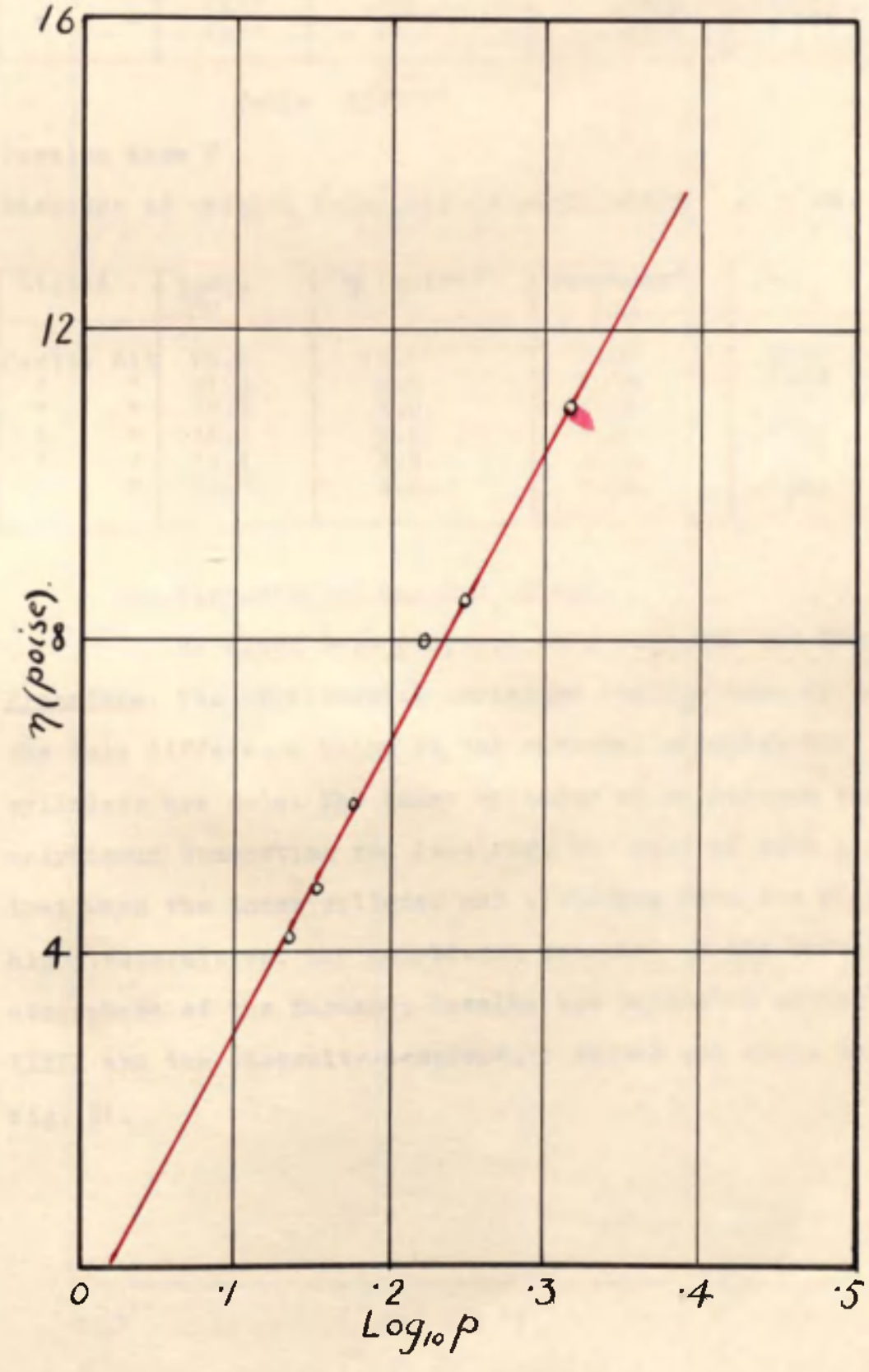

fig. 80.

Table XXXVII

Torsion tape IV

Distance of weights from axis of oscillation = 5 cm.

Liquid	Temp. °C	η (poise)	Decrement (p)	$\log_{10} p$
Glycerine sol.	28.4	1.65	1.42	.1523
Castor oil	30.0	4.1	1.94	.2878
" "	27.8	5.20	2.20	.3424
" "	25.5	6.0	2.43	.3856
" "	22.8	7.6	2.90	.4624
" "	20.0	9.75	3.95	.5966

Table XXXVIII

Torsion tape V

Distance of weights from axis of oscillation = 5 cm.

Liquid	Temp. °C	η (poise)	Decrement (p)	$\log_{10} p$
Castor oil	18.6	11.1	2.07	.3160
" "	21.7	8.5	1.78	.2504
" "	22.4	8.0	1.66	.2201
" "	26.2	5.8	1.49	.1732
" "	28.4	4.8	1.42	.1523
" "	29.2	4.2	1.36	.1335

The Viscosity of MnO-SiO_2 Slags.

The slags were prepared from pure MnO and SiO_2 sand. Procedure. The experimental procedure was the same as before, the only difference being in the material of which the cylinders are made. The inner cylinder of molybdenum and molybdenum connecting rod (see fig. 76) were of such a length that when the inner cylinder was withdrawn from the slag at high temperatures, the molybdenum remained in the reducing atmosphere of the furnace. Results are tabulated in table XXXIX and the viscosity-temperature curves are shown in fig. 81.

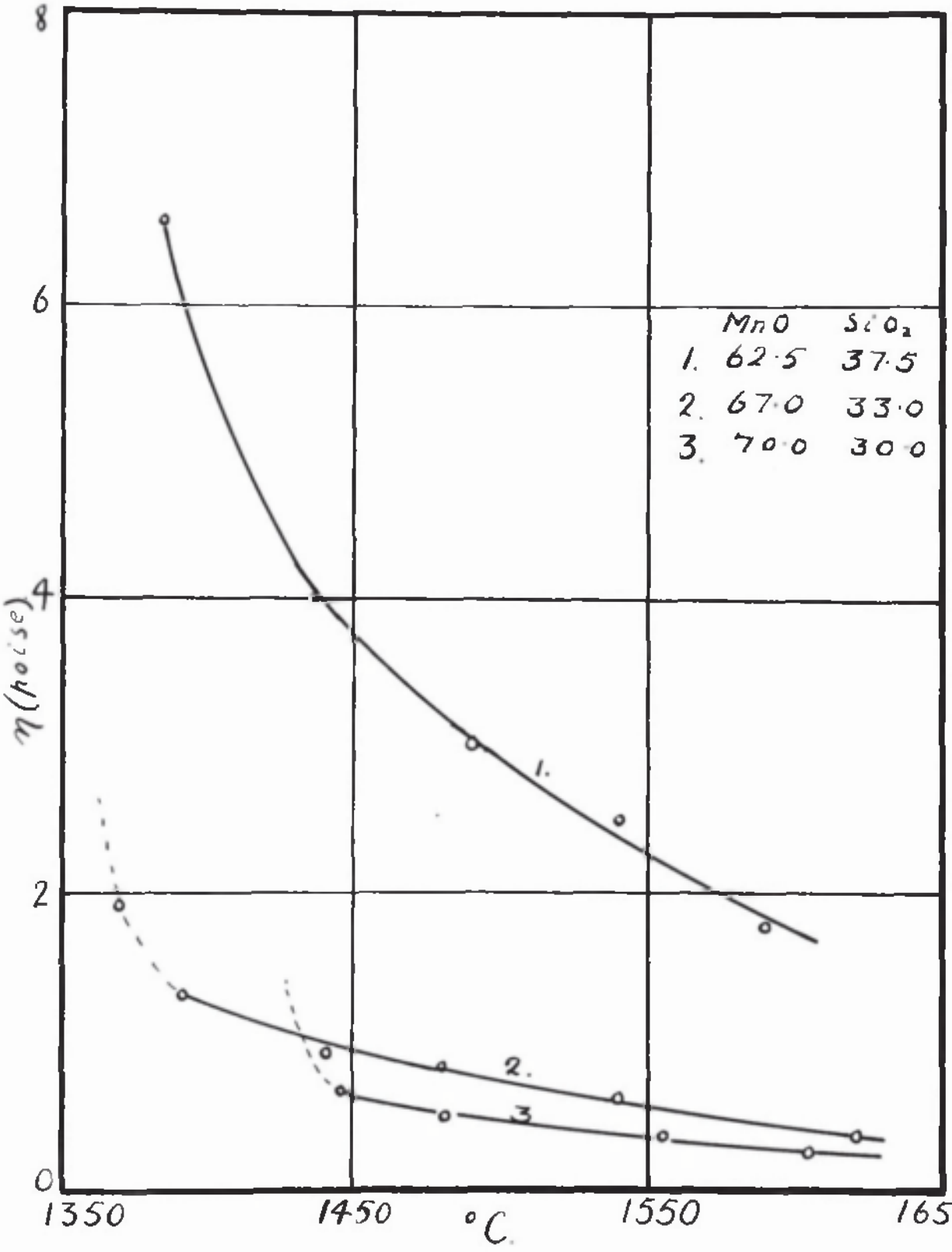
8
6
4
2
0
η (poise)
MnO SiO₂
1. 62·5 37·5
2. 67·0 33·0
3. 70·0 30·0
1.
2.
3
1350
1450
°C.
1550
1650

Fig. 81.

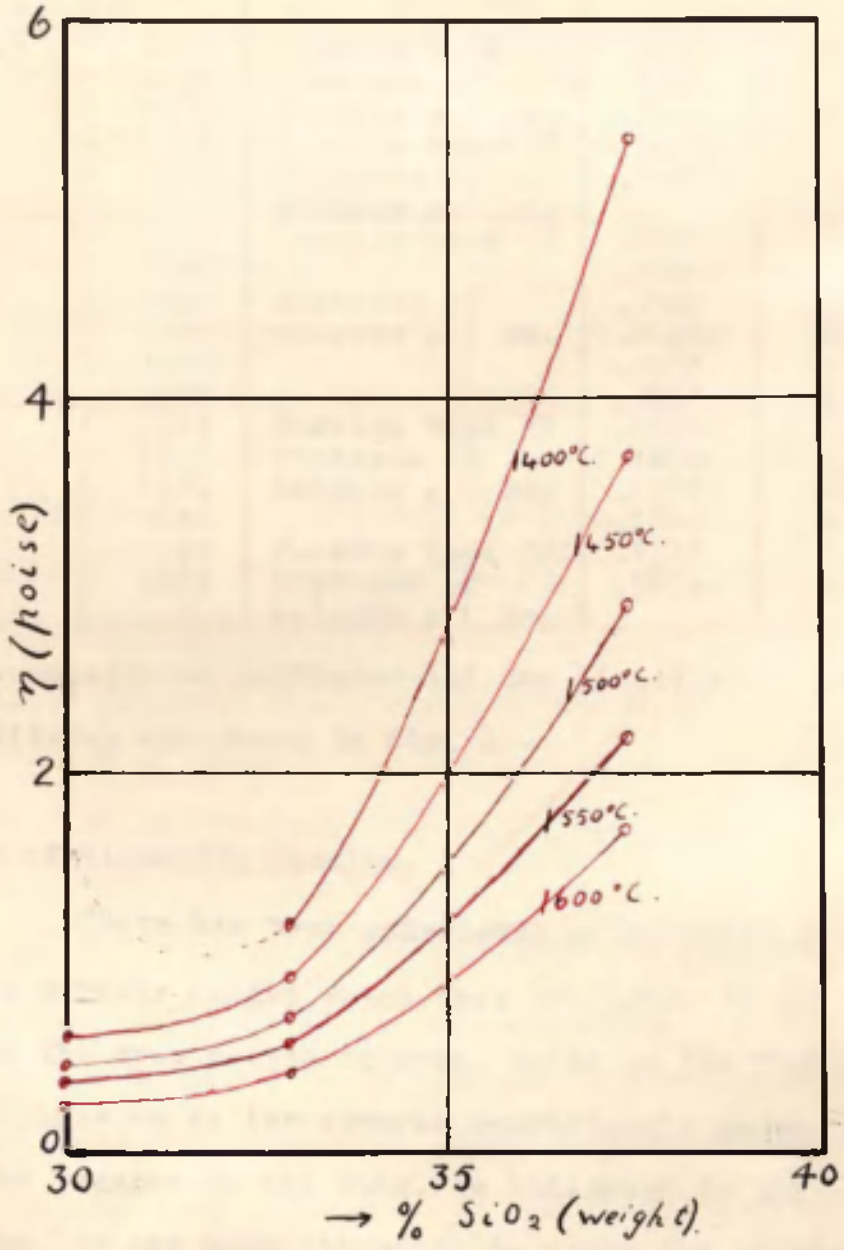
6
4
2
0
η (noise)
1400°C.
1450°C.
1500°C.
1550°C.
1600°C.
30
35
40
→ % SiO2 (weight)

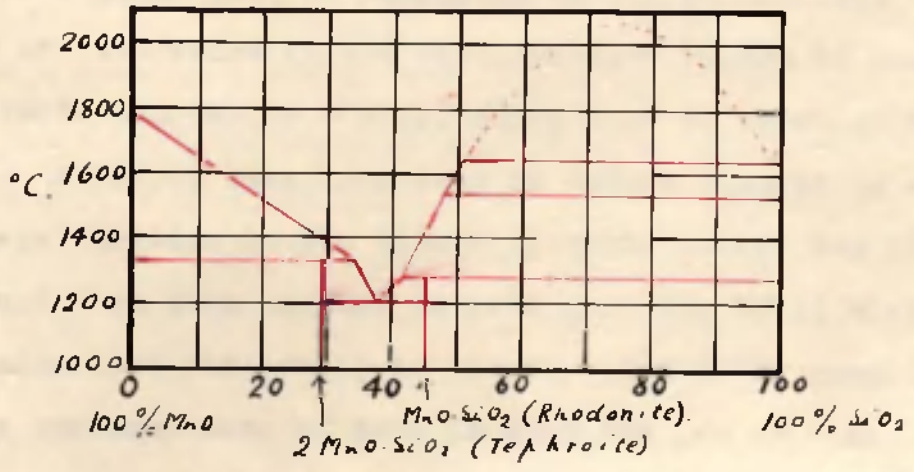
2000
1800
°C.
1600
1400
1200
1000
0
20
40
60
80
100
100 % MnO
MnO·SiO2 (Rhodonite)
100 % SiO2
2 MnO·SiO2 (Tephroite)

fig. 82

Table XXXIX

% Composition MnO	% Composition SiO_2	Temp. °C	Experimental Details	$Log_{10}\eta$	η (poise)
62.5	37.5	1490	Torsion tape V.	.1072	3.0
		1435	Distance of	.1303	4.0
		1370	weights = 5 cm.	.1959	6.6
		1590	Torsion tape IV	.1614	1.75
		1540	Distance of	.2041	2.50
			weights = 5 cm.		
67	33	1520	Torsion tape IV	.0969	0.32
		1540		.1584	0.61
		1480	Distance of	.1987	0.80
		1440	weights = 1 cm.	.2304	0.95
		1392		.3075	1.32
		1370		.4533	1.97
70	30	1605	Torsion tape IV	.0828	0.25
		1555	Distance of	.1038	0.35
		1480	weights = 1 cm.	.1271	0.47
		1435		.1761	0.70
		1590	Torsion tape III	.1761	0.26
		1435	Distance of	.3979	0.72
			weights = 1 cm.		

Viscosity-composition isotherms and the liquidus of the $MnO-SiO_2$ diagram are shown in fig. 82.

Discussion of Viscosity Results.

There has been considerable discussion as to whether the various oxides which form the slags in the blast furnace and the open hearth furnace, exist in the liquid slag as simple oxides or as the mineral constituents which have been proved to be present in the slag. As indicated in the introduction, it has been attempted to prove the existence of compounds from viscosity data.

The viscosity of ordinary liquid mixtures has received a great deal of attention as can be realised from the number of references in the supplementary volume of Landolt and Börnstein's Tables (1927), which runs to about eleven hundred. Attempts have been made to deduce changes in a mixture from peculiarities in the viscosity-ratio curves and their departure from laws assumed to hold good for ideal mixtures. The fundamental difficulty in the way of drawing conclusions from an enormous mass of data is that the law of "ideal" mixtures is not known. Hatschek in "Viscosity of Liquids" states that "the viscosity-concentration function for a mixture approaching the ideal as closely as possible is not known, but

is certainly not linear. It is, therefore, obvious that all attempts to deduce changes in the molecular complexity or chemical composition of mixtures from peculiarities of the viscosity-ratio curves and their deviations from an arbitrarily assumed law must be viewed with caution, unless there is independent evidence of such changes." It has been shown that, generally speaking, associated liquids - and particularly those containing hydroxyl groups - have relatively high viscosities, and therefore a maximum in the viscosity curve indicates further association and eventually complex formation. Hatschek points out that although "maxima are held to occur whenever there is chemical combination; it is questionable whether the converse can be safely assumed that all maxima are due to the formation of compounds." There is fairly general agreement that the particular ratio at which a viscosity maximum occurs does not necessarily, or even probably, indicate the compound or complex causing the maximum. FINDLAY[55] has suggested that it is not the position of the maximum, but the maximum deviation from the ideal mixture law, which is the important factor. As long as the ideal law of mixtures is unknown, this maximum deviation is necessarily unknown. Hatschek gives viscosity-composition curves for mixtures of ethyl formate and stannic chloride. The viscosity-composition curves have each a very sharp maximum at the composition corresponding to one molecule of stannic chloride to two of ester. A mixture of stannic chloride and acetic acid behaves similarly. At the composition $SnCl_4 \cdot 3CH_3COOH$, the viscosity-composition curve has a sharp maximum. There is evidence of the formation of this compound as there is marked evolution of heat on mixing and a decrease in volume.

ENGLISH[31] found that the viscosity-composition curve of glasses composed of soda, borax and silica showed a maximum at a temperature of 600°C corresponding to the composition $3Na_2O.2B_2O_3.xSiO_2$. At 700°C the viscosity peak was less marked and at 800°C had disappeared. This was taken as indicating that the compound was unstable at 800°C.

When there is thermal or other evidence for the existence of a compound at its melting temperature, a maximum in the viscosity-composition curve at the composition of the compound might be taken as evidence of the existence of the complex in the liquid state. However, since the ideal law of mixtures is not known, absence of a maximum in the viscosity-composition curve cannot be assumed to indicate the absence of the compound.

Examination of the viscosity-composition isotherms in fig. 56 shows that increase of CaO decreases the viscosity of $CaO-SiO_2$ slags in the range 52-44% CaO. Thermal evidence shows that a mixture of 48.28% CaO and 51.72% SiO_2 melts as the compound $CaO.SiO_2$ (calcium bisilicate). However, no maximum appears in the viscosity-composition isothermal curves.At 44% CaO, the slag melts as a mixture of $CaO.SiO_2$ and SiO_2. This mixture has a higher viscosity than the compound. The most fluid mixture found in this range consisted of calcium sesquisilicate and calcium bisilicate. In this range, the mixture with the highest melting point (1540°C) has the composition of the compound $CaO.SiO_2$ and is less viscous than the eutectic mixture of calcium bisilicate and silica with the melting point of 1500°C.

The viscosity-composition isotherms shown in fig. 82 indicate decreasing viscosity with increasing MnO in the system $MnO-SiO_2$. The eutectic mixture has the highest viscosity and the lowest melting point of the three melts examined. Thermal evidence shows that the compound tephroite ($2MnO.SiO_2$) undergoes peritectic dissociation and in the liquid state will be largely dissociated. It has the lowest viscosity of the three melts examined. The viscosity-composition curves have a decided sag, indicating that with increasing SiO_2 beyond the eutectic composition, the viscosity increases rapidly.

Thermal evidence indicates that the liquidus in the system $CaO-Al_2O_3$ has a very sharp maximum at the composition $5CaO.3Al_2O_3$. The viscosity-composition isotherms in fig. 58 show a maximum at this composition decreasing with increase

in temperature until at 1600°C the maximum has disappeared. At 1500°C, the maximum depends on one result and more evidence would be required. At 1550°C the maximum is not pronounced. As shown in fig. 57, the viscosity-temperature curves are very steep, an error of 10 C° in temperature introducing a large error in viscosity. In further work in this system careful temperature control would be required. However, since the temperature control was within 10°C, these results might be explained as indicating the break down or the complex $5CaO.3Al_2O_3$ with increasing temperature above the liquidus.

The ternary system $CaO-SiO_2-Al_2O_3$ is much more complicated; the law for ideal mixtures of two components is not known and is certainly not known for three components. McCAFFERY[12] found that slags composed of CaO, SiO_2, Al_2O_3 and MgO showed large changes in viscosity with composition at 1400°C, but as the temperature was increased these changes with composition decreased. He suggested that at 1400°C, complexes existed in the liquid state, but at high temperatures (over 1600°C), the slags were mixtures of the simple oxides.

According to FINDLAY[56] association of molecules in many liquids and the existence of liquid crystals in certain organic compounds has been recognised. Examination by polarised light of such substances as p-azoxyanisole and p-azoxyphenetole showed that the liquid exhibited turbidity, double refraction and interferance colours at temperatures just above the melting point. No evidence of a true space lattice was found by x-ray analysis, but there is an orientation of the molecules with their axes parallel, into aggregates or swarms. On further heating they become isotropic at definite temperatures, and on cooling, the reverse series of changes occur; the process is enantiotropic. In 1933, the Faraday Society published a Symposium on Liquid Crystals. ORNSTEIN and KAST[57] suggested that every liquid which has not perfectly symmetrical molecules, forms swarms in the immediate neighbourhood of the melting point, of the same kind as are stable for liquid crystals over a larger temperature range. The size of the swarms decrease

with increase of temperature as measured from their double refraction and diamagnetic and dielectric anisotropy. This was confirmed by a number of other authorities[58]. SOSMAN[59] states that the unit of structure in liquid silica is larger than the simple atom triplet SiO_2. LAWRENCE[60] suggested that any solution having a structure would be expected to have a high viscosity.

In the $CaO-SiO_2$ and $MnO-SiO_2$ slags, the viscosity was decreased with decreasing silica as shown by the viscosity-composition isotherms. Examination of the viscosity-composition isotherms in figs. 68-73 and the constitution diagram in fig. 75 shows that the viscosity of $CaO-SiO_2-Al_2O_3$ slags increases very rapidly with increasing free silica even at a temperature of 1600°C. A striking feature of the viscosity-temperature curves for $CaO-SiO_2-Al_2O_3$ slags (figs. 59-67) is the convergence of the curves with increasing temperature. It would appear that at a temperature about 1700°C the variation of viscosity with composition would be greatly reduced. This could be explained by the existence of complexes in the $CaO-SiO_2-Al_2O_3$ slags at the lower temperatures and their break down with increasing temperature. Slags with high percentage of anorthite, gehlinite or free silica show a very rapid decrease in viscosity and converge with increasing temperature. In the $CaO-SiO_2$ slags, the viscosity does not increase very rapidly at temperatures just above the liquidus, but examination of the viscosity-composition curves figs. 59-67 shows that the viscosities of the $CaO-Al_2O_3-SiO_2$ slags approach the viscosity of the $CaO-SiO_2$ slags at about 1700°C. The viscosity-temperature curves of the $CaO-Al_2O_3$ slags (fig. 57) are very steep, but at temperatures of over 1600°C they appear to be approaching the viscosity of $CaO-SiO_2$ and $CaO-SiO_2-Al_2O_3$ slags. It is probable that at such temperatures (about 1700°C), the aggregates or swarms have disappeared and the slags are composed of the simple oxides CaO, SiO_2 and Al_2O_3.

In fig. 49 is shown the effect of fluorspar on a blast furnace slag composed chiefly of CaO, SiO_2, Al_2O_3 and MgO. If the rapid rise in viscosity is due to the existence of aggregates or molecules, the effect of fluorspar may be to inhibit their formation or to displace their growth to a lower temperature. It is interesting to note that as the temperature is increased, the curves converge. At 1600°C, the fluorspar reduced the viscosity from 3 to 1.7 poise while at 1450°C it is reduced from 30 to 5.4 poise. SCHWERIN[61] and MATSUKAWA[47] also found that fluorspar lowered the viscosity of slags. Schwerin investigated blast furnace slags differing in composition from the one investigated here, but the form of the curves are very similar to those in fig. 49. Schwerin's curves converged with increasing temperature. The effect of adding fluorspar is analagous to increasing the temperature.

RANKIN and WRIGHT[10] have shown that the melting points of mixtures of lime, silica and alumina in the range of compositions found in blast furnace slags are typical of eutectic forming compounds or minerals. The viscosity results seem to indicate that even at temperatures about 1600°C, the slag does not behave as a simple solution of the oxides, but as a mixture of compounds. Details of the compounds occurring in this range are given in table XL.

Table XL

Compound	Composition	Analysis CaO	Al_2O_3	SiO_2	Melting point.
Calcium bisilicate	$CaO.SiO_2$	48.28	---	51.72	1540
Calcium sesquisilicate	$3CaO.2SiO_2$	58.34	---	41.66	1700
Calcium orthosilicate	$2CaO.SiO_2$	65.12	---	34.88	over 1700
Anorthite	$CaO.Al_2O_3.2SiO_2$	20.16	36.65	43.19	1550
Gehlinite	$2CaO.Al_2O_3.SiO_2$	40.91	37.18	21.91	1590

As shown in fig.75, three of these minerals can only be present in any one slag.

It will be observed that in this range CaO and SiO_2 may combine to form one or two of the three silicates in any

one slag. The Al_2O_3 always forms a ternary compound containing CaO and SiO_2. In any slag, one or both of these ternary compounds is formed. These compounds can be considered as bisilicates of lime. In anorthite the Al_2O_3 molecule replaces a molecule of lime, alumina thus acting as a base. In gehlinite, the molecule of Al_2O_3 acts as an acid replacing the molecule of SiO_2. The formation of these compounds and their relative proportions depend on the relative amounts of lime and silica available for combination with the alumina.

The Variation of Viscosity with Basicity $(\frac{CaO}{SiO_2})$ for Constant Alumina Contents.

As shown in fig. 75, slags containing 10% Al_2O_3 and with a basicity between .4 and .8 consist of silica, anorthite and calcium bisilicate. As the basicity is increased from .4 to .8, the silica is reduced and at a basicity of .8, the slag consists chiefly of bisilicate and anorthite (about 73% bisilicate and 27% anorthite). The viscosity decreases rapidly at 1500°C (see fig. 68). Between the basicity ratios of .8 to 1.0, the constituents are bisilicate, anorthite and gehlinite. From .8 to 1.0, the anorthite is replaced by gehlinite, the amount of calcium bisilicate remaining approximately constant. The decrease in viscosity is not marked. On increasing the basicity beyond 1.0, the slag composition passes into area 2 of fig. 75, calcium sesquisilicate replacing the bisilicate and the viscosity begins to increase rapidly.

The isotherms at 15% Al_2O_3 are very similar to those at 10%. There is a rapid decrease in viscosity with decreasing silica. In area 1, the constituents are bisilicate, anorthite and gehlinite with the latter two in greater proportion. With increasing basicity, the anorthite is replaced by gehlinite with a gradual decrease in viscosity. In this range a small change in basicity does not affect the viscosity greatly. At a basicity greater than 1.1, the anorthite disappears, sesquisilicate appearing, accompanied by an increase in viscosity. In this region a small change in basicity brings about a change in the constitution of the slag and a distinct change in viscosity.

At 20% Al_2O_3, the viscosity decreases rapidly with increasing basicity from 0.4 to 0.7 as shown by the isotherms in fig. 70. This corresponds to a decrease in silica content. At the CaO to SiO_2 ratio of 0.7 the free silica has disappeared and the slag consists of approximately 55% anorthite and about 45% bisilicate. Increasing the basicity from 0.7, anorthite is replaced by gehlinite while the bisilicate remains practically constant until at 1.3, the anorthite has disappeared. The decrease in viscosity is not marked and up to a lime to silica ratio of 1.174 the viscosity has not commenced to increase. At 35% Al_2O_3 passing from a basicity of 0.428 to 1.3 the anorthite is gradually replaced with gehlinite, the small amount of bisilicate remaining practically constant. The slags contain over 90% gehlinite and anorthite. With increasing basicity, the viscosity at 1500°C falls rapidly to about 28% CaO. From 28% to about 32% CaO there is not much change in viscosity, but with further increase in CaO the viscosity increases rapidly.

It is obvious from these results that anorthite is the most viscous of the slags examined. Gehlinite is also very viscous.

The Influence of Alumina on the Viscosity.

For all the CaO to SiO_2 ratios examined, it was found that increasing alumina increased the viscosity at any given temperature above the liquidus, the effect being greater the lower the temperature. This corresponded to an increase in anorthite or gehlinite.

However, for a ratio of 1.3 this is not the case. From the thermal diagram it is seen that such melts from 0 to 10% Al_2O_3 have high melting points and are not in the liquid state at 1500°C. At 15-20% Al_2O_3, the melting point is somewhere in the region of 1400°C and this composition of slag is near the minimum viscosity for this alumina content as seen from the isotherms. With further increase in alumina the viscosity and the melting point rise due to increase in gehlinite and anorthite. In actual blast furnace practice, the basicity usually employed is 1.4 with about 15-18% Al_2O_3. The above

shows that this composition is not far removed from the minimum viscosity for this alumina content and has a low melting point. In actual blast furnace slags, however, there is about 5% MgO, but McCaffery found that increasing MgO lowered the viscosity and melting points of all the slags in this region. Such slags, therefore, will be molten and free running at 1400°C and will melt above the tuyeres zone of the furnace.

However, with an alumina content from 0 to 10%, the slag will not be completely molten at the tuyeres zone due to the presence of sesquisilicate and orthosilicate. Hence higher hearth temperatures are required with the consequent difficulty of preventing too great a reduction of SiO_2 in the slag. With alumina greater than 20%, the constituents are chiefly gehlinite with some bisilicate and anorthite. The melting point is increased and the viscosity increased. COLCLOUGH[17] states that such slags in practice can be melted and the furnaces operated smoothly only if the hearth temperature is raised above the normal by operating with a low ratio of coke to ore. This results in an increase in the reduction of silica to silicon which passes into the iron. As a result, ores with 20-30% Al_2O_3 and basicity of 1.4 have been used to produce iron high in silicon and suitable for foundry practice. To produce basic iron, a lower hearth temperature is necessary to decrease the reduction of silica. Under such conditions, the furnace forms scaffolds and sticks. These difficulties are due to the excessive proportion of the mineral gehlinite.

A feature of the viscosity isotherms (figs. 68-73) is that for each alumina content there is a minimum viscosity. McCAFFERY[12] found that the CaO, SiO_2, Al_2O_3 and MgO slags showed this feature. The compositions of slags of minimum viscosity for each alumina content are shown in table XLI.

Table XLI

	% Alumina					
	10	15	20	25	30	35
SiO_2 %	43	40	36	37	35	35
CaO %	47	45	44	38	35	30
$\frac{CaO}{SiO_2}$	1.09	1.12	1.22	1.02	1.00	.86
Viscosity (poise)						
1500°C	4.0	5.4	10.0	15.0	17	18
1550°C	3.0	3.4	7.0	9.5	11.5	--
1600°C	1.9	2.4	4.5	6.0	7.5	--

Table XLII shows the composition of slags of minimum melting point for each alumina content.

Table XLII

	% Alumina					
	10	15	20	25	30	35
SiO_2 %	41.6	41.5	42	39.5	37	34.5
CaO %	48.4	43.5	38	35.5	33	30.5
$\frac{CaO}{SiO_2}$	1.16	1.05	.9	.9	.89	.88
Temperature °C (approx.)	1330	1316	1265	1310	1350	1370

It will be noted that the compositions of minimum viscosity do not occur at the compositions of lowest melting, but with the exception of 20% Al_2O_3 they are in very close proximity.

It is obvious, therefore, in blast furnace practice that a basicity of 1.4 cannot be employed irrespective of the alumina content. As suggested by COLCLOUGH[27], it is necessary to vary the basicity with alumina content so as to obtain the most suitable melting point and viscosity in the slag. With slags containing more than 20% Al_2O_3, Colclough found that the most suitable basicity was about 1.0 and employing such a factor, was able to produce basic iron from ores containing about 25% Al_2O_3.

The chief constituents of an acid open hearth furnace slag are FeO, MnO, CaO and SiO_2 . During the refining

action, the slag dissolves silica from the hearth tending to form a saturated solution. For the furnace temperature, the composition of a saturated slag composed of FeO, MnO and SiO_2 can be obtained from the ternary equilibrium diagram FeO-MnO-SiO_2 published by HAY and his co-workers[20]. The rate of the refining actions are decreased, and, for successful operation, it is necessary to maintain a proper amount of FeO and MnO in the slag by charging scale, iron ore or manganese ore. The viscosity-composition isotherms for MnO-SiO_2 slags show that the viscosity increases with increasing SiO_2. An increase in viscosity would explain the decrease in the rate of the chemical reactions of refining. MATSUKAWA[47] found that MnO-SiO_2 slags were fluid and that the viscosity of open hearth slags decreased with increasing MnO. Since his results are not expressed in absolute units, they cannot be compared quantitatively with my results. Endell in a private communication gives a viscosity-temperature curve for a slag composed of MnO and SiO_2, which agrees very closely with the curves shown in fig. 81. He encountered difficulties which he does not describe and was unable to obtain further results in this system. Endell's investigations were carried out with a platinum cylinder and the close agreement with my results is a further proof that the molybdenum does not contaminate the slag.

The probable explanation of the stability of the silica hearth in the acid furnace is, that as the slag attacks the hearth it takes silica into solution forming a viscous layer on the surface of the hearth. The rate of diffusion of FeO and MnO to the silica will, therefore, be decreased with a subsequent decrease in the rate of attack of the hearth.

Further application of viscosity to acid open hearth practice cannot be made until results are obtained for FeO-SiO_2, FeO-MnO-SiO_2 and FeO-MnO-SiO_2-CaO slags. An apparatus in which the viscosity can be determined in a controlled atmosphere has been designed but results have not yet been obtained.

BIBLIOGRAPHY

1 COLCLOUGH.....'A Study of the Reactions of the Basic Open Hearth Furnace' Symposium of The Faraday Society--1925.

2 McCANCE.....Trans. Faraday Soc., 1918, Vol. 14, p. 213. and 1925, vol. 26, p.176. Jour. West of Scot. I.S.I. 1933 vol. XL and 1933-34 vol. XLI.

3 FERGUSON.....Jour. West of Scot. I.S.I. 1934-35, vol. 42, p. 13.

4 BENEDICKS and LOFQUIST....."Non-Metallic Inclusions in Iron and Steel."

5 VOGT.....Die Silikatschmelzlosungen mit besonderer Rucksicht auf die Mineralbildung und die Schmelzpunktemiedrigung. Christiana 1903-04

6 DOERINCKEL.....Metallurgie, 1911, viii, p 204.

7 SOSMAN.....Trans. Faraday Soc. xii,1917.

8 WHITELY and HALLIMOND.....J.I.S.I. 1919, xcix., p. 199.

9 HERTY.....Co-operative Bull. No. 36 U.S. Bureau of Mines, 1928 and Metals and Alloys, Decr., 1930, vol. 1,p. 883.

10 RANKIN and WRIGHT.....Amer. Jour. of Sci., 1915, 39, page 88.

11 FEILD and ROYSTER.....Bureau of Mines, Technical Papers nos. 187 and 189.

12 McCAFFERY.....Trans., A.I.M.E., 1931 (Iron and Steel Division), p. 60 and 1932, vol. 100, p.64. American Institute of Mining and Metallurgical Eng. 1931, Tech. publ. no. 383

13 MATHEWSON, SPIRE and MILLIGAN...Amer. Soc. Steel Treaters, 1931, 19, p. 66.

14 JETTE and FOOTE.....Trans. A.I.M.E. 1933, vol. 105, p. 276.

15 TRITTON and HANSON.....J.I.S.I. 1924, vol. cx., p. 90

16 HAY, HOWAT and WHITE.....Jour. West of Scot. I.S.I., 1933-34, vol. , p. 97-105.

17 BOWEN and SCHAIRER.....Amer. Jour. Sci. 5th. series, vol. 24, 1932, p. 177.

18 BOWEN and GREIG.....Journal of the American Ceramic Society, vol. 7, 1924, p. 238.

19 ANDREW, MADDOCKS and HOWAT.....Jour. I and S., 1931, cxxxiii, 283.

20 WHITE, HOWAT and HAY.....Jour. Royal Technical College, Glasgow, 1934, vol. 3, part 2, p. 231 and

HAY, HOWAT and WHITE.....Jour. West of Scot. I.S.I 1933-34, vol. 41, p. 97-105. and

HAY, WHITE and McINTOSH.....Jour. West of Scot. I.S.I. 1934-35, vol. 42, p. 99-104.

and HAY, McINTOSH, RAIT and WHITE.....Jour. West of Scot. I.S.I. 1936-37, vol. 44 , p.85-92.

and McINTOSH, RAIT and HAY.....Jour. Royal Technical Coll, Glasgow, 1937, vol. 4 Part 1 , p. 72.

21 ESSER, AVERDIECK and GRASS.....Archiv. fur das Eisenhuttenwesen, vol. 6, 1932-33, p.269.

22 EPSTEIN ....."Alloys of Iron and Carbon" vol. 1

23 MATSUBARA and SCHENK....."Jour. Amer. Inst. of Mining and Metallurgical Eng." 1922, vol. 67, p. 3.

24 HERTY.....Metals and Alloys, Dec. 1930

25 MASING.....Ternäre Systeme.

26 MARSH.....Principles of Phase Diagrams

27 COLCLOUGH.....Jour. Iron and Steel Inst. Sept. 1936

28 KRINGS and SCHACKMANN.....Z An Org. Allg. Chem. 1931 vol. 209, p. 99.

29 C.H. HERTY.....Min. Metallurg. Invest. Bull. 47, 1930.
Stahl. u. Eisen 51 (1931) S 463/65.

30 ENDELL.....Archiv. fur das Eisenhuttenwesen Heft. 3 Sept. 1936.

31 ENGLISH.....Jour. Soc. Glass Techn. 1924, vol. 8.

32 V.H. STOTT.....Jour. Soc. Glass Techn. 1925, vol. 9.

33 MARGULES.....Sitz. Wiener Akad, 1881, 83, 588.

34 COUETTE....."Viscosity of Liquids" Hatschek.

35 HATSCHEK....."Viscosity of Liquids" Bell & Sons Ltd., London , 1928.

36 LADENBURG.....Ann, Physik, 1907, 22, 287.

37 SCHOTTENER.....Sitz. Wiener Akad., 1879, 79 47.

38 GREINER.....Inaug. Diss. Jena, 1907.

39 ARNDT and GESSLER.....Zeitsch., Elektrochem., 1907 13, 580.

40 DOELTER.....Sitz. Wiener Akad., 1905, 114, 529

41 STALEY.....Eighth Inter. Cong. App. Chem. 1912, sect. IIIc. 5, 127.

42 TROUTON and ANDREWS, Phil. Mag. 1904, 7, 347.

43 ENDELL.....z. Metallkunde, 17 (1932)368

44 GEHLOFF and THOMAS.....z. Tech. Phys., 7, 1926

45 PROCTER and DOUGLAS.....Proc. Phys. Soc. 41, 1929 500.

46 SAITO and MATSUKAWA.....Memoirs College of Eng. Kyoto Imp. Univ. 2 (1932) 49.

47 MATSUKAWA.....The Taniguchi Foundation for the Promotion of Industrial Progress, March, 1935.

48 FAWSITT.....Proc. Roy. Soc., 1908, vol. 80, p. 290.

49 GUYE and VASILEFF.....Arch. des Sciences Phys. and Nat. Geneve, 1914, 37, 214.

50 OBERHOFFER and WIMMER.....Stahl u Eisen, 1925, vol. 45, pp. 969-977.

51 THIELMANN and WIMMER.....Stahl u Eisen, 1927, vol. 47, pp. 389-399.

52 ESSER, GREIS and BUNGARDT.....Archiv. fur das Eisenhuttenwesen, 1934, vol. 7 pp.385-388

53 STOTT.....Proc. Phys. Soc. 1933, vol 45, pp. 530-544.

54 ENDELL.....Archiv. fur das Eisenhuttenwesen Heft. 3 Sept. 1936.

55 A. FINDLAY....."Viscosity of Liquids". Hatschek.

56 A. FINDLAY.....The Phase Rule and its applications. Longmans, Green & Co., New York., sixth edition, 1927, pp. 65-67

57 L.S. ORNSTEIN and W. KAST.....New arguments for the Swarm Theory of Liquid Crystals. Trans. Faraday Soc. Vol. 29, 1933, pp. 931-944.

58 Liquid Crystals and Anisotropic Melts.- A general discussion. Trans. Faraday Soc., vol. 29, 1933, pp. 881-1085.

59 R.B. SOSMAN.....The Properties of Silica. Chemical Catalogue Co. New York, 1927.

60 A.S.C. LAWRENCE.....Lyotropic Mesomorphism. Trans. Faraday Soc. vol. 29, 1933, pp. 1008-1015.

61 L. SCHWERIN.....Metals and Alloys June 1934 p. 118.